NASA SP–5103

SELECTED TECHNOLOGY FOR THE GAS INDUSTRY

A conference held at
LEWIS RESEARCH CENTER
Cleveland, Ohio
March 19–20, 1975

NATIONAL AERONAUTICS AND SPACE ADMINISTRATION

NASA SP-5103

SELECTED TECHNOLOGY FOR THE GAS INDUSTRY

The proceedings of a technology utilization conference held at Lewis Research Center, March 19–20, 1975

Prepared by Lewis Research Center

Technology Utilization Office 1975
NATIONAL AERONAUTICS AND SPACE ADMINISTRATION
Washington, D.C.

FOREWORD

In welcoming you to the Lewis Research Center and this Conference, I would like to acquaint you with the Center and its work.

Lewis Research Center was established in 1941 as the Aircraft Engine Research Laboratory of the National Advisory Committee for Aeronautics. As the propulsion research center of NACA until 1958, its task was to advance the technology of our Nation's aircraft engines. From this effort, in partnership with other research laboratories and the American industry, came many benefits to our Nation. The air arm of our military forces was strengthened, a new level of mobility was provided to our people and their goods, and American aircraft came to dominate the commercial fleets of the free world.

In October 1958, Lewis became part of the National Aeronautics and Space Administration with a broadened responsibility in the fields of propulsion and power for both aeronautical and space applications. Here our technologies have helped explore the planets, place men on the Moon, measure the stars, and view the resources and environment of our Earth from a vantage point in space. The ultimate benefits of this new knowledge and these new technical capabilities are truly immeasurable.

Lewis Research Center occupies 350 acres adjacent to Cleveland Hopkins International Airport and 8000 acres at the Plum Brook Station near Sandusky, Ohio, about 50 miles west of Cleveland. The physical plant comprises a number of unique major facilities such as altitude chambers, wind tunnels, huge vacuum tanks, and a 500-foot deep chamber for free-fall experiments, as well as laboratories for chemical, metallurgical, physical, and electrical research. The total capital investment is about $270,000,000; the staff numbers about 3000, including 1200 scientists and engineers.

Currently, about half of the program activities at Lewis are in the field of aircraft propulsion. The utility of civil aircraft is being improved by making them quieter, cleaner, more efficient, and more versatile. Another objective is to increase the effectiveness of military aircraft. Noise and

pollution reduction, propulsive lift systems for aircraft to ease future airport traffic congestion, and technology for supersonic flight are all areas of intensive work. The effort to improve engine performance and efficiency requires continuing research on compressors, combustors, turbines, and controls for turbomachinery.

For space flight, Lewis is responsible for the overall management of the development and operational use of the Atlas/Centaur and Titan/Centaur launch vehicles. The hydrogen-fueled Centaur upper stage, which was our Nation's first high-energy rocket vehicle, was a natural outgrowth of the pioneering work that Lewis performed in high-energy propellants in the late 1940's and early 1950's. This work has helped make it possible to select and apply liquid hydrogen for the upper stages of the Saturn rockets as well. The Titan/Centaur launch vehicle, with an initial thrust of 2 400 000 pounds, will be our Nation's largest launch vehicle for the rest of this decade. Atlas/Centaur and Titan/Centaur will provide launch services for public and private corporations, NASA and other government agencies, and foreign governments; payloads will include communications satellites, scientific probes, and spacecraft to explore other planets.

New technology for advanced spacecraft is also being developed at Lewis. A communications technology satellite sponsored jointly by the United States and Canada is based on advances in technologies such as broadcast tubes, antennas, and solar cells. The satellite, to be launched this summer, will broadcast television and audiosignals to small, inexpensive ground receiving stations in isolated regions of North America.

Another major area of work at Lewis is space electric power generation. Solar cells, batteries, fuel cells, thermionic converters, magnetohydrodynamic generators, and turbine systems driven either by boiling fluids (Rankine cycle) or heated inert gas (Brayton cycle) are subjects of study.

About 10 to 15 percent of the technical effort at Lewis can be categorized as basic research in support of present and future propulsion and power tech-technology. Areas of particular strength include materials research (lubrication, friction, and wear), plasma physics, and fluid mechanics.

More and more the technical capabilities from the aerospace program and the many needs of people here on Earth are coming together. Besides improved air travel, the long experience with gas turbines and other propulsion systems can be related to prime movers for ground or sea transporta-

tion. And the complex disciplines of power generation and energy conversion for space have much in common with energy problems here on Earth. Accordingly, these technologies are beginning to be put to productive use in achieving economic, clean transportation and abundant clean energy for all our people.

Emerging with these kinds of technical activity are many productive relationships with other government agencies - federal, state, and local. Several of the agencies with which Lewis has joined forces to assist the Nation toward energy self-sufficiency - Atomic Energy Commission, Department of Interior, Environmental Protection Agency, and the National Science Foundation - have recently transferred their energy research function to the newly created Energy Research and Development Administration. We look forward to a continuing, productive, working relationship with that agency.

This broadening use of aerospace technology is an exciting trend. It dramatizes Lewis' traditional role of technical service to others. We hope that this Conference will lead you and others in your industry to useful aerospace technology.

Bruce T. Lundin
Director
Lewis Research Center

Page intentionally left blank

Page intentionally left blank

INTRODUCTION

This Conference is motivated by an important objective of NASA - to ensure maximum value from national aerospace activities.

At its present level of $\$3\frac{1}{4}$ billion per year, the aerospace program is only a penny out of the Federal budget dollar, but it is a large part of the $18 billion that the Federal Government invests annually in research and technology. Federal research and technology expenditures represent about three quarters of the national total. Thus, it is important that this Nation use the results of all these expenditures as effectively as possible. In fact, the legislation that established NASA stipulates that NASA shall "provide for the widest practicable and appropriate dissemination of information concerning its activities and the results thereof."

A problem of first importance is that of usefully disseminating the technical information being generated in our country, especially when this information is so profuse, so fragmented, and so isolated from many potential users by company, industry, geography, and other factors - such as the form in which it appears. NASA has addressed itself to this communication problem in a variety of ways. This Conference is one such attempt at communication.

The underlying premise of this Conference is that advances made in one technical field can contribute to other fields. Anyone will immediately think of his own examples. For instance, space exploration was made possible by the development of rocket propulsion, the computer, and miniaturized electronics. To continue the example, the modern rocket engine evolved from engines developed for military purposes, and it traces its antecedents to Chinese pyrotechnics. But along the way it has both adapted and helped create turbopump technology, modern metallurgy, new understanding in fluid mechanics and thermodynamics, and advanced control systems.

Based on this premise, then, we have selected and will describe technical topics from aerospace activities that might have value for the gas industry.

There are several reasons for having chosen the gas industry for this effort. It is a large industry and it is vital to our Nation's well being. As one of the energy industries, its ingenuity will be increasingly challenged to keep up with growing energy demands. And, most compelling, perhaps, technical people from your industry expressed the belief that NASA information might be helpful to you.

The choice of the specific technical topics for this Conference was guided by meetings and consultations between members of our staff and members of the staff of the Institute of Gas Technology under the auspices of the American Gas Association. We are grateful for their help, and we thank them for it. In particular, acknowledgments are due Philip J. Anderson, Derek P. Gregory, Alex J. Konopka, Dennis H. Larson, George M. Long, Robert A. Macriss, Robert B. Rosenberg, Donald R. Shoffstall, Jerry Wurm, and Gene G. Yie, all of the Institute of Gas Technology.

The Institute's efforts were supported with funds provided by the American Gas Association under the direction and counsel of the Research and Development Executive Committee (REDEX) and the Research Review Committee; the American Gas Association Staff Project Manager was A. H. Rausch.

Finally, what NASA is doing and learning is, after all, yours. If additional value can be derived from the results, it should be. We want you to use whatever is useful to you.

But technology transfer is a push-pull game. This Conference can only give you an overview of the types of information available. We invite your further inquiry on whatever may interest you.

Water T. Olson
Director, Technology Utilization
and Public Affairs

CONTENTS

I. A PERSPECTIVE ON ENERGY

Robert E. English

A considerable technology already exists for solving some of our nation's problems concerning energy. A number of these technologies of special interest to the gas industry are described in this collection of papers.

The following are the areas of technology within which Lewis Research Center has conducted research on gas-turbine engines for aircraft during its 30 years of existence:

- Design of gas-turbine engines
- Compressor aerodynamics
- Turbine aerodynamics
- Combustion
- Materials
  - High-temperature alloys
  - Fracture mechanics
  - Corrosion
  - Low-cycle fatigue
  - Ceramics
  - Composites
- Turbine cooling
- Hydrogen as fuel

Our principal role has been in research on gas-turbine engines for aircraft. Special emphasis is herein placed on the range of application of this work, since many of the problems that have confronted us in the aeronautical field also face those in other endeavors. This range of application will be illustrated by discussing some other technologies that are beneficiaries of aircraft gas-turbine technology.

Figure I-1 shows a typical research compressor. It has eight stages, is about 20 inches in diameter, and is driven by a 15 000 horsepower motor. The technology which has evolved from research on such compressors has

been used in designing very different compressors, such as that shown in figure I-2. This compressor is 20 feet in diameter and supplies pressurized air to one of our wind tunnels. A 150 000-horsepower motor drives this compressor and demands about 120 megawatts of electric power. Compressors at the opposite end of the power spectrum were required for our space power program; two examples are shown in figure I-3. Driving each of these compressors at its design operating condition requires only 14 kilowatts, about 1/10 000 of the power of the wind tunnel compressor. The axial-flow compressor is 3.5 inches in diameter, and the radial compressor is 6 inches in diameter. Radial compressors having diameters as small as 3.2 inches have also been investigated. A wide range of applicability exists for such component research. For example, the AEC needed for their gaseous diffusion plants for separating U-235 from natural uranium very efficient compressors to compress the UF_6 gas. This gas has a molecular weight of 352 and, for that reason, requires a very different compressor design. But we applied the same basic technology in designing these compressors back in 1953.

NASA was confronted by a similar problem in its research for the space program. We were investigating gas-turbine power systems for use in space that would use nuclear energy as their basic energy source. In that program the gas-turbine powerplant shown in figure I-4 was built and tested. This 10-kilowatt powerplant is shown being prepared for testing in a large vacuum chamber (100 ft diam). By terrestrial standards, 10 kilowatts is a low power. Because the gas turbine was intended for operation in space, the gas loop is hermetically sealed and the gas that is the working fluid recirculates continuously within the powerplant. This gas-turbine engine is a complete powerplant that is capable of starting and stopping on command. It has recently completed 2 years of endurance testing.

As an example of the other constituent technologies listed previously, a corrosion problem of gas-turbine blades is shown in figure I-5. This corrosion resulted from sulfidation, a consequence of sulfur in the fuel that is a current problem for gas turbines in stationary powerplants here on Earth. In our application, this problem was solved by coating the blades with aluminum.

Hydrogen has been studied as a fuel for rockets and turbojet engines for over 20 years. Figure I-6 shows a B-57 aircraft modified to operate one of

its engines on liquid hydrogen. This aircraft was test flown here in 1956.

As a consequence of this background of research on the problems of converting energy from one form to another, we were asked by several agencies to participate with them in the evaluation and formulation of several energy programs. Some of these are the following:

(1) Evaluation of advanced engines for trains and buses - DOT
(2) Studies of energy research and development goals, sponsored by the Federal Council on Science and Technology -
    (a) Panel on Transportation Energy R & D Goals
    (b) Panel on Advanced-Cycle Central-Station Powerplants
(3) Solar energy as national energy resource - NSF/NASA Solar Energy Panel
(4) The Nation's Energy Future - report to the President by Dixy Lee Ray

The program set down by the NSF/NASA joint panel on solar energy provided the basis for the government's present program on solar energy. In the fall of 1973 the AEC assembled 16 panels to formulate the recommend programs of research and development in energy. NASA personnel contributed to a number of those panels. Dr. Ray used the reports from those panels in preparing her report to President Nixon in December 1973.

Through participation in these various program reviews we have become informed on various viewpoints concerning the supply of and demands for energy. Furthermore, we have had to probe more deeply and to evolve a perspective of our own in order that we could guide our own programs wisely.

The following topics are discussed in this paper:

(1) Supplies of fossil fuels
(2) Competition of electric power and synthetic natural gas as heat sources
(3) Use of wasted heat from power generation
(4) Present efforts to increase efficient use of energy

SUPPLIES OF FOSSIL FUELS

The sources of our energy in 1972 are listed in table I-1. Throughout this discussion, 1 quadrillion Btu's will be called "1 quad." One thousand

quads, or 10^{18} Btu, will be called "1 Q." Total energy used in 1972 was 72 quads, or a little less than 0.1 Q per year. The energy shown for hydroelectric power is the amount of fuel a conventional powerplant would require to produce the same amount of electrical energy. Gas and oil together constitute 79 percent of the energy used while coal constitutes 17 percent. Figure I-7 shows the known recoverable reserves of our fossil fuels. Shale oil is shown with a question mark because of the uncertainties of the economics, technology, and environmental impact of extracting shale oil. The reserves of oil and natural gas are shown as roughly 0.5 Q each, reserves adequate for about 20 years at the present use rates. We are aware of the present controversy concerning the supplies of these fuels from which so much of our energy comes, and we recognize that the amounts to be produced may exceed these amounts several times. I would rather focus our attention on the heights rather than the shortness of some of the bars.

Our coal reserves of 4 Q are sufficient for 325 years at the present rate of use. Because of the large reserve shown for coal, let us explore in more detail the resources of coal already mapped and explored (table I-2). The amounts of coal are given for various depths of coal deposits and for various seam thicknesses. The seam thicknesses are defined in the bottom section of the table; seams thinner than those listed have been ignored. To obtain the estimated coal reserves shown in figure I-7, only coal in thick seams and at depths less than 1000 feet was considered. Then half of this coal was estimated to be recoverable at roughly present costs and with present technology; the rest of the coal was neglected. But the total quantity of coal already mapped and explored is eight times the 4 Q amount, sufficient for 2500 years at the present use rate. The distribution of this coal is shown according to rank in figure I-8 and by location in figure I-9.

Of the coal whose location is known, 89 percent is within 1000 feet of the Earth's surface (table I-2). The main reason for this concentration of coal in shallow deposits is probably economic rather than geologic; that is, our exploration for coal has largely been confined to small depths. Why look deeply for coal if a 2000-year supply (at the present use rate) has already been located at depths of less than 1000 feet? Averitt of the U.S. Geological Survey makes the following statement concerning the deficiency in our knowledge about the amount of coal actually contained in the ground:

> The pronounced concentration of identified resources in the 0-1000-foot overburden category . . . results in part . . . from the fact that progressively less information is available for the more deeply buried beds . . . . As exploration and development are carried to greater depth it is certain that the identified resources will be considerably increased by addition of tonnage in the deeper overburden categories.

Thus, further exploration for coal may add substantially to the 32.6 Q shown.

As stated earlier, this 32.6 Q reserve of coal would last 2500 years if we would continue to use coal at the present rate. However, our rate of using coal is expected to rise. So, let us assume that we get all our energy from coal and that we continue to use coal at the present total energy-use rate. Then 32.6 Q would last over 400 years, a rather substantial period of time when we consider the paces at which both our technology and our economy move to create new options.

Figure I-10 shows our identified resources of shale oil. The practicality of using shale oil depends greatly on the concentration of oil in the shale, expressed here as gallons of oil per ton of shale. For the highest concentration, 8 Q have been identified. If we can extract just half of this 8 Q of oil from the ground, it would fulfill our present need for oil for over 100 years. The total of 65 Q is twice the energy shown for coal in table I-2. In table I-3 Duncan and Swanson of the Geological Survey make an informed judgment concerning the deposits of shale oil as yet undiscovered. The "known resources and possible extensions" shown in this table duplicate the data presented in figure I-10. Let us assume that we can get half of the 941 Q out of the ground. The resulting 470 Q is enough to fulfill our present needs for energy of all kinds for 6500 years. Present technology and present economic conditions will not permit extraction of all this fuel at present, but that is not the point. Large reserves of fossil fuels are in the ground, and before we run out of them, we may be able to evolve the technology to make these fuels available for our use.

In summary:

(1) We are not about to run out of fossil fuels. These supplies should last for several centuries.

(2) Exploration could more certainly define the magnitude of these resources, and such data are vital when formulating long-range energy plans.

(3) Two crucial factors are the technology and the construction of the physical facilities to make these resources available, low in cost, and socially acceptable.

Next, let us briefly consider waste as a possible energy source. The nation's total supply of organic wastes is shown in table I-4 in millions of tons of dry waste each year. If we take the optimistic view that we will collect all this waste and use it all to produce energy, then we might obtain about 9 quads of energy per year. This is about one-eighth or our present demand for energy. Although this is a significant number, it is not a cure for our energy crisis. In summary:

(1) The energy potential in waste is small in relation to our demand for energy.

(2) Recovery of energy from our waste might diminish the cost of waste disposal, thereby making a virtue of necessity.

Fortunately, we have very large resources of fossil fuels and can plan on their use for several centuries. This knowledge of our large resources of fossil fuels will now be used as a background for discussing our energy demands.

HEAT FROM ELECTRIC POWER OR SYNTHETIC NATURAL GAS

Our energy demands for 1972 can be classified into four categories. About 26 percent (18.6 quads) of our energy is consumed in producing electric power. Transportation consumes 25 percent (18.1 quads) and is utterly dependent on liquid hydrocarbons, all from petroleum at present. The residential and commercial and the industrial energy demands are in addition to their demands for electric power; these two demands total 49 percent (35.5 quads), essentially half of our present energy use. Because of the large size of these two demands, they are now analyzed in more detail.

Table I-5 shows the four demands and the energy sources for each demand as of 1972. In the residential and commercial sector and the industrial sector, 51 percent of the energy comes from gas and 35 percent from oil. Expressed another way, these two sectors make up 78 percent of the demand for gas. Therefore, because of their respective demands, each of these two sectors is considered in greater detail.

Table I-6 shows various residential and commercial uses for energy including electric power. For space heating alone, 12.8 quads are required each year; this is about 70 percent of the total demand in the residential and commercial sector. The industrial sector is similarly broken down in table I-7. Again electric power is included. Although most of this power is purchased, about 5 percent is generated by industry itself. The two largest demands are for heat - process steam alone demanding 11 quads per year.

Whether or not heat for residential and commercial buildings and for industrial processes should be shifted to electric power, since 17.7 quads are needed for industrial heat and 12.8 quads are required for heating residential and commercial buildings, has already received considerable attention nationally, and divergent opinions have been given as answers. The three criteria used herein to evaluate the competition between electric power and synthetic natural gas (SNG) for this market are as follows:

(1) Customer's cost for energy

(2) Magnitude of capital investment

(3) Overall efficiency

Table I-8 shows the electric-power-generating capacity required to fulfill these demands. Since the residential and commercial heating load is seasonal, it was assumed that the demand would extend over 3000 hours per year or just over one-third of a year. Furthermore, since the heating demand is not constant over this period, some allowance must be made for cold days; therefore, it was assumed that the peak demand would be twice the average during the heating season. Under these conditions, 1900 gigawatts of power-generating capacity are required to replace the 12.8 quads supplied by fossil fuels; this demand alone is roughly five times the entire power-generating capacity of the United States. This required capacity is so high because of the greatly varying demand imposed by the variableness of weather.

By way of contrast, the industrial process heat was assumed to be constant over 6000 hours a year. If this industrial heat were demanded during a normal 40-hour week for 50 weeks a year, the required electric generating capacity would also be 1900 gigawatts, the same as for the space heating of residential and commercial buildings. Because such heat would be costly, it was assumed that the economic incentive provided by such costly energy

would encourage industry to flatten its demand. So, it was assumed as an extreme case that the demand would be absolutely flat over 6000 hours per year. In that case, 600 gigawatts of power are required, a 150 percent addition to the presently installed capacity to generate electric power. The total cost of building the 2500 gigawatts of power-generating capacity would be of the order of $500 billion.

Table I-9 compares SNG and electric power as competitive means of meeting the residential and commercial demand for heat. The electric heat from fossil-fueled powerplants would cost the customer about 3 times as much per million Btu's as would SNG, and the required capital investment would be roughly four times as great. Although this electric power for heat could be obtained from nuclear rather than fossil powerplants, the cost to the customer would nearly double again because of the high capital cost of nuclear powerplants. Inasmuch as the electric powerplants for this service would have a capacity factor of only 17 percent under these conditions, a low-cost but inefficient powerplant would be installed; in spite of this, the capital investment for electric power is high. For SNG, on the other hand, gas produced would be stored against seasonal demand just as is done with natural gas at present. The overall efficiency of electric heat considers production of clean fuel from coal at 75 percent efficiency and a 25 percent efficiency for the low-cost power-generating system. The overall efficiency of 50 percent for SNG is the product of 70-percent efficiency of making SNG and 70-percent efficiency of transmission and use. SNG is seen to be superior to electric heat on all three measures of merit.

Heat pumps can diminish the disadvantages of electric power by providing twice as much heat for a given amount of electrical energy. Although this would cut the costs of electric heat by a factor of two and double its overall efficiency, SNG would still be superior on all three counts. Gas-driven heat pumps are being investigated by the American Gas Association and they are shown to improve the competitive advantage of gas over electricity.

The industrial demand is evaluated in table I-10. Use of electric power for typical industrial demands would cost about $9 per million Btu's, three times as much as SNG. Off-peak demands for electric heat might compete in unit cost with SNG. For the high hours of industrial demand each year, an

efficient but costly electric powerplant would be justified. Thus, the advantage of SNG concerning capital investment is the same as for the residential and commercial case but the efficiency advantage is narrowed.

To summarize:

(1) SNG will usually cost the customer less.

(2) SNG will require less capital investment.

(3) SNG will be more efficient.

USE OF WASTED HEAT FROM POWER GENERATION

Figure I-11 illustrates the problem posed by even our most efficient powerplants having an overall efficiency of 40 percent. For each 100 Btu's of energy consumed by the powerplant, 40 Btu's of useful energy are produced and 60 Btu's are wasted. In existing steam powerplants, the steam from the turbine is condensed at temperatures from 70^{o} to 100^{o} F. At such a low temperature not much can be done with this waste heat, and it is generally rejected to a nearby body of water. In some industrial applications, the temperature of the condensing steam is raised to 200^{o} to 400^{o} F in order to make this heat suitable for use, and a corresponding penalty in efficiency of producing power is accepted. As the costs of fuels rise, we should expect to see more use of this otherwise wasted heat from power generation.

Therefore, to decide whether an extensive use of the presently wasted heat will be practical, the following factors must be considered:

(1) The demand

(2) Economical transport of heat from powerplant to user of heat

(3) Nature of the power generator

(4) Characteristics of the energy source

As previously shown in table I-6 residential and commercial buildings require per year about 2.5 quads for heating water and about 12.8 quads for space heating; both of these demands for heat are at low temperatures. Also shown previously (table I-7), industrial process steam alone consumes 11 quads a year. The nature of the process steam is shown in figure I-12. Forty-five percent of the energy is used to produce steam at temperatures below 340^{o} F (the boiling temperature for water at 100 psi), and 43 percent of the energy is consumed in boiling water at temperatures from 340^{o} to

390° F (i. e., from 100 to 200 psi). Twelve percent of the energy is used at higher temperature. But we want now to focus our attention on the 88 percent at temperatures of 390° F and below, or 9.7 quads. The following shows these three demands for low-temperature heat to total 25 quads per year, which is 35 percent of our total energy demand and greater than all the energy we use to produce electric power:

	quad/yr
Residential and commercial:	
Space heat	12.8
Heat water	2.5
Industrial process ($T<400^{\circ}$ F)	9.7
Total	25.0

This demand is so large that a nation conscious of the needs for efficient use of its energy should focus considerable attention on how best to meet the demand.

In some industrial applications large demands for low-temperature heat will be located right next to a site at which electric power might be produced. In other cases, the demands for heat are themselves distributed or are not located near the site of power generation; in these cases, the costs of transporting the heat must be considered. Figure I-13 shows that hot water is three or four times as effective in transporting heat as is steam in the temperature range of interest from 300° to 390° F.

Heating the water to supply this waste heat usually imposes a penalty in the efficiency with which power is generated as shown in figure I-14. Nuclear-steam powerplants suffer the greatest penalty and gas turbines the least. The basic reasons are as follows: In order to heat water to, say, 375° F, a steam powerplant must condense its steam at about 400° F rather than at 80° F or so for best efficiency; the steam powerplants thus lose efficiency. On the other hand, the exhaust temperature for a recuperated gas turbine is about 500° F, so water can be heated to 400° F with essentially no penalty in efficiency; although at still higher water temperatures the design and efficiency of the gas turbine would require some compromise, its efficiency would still be the highest.

In summary, the demand for heat at low temperatures is large, about

35 percent of our total demand for energy. Fulfilling this demand by using normally wasted heat from power generation will generally require decentralization of power generation, proximity of power generation to industrial and population centers, and distribution of hot water rather than steam. The power generator will be both cheaper and more efficient if it is a gas turbine rather than a steam turbine. For such service, the energy source should be safe, nonpolluting, and suitable for distribution to decentralized power generators, all characteristics of clean fossil fuels.

PRESENT EFFORTS ON INCREASING EFFICIENCY OF ENERGY USE

The following are some of NASA's current programs concerned with energy:

(1) Modular integrated utility systems (MIUS) - HUD
(2) Solar heating and cooling of buildings - NSF, HUD
(3) Wind power - NSF
(4) Production and use of hydrogen - AEC
(5) Test of helium gas turbine for high temperature gas reactor (HTGR) - AEC
(6) Automotive gas-turbine technology - EPA
(7) Aeronautics
(8) Study of advanced power-conversion systems - DOI, NSF

Many of these programs are being conducted in cooperation with other government agencies. In a number of cases, the programs have been transferred to ERDA, but the agency with which our cooperative effort began is listed to identify just which group we are working with.

The MIUS is a total-energy concept for producing power and using waste heat; in addition, waste materials for a residential community are consumed as fuel, and water and energy cascade through multiple uses in an attempt to conserve both of these scarce resources. This concept plus the use of solar energy to heat and cool buildings, generation of power from the wind, and the production and use of hydrogen are discussed in paper XI.

With the AEC we are studying a helium gas-turbine for use with the high-temperature gas-cooled reactor (HTGR). This closed-cycle gas turbine will be tested on fossil fuel before being used with the nuclear reactor. Our work

with the AEC will define the most economical test facility for this purpose.

In combination with EPA we are investigating the advancement of technology for automotive gas turbines. Figure I-15 shows the Chrysler gas turbine that is the starting point for this program. The technology program involves several ways the fuel economy, atmospheric emissions, and cost of the engine can be improved. For example, we are redesigning the compressor and turbines to achieve higher efficiency. An experimental variable-geometry combustor for the gas turbine has met the 1978 emissions standards that the spark-ignition engines have not been able to meet, and a laboratory model of a catalytic combustor has shown the possibility of surpassing even these standards by a factor of 50 or so. Some of our gas-bearing technology is being studied as a way to avoid carburization of oil in the engine's hottest bearing. And, as ways to lower cost, ceramic heat exchangers and low-cost methods to manufacture turbine wheels are both being explored.

Table I-11 shows some ways in which the fuel economy of autos might be improved. Although radial tires can increase fuel mileage by 5 percent, substantially larger gains are possible by using lighter cars and engines with a small piston displacement. Computer control of traffic flow can increase fuel mileage in urban situations, and streamlining can extend mileage by a similar amount under highway conditions. Improved transmissions could do a better job of operating the engines at the point of best fuel economy for any given power requested by the driver. The fuel economy and emissions of spark-ignition engines might both be improved by lean operation. We are investigating the on-board reforming of fuel to produce hydrogen and then using this hydrogen to extend the flammability limits to fuel-air ratios only 50 or 60 percent of stoichiometric. For automotive gas-turbines, liquid cooling of the turbine or perhaps ceramic turbines might permit turbine operation at 2000^{o} to 2500^{o} F; not only would fuel mileage be increased, but the cost of materials from which the turbine is built might be diminished. Fuel mileage of the order of 50 or 60 miles per gallon appears achievable as a consequence of such advances in technology.

Some means for increasing the fuel mileage of aircraft are shown in table I-12. Improved air traffic control can diminish both the amount of time spent idling the engines on the ground prior to takeoff and any time spent orbiting an airport in a holding pattern while awaiting clearance to

land. Flight speeds and flight altitudes can be chosen for best fuel economy; these measures are already being pursued to a significant degree by the airlines. In the area of aircraft design, a supercritical wing can decrease aircraft drag. An active control system and stability augmentation will permit some reduction in size of the aircraft's control surfaces located in the tail and some reduction in drag through improved trim of the aircraft.

Composite materials permit design of lighter aircraft and thereby save fuel. And providing motive power to the aircraft's wheels would obviate the need to run the powerful main engines simply to taxi across the airport. Engine fuel consumption can be diminished by increasing both turbine inlet temperature and compressor pressure ratio. Fuel mileage can also be increased by increasing the fraction of airflow that passes through the fan and bypasses the main compressor and turbine.

Although turboprop engines have been largely superseded for passenger service, advanced turboprop engines offer as much as a 50 percent increase in fuel mileage. This feature can readily be exploited in the movement of air freight, itself a rapidly growing field. But whether or not this improved mileage can be realized in passenger service depends on passenger acceptance of somewhat lower flight speeds and this is difficult to foretell.

For large, central power stations, we are conducting an intensive study of advanced power-conversion systems. The principal participating agencies are the Department of Interior, the National Science Foundation, and the National Aeronautics and Space Administration; furthermore, the Environmental Protection Agency and the Office of Management and Budget also review this work. Three principal study efforts are underway by General Electric, Westinghouse, and NASA-Lewis. General Electric and Westinghouse each have a contract for $1 million to analyze and prepare preliminary designs of a variety of power conversion systems. NASA-Lewis supplements these studies with exploratory studies of its own and assesses the impacts and benefits of these various power systems on the nation. A contract with an architect-engineering firm supplies background and evaluations in areas where our research laboratory lacks experience. A panel drawn from the electric utility industry reviews this work and advises us.

The fuels being investigated are several forms of coal - bituminous, sub-bituminous, and lignite - and clean fuels derived from coal. The coals will be burned in conventional furnaces or fluidized beds (atmospheric and

pressurized). In the case of low-Btu gas, the gasifier is integrated with the powerplant and into the study as well. The intermediate- and high-Btu gas as well as the clean liquid fuels are considered to be obtained from an industrial supplier. Hydrogen is also included as a fuel.

Several types of power systems are being evaluated. A necessary starting point is the steam powerplant with modest improvements. Gas turbines operating on air and combustion products as well as a closed gas turbine operating on carbon dioxide are being evaluated. Fuel cells operating on several fuels are also included. Three types of topping cycles are being studied; the essential features of a topping cycle are shown in figure I-16. A conventional steam cycle is the basis for all the topping cycles, but the distinguishing feature is that heat for the steam boiler is the waste heat from the cycle placed on top - on top, that is, in the sense of high temperature. For the gas- and steam-turbine combined cycle shown here, air is first compressed, then heated to high temperature in the burner, and finally expanded through a turbine; this turbine drives both the compressor and a generator. The hot exhaust gas from the gas turbine at about 1100° F is used to boil and superheat water in the boiler. The resulting steam drives a turbine and thereby a generator. It is then condensed in the condenser and pumped back into the boiler once more.

The reason for the interest in this class of powerplant is the higher efficiency shown in figure I-17. At present, the best steam powerplants are 40 percent efficient. If the existing technology for cooling aircraft gas turbines is applied, maximum efficiencies of about 49 percent possible appear with turbine inlet temperatures of 2400° F. A higher efficiency would be possible if the ceramic materials presently being investigated would permit operation at these high temperatures without cooling. Water-cooled turbines have not received much research attention so far, and they may provide a way to obtain efficiencies in the range of 50 to 55 percent.

The various types of powerplants are evaluated on the basis of multiple measures of merit; among these are overall efficiency, cost of power produced, and the magnitude of capital investment required. The cost of capital as well as interest on the investment during the period of construction are included. The various emissions, including oxides of nitrogen and sulfur, discharged particles, and waste heat, are also considered. The disposal and possible use of waste products (such as uranium in coal ash) and the

requirements for water and land are additional variables. The study encompasses the geographical factors of powerplant and fuel-source locations, any conversion of fuel to another form (as coal to SNG), and the mode and cost of transporting the fuel. Emphasis is placed on identifing key factors limiting widespread application of each power-conversion concept, such as the supply of critical materials or the need for specially trained manpower or special manufacturing capabilities. Overall, an attempt is being made to have a comprehensive basis for evaluating the various power-conversion concepts.

CONCLUDING REMARKS

Our nation has very large resources of fossil fuels, sufficient to last several centuries or perhaps longer. A statement that we are about to run out of fossil fuels is patently wrong. But we must make these fuels available for our use. This means that we must create the technology for extracting these fuels from the ground and for their conversion and use in ways that are acceptable to society. An important aspect of the problem is that we must also supply the capital investment and build the physical plant to extract and convert these fuels and then transport them to market.

As we look for ways to satisfy our future demands for heat in residential, commerical, and industrial applications, electric power appears to be a poorer choice than synthetic fuels. Synthetic fuels will be cheaper for the customer to buy, will require less capital investment, and will save energy.

Finally, our nation needs to place an increased emphasis on the efficient use of energy. We must find ways to save energy without refusing people the things they would really like to have. For example, although a transistor radio uses less energy than a tube-type radio it is not a poorer radio but a better one. Radial tires decrease the rolling resistance of automobiles and thereby save fuel, but their improved adhesion to the road and their improved lateral stability make them better tires not poorer ones. For aircraft, turbofan engines consume less fuel, provide more takeoff thrust, and produce less noise than turbojets. Although turbofans use less energy, they are actually better aircraft engines.

Many buildings are heated by the burning of natural gas; these buildings would be no less comfortable if the heat used were the waste heat from power generation. The rising costs of energy will provide the economic incentive for us to search for ways in which processes might be combined and thereby save energy. The energy required by industry and by residential and commercial buildings is half our total energy use, quite apart from their demands for electric power; their demand for low-grade heat alone is 35 percent of our total energy use. Fulfilling this large demand for heat by using waste heat from power generation appears to be a market with great economic potential. Getting the power generator close to the demand for heat may require decentralization of power generation and a clean fuel such as SNG.

BIBLIOGRAPHY

Averitt, Paul: Coal. In United States Mineral Resources - Assessment of U.S. Potential and Worldwide Deposits, D. A. Brobst and W. P. Pratt, eds., U.S. Geological Survey, 1973, pp. 133-142.

Averitt, Paul: Coal Resources of the United States, 1 January 1967. BULL-1275, U.S. Geological Survey, 1967.

Duncan, Donald C.; and Swanson, Vernon E.: Organic-Rich Shale of the United States and World Land Areas. Circular 523, U.S. Geological Survey, 1967.

Linden, H. R.: Testimony at Public Seminar, Energy Policy and Resource Development. President's Energy Resources Council, Dept. of State, 1974.

Project Independence Report. Federal Energy Administration, 1974.

TABLE I-1 - ENERGY SOURCES IN 1972

SOURCE	QUADS[a]	PERCENT
GAS	23.1	32
OIL	33.0	46
COAL	12.5	17
NUCLEAR	.6	1
HYDRO (FUEL EQUIVALENT)	3.0	4
TOTALS	72.1	100

[a]1 QUAD = 10^{15} BTU; 1 Q = 1000 QUADS = 10^{18} BTU.

TABLE I-2.- ULTIMATE RESOURCES OF COAL

MAPPED AND EXPLORED

[UNIT: 1 Q = 1000 QUADS.]

DEPTH, FT	SEAM THICKNESS			TOTALS	PERCENT
	THICK	INTERMEDIATE	THIN		
0-1000	8.1	7.5	13.4	29.0	89
1000-2000	1.0	1.3	.8	3.1	9.5
2000-3000	---	---	.5	.5	1.5
TOTALS	9.1	8.8	14.7	32.6	100.0

	SEAM THICKNESS		
	THICK	INTERMEDIATE	THIN
ANTHRACITE, BITUMINOUS	OVER 42 IN.	28-42 IN.	14-28 IN.
SUB-BITUMINOUS, LIGNITE	OVER 10 FT	5-10 FT	2.5-5 FT

TABLE I-3.- PROJECTION OF RESOURCES OF SHALE OIL

[UNIT : 1 Q = 1000 QUADS.]

	CONCENTRATION, GALS/TON			TOTALS
	25-100	10-25	5-10	
KNOWN RESOURCES	3	9	12	24
POSSIBLE EXTENSIONS	5	14	22	41
UNDISCOVERED AND UNAPPRAISED	3	123	750	876
TOTAL				941

TABLE I-4.- WASTE AS AN ENERGY[a] SOURCE

SOURCES OF WASTE	ULTIMATE POTENTIAL, 10^6 TONS/YR
AGRICULTURE AND FOOD	390
ANIMALS	200
URBAN WASTE	129
LOGGING AND WOOD MANUFACTURING	55
INDUSTRY	44
SEWAGE	12
MISCELLANEOUS	50
TOTAL	880

[a]ENERGY CONTENT, 9 QUADS/YR AT 5000 BTU/LB.

TABLE I-5. - 1972 ENERGY USE

	ENERGY SOURCE					TOTAL AMOUNT OF ENERGY SOURCE REQUIRED, QUADS/YR	PERCENT OF DEMAND
	GAS	OIL	COAL	NUCLEAR	HYDRO		
	AMOUNT OF ENERGY SOURCE REQUIRED, QUAD/YR						
ELECTRIC POWER	4.1	3.1	7.8	0.6	3.0	18.6	26
TRANSPORTATION	.8	17.3	---	---	---	18.1	25
RESIDENTIAL AND COMMERCIAL	7.6	6.7	.4	---	---	14.7	20
INDUSTRIAL	10.6	5.9	4.3	---	---	20.8	29
TOTALS	23.1	33.0	12.5	0.6	3.0	72.1	100
PERCENT OF SUPPLY	32	46	17	1	4	100	---

TABLE I-6. - RESIDENTIAL AND COMMERCIAL ENERGY USE IN 1972

	ENERGY SOURCE				TOTAL AMOUNT OF ENERGY SOURCE REQUIRED, QUAD/YR
	GAS	OIL	COAL	ELECTRICITY	
	AMOUNT OF ENERGY SOURCE REQUIRED, QUAD/YR				
SPACE HEAT	5.0	6.7	0.4	0.7	12.8
AIR CONDITIONING	.1	---	---	.9	1.0
HEAT WATER AND COOK	2.5	---	---	.6	3.1
MISCELLANEOUS ELECTRICITY	---	---	---	1.0	1.0
TOTAL	7.6	6.7	0.4	3.2	17.9

TABLE I-7. - INDUSTRIAL ENERGY USE IN 1972

	ENERGY SOURCE				TOTAL AMOUNT OF ENERGY SOURCE REQUIRED, QUADS/YR
	GAS	OIL	COAL	ELECTRICITY	
	AMOUNT OF ENERGY SOURCE REQUIRED, QUADS/YR				
PROCESS STEAM	6.6	2.6	1.8	---	11.0
DIRECT HEAT	3.2	1.1	2.3	.1	6.7
FEED STOCK	.5	2.1	.1	---	2.7
POWER GENERATION	.3	.1	.1	(.1)	.4
ELECTRIC DRIVE	----	---	---	1.9	1.9
ELECTROLYSIS	----	---	---	.3	.3
OTHER	----	---	---	.1	.1
TOTAL	10.6	5.9	4.3	2.3	23.1

TABLE I-8. - ELECTRIC POWER DEMAND

	PRESENT FUEL DEMAND, QUAD/YR	HR/YR	PEAK DEMAND / AVERAGE DEMAND	PEAK DEMAND FOR ELECTRIC POWER, GW
RESIDENTIAL AND COMMERCIAL SPACE HEAT	12.8	3000	2	1900
INDUSTRIAL PROCESS HEAT	17.7	6000	1	600
PEAK POWER DEMAND, GW	----	----	----	2500

TABLE I-9.- SUPPLYING RESIDENTIAL AND COMMERCIAL HEAT

	ENERGY COST, $/MBTU	INVESTMENT, $/MBTU/DAY	OVERALL EFFICIENCY, PERCENT
ELECTRIC HEAT	14.65	7100	18
SNG	4.70	1800	50
ELECTRIC HEAT PUMP	7.30	3600	36
GAS HEAT PUMP	2.90	1100	70-100

TABLE I-10.- SUPPLYING PROCESS HEAT TO INDUSTRY

[ENERGY DEMAND, 6000 HR/YR.]

	ENERGY COST, $/MBTU	INVESTMENT, $/MBTU/DAY	OVERALL EFFICIENCY, PERCENT
ELECTRIC HEAT (1-3¢/kW-HR	3-9	7100	34
SNG	3	1800	50

TABLE I-11.- AUTOMOTIVE FUEL ECONOMIES

	IMPROVED MILEAGE, PERCENT
RADIAL TIRES	5
LIGHTER CARS	30
SMALL-DISPLACEMENT ENGINES	30
COMPUTER-CONTROLLED TRAFFIC FLOW	5
STREAMLINING	5
IMPROVED TRANSMISSIONS	10
MORE EFFICIENT ENGINES	20

TABLE I-12.- INCREASED MILEAGE IN AIR TRANSPORTATION

	IMPROVED MILEAGE, PERCENT
FLIGHT OPERATIONS:	15
AIR TRAFFIC CONTROL	
REDUCED FLIGHT SPEEDS	
OPTIMUM ALTITUDES	
AIRCRAFT DESIGN:	20
SUPERCRITICAL WING	
ACTIVE CONTROL SYSTEM	
STABILITY AUGMENTATION	
COMPOSITE MATERIALS	
POWERED WHEELS	
ENGINE DESIGN:	20
INCREASED TURBINE TEMPERATURE	
HIGHER PRESSURE RATIO	
HIGHER BYPASS RATIO	
COMPOSITE MATERIALS	
ADVANCED TURBOPROP ENGINE	50

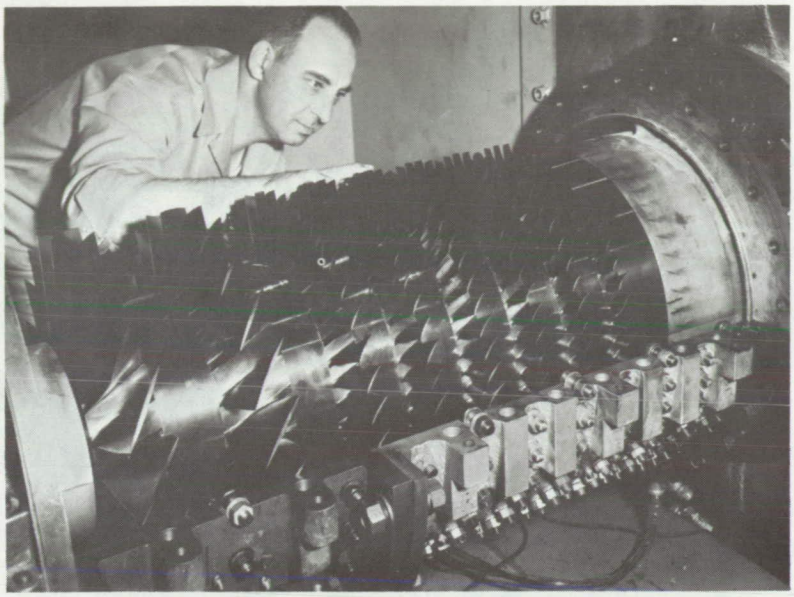

Figure I-1. - Research compressor. Efficiency, ~90.5 percent.

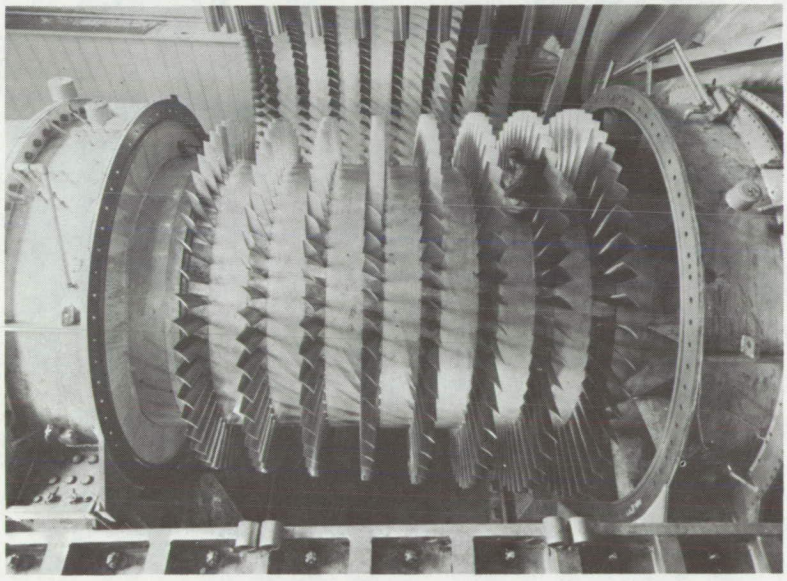

Figure I-2. - Twenty-foot-diameter compressor. Efficiency, ~91 percent.

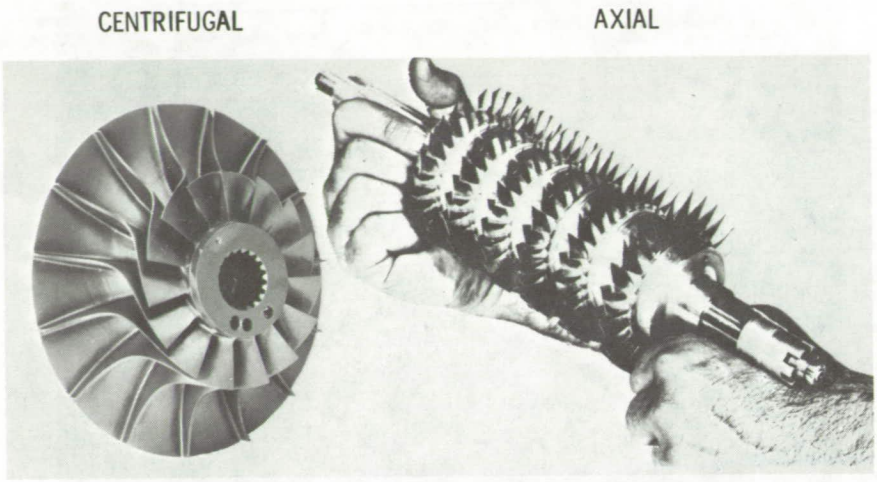

Figure I-3. - Brayton cycle compressor.

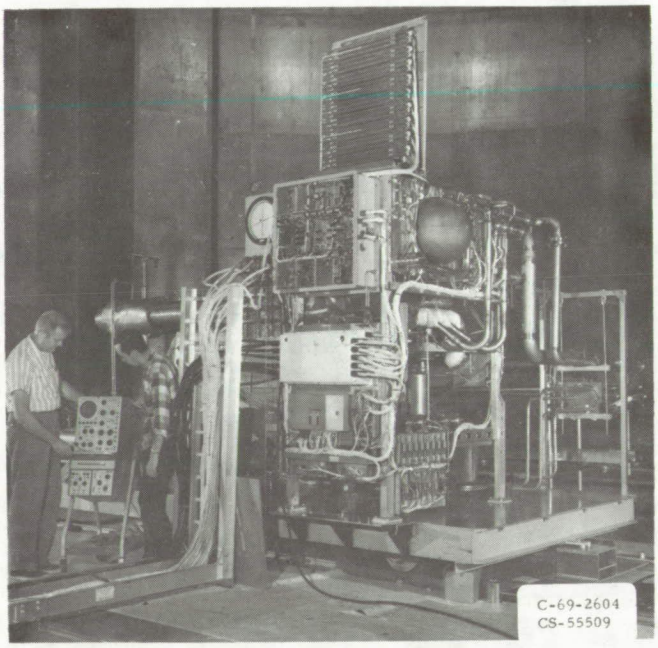

Figure I-4. - Brayton power system test engine.

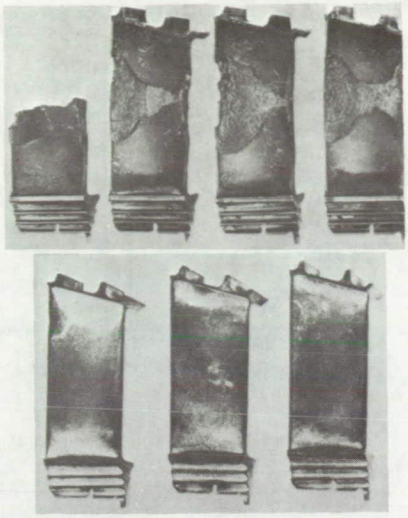

Figure I-5. - Hot corrosion of nickel turbine blades: 500 engine hours (top row); aluminized blades (bottom row).

Figure I-6. - B-57 aircraft fueled with hydrogen.

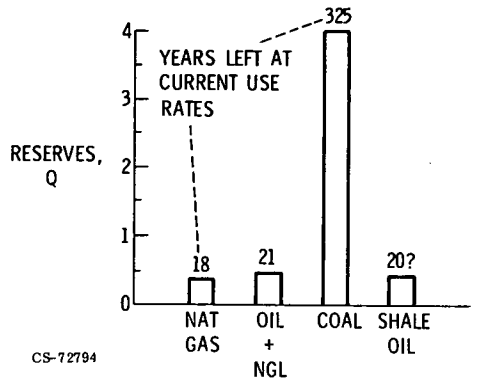

Figure I-7. - Fossil fuel reserves of U. S. (1 Q = 10^{18} Btu = 1000 quads).

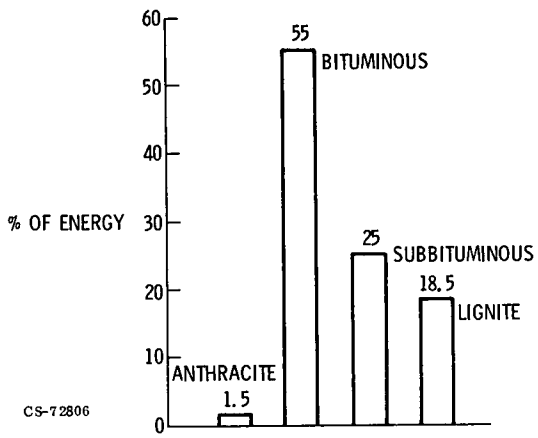

Figure I-8. - Coal according to rank.

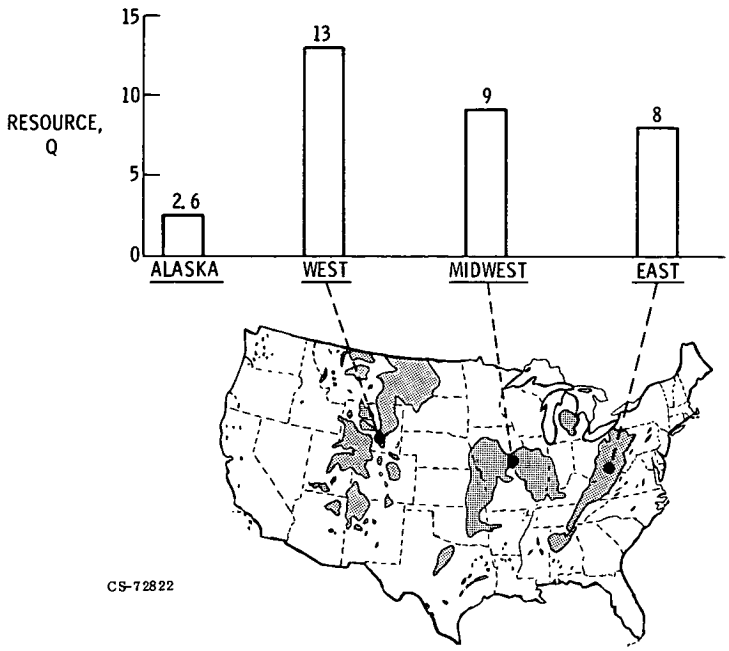

Figure I-9. - Location of coal resources.

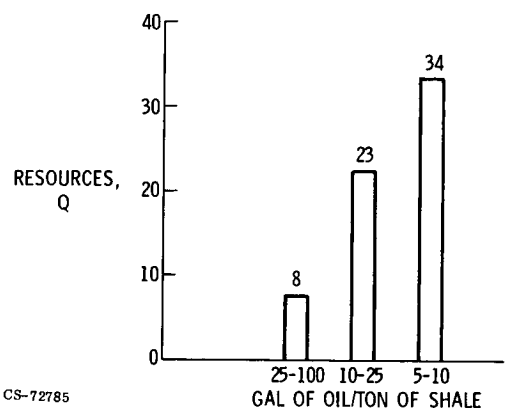

Figure I-10. - Identified resources of shale oil.

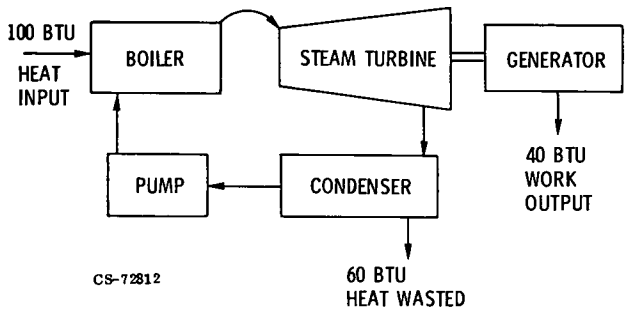

Figure I-11. - Heat wasted in power generation.

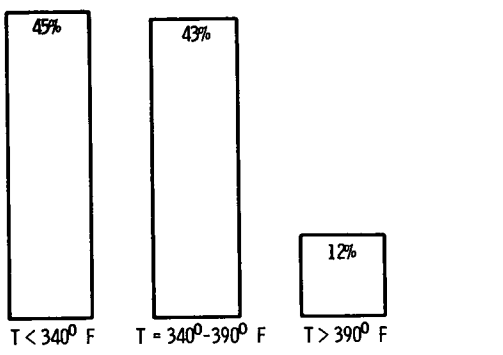

Figure I-12. - Industrial process steam at various temperatures.

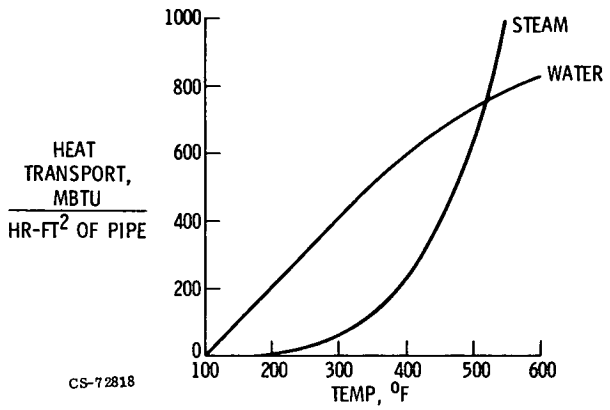

Figure I-13. - Effectiveness of water in heat transport.

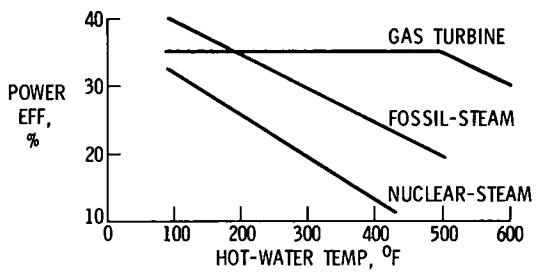

Figure I-14. - Heating water affects efficiency.

CS-72783

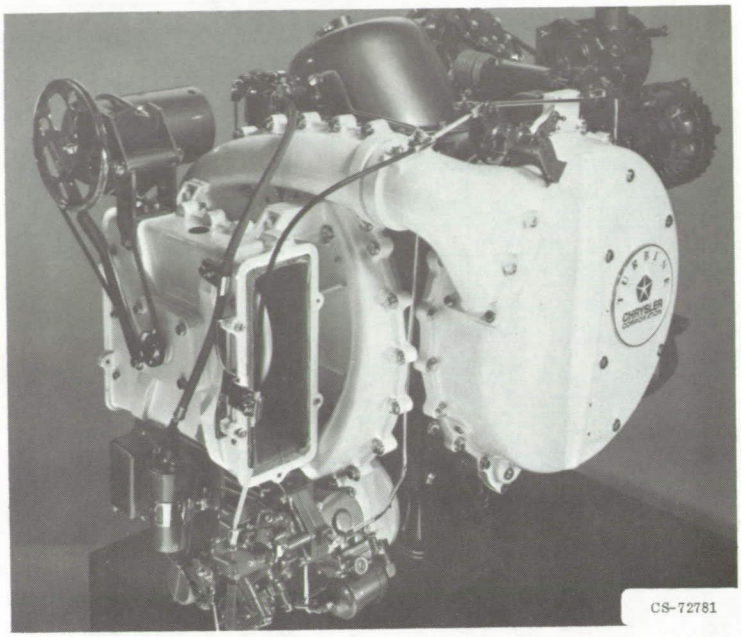

Figure I-15. - Automotive gas turbine engine.

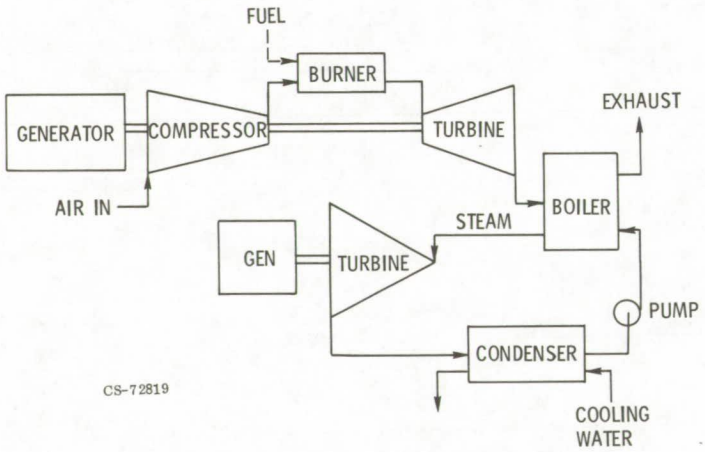

Figure I-16. - Gas- and steam-turbine combined cycle.

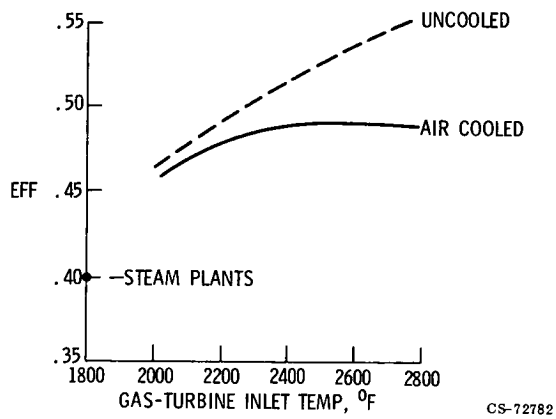

Figure I-17. - Efficiency of combined cycle.

Page intentionally left blank

Page intentionally left blank

II. EXPLORATION FOR FOSSIL AND NUCLEAR FUELS FROM ORBITAL ALTITUDES

Nicholas M. Short*

Sources of fossil fuel must be found before they can be developed and used. Under some circumstances, useful information pertaining to the search for oil and gas can be obtained from orbiting satellites. This is particularly true if the premise that oil and gas fields sometimes leak, and express that leakage at the surface, is valid. The systems now in use may also aid in the search for oil shale, uranium, geothermal sources, and coal - but with less optimistic results to date. NASA is now operating a spacecraft system that has already proved useful in the search for gas and oil. This system is the earth resources technology satellites (ERTS) now called LANDSAT. The first such satellite is shown in figure II-1; a second satellite in the series was launched in January 1975. The satellite shown here is actually a NIMBUS satellite taken from the meteorology program and modified. It contains two sensor systems: a set of television cameras, and a multispectral scanner. The scanner is the system that has been used for practical operations. The results of those operations are discussed in this paper.

LANDSAT-1 is operating at an altitude of 570 miles in a near-polar orbit, traversing an identical area of the earth every 18 days. It produces an instantaneous image that covers approximately 13 000 square miles, providing useful data at a resolution of approximately 270 feet. It operates in a multispectral mode. Figure II-2 is an aerial photomosaic showing approximately the same aerial coverage as a LANDSAT image. It shows the Wind River Basin of Wyoming, an energy-rich basin with a considerable amount of oil and gas production. Some of the major uranium fields in the United

*NASA Goddard Space Flight Center, Greenbelt, Maryland 20771.

States are here, as well as coal deposits. This photomosaic is made from approximately 12 000 individual aerial photographs, at a cost today of about $1/4 million. There is a lot of information contained here. But a great deal of potential informational content is missing because a mosaic does not give the strong photographic contrast that has proved to be so useful in LANDSAT images. Figure II-3 is a LANDSAT frame taken essentially of the same area. This image taken from space, 570 miles up, is much more sharply defined. The Wind River Basin stream systems, agricultural regions, and surrounding mountains stand out much more clearly than in the photomosaic. This LANDSAT image costs roughly $2500, or 1/100th the cost of the photomosaic. Thus, the cost of a single frame is quite low in comparison with conventional aerial photography, and the product contains much more information.

Figure II-4 gives the basic principles for using the LANDSAT data to extract useful information about the ground scene. This series of spectral curves shows the amount of reflected light energy as a function of wavelength, ranging from the lower end of the visible spectrum ($\sim$0.5 μm) through the near infrared ($\sim$1.2 μm). Various major surface features have different spectral signatures, according to the different amounts of energy returned. There is a characteristic signature for each major type of surface feature. By using these spectral signatures, plus information about the shape or appearance of the feature in a photograph, the major features can be effectively identified. As yet, a spectrometer cannot be used in space. The multichannel scanner which is used is effectively a radiometer. It measures the average amount of light energy being reflected in each one of these waveband intervals. These average values can be reduced to an equivalent of spectral signatures. By that means, and by using computer processing in particular, specific features on the ground are selected for identification and for careful measurement.

Figure II-5 is included as an example of the color imagery process used on LANDSAT photographs. These three images of the same area around the Salton Sea in southern California were taken during the Apollo 9 multispectral camera experiment. Film and filter combinations were used that provided narrowband images; one in green, one in red, and one in infrared. By taking these three images, which show different kinds of total variation related to the objects on the ground, and putting them through color filters, a false-color infrared photograph or image was constructed. This image

compares quite favorably with one that was taken with false-color film. The same thing can be done with the LANDSAT system, for example, in figure II-6, which shows the Salt Lake area of Utah. The LANDSAT system has four channels that produce a green image, a red image, and two near-infrared images. By combining any three of these through blue, green, and red filters a false-color composite can be produced that gives additional information helpful to the interpreter of the ground scene. One of the remarkable advantages of LANDSAT is that the system provides quantitative radiometric data. Individual images taken at different times of the year can be adjusted to conform to the total character of the ground scene. Individual frames taken under different lighting and atmospheric conditions can be corrected and matched. These can then be made in color and put together in mosaic form.

An example of a mosaic produced from LANDSAT images is figure II-7, which shows the entire state of California. Mosaicking is one of the special characteristics of this satellite system. Another is the ability to enlarge individual LANDSAT images to gather information in detail about specific areas. For example, the San Francisco Bay area is shown in figure II-8. This is typical of the enlargements that can be made from the standard LANDSAT image, which normally is 1:1 million scale. Such images can be effectively enlarged to a scale of about 1:150 thousand just by photographic processes. By using computer processes, even larger-scale imagery can be achieved.

Another advantage of LANDSAT is the simple fact that it is operating on a repeating cycle. In principle, with cloud-free conditions, the same part of the world would be viewed every 18 days. On the average, information on the same area is repeated every 54 days. This, of course, affords seasonal coverage, which is quite valuable in such disciplines as agriculture, forestry, and flood control. Seasonal coverage also turns out to be useful to geology. Figures II-9 and II-10 indicate specifically the very sharp contrast achievable on a seasonal basis, largely due to the interaction between geological soils and vegetation. Figure II-9 shows the Witwatersrand region of South Africa, one of the major gold-mining regions in the world. Some of the geological features of the region are expressed in this southern hemisphere winter scene. But in general, the image is rather washed out; in a color reproduction the brown pervades and overprints the entire image. The

very same region in the summertime (fig. II-10) shows the very sharp differences in vegetation related to the geological soils. Details appear that were completely missed in the winter scene. Aerial photography is too expensive to be repeated in the same area several times in the course of a year. LANDSAT provides this repetition automatically and thus can be very useful in geological mapping.

In this paper, LANDSAT imagery will be applied to general geological problems and then specifically to one of interest to the oil and gas industry. The University of Wyoming had a project to see how effectively they could produce a simple general geological map from LANDSAT imagery. In exploring for metals and fossil fuels, one of the most important tools is a good map. The maps of many parts of the world are quite good because of extensive mapping over the years. But maps of some areas, the small-scale maps in particular, are too general and too incomplete to be useful. The purpose of this project was to see if it were possible to make a reasonable approximation of a good small-scale map by using space imagery. So an area was chosen for the demonstration that has a rather complex geology, the Wind River Basin of Wyoming. The result is shown in figure II-11, which is a simple photointerpretation of that same region. It is a rock units map made exclusively from the LANDSAT image shown in figure II-3. A considerable amount of detail is provided, both in the rock units and in the structural geology, that is, the faulting and fracturing of the rocks exposed in the mountain range. A very large amount of detail in the arch and in the basins had not been adequately mapped after 50 to 75 years of detailed mapping on the ground. If figure II-11 were compared to the geological map of the state of Wyoming (fig. II-12) produced by that 50-year mapping program, it could be seen that generally the two mapping systems are compatible. Perhaps some of the mapping by space imagery is less accurate than the ground mapping, but some areas have actually proved to be more accurately mapped from space than by the standard conventional techniques used on the ground. So LANDSAT has a great deal of practical application in geological mapping, primarily in parts of the world where mapping has not progressed to the extent that it has in the United States.

LANDSAT images can be computer processed quite effectively. The data from the scanner are telemetered in a digital mode, computer-compatible tapes are produced, and programs are written to effectively

enhance the data to bring out information that is not there in the normal color product produced by the methods previously shown. For example, figure II-13 shows the Coconino Plateau which encompasses the Grand Canyon. Variations in rock type in the Coconino Plateau are shown by shading. A computer-processed version of that same scene (fig. II-14) show (would show if reproduced in color) yellow, white, and green patterns in that same area of the Coconino Plateau. These patterns represent different rock units that have not been adequately mapped in the field and that vary between sandstones and limestones. The particular application of this imagery was to map these rocks and the associated fracture systems and then to use that information to prospect for ground water. The program has had surprisingly high success, to the point where cattle are now being watered as a result of drilling that was based entirely on the information from this kind of an analysis.

Another area of application that has direct bearing on fossil fuel exploration is enhancement of certain types of surface alterations. The example used here is metal exploration, but the process applies equally well to oil, gas, uranium, and geothermal source exploration. All these have related surface alteration effects that can be diagnostic guides to the location of subsurface energy sources. The example shown in figure II-15 is a LANDSAT image of a gold and silver mining district. Associated with gold and silver mining is a surface alteration consisting of iron sulfite or pyrite, which leads to simple hydrated iron oxide, or rust. This surface stain actually shows up in many places in this color composite from LANDSAT, which is a portion of a single frame. By special processing techniques, figure II-16 was produced from the normal LANDSAT imagery. The iron oxides have been enhanced and are now shown in a rust color (would appear, in a color reproduction, as a rust color). They form a circular "halo" around the gold field. This halo represents a surface alteration zone directly related to the mineralization. Such false-color enhancement of space imagery is probably the best single guide to ore prospecting for many metals. And it is something that can be done now, with existing data being produced by satellites. It can also be applied to oil and gas exploration.

Perhaps the most important single use of LANDSAT imagery for geological exploration is the detection of fractures, or lineaments. (They are called "linears," until they are proved to be geologic in nature.) Because

of the uniform lighting and the synoptic overview, many fracture systems which are missed in ground mapping and in aerial photography show up in space imagery. The example used to make this point is again in Wyoming (fig. II-17). The Wind River Mountains are very rugged and practically inaccessible. Also they belong, by treaty, to the Shoshonee and Irapahoe Indians, who must give their permission for any ground mapping. A geologist at the University of Wyoming had such permission. In five summers of field work, representing about $1\frac{1}{2}$ man-years, he produced the amount of information about major fractures in the exposures of the Wind River Mountains that is shown at the upper left of the mountain range in figure II-18. An aerial flight across the center of the Wind River area provided the additional information shown by the band in figure II-18. Using the LANDSAT image shown in figure II-17, the investigator produced the map shown in figure II-19 in 3 hours, and that included a coffeebreak. The practical point here is that this type of mapping process has been speeded up by orders of magnitude. Of course, the key is, do these fractures really exist? Field investigations of several areas in the Wind River Mountains have shown that the fracture systems exposed in figure II-19 indeed are real geological features. Thus, the LANDSAT map (fig. II-19) is a bonafide detailed fracture map of a major mountain range.

Again this process can be automated by using special filtering techniques. An image of the Coconino Plateau near the Grand Canyon has been reprocessed by using a technique called edge enhancement to produce a number of what appear to be zig-zags (fig. II-20). They are actually combinations of stream channels and fracture systems. People exploring for ground water actually used this map to locate shallow perched water zones.

Figure II-21 shows a spectacular scene - the first mosaic of an entire nation. It is a mosaic of the United States made from 570 LANDSAT images. This mosaic, by the way, is available from the U.S. Soil Conservation Service. As a general overview the mosaic is interesting, but it also happens to contain much practical information. Several investigators have been using this data base to identify fracture systems that apply to the entire United States. The first such map that was produced is shown in figure II-22. It took an investigator of the U.S. Geological Survey less than 2 weeks to produce this particular map, and it is probably the most detailed fracture, or lineaments, map of the United States in existence. The

significance of this process for geological exploration is that fractures are, in many cases, instrumental in localizing deposits of ore, oil, gas, and other energy sources.

A specific example of how LANDSAT data have been used in a test program is a pilot study of the usefulness of space imagery in fossil fuel exploration. The approach was to take a known producing region and see what, if anything, could be found in space imagery that would relate to oil and gas production. The study was carried out by a company called Eason Oil of Oklahoma City. The study area (fig. II-23) was the Anadarko Basin, which extends from southwest Oklahoma into the Texas Panhandle and is one of the oldest producing fields in the United States. It is a tightly folded basin with very deep production. At one time, perhaps still, the deepest oil well in the world, some 30 000 feet deep, was drilled in this particular basin. Production has occurred both in anticlines and in fractures or fault traps, as well as in stratographic traps. All of these features or evidence concerning them have been recognized from the LANDSAT data. A (color) composite of a large part of the Anadarko Basin is shown in figure II-24. The South Canadian River meanders through this area, crossing the Oklahoma-Texas border. A particular type of anomaly, called the hazy anomaly, is shown at a bend of the South Canadian River. Hazy anomalies turned out to be the most exciting results to date in oil and gas exploration from space, although they are still very questionable.

The hazy anomalies themselves and other information about the area vary from season to season. The image shown in figure II-24 was taken in April. Vegetation is just beginning to come forth. Some of the winter wheat fields have already been harvested, and other fields are just coming into production. The grasses and sage are beginning to grow. By summertime (fig. II-25), the area has changed quite dramatically. The appearance of the major hazy anomaly is completely different from what it was before. One would not be able to recognize that the hazy anomaly existed. This is a strong argument again for having repetitive coverage, which is routinely provided from space. Figure II-26 shows a fall scene, and it is, in turn, quite different from the summer scene. The seasonal variations are important because changes in vegetation may serve as very subtle but important clues to the presence of either fractures or other surface manifestations which may be related to escaping oil and gas.

A geological map of the area made exclusively from LANDSAT imagery is shown in figure II-27. It is not a geological map in the standard sense because age is not assigned to the rock units. However, the outcrop patterns of the different rock units can be recognized, especially by using the multiseasonal coverage as an additional aid. This map, produced exclusively by LANDSAT imagery, corresponds quite well with the published conventional geological oil and gas map of the state (fig. II-28). In some cases, the detail in the LANDSAT imagery is greater than that in the conventional geological map. However, as previously mentioned, the conventional map has a distinct advantage in showing certain other features for which a higher level of accuracy is required.

In the Anadarko Basin, as in many oil and gas fields, fracture systems, such as those shown in this conventional geological map (fig. II-29), are used by the exploration geologist in planning where to carry out seismic surveys and eventually in planning drilling programs to determine whether or not there is trapped oil and gas. The heavy lines in figure II-29 indicate the published major fracture systems for this part of the Anadarko Basin. As far as is known, that was the principal information available before the LANDSAT program. The many lighter lines in the figure represent linears that were detected exclusively from LANDSAT imagery. Many of these linears have proved to be false, and others are joints or other fractures of significance geologically. Others were uncertain and may be artifacts or cultural features. But they are at least of interest and may be potential clues to structure. Some of these linears have proved to be fractures that have localized several of the major producing fields in that part of Oklahoma.

There are dangers in using this information. The Goddard Space Flight Center is presently assessing the potential for oil and gas exploration from space imagery. First, the validity of the data that the investigators are producing must be determined. A rather intriguing experiment was run which showed that we still have a long way to go. There is presently too much subjectivity in making the kinds of interpretation shown in the preceding figures. The April image of the Anadarko Basin (fig. II-24) was examined by four trained geologists. Each one attempted to find the linears which he thought existed in the image. As shown in figure II-30, there was considerable variation in what each geologist picked as linears. Combining these data (fig. II-31) showed their agreement. A grand total of 723 linears

were picked out. All four geologists found only four linears in common, which was a great shock to us. Three of the four found 73 linears in common, two found 128 in common, and approximately 500 were a cumulative sum of the individual findings. These results were disturbing. Furthermore, when compared with the Eason Oil results (fig. II-32), there was only 28 percent agreement between the Goddard choices of linears and the Eason choices. Goddard found about 35 percent of linears that Eason did not find, and Eason found about 30 to 40 percent that Goddard did not. Thus, caution must be exercised in that we have just begun to learn how to use these space imagery data effectively.

Linears are extremely important in geological exploration. Objective approaches, either computer- or instrument-based, and other criteria must be developed to produce maps that show linears with a relatively high degree of confidence. Otherwise, oil companies may discover that they are drilling on some subtle surface feature that has no bearing whatsoever on geological information. This has already happened once in using LANDSAT data. In the state of Wyoming an independent firm used a linear map to drill, found nothing, and discovered later that they had been looking at a surface feature caused by the wind.

Let us return to the subject of hazy anomalies shown here in figure II-33. Are they really related to the known locations of oil and gas deposits? The Eason Oil investigators, after about a year, came up with a map that showed the distribution of several types of surface features (fig. II-34). These were drainage patterns, hazy anomalies, and total differences that could not be explained by any conventional techniques or by any known map information. This anomalies map was correlated with the most up-to-date maps of oil- and gas-producing fields in the Anadarko Basin. Their results were staggering; they were astounding. If they were correct, it appeared that a major new exploration tool has been discovered. From one test area (table II-1) there were 76 anomalies. Fifty-nine of the 76 correlated with producing fields. Eleven more related to nonproductive geological structures. Only 6 of the 76 had no relation, according to their criterion, to producing oil and gas fields. Of the hazy anomalies in that area, 33 of the 35, according to their broadly defined criterion (discussed later in this paper), coincided with a field or a structure.

It was decided to analyze another test area which also showed a very high degree of correspondence between hazy anomalies and geological features. An aerial photograph of that area taken at an altitude of 50 000 feet is shown in figure II-35. A large hazy anomaly appears in the bend of the South Canadian River. A network of roads go to different drilling sites since it is a producing gas field and has a limited amount of oil production as well.

The blotchy graininess in the river bend was shown in both aerial photographs and conventional ground maps. This is a region where in winter and spring the soils are well exposed and quite sandy, a point of considerable interest. Sandy soils were also found at the sites of other hazy anomalies. It may be that the sandy soils in some way relate to escaping oil and gas which affect vegetation. The change in vegetation might permit wind to blow away the fine silt and leave behind the sandy soils. If so, there is a direct relation between sandy soils and the presence of oil and gas fields.

A LANDSAT image (fig. II-36) was taken of the scene shown in the preceding aerial photograph. Whereas the aerial photograph was taken at an altitude of 10 miles, the LANDSAT image was made at an altitude of 570 miles. The same, and in some respects even more, information is provided by the LANDSAT image. The primary advantage of LANDSAT is the ability to take the multispectral data and computer process it to extract more information.

By using a special computer program, enhanced images (fig. II-37) were produced in which the anomaly that was associated with the gas- or oil-producing field was color coded. The hazy anomaly at the bend in the South Canadian River would appear in a color reproduction as an orange-brown tone. However, that orange-brown tone merely denotes barren soil. Farmland where the fields are fallow exposes a highly reflective sandy soil and thus appears as the same orange-brown tone. Figure II-38 is another LANDSAT image of that same area in which the (color) tones that are associated with hazy anomalies are even better enhanced. Another computer enhancement of a larger view of that same area using the color-coding system is shown in figure II-39. Again, the large hazy area which had been identified by photointerpretations is shown. But the same orange-brown color also appeared in many other places, denoting highly reflective soils not necessarily associated with the presence of oil or gas fields. The reasons for the appearance of the orange-brown tones can be distinguished by looking at

the pattern - not just the color but the pattern of color. A regular pattern is associated with agriculture and obviously would eliminate the area from consideration.

A map produced by Eason of the hazy anomalies (fig. II-40) was examined at Goddard to determine how their choice of hazy anomalies corresponded to the producing oil and gas fields. A 1972 oil and gas map of the same area (fig. II-41) shows the bend in the South Canadian River that we have been looking at and a number of large fields. Superposing the hazy anomalies picked out by LANDSAT imagery on the producing oil and gas fields shows that many of the hazy anomalies have no relation to the known oil and gas fields (fig. II-42). The oil and gas fields in the bend of the river do not correspond too well to the outline of the hazy anomaly. In some cases only a small part of a hazy anomaly is associated with an oil and gas field. Or conversely, a small hazy anomaly may be associated with a large oil and gas field. These results did not correspond to those previously claimed by Eason. It seems that their criterion was that, if any part of one touched any part of the other, a correlation was assumed. Goddard is presently attempting a statistical analysis to prove or disprove that the correlation between hazy anomalies and the presence of oil and gas is as valid as Eason claims. The results are not yet available. As was shown in figure II-42, solely on a visual basis, there is some question about the high correlation that was indicated in their report.

The last case to be covered is a study made by Dr. T. J. Donovan of the U.S. Geological Survey in the Anadarko Basin. This basin contains a large, gas- and oil-producing geological structure called the Cement Field (fig. II-43). It is an anticline running northwest and having about a 25-mile surface expression in rock units that are primarily limestone and red beds dating from the Permian age. Dr. Donovan found that toward the center of the structure the Permian red beds bleached out to a much lighter yellow (e.g., as shown by the lighter tones in the road toward the top of fig. II-44). Figure II-45 shows a rock sample from a normal (unbleached) Permian red bed, a rock sample from the bleached Permian red bed, and a piece of Permian gypsum that was chemically altered to sandstone.

The question is, why do these changes occur? The answer, which is very exciting, is published in reference 1. A map of color change in terms of changing iron contents is shown in figure II-46. Toward the center of

Cement Field there is a decrease in iron oxide content, which is related to the bleaching effect. Dr. Donovan postulated that that particular field, which produces oil and gas from a depth of 8000 to 9000 feet, leaked and that as the hydrocarbons leaked they interacted with the surface rocks and brought about the various kinds of color alterations. He proved this by measuring isotope ratios of carbon 12 to carbon 13 and oxygen 16 to oxygen 18 (fig. II-47). In two crestal areas where production was heavy, there was a very strong change in isotope ratios - so dramatic that this could only be caused by interactions with methane and other hydrocarbons. Dr. Donovan set up a model which seems to prove convincingly that this is a case where oil and gas leakage have definitely been responsible for the surface changes observed. By implication, there must be other places in the world where oil and gas leakage could bring about similar alterations. Such alterations in the color or composition of rocks and in their light reflectance properties should be able to be identified by using space imagery.

A very recent view of Cement Field is shown in a computer-processed LANDSAT image (fig. II-48). The surface features are enhanced here by conditions not seen in other images of this area. There is a very light snow cover over the entire region that brings out certain features. Also the image was taken in midwinter when the sun angle is low, and this enhances other features. Presently, a computer analysis is being made to see if the color changes noted by Dr. Donovan can be distinguished in LANDSAT imagery.

On the basis of visual analysis alone, it would seem the LANDSAT data can be quantified to serve as another guideline in exploring for oil and gas. However, we are still in a very preliminary evaluation of the usefulness of this technique. The case history in the Anadarko Basin must be examined to see whether or not the results stand up under close scrutiny. Before exploration geologists will become enthusiastic about the potential of space imagery as an added tool for exploration, its general applicability must be demonstrated. Other regions of the United States and other parts of the world must be studied to see if this type of data is fairly universal. Can analysis of linears be used as a general approach to looking for oil or gas traps? Can the surface alteration effects previously described be used, at least in certain parts of the world where vegetation is relatively sparse, as

indications of escaping hydrocarbons? In the next year, through a combination of studies in the earth resources and energy programs of NASA, we may be able to come up with results that will encourage the gas industry to seriously consider this exploration technique.

REFERENCE

1. Donovan, Terrence J.: Petroleum Microseepage at Cement Oklahoma: Evidence and Mechanism. Amer. Assoc. Petroleum Geologists Bull., vol. 58, no. 3, Mar. 1974, pp. 429-446.

TABLE II-1. - COMPARISON OF ANOMALIES FOUND BY GODDARD AND BY EASON OIL COMPANY

SURVEY 1 - GEOMORPHIC, TONAL AND HAZY ANOMALIES	
76	TOTAL ANOMALIES
59	PRODUCING FIELDS
11	NONPRODUCTIVE STRUCTURES
6	NO COINCIDENCE
33 OF 35	HAZY ANOMALIES COINCIDENT WITH FIELD OR STRUCTURE
SURVEY 2 - HAZY ANOMALIES	
57	TOTAL ANOMALIES
42	PRODUCING FIELDS
6	NONPRODUCTIVE STRUCTURES
9	NO COINCIDENCE

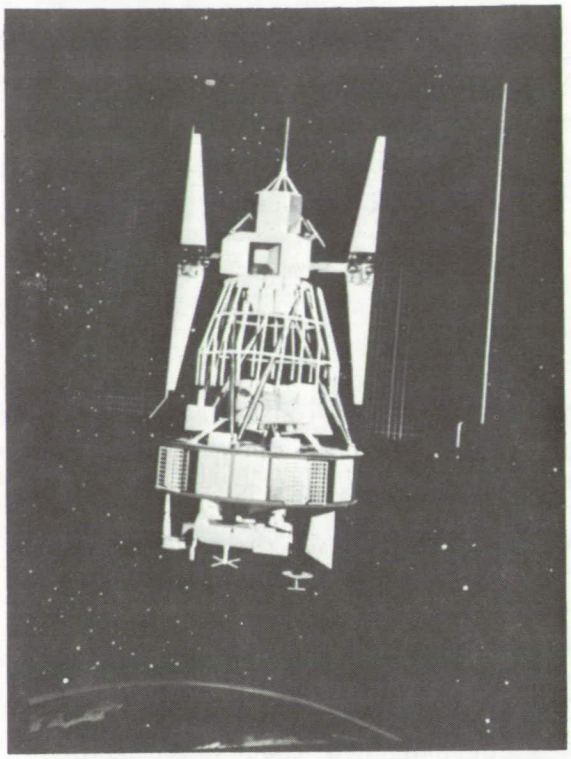

Figure II-1. - ERTS satellite.

Figure II-2. - Aerial photomosaic of Wind River Basin of Wyoming.

Figure II-3. - LANDSAT image of Wind River Basin.

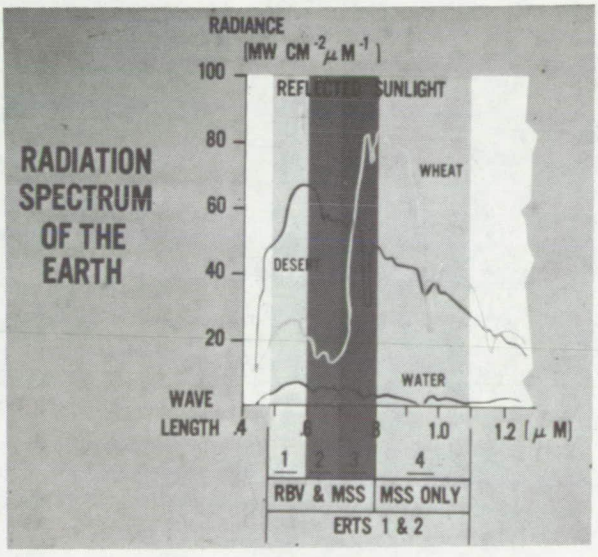

Figure II-4. - Radiation spectrum of the earth.

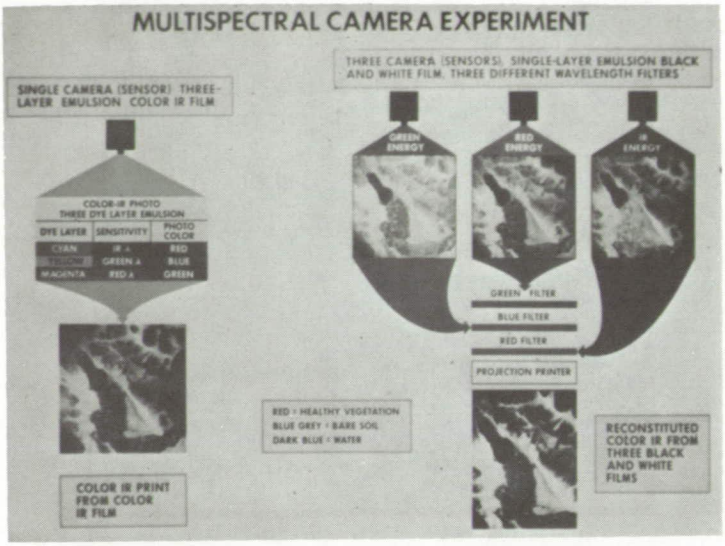

Figure II-5. - Explanation of multispectral imagery techniques.

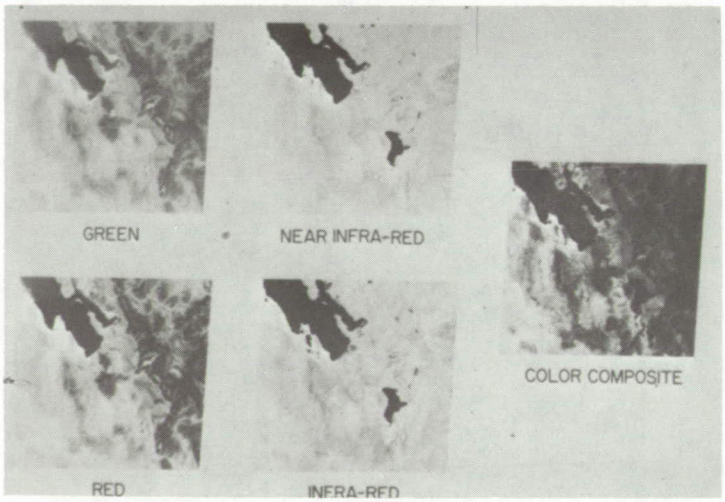

Figure II-6. - Multispectral scanner bands used on LANDSAT.

Figure II-7. - Mosaic of California created from LANDSAT multi-spectral images.

Figure II-8. - Typical enlargement of LANDSAT image, showing San Francisco Bay area.

Figure II-9. - Witwatersrand region of South Africa (LANDSAT image taken in winter).

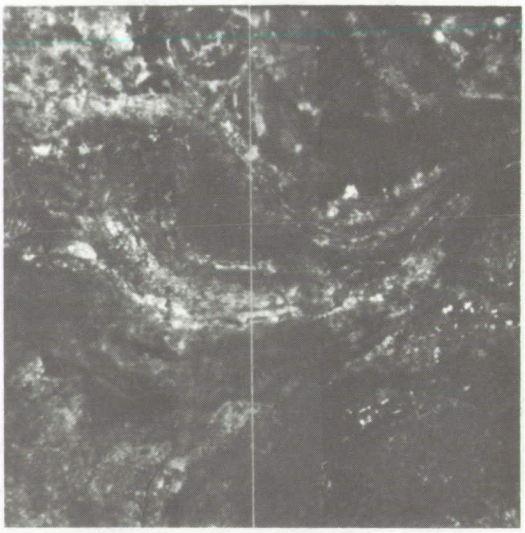

Figure II-10. - Same scene as in figure II-9, but taken in summer.

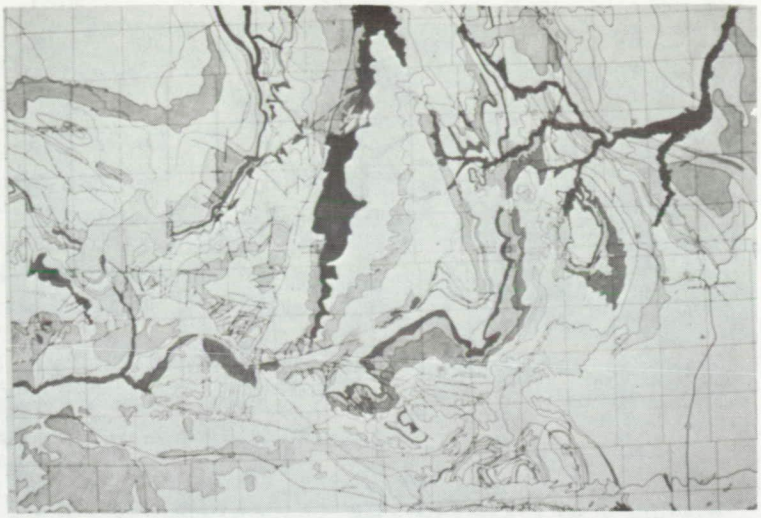

Figure II-11. - Rock units map of Wind River Basin made from interpretation of LANDSAT image.

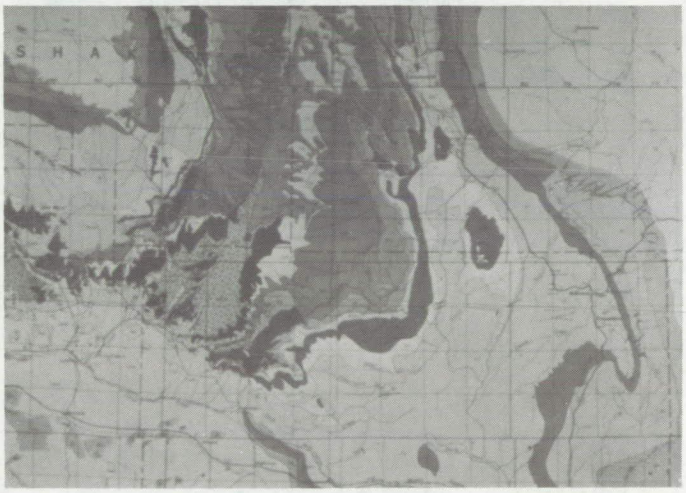

Figure II-12. - Geological map of Wyoming produced from 50 years accumulation of ground surveys.

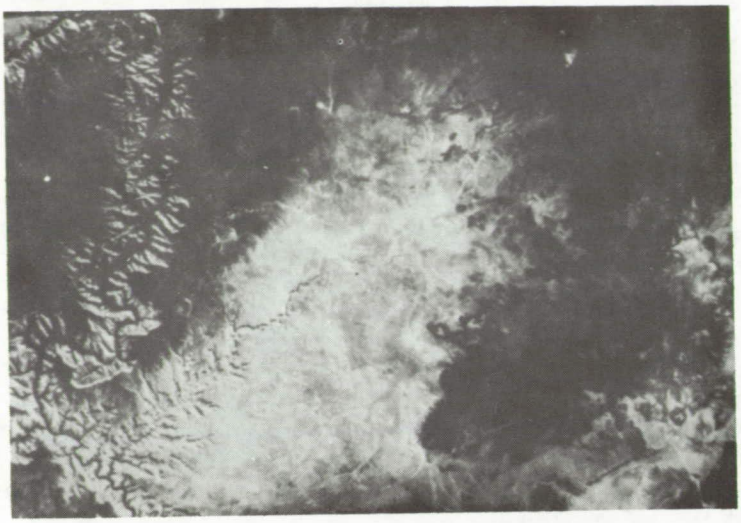

Figure II-13. - LANDSAT image of Coconino Plateau in Arizona, showing Grand Canyon at left edge.

Figure II-14. - Computer-enhanced, false-color image of area shown in figure II-13.

Figure II-15. - LANDSAT image of a gold and silver mining area.

Figure II-16. - Same area as in figure II-15, but with computer-enhanced false color.

Figure II-17. - LANDSAT image of Wind River Mountains of Wyoming.

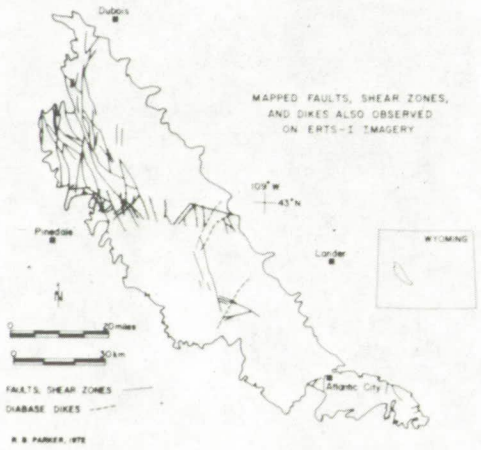

Figure II-18. - Map showing linears determined by $1\frac{1}{2}$-man-year ground survey plus one strip of aerial survey information.

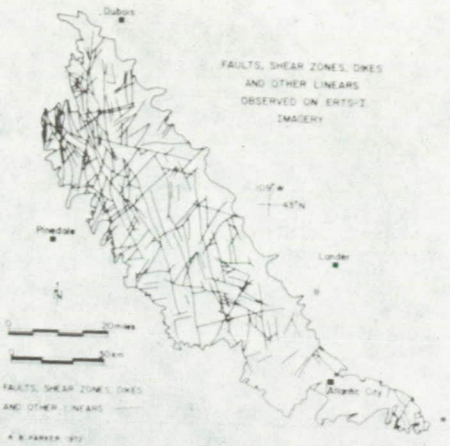

Figure II-19. - Linears map drawn in 3 hours from one LANDSAT image.

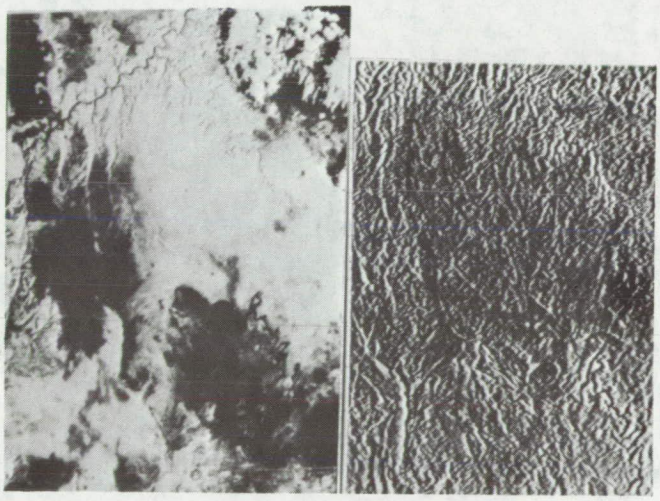

Figure II-20. - Comparison of regular image with edge-enhanced image (Coconino Plateau).

Figure II-21. - Mosaic map of United States made from 570 LANDSAT images.

Figure II-22. - Fractures map of United States produced from map in figure II-21.

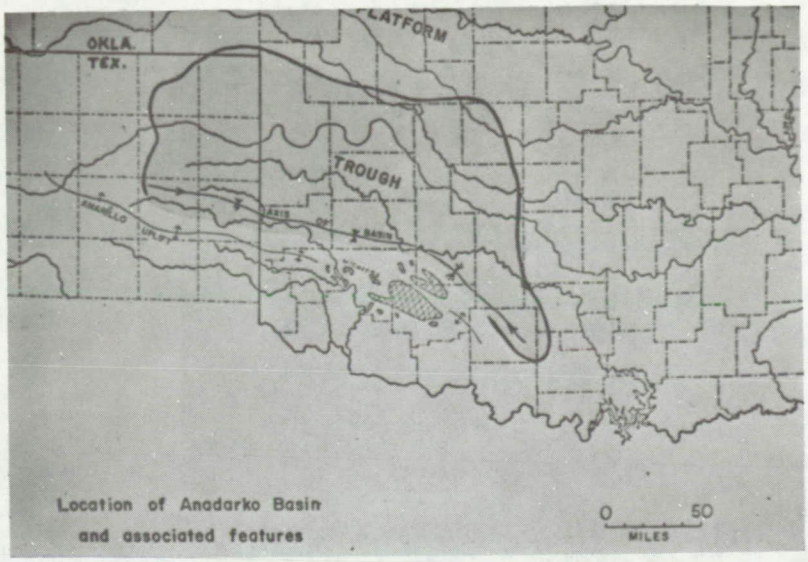

Figure II-23. - Anadarko Basin, along Texas-Oklahoma border.

Figure II-24. - Color composite of Anadarko Basin from LANDSAT imagery (April image).

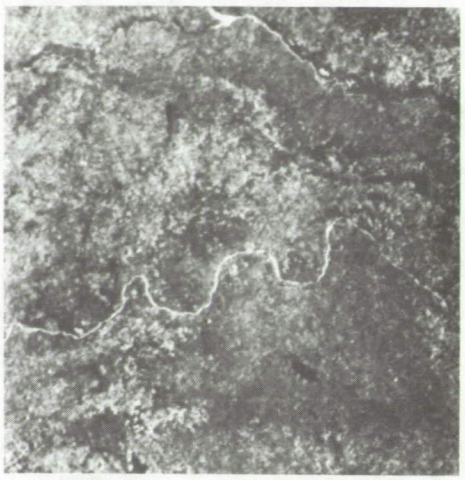

Figure II-25. - LANDSAT image of Anadarko Basin taken in summer.

Figure II-26. - LANDSAT image of Anadarko Basin taken in fall.

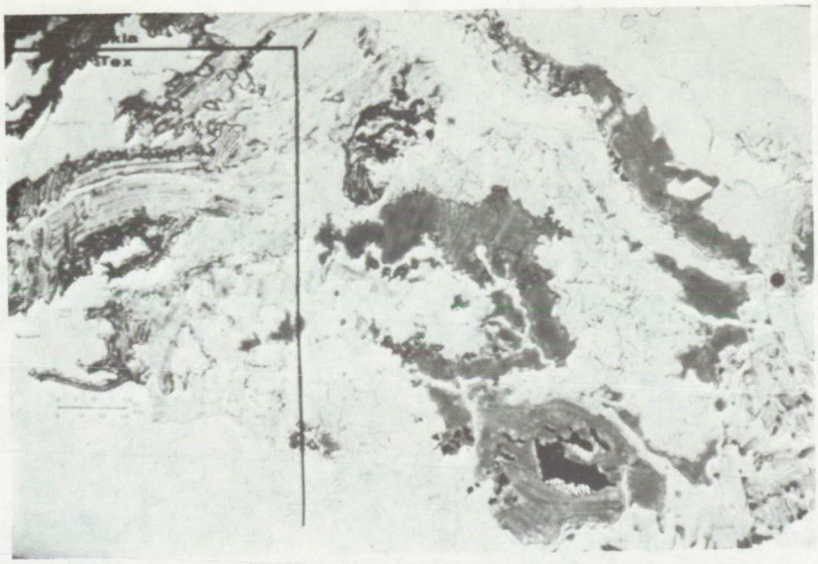

Figure II-27. - Geological map of Anadarko Basin made from LANDSAT imagery.

Figure II-28. - Conventional oil and gas geological map of Anadarko Basin.

Figure II-29. - Major-fractures map of Anadarko Basin from ground surveys.

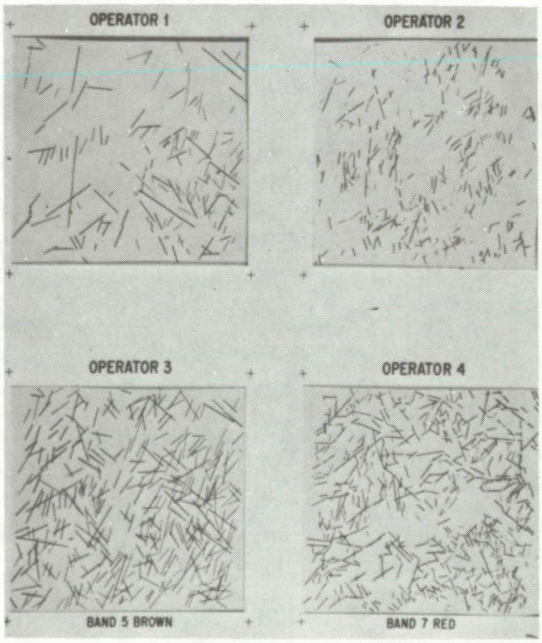

Figure II-30. - Comparison of linears deduced from LANDSAT imagery by four geologists from NASA Goddard Space Flight Center.

Figure II-31. - Agreement among four geologists' selections shown in figure II-30.

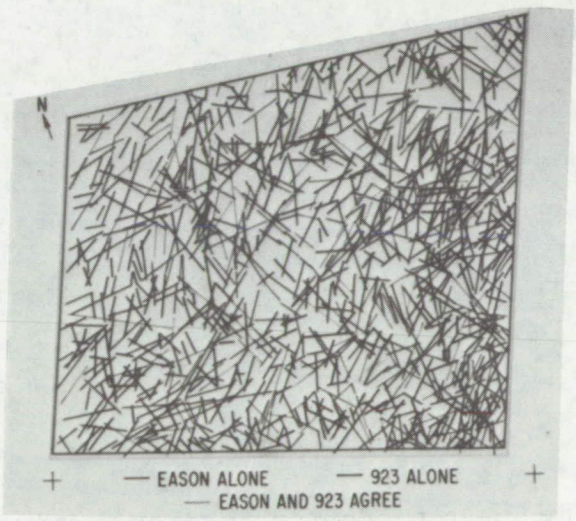

Figure II-32. - Comparison of Eason Oil Company data with Goddard geologists' data.

Figure II-33. - Hazy anomalies (lower center) shown in bend of South Canadian River.

Figure II-34. - Eason Oil Company map of all types of anomalies in Anadarko Basin.

Figure II-35. - Aerial photograph of South Canadian River bend, taken from 50 000 feet, showing a hazy anomaly.

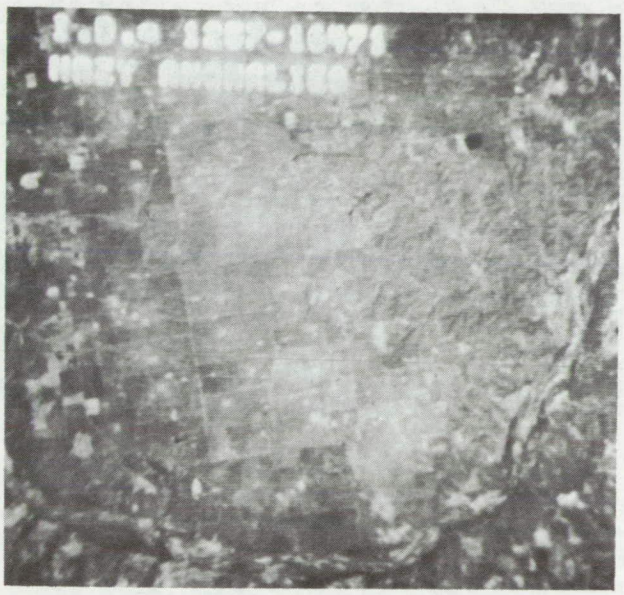

Figure II-36. - Enlargement of LANDSAT image, taken from 570 miles, of area shown in figure II-35.

Figure II-37. - False-color, computer-enhanced image of area shown in the two preceding slides.

Figure II-38. - Same area as in figure II-37, but with different color treatment.

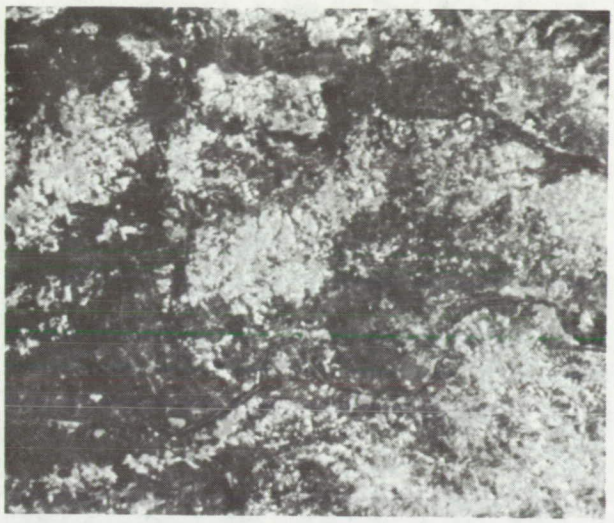

Figure II-39. - Additional false-color image of larger area of Anadarko Basin than shown in figure II-38.

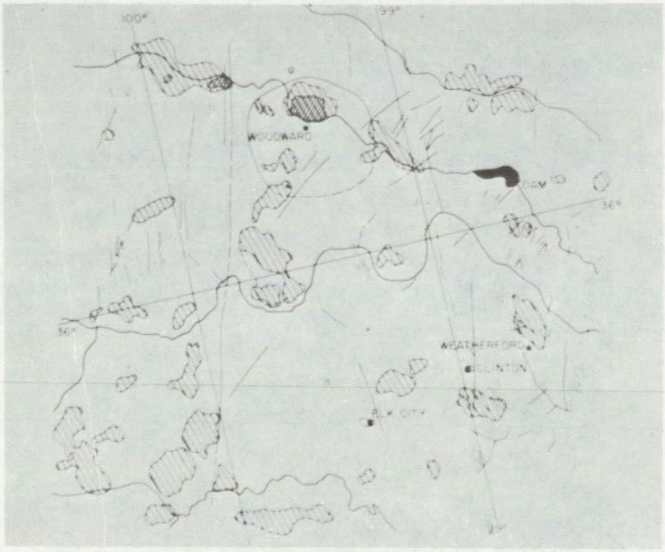

Figure II-40. - Hazy-anomalies map produced by Eason Oil Company.

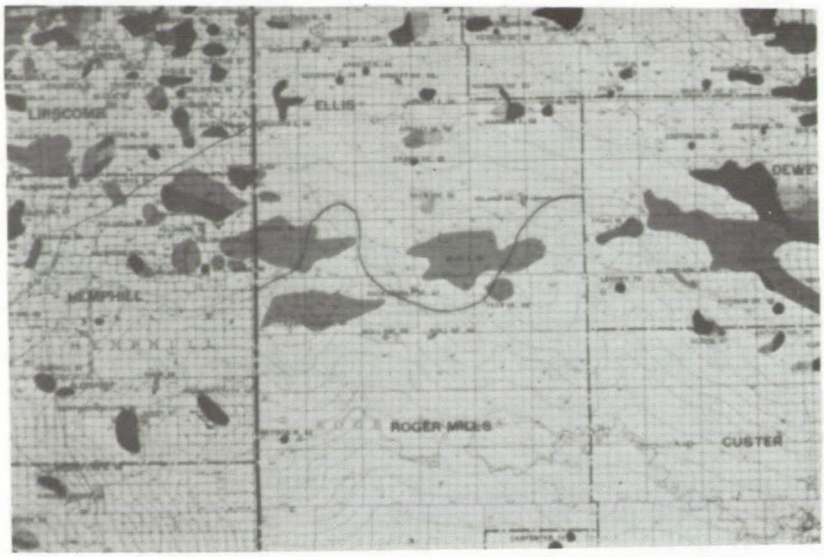

Figure II-41. - Oil and gas map of Anadarko Basin from 1972.

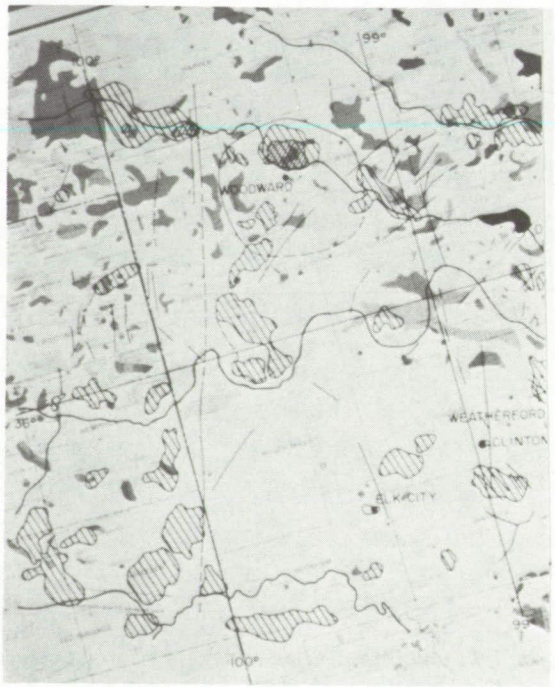

Figure II-42. - Hazy anomalies of figure II-40 superposed on gas and oil fields of figure II-41.

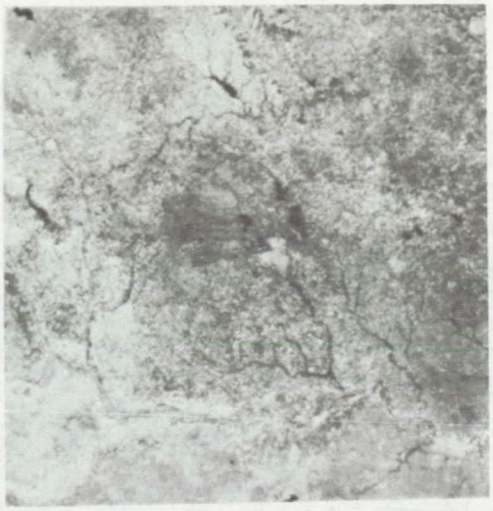

Figure II-43. - "Cement Field" region of Anadarko Basin from LANDSAT imagery.

Figure II-44. - Road in "Cement Field."

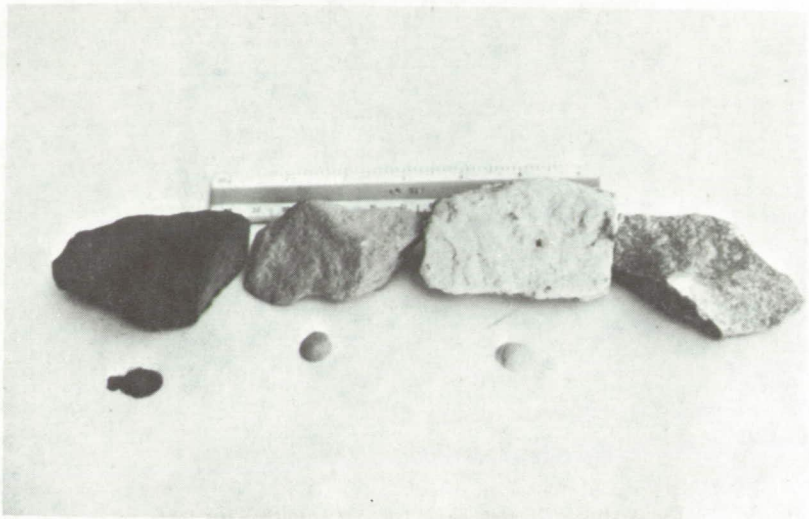

Figure II-45. - Rock samples. From left to right: unbleached Permian red bed, bleached Permian red bed, second bleached Permian red bed, and Permian gypsum altered to limestone.

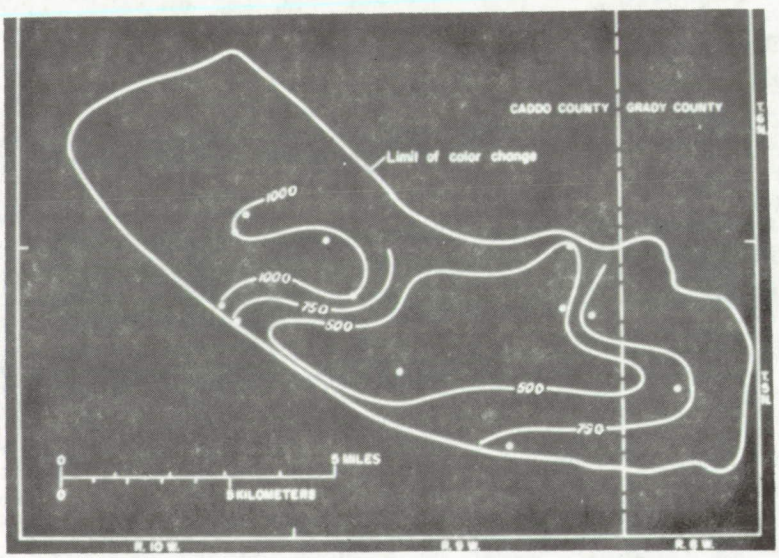

Figure II-46. - Map of "Cement Field" depicting color-change regions.

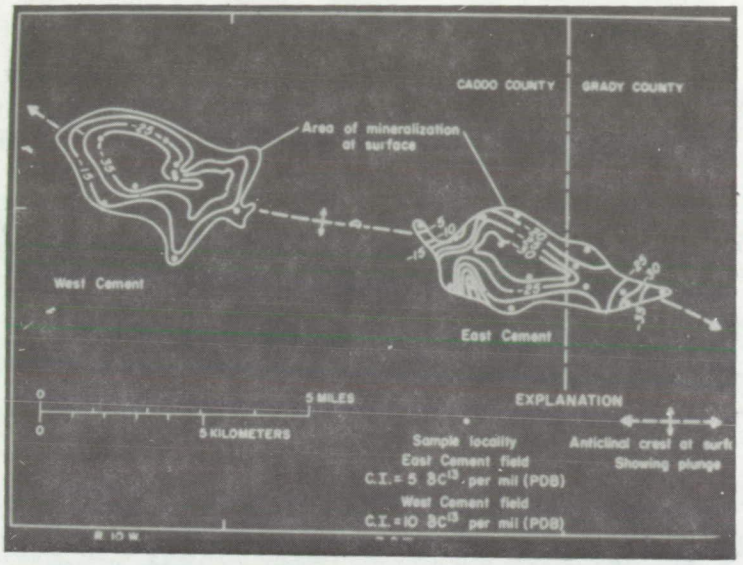

Figure II-47. - Map of "Cement Field" showing various isotope ratios.

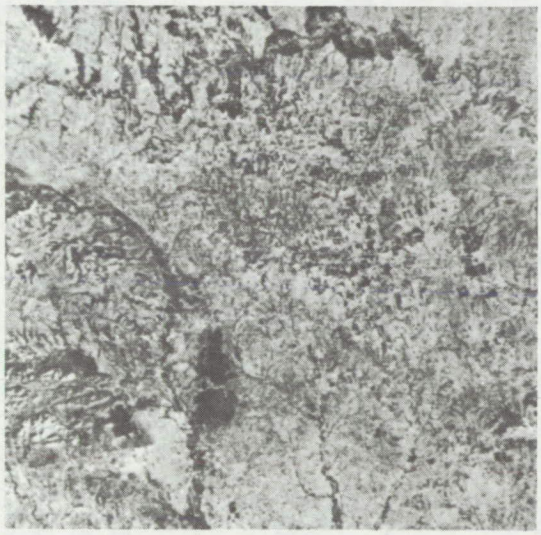

Figure II-48. - Recent computer-processed LANDSAT image of "Cement Field."

Page intentionally left blank

Page intentionally left blank

III. TECHNOLOGY FOR LIQUEFIED GAS

Donald A. Petrash, James R. Barber, Rene Chambellan,
and David R. Englund, Jr.

An example of NASA developed aerospace technology applied to the ground-based storage of cryogenic fluids is shown in figure III-1. This figure shows a 200 000-gallon liquid hydrogen storage tank and two 34 000-gallon railroad cars which are insulated with multilayer insulation. The 200 000-gallon storage vessel probably has the lowest heat leak of any large storage vessel in existance. Its design boiloff loss is about 0.05 percent per day; thus, almost 6 years would be required for the entire contents of this vessel to boil away. This represents a total heat leak of only 12 000 Btu per day.

High performance insulation technology such as that just described, as well as new technology in the areas of storage, transfer, and transport of cryogenic fluids will be discussed herein. Figure III-2 indicates the scope of the discussion. Spacecraft and aircraft insulation systems technology which has application to ground storage and transport systems will be covered. In addition, the technology of low heat leak tank supports developed for spacecraft systems is described. The instrumentation discussed covers a broad spectrum from the measurement of storage tank pressure and quantity to the measurement of the bulk transfer of known quantities of the cryogens.

The significance of applying advanced technology to the storage of cryogenic fluids and in particular liquefied natural gas (LNG) can be illustrated by the data in figure III-3. Imported liquefied natural gas, as shown on the figure is projected to increase from 1 percent of 1970's supply to about 15 percent of the total supply by 1990. A cost savings of about 600 million dollars could be realized over the next 15 years if new insulation technology could be used to reduce the boiloff loss by only 1 percent.

MICROSPHERE INSULATION TECHNOLOGY

An insulation system currently being developed is one capable of supporting compressive loads while also exhibiting low heat-transfer characteristics. The insulating system consists of small, hollow glass spheres confined within an evacuated space around the fluid to be insulated. These spheres, called microspheres, are 0.001 to 0.003 inch in diameter with a wall thickness about one-fiftieth of its diameter (fig. III-4).

An illustration of an upper stage spacecraft with microsphere insulation is shown in figure III-5. The inner tank contains the cryogenic propllent and is designed to withstand internal pressure loads. The vacuum jacket is designed to flex in order to allow for thermal contraction and expansion of the propellant tank. The microspheres are confined within the space between the vacuum jacket and the inner tank. Separation barriers are used to keep the microspheres from shifting under flight loads.

A comparison of several insulation systems is shown in figure III-6. Effective thermal conductivity is plotted against insulation hot side temperatures. Cold side temperature is maintained constant at -260° F. The top curve is for a polyurethane foam. Gas-filled polyurethane foam is commonly used inside LNG tanks as insulation. The conductivity curve for methane is shown for comparison. The lower two curves are for microsphere insulation systems. The curve for the case where the voids between microspheres are filled with methane gas shows a substantial improvement over gas-filled polyurethane foam. The other shows the best performance that can be expected from microspheres and that is when they are in an evacuated space. (Information obtained from a private communication with G. R. Cunnington of Lockheed Palo Alto Research Laboratory.)

Figure III-7 shows how microsphere insulation could be used on an LNG storage tank. The concrete floor and wall of the tank are lined with microspheres in a carbon dioxide atmosphere encased under a flexible sheet which serves as a seal. Carbon dioxide cryopumps to a relatively low pressure, approximately 3.5×10^{-3} torr at -260° F, and this eliminates the need for maintaining sophisticated vacuum pumping equipment at the storage site. The concrete cover is insulated by suspending polyurethane foam on hangers. Even if leaks should develop over a period of time in the internal seal so that the spaces around the microspheres became filled with gas, the heat-

transfer losses would be less than with an equal thickness of gas-filled foam.

The potential benefit of using an insulation of better performance is that lower boiloff will occur for any given thickness of insulation or alternately a thinner insulation will allow more storage in a tank of fixed dimensions.

An extension of the microsphere insulation concept to LNG pipelines is shown in figure III-8. As in the case of the LNG storage tank, microspheres and carbon dioxide are enclosed between an outer structural shell and an internal stainless steel liner. By keeping the outer structural shell warm, materials less costly than stainless steel can be used. A warm outer shell will allow installation underground or underwater as well as over land. Although not as thermally effective as a vacuum jacketed line, the microsphere line should be less expensive, easier to maintain, and more rugged.

OPACIFIED FIBERGLASS INSULATION TECHNOLOGY

Supersonic airplanes cruising at three times the speed of sound will sustain temperatures approaching 700^{o} F, even though the air through which the plane cruises is at -65^{o} F. The high skin temperatures are due to the impact and scrubbing action of the air on the airplane. Storing LNG in such an aircraft presents a difficult insulation problem since the temperature difference between the liquid and the heated airplane structure is about 960^{o} F. This temperature difference is a high potential for driving heat into the fuel. The difficulty in producing a satisfactory insulation system is that, in addition to maintaining light weight and high resistance to heat transfer, the material must also withstand extended exposure to 700^{o} F and dynamic loading conditions encountered in aircraft operations. One material that meets the challenge is a glass wool type insulation, usually called fiberglass.

There is nothing very new about ordinary fiberglass insulation; however, if it is treated in such a way as to block radiant heat, there results an opacified insulation material with improved performance. Opacification is accomplished during the manufacturing process of the fiberglass wool by dispersing a highly reflective metal powder into the wool along with a bonding agent at the same time that the glass filaments are being formed. Such

an insulation was produced for a Lewis Research Center program for developing high performance insulation systems for a supersonic cruise aircraft using cryogenic fuels. In this program fiberglass batting was used with a specific weight of 0.6 pound per cubic foot and opacified with 2 percent by weight of aluminum powder, such as used in paint, and 25 percent by weight of a silicone resin.

In concept, the randomly oriented aluminum flakes, constituting the powder, behave like myriads of tiny mirrors and reflect the radiant heat energy as shown on the right side of figure III-9. Results of tests to measure and compare the effective thermal conductivities of opacified and unopacified fiberglass insulations are also shown in figure III-9. These tests were performed with a cold side temperature at room ambient and the hot side temperature varied from 100^{o} to 700^{o} F. At low temperatures the effect of opacification is negligible; however, as the temperature increases the effect becomes increasingly pronounced. At 700^{o} F the thermal conductivity of the opacified fiberglass is about one-third that of the ordinary fiberglass.

It is felt that opacified fiberglass has a significant potential as an insulating material. A cross-sectional view of an external insulation system for an LNG supersonic aircraft fuel tank is shown in figure III-10. This system is composed of opacified fiberglass batting interspersed with aluminized radiation barriers. The latter raises the performance over that with no barriers by about 20 percent. The insulation is held against the tank wall by a fiberglass netting which also holds a perforated aluminum foil cover over the batting laminates. Before the insulation is applied, dry nitrogen gas purge lines are placed next to the tank wall in order to maintain a flow of dry gas outward through the insulation blanket. A vented insulation system is required for an aircraft application to allow the insulation to "breathe" as altitude changes. For a ground application, a hermetically sealed cover would probably be used over the insulation materials. The dry gas purge would, most likely, not be used.

Applications of opacified fiberglass insulation generally become apparent when problems occur. One possible use could be as a protection against fires with high radiosity. With a suitable outside cover, holding the opacified fiberglass against atank containing LNG could produce an effective protection against fire. An insulation system for this purpose would have to be

developed and tested. Other potential applications could be in self-cleaning ovens, in portable appliances such as broilers, in gas turbines, and central power plants.

Opacified fiberglass can also be used in an internal wet insulation system as shown in figure III-11. This system uses a fiberglass-polyimide flexible-honeycomb core. The flexibility feature permits installation on compound curved surfaces. The honeycomb is bonded to the inner surface of the tank wall, care being exercised to produce a continuous bond, thus preventing intercell leakage. Each cell is packed with dry opacified fiberglass in order to reduce convective heat transfer and radiation. The surface of the honeycomb core facing the liquid is covered with a thin face sheet of polyimide which is dimpled and bonded to the edges of the honeycomb. Dimpling provides the flexibility needed to accommodate shrinkage when the face sheet is exposed to the cold liquid. Here also a continuous bond is required between the face sheet and the edges of the honeycomb to prevent intercell leakage. The face sheet is perforated at each cell by a single small hole. This penetration is made by locally melting the face sheet with a hot needle, thus preventing tears in the sheet during the perforation process. Another benefit derived from using the hot needle is that a bend is formed around the edge of the hole, thus providing reinforcement at a region of high stress concentration.

A vertical cross section of the internal insulation just described is shown in figure III-12. During operation the liquid penetrates the face sheet through capillary holes and enters the insulation. As the liquid absorbes heat from the insulation material, it vaporizes and pressurizes the cell until the cell internal pressure and tank pressure equalize. At each hole a vapor-liquid interface is established which is dependent on surface tension and hole diameter. The net result is that the insulation effective thermal conductivity will be the aggregate of the conductivities of the cell walls, fiberglass batting, and the gaseous fuel.

In the application of the internal wet insulation system to aircraft tanks, which generally are not round, the problem of sharp changes in curvature is encountered. This results from the necessity of shaping the fuel tanks to fill the limited available space. The problem of sharp corners can be haddled in several ways; one arrangement that worked is shown in figure III-13. The bottom insulation is brought out to the sidewall and terminated, being

bonded both to the tank bottom and sidewalls. The vertical insulation is brought down to within 0.5 inch of the bottom insulation. The remaining space is filled with fiberglass wool and covered with a polyimide dimpled facesheet. A pressure balance is achieved by venting this space into the bottom insulation cells; this produces, in effect, a large cell connecting sides and bottom.

A comparison of the effective thermal conductivity of the two insulation systems just described for a supersonic aircraft application and the conductivity of high performance insulation for spacecraft applications can be made by studying figure III-14. Also included, as a benchmark, is a curve for polyurethane foam. Spacecraft insulations are the two bottom curves. It should be noted that the cold side temperatures for the aircraft and spacecraft applications are essentially the same whereas the hot side temperatures are quite different.

The internal wet-insulation system has the highest conductivity of all the systems, as indicated by the uppermost curve. But it has one advantage in that the tank skin and support structures are at the outside ambient temperature. Therefore, heat leaks and thermal shrinkages are greatly reduced.

The opacified fiberglass five-radiation barrier insulation has a conductivity lower than that of the internal wet insulation and just slightly below that of the 2 pound per cubic foot polyurethane foam.

Even though the insulation systems described were designed for aircraft and spacecraft application, the concepts, if adapted to ground-based applications, could provide improved performance where needed.

INSTRUMENTATION FOR QUANTITY MEASUREMENT

There are a great number of ways available for measuring the quantity of liquid in a tank. These include liquid level sensing and methods that directly measure the mass of fluid in a tank. The following discussion covers some methods which have been used with good success in NASA programs.

A capacitance probe can be used to measure the quantity of fluid in a tank. In fact, this method has been proposed for liquid level and liquid density measurements in LNG tanks on ships. NASA has used this method to

measure the quantity of liquid hydrogen and liquid oxygen propellants on the Centaur launch vehicle. The Centaur is an upper stage vehicle used with the Atlas, as shown in figure III-15, or with the Titan. The Centaur can be shut down and restarted in space so that it can coast or be put in a parking orbit for a time and then be restarted to continue the mission. On Centaur the amount of propellant in each tank is measured during the flight and the flow rate is adjusted so that as little propellant as possible is left at burnout. This is necessary to get the maximum payload capability from the vehicle. This system is called a propellant utilization system. Figure III-16 shows a schematic diagram of the system. Capacitance probes are mounted in both the liquid hydrogen and liquid oxygen tanks. Figure III-17 shows a liquid hydrogen probe being installed; it is about 15 feet long and 3 inches in diameter. Signals from these probes are used to adjust mixture ratio valves which control the liquid oxygen flow to the engines. A measure of the success of this system is given by the average uncertainty in the amount of propellant left at burnout. Experience from many flights shows that this uncertainty is just 13 pounds. This is less than 5/100 of a percent of the 30 000 pounds of propellant that the vehicle carries when full.

Figure III-18 shows a schematic diagram of a capacitance measuring system. A capacitance probe is mounted vertically in a tank. The probe consists of two hollow concentric cylinders open at both the top and the bottom. The electrical circuit for measuring the capacitance requires that both cylinders be insulated from ground and, of course, from each other. The probe supports must have low heat leakage and allow for thermal contraction of the probe.

The probe operates on the principal that the capacitance of two conducting surfaces separated by a gap depends on the density of the dielectric fluid within the gap. The relative amount of liquid and vapor within the probe will indicate the liquid level. This is true if the liquid density is constant. But the probe is sensitive to variations in liquid density and this means that the probe actually provides a signal proportional to the mass of liquid in the tank. Furthermore, if the probe is totally submerged in liquid, a measurement of the density of the liquid can be obtained. This type of system can provide measurements of liquid hydrogen quantity to within about 1 percent. Sensitivity of the probe is a problem with hydrogen because liquid hydrogen

has a small dielectric constant. Sensitivity should not be as much of a problem with LNG.

Some factors to be considered when using this system are the following. First, if the tank area is constant with height, the measurement is proportional to the quantity in the tank. If the tank area is not constant, the variation can be accounted for by shaping the probe. In any event, the tank area must be accurately known. Second, thermal contraction of the tank area and the length of the probe must be accounted for. Third, leakage resistance to ground at the electrical feedthrough must be avoided because of the high electrical impedance of the probe. One source of leakage resistance is moisture; this can be minimized by keeping the feedthrough warm and free of frost or condensation. Finally, the dielectric constant-density relationship is the basis for this measurement. Data are available for most pure fluids including methane, ethane, and other components of LNG. However, accurate data for various mixtures of LNG must be obtained.

Another method for measuring the mass of liquid in a tank is the classical buoyant force method. This technique has been used in the NASA Lewis liquid-hydrogen flow stand to determine mass flow rate to within 0.25 percent.

Figure III-19 shows a schematic diagram of this method. A buoyant float is suspended in the tank. The buoyant force due to the liquid and the vapor displaced by the float is measured with a load cell. In pressurized tanks where the density of the vapor may be appreciable, the buoyancy due to the vapor must be considered.

The following are some factors to consider with this method. First, the ratio of the cross-sectional areas of the tank and the float should be constant at all levels in the tank. If the tank does not have a uniform cross-sectional area, the float can be shaped to maintain a constant area ratio. Second, thermal contraction of the tank and float should be accounted for. Third, the float will usually be hollow to minimize the float tare weight. It should be filled with a noncondensible gas and sealed. Fourth, since buoyancy measurements are sensitive to both vibration and slosh, these should be minimized. Finally, to prevent calibration drift, the load cell should be kept at a uniform temperature, preferably near room temperature.

The buoyant float technique can also be used to measure liquid density

by using a completely submerged float. Liquid hydrogen density has been measured to within 0.15 per cent with this technique.

LOW HEAT LEAK TANK SUPPORTS

The design of a tank to contain cryogenic fluids must consider not only insulation but also the contribution to total heat flow of tank supports and propellant lines. The tank supports shown in figure III-20 are typical of those used in upper stage spacecraft tankage. These supports are designed to provide a minimum contact area between the cold tank and the warm structure. The heat path is also long which increases resistance to heat flow. Closeups of two of these struts are shown in figure III-21. Self-alining ball end bearings are used to assure the proper load alinement along the axis of the strut. The center portion of the strut is made by winding continuous resin impregnated glass fibers on a dissolvable mandrel. Once the resin has been cured, the mandrel is dissolved in remove it.

Figure III-22 shows heat transfer plotted against strut length for a composite strut and a metal strut of equal strength. These struts are also about equal in weight. Therefore, a support system can be designed using the composite strut in shorter lengths that has both a lower heat leak and is lighter in weight then a metal strut. This allows installation in more confined areas.

In order to take full advantage of the strength capability of the composite structure, it was necessary to devise special techniques to transfer loads from the metal ends to the composite structure. Line loadings as high as 2500 pounds per inch of strut circumference were encountered. The problem was made for difficult by the fact that the composite material is at times only 0.030 inch thick. Figure III-23 shows two concepts for load transfer that were developed where continuous resin impregnated glass filaments are wound so as to lock in specially designed end fittings. This allows both tension and compression loads to be transferred effectively to the longitudinal load carrying filaments.

Another source of heat leak to a cryogenic propellant tank is the lines that are required to transfer propellant and provide venting and pressuriza-

tion. Because interval pressures are quite low, propellant lines on a spacecraft are usually not designed on the basis of internal pressure, but rather, they are designed to resist rough handling and accidental damage. If, for these low pressure applications, rugged propellant lines could be designed for minimum weight based on internal pressure, substantial weight savings could be achieved. NASA has been applying the techniques of filament winding and composite technology to this problem; the concept is illustrated in figure III-24. An internal liner of thin stainless steel is designed to carry the longitudinal load while an overwrap of glass fibers impregnated with epoxy resin carries the circumferential loads and provides a tough protective outer covering. The metal ends are built up in thickness as part of the metal liner. This allows sections of line to be joined by conventional methods. In addition to saving weight, the total thermal mass is reduced. The result is much lower chill-down boiloff losses and a quicker attainment of single phase liquid at the delivery end of the line. Another advantage is that the thermal conductance along the line is greatly reduced. This means reduced heat transfer back to the cryogenic propellant tank.

Shown in figure III-25 is the wrapping operation of a thin wall tube 15 inches in diameter and 10 feet long. The tube is pressurized internally to prevent it from buckling while it is being wrapped. After the wrapping operation is complete and the resin has been cured, the internal pressure is removed. The resulting line is light, strong, and rugged.

Shown in figure III-26 is a weight comparison between an all metal liquid line and a composite line. Weight per inch of line is plotted against line size. For a 50-psi service pressure, the all metal line is designed, not on pressure, but to withstand roughness in handling. Thus, the composite line which can be designed to minimum thickness based on pressure and still be rugged enough to withstand rough handling shows substantial savings in weight. Weight reductions are also possible in larger sizes and for lines designed for higher pressures; but, in the higher pressure regime, where metal lines are designed for purely pressure considerations, the weight comparison is less dramatic than shown here.

There is no technical reason why thin-wall composite overwrap lines cannot be constructed in larger sizes and for higher operating pressures. Thus, it is possible to speculate on how a high pressure gas transmission line might be constructed. Such a line would consist of an inner metal shell

designed to carry all the longitudinal load and approximately half of the circumferential load. A composite overwrap, matched to the strain produced in the metal shell, would carry the remaining circumferential load. The connecting ends of each pipe section would be welded in the field. After welding is complete, the joint would be wrapped with fiber impregnated with a resin that can cure at the site temperature.

The potential advantage of using this concept is that the metal liner is thinner than would normally be required; thus, it would be lighter and easier to ship and handle. The composite fiber-resin overwrap would provide protection from corrosion which should result in longer pipeline service life and lower maintenance costs.

INSTRUMENTATION FOR FLOW MEASUREMENT

A variety of temperature sensors are available for cryogenic temperature measurements. Some of the more common ones are shown in figure III-27. At the top of the figure is the carbon resistance thermometer, which is a simple carbon composition resistor of the type used in electronic circuitry. In the center of the figure is the germanium resistance thermometer in which the sensing element is a thin bar of germanium treated to make it a semi-conductor. In the platinum resistance thermometer the sensing element is a platinum wire. Both a surface-mounted and a probe-type element are shown. The characteristics of these sensors are shown in figures III-28 and III-29.

Figure III-28 shows typical resistance values plotted against temperature. On the temperature scale the normal boiling points for hydrogen, nitrogen, and methane are also shown. Note that for the carbon and germanium semi-conductor sensors the resistance decreases with increasing temperature, while for the metal platinum sensor the resistance increases with temperature. Note also that the germanium sensor has a rather low resistance at the methane boiling point which makes resistance measurements somewhat more difficult.

Figure III-29 shows the sensitivity of these sensors plotted against temperature. The sensitivity is defined as the percentage change in resistance per ^{o}F. In the region of the methane boiling point the platinum sensor has

roughly twice the sensitivity of the germanium sensor and seven times the sensitivity of the carbon sensor. Thus, the platinum sensor is superior for this temperature range from the standpoint of sensitivity and also resistance value.

There are additional reasons for preferring the platinum sensor. For example, a two-point calibration, perhaps at the nitrogen boiling point and the freezing point of water, is sufficient for good quality platinum sensors. This is a significant advantage over the germanium sensor which requires a number of calibration points in the temperature range of interest. Not only is the calibration procedure simpler, but the calibration is very stable and can be repeated to within one degree F. Also, the platinum sensors can be easily interchanged by using a calibration based on the resistance difference ratio technique.

The cost of these sensors should be compared on the basis of the cost of a calibrated probe ready to use. Platinum probes range in cost from less than $100 to more than $500. Platinum probes used at Lewis cost about $250. Germanium probes will be somewhat more costly because of the higher calibration cost. The cost of a carbon resistor probe will be less than $100. However, the low sensitivity and relatively poor stability make the carbon sensor a poor choice for this temperature range.

A low cost alternative to these sensors is the type E thermocouple, which is Chromel-constantan. This thermocouple has a very acceptable sensitivity of 16 microvolts per degree Fahrenheit in this temperature range. The measurement accuracy with the thermocouple will not be as good as with the platinum sensor, but it may be sufficient for use in LNG.

As in most cryogenic instrumentation, the details of the installation have a great bearing on the results obtained. Consider the following examples. Most measurements of the temperature of the fluid in a cryogenic line involve the use of a thermometer well so that thermometers can be removed and changed without opening the line. In the case of a vacuum-jacketed or double-wall insulated line such as the microsphere concept, the preferred installation is as shown in figure III-30. A thermometer well is installed in the cryogenic line and the sensor lead wires are wrapped loosely around the cryogenic line before going to the access port in the jacket which contains the electrical feedthrough. This eliminates an error due to heat conducted down the sensor lead wires and allows for relative motion between

the jacket and the thermometer well.

The case of a conventionally insulated line is shown in figure III-31. Here it is important to immerse the well as deeply as possible so as to minimize the heat conducted to the sensor along the walls of the well and the thermometer probe. One technique is to use a standoff leg to increase the immersion depth and to reduce heat leaks to the probe tip. A liquid-vapor interface may be formed in the standoff leg. In both cases it is important to get good thermal contact between the thermometer probe tip and the inside wall of the well. A spring-loaded sleeve or copper wool can accomplish this.

When it comes to measuring flow rates, cryogenic fluids are not like any other liquids, the cryogens are handled under conditions close to their boiling points and the fluids, in general, have low heats of vaporization which means they boil easily. Thus, the possibility of two-phase flow - that is, a mixture of liquid and gas - must always be considered in designing a flow measuring system.

Figure III-32 is a picture of two-phase flow in which the volume flow rate of gas is 1.6 percent of the total volume flow rate. In this picture light is being transmitted through a transparent flow line. Some of the bubbles show up clearly while others appear as dark shadows. If this two-phase fluid were methane at 45 psi absolute, where the density of the saturated liquid methane is 80 times that of the vapor, the vapor bubbles in this picture would represent a mass quality of only 0.02 percent. This sounds like a negligible amount of boiling, but if it occurred in - or shortly upstream of - a volume flow rate measuring station, sizable error in total quantity transfer could result. The point is that special care must be taken to eliminate sources of local boiling when designing flow metering stations.

With regard to cryogenic flowmeters, most of the NASA experience has been obtained with turbine-type flowmeters. Some typical turbine flowmeters are shown in figure III-33. At the upper left is a meter with end flanges. The smaller meters to the right have flare end fittings. At the bottom is a cutaway view of a meter and one with the turbine assembly removed. The heart of the meter is a small free-running turbine which rotates at a speed proportional to the velocity of the fluid passing through the meter. The speed of the turbine is measured with a magnetic pickup which generates a signal each time a turbine blade passes the pickup. The turbine is mounted in ball bearings that have glass-filled-Teflon ball retainers.

The discussion that follows is based primarily on results obtained with small turbine meters, meters with diameters from 3/4 to 2 inches.

Figure III-34 shows the type of calibration curve obtained for these meters. The vertical scale is the calibration factor with dimensions of pulses per gallon. The horizontal scale is the pulse rate which is proportional to the rotational speed of the turbine. The calibration factor rises from zero at low flow rates and asymptotically approaches a constant value. The range over which this calibration factor is constant to within some acceptable tolerance is the so-called linear range of the flowmeter. Turbine meters have been used in liquid hydrogen over a linear range of 6 to 1 based on the criterion that the calibration factor be constant to within 1/2 percent. Repeated calibrations in liquid hydrogen have indicated that a meter of good quality will have a reproducible calibration curve to within ±1/3 percent.

There are some factors to consider when planning to use turbine-type flowmeters. First, regarding the calibration fluid, the primary question is whether or not it is necessary to calibrate with LNG. Obviously, this depends on what error is acceptable. With liquid hydrogen if errors of less than ±1/2 percent are desired, calibration with liquid hydrogen is mandatory. Second, bearing replacement after 50 to 100 hours of operation is recommended since life tests on small turbine meters have indicated that calibration shifts of from 1/2 to 1 percent may occur after 50 hours of operation in liquid hydrogen. Third, meter chilldown can present problems. Uncontrolled two-phase flow through the meter during chilldown of the line and meter will cause the turbine to overspeed; this leads to bearing failure. Some acceptable method of obtaining meter chilldown must be included in the design of the installation. Finally, with regard to size, it should be noted that good results have been obtained using small turbine meters here at Lewis. Limited bearing life has not been a big problem because the tests involve fairly short times and because removal and replacement of small meters is not difficult. Some experience has also been obtained with large size turbine meters. In the one-million-pound thrust M-1 rocket engine program a 20-inch-diameter turbine meter was built and used in liquid hydrogen. If full size turbine meters are to be used in large LNG transfer lines, the problems to be solved are calibration and bearing life. Whether

or not it will pay to solve these problems depends on what alternatives are available.

In general, there are two alternatives. One is to avoid direct measurement of flow rate and rely on quantity measurements in storage tanks. This is the practice in ground-based storage and handling facilities for cryogenic propellants. The other alternative is to find a different flowmeter, preferably one with no moving parts. One such meter is the vortex shedding meter which is being evaluated for use in LNG by the National Bureau of Standards.

If a volumetric flowmeter is used to measure quantity transfer, a secondary measurement of liquid density is needed to determine the total mass transfer. Two methods that can be used to measure liquid density have previously been mentioned: One method is the buoyant force technique using a totally submerged float; the other is the capacitance technique.

Another device for measuring the density of liquid hydrogen has been developed which is similar to the capacitance method in that it uses the relation between the relative dielectric constant and the density. In this device, the sensing element is an open-ended microwave cavity built into a flow line as shown in figure III-35. This figure shows a section of flow line with a pair of axially oriented hollow cylinders held in place by radial vanes. The cavity consists of the section of line between these cylinders. By properly sizing these cylinders a highly resonant cavity can be formed and yet fluid can flow through the device. Small coupling loop antennas are mounted in the walls of the cavity. Each loop is formed on the end of a piece of metal sheathed co-axial signal line by bending the center conductor into a loop and grounding the end to the sheath. The sheath is then soldered to the wall of the cavity. These loops are used to excite the cavity and pick up a signal which can be used to measure the resonant frequency of the cavity. The resonant frequency of the cavity is a function of the average dielectric constant of the fluid which, in turn, can be related to its average density.

The advantage of the cavity over the capacitance sensor is that in the cavity frequency is measured rather than capacitance. It is easier to get highly precise measurements of frequency than it is to get precise measurements of capacitance. Precise measurements are important to get accurate measurements of density. For example, in order to measure liquid hydrogen density to within 1 percent the dielectric constant must be measured to within 1/5 percent. For liquid methane the problem is less severe; the

ratio of errors is then about 2 to 1 rather than 5 to 1.

The cavity can be scaled to different size lines. The larger the cavity, the lower the frequency. The cavity tested by NASA was approximately 1.6 inches in diameter and had a resonant frequency of 10 gigahertz.

This resonant cavity device has not been used on operating systems in the field. However, reports are available describing the construction of the cavity and giving the theory for its design. Also, experiments have been run in which the density of liquid hydrogen has been measured to within 0.15 percent.

Finally, if two-phase measurements are required, it should be noted that, in theory at least, both the cavity and the capacitance sensor can be used. For two-phase measurements, however, the accuracy depends on having small bubbles that are uniformly dispersed throughout the liquid.

GELLED LIQUID METHANE

A major problem encountered in using LNG as a fuel for a supersonic cruise aircraft is boiloff due to the decrease of pressure with altitude. The boiloff can be controlled by storing in pressurized tanks or by loading subcooled LNG at ground level and pressurizing with a nonsoluble gas. However, pressurant gases with low solubility in LNG are rare and expensive. Nitrogen would be an excellent pressurant if its solubility in subcooled LNG could be controlled. Liquid methane, a major component of LNG, can absorb nitrogen up to 8 percent by weight in an hour at a liquid temperature of -284° F.

One method for reducing nitrogen absorption is to gel the LNG. Satisfactory gels of liquid methane have been accomplished using either water or methanol. The absorbed percent by weight of nitrogen plotted against percent by weight gellant concentration is shown in figure III-36. Even at gellant concentrations as low as 1 percent by weight the nitrogen absorption after 1 hour is less than 1 percent. The reason for this is that the upper regions of the gel become nitrogen saturated and act as a seal which effectively stops the absorption process.

The selection of water or methanol as a gelling agent depends on customer usage. Less water than methanol is required to provide the same reduction in

nitrogen adsorption. On the other hand, the water, as opposed to methanol, does not contribute to the heat of combustion. Also, the presence of even small quantities of water may be detrimental at the point of consumption.

The control of slosh in partially filled transport tanks is a particularly interesting application for gelled liquid. Reduced heat transfer, due to convection, during shipment and improved stability of the transport tanker are benefits to be gained by gellation.

Pinning down the mechanical properties of a cryogenic gel is very difficult; however, a rudimentary index of the stiffness or solidity can be obtained by measuring a property called "structure index". Gellant concentration plotted against structure index for gelled liquid methane at -284° F is shown in figure III-37. This index could be considered as somewhat analogous to a yield stress. The index is obtained by placing weighted spheres of various sizes on the surface of the gel and measuring the projected contact area when the spheres no longer sink. The structure index is simply the sphere weight, corrected for buoyancy effects, divided by the projected contact area of the sphere. Even at low gellant concentrations such as 3 percent, for example, the gel can support a loading of 1/2 pound per square foot. The gel has a consistancy like that of yogurt or a soft custard. Gelled liquid methane is easily transferred from tank to tank. The gels are stable and readily reformed again after being transferred.

Gels of liquid methane can be formed at the normal boiling point of -260° F. Samples of gelled methane when dumped on a floor persisted as amorphous lumps. This property should be important when spill hazards are considered. Work has just begun in the area of gelling cryogens, and it appears that there are some important potential benefits to be gained from this process.

CONCLUDING REMARKS

In summary, the results of recent work in the areas of storage, transfer, and transport of cryogenic fluids have been reviewed. Although this work has been directed at the problems encountered in spacecraft and aircraft, there appear to be many areas where this technology can be transferred to terrestrial applications.

BIBLIOGRAPHY

Barron, Randall: Cryogenic Systems. McGraw-Hill Book Co., 1966.

Brady, H. F.; and Del Ducca, D.: Insulation Systems for Liquid Methane Fuel Tanks for Supersonic Cruise Aircraft. (MCR-72-42, Martin Marietta Corp.; NAS3-12425.), NASA CR-120930, 1972.

Bullard, B. R.: Cryogenic Tank Support Evaluation. (LMSC-K-16-68-1, Lockheed Missiles and Space Co.; NAS3-7979.), NASA CR-72538, 1969.

Hall, C. A.; Pharo, T. J.; Phillips, J. M.; and Gille, J. P.: Low Thermal Flux Glass-Fiber Tubing for Cryogenic Service. (Martin Marietta Corp.; NAS3-12047.), NASA CR-72797, 1971.

Haskins, J. F.; and Hertz, J.: Thermal Conductivity of Plastic Foams From -423° F to 75° F. Advances in Cryogenic Engineering, vol. 7, K. D. Timmerhaus, ed., Plenum Press, 1962, pp. 353-359.

Johnson, V. J., ed.: A Compendium of the Properties of Materials at Low Temperature (Phase 1). Part 1. Properties of Fluids. WADD-TR-60-56-PT-1, Wright Air Development Division, National Bureau of Standards, Cryogenic Engineering Lab., 1960.

Scott, Russell B.: Cryogenic Engineering. D. Van Nostrand Co., Inc., 1959.

Siegel, Robert; and Howell, John R.: Thermal Radiation Heat Transfer. Vols. 1 to 3, NASA SP-164, 1971.

Smetana, Jerry; and Wenger, Norman C.: Two-Phase Hydrogen Density Measurements Using an Open-Ended Microwave Cavity. NASA TN D-6212, 1971.

Smetana, Jerry; and Wenger, Norman C.: Instrumentation for Liquid Hydrogen Density Measurements Using an Open-Ended Microwave Cavity. NASA TN D-6415, 1971.

Vander Wall, E. M.: Investigation of the Suitability of Gelled Methane for Use in a Jet Engine. (Aerojet Liquid Rocket Co.; NAS3-14305.), NASA CR-72876, 1971.

Wenger, Norman C.: Theory of Open-Ended Circular Cylindrical Microwave Cavity. NASA TN D-3514, 1966.

Wenger, Norman C.; and Smetana, Jerry: Liquid-Hydrogen Density Measurements Using an Open-Ended Microwave Cavity. NASA TN D-3680, 1966.

Wenger, Norman C.; and Smetana, Jerry: Hydrogen Density Measurements Using an Open-Ended Microwave Cavity. IEEE Trans. Instru. Measurement, vol. IM-21, no. 2, May 1972, pp. 105-114.

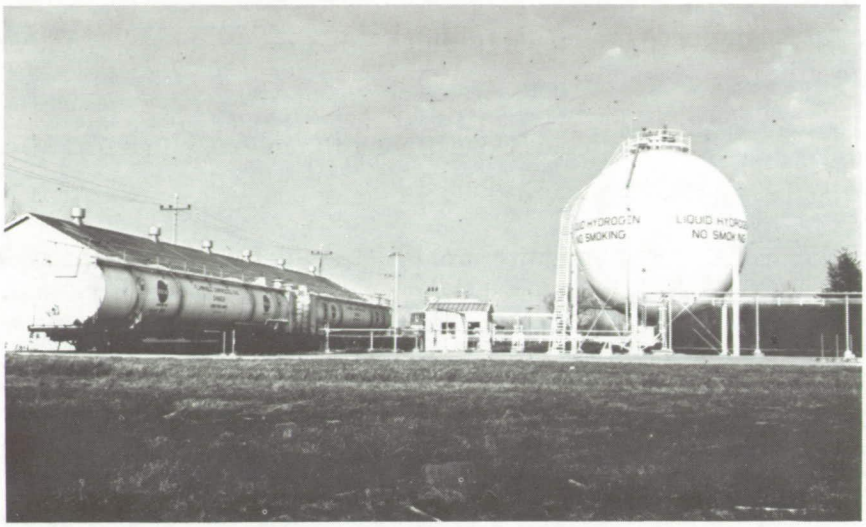

Figure III-1. - Liquid hydrogen storage facility.

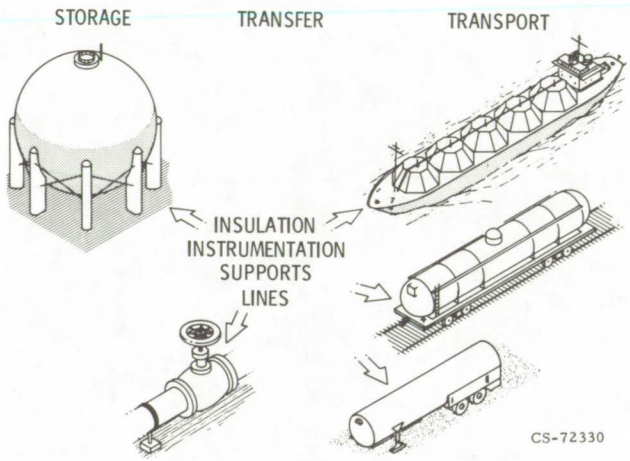

Figure III-2. - Terrestrial applications of aerospace technology.

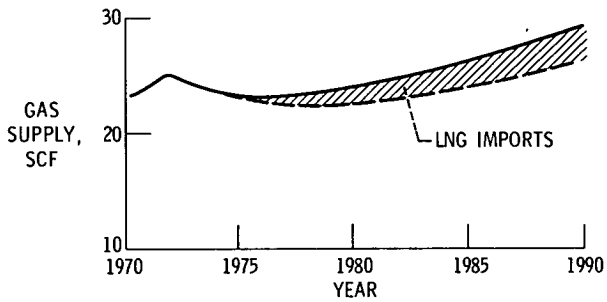

Figure III-3. - Federal Power Commission projection of total United States gas supply.

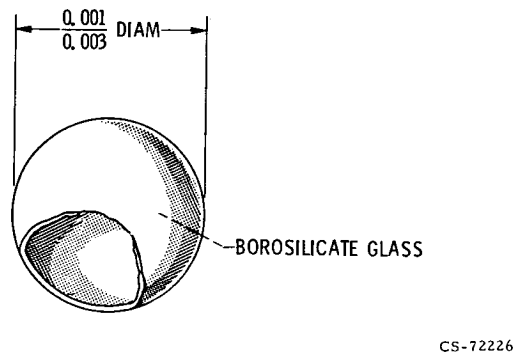

Figure III-4. - Microsphere.

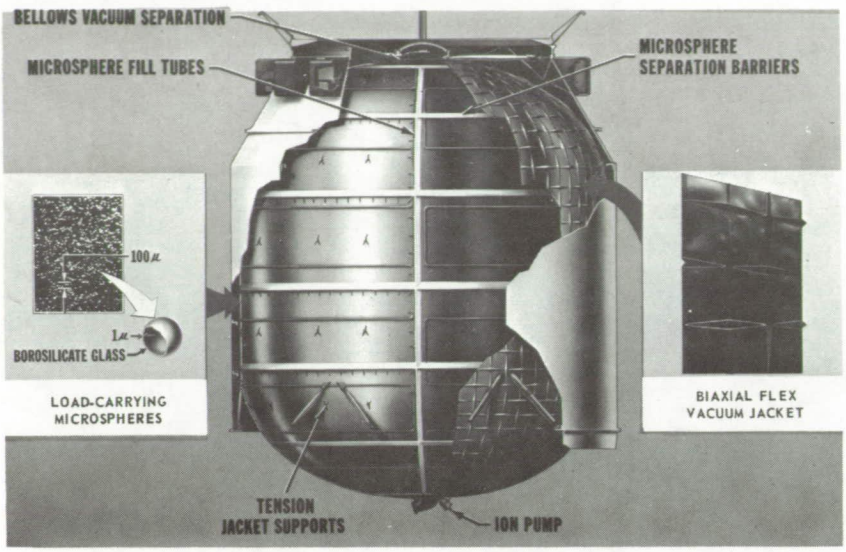

Figure III-5. - Microsphere insulation system.

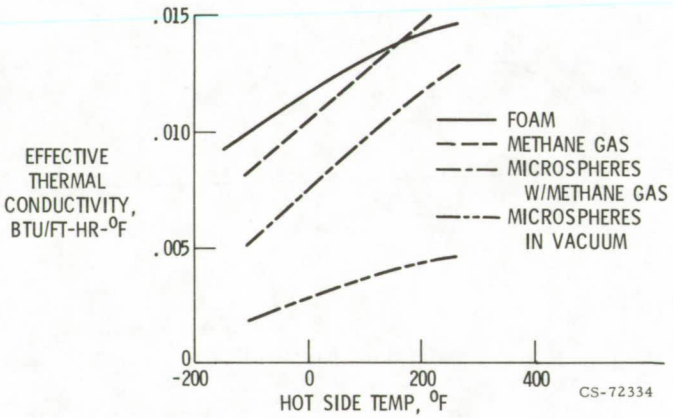

Figure III-6. - Effective thermal conductivity for several insulations. Cold side temperature, -260° F.

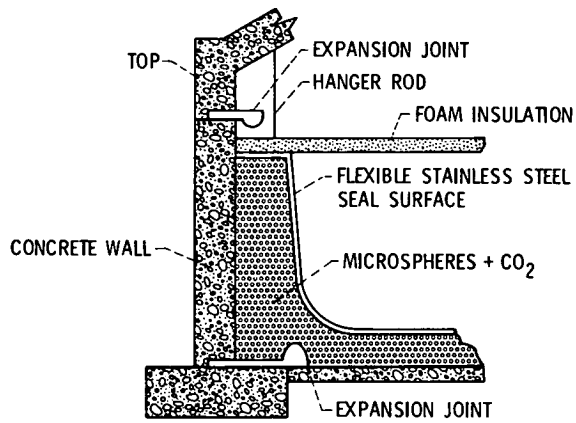

Figure III-7. - Liquid natural gas storage tank using microsphere insulation.

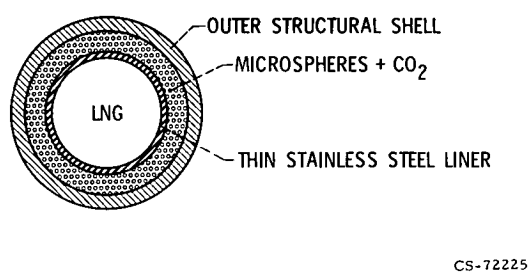

Figure III-8. - Liquid natural gas pipeline using microsphere insulation.

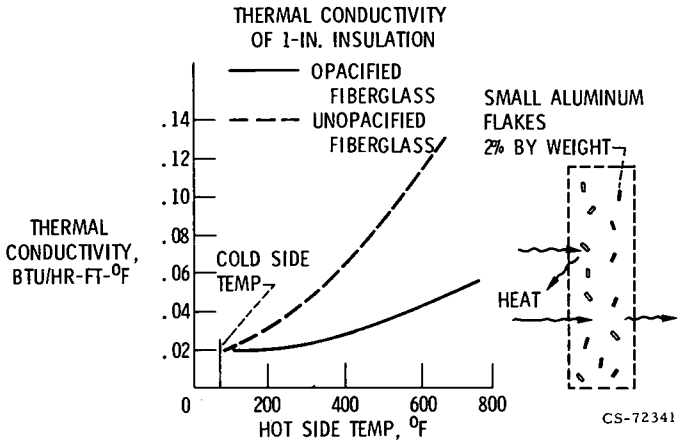

Figure III-9. - Opacified fiberglass.

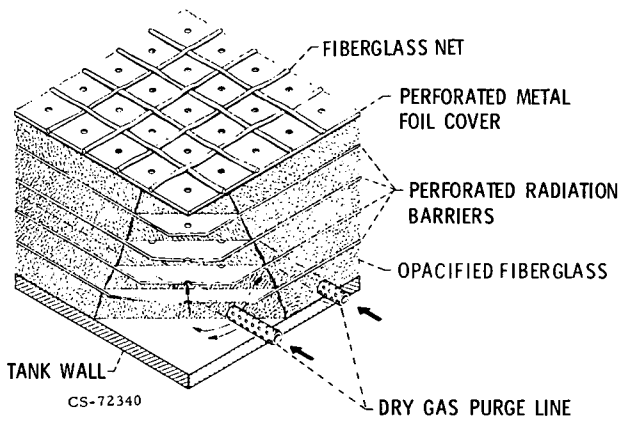

Figure III-10. - External insulation.

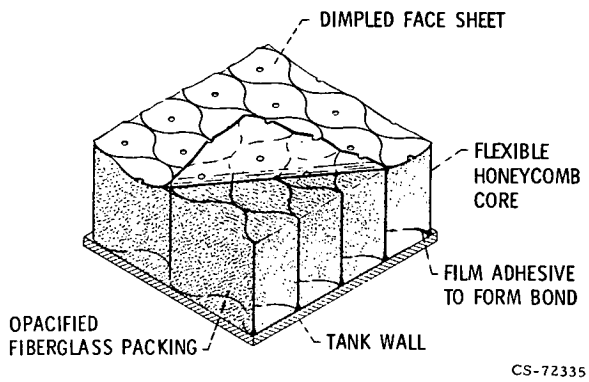

Figure III-11. - Internal insulation.

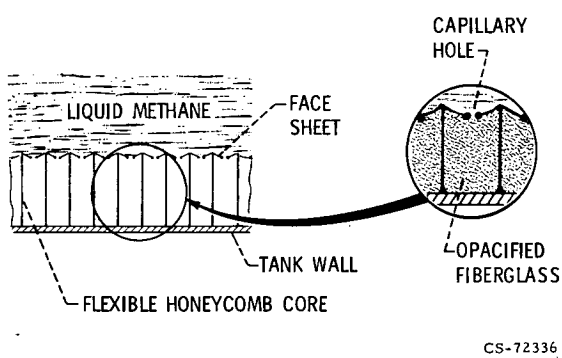

Figure III-12. - Internal insulation configuration.

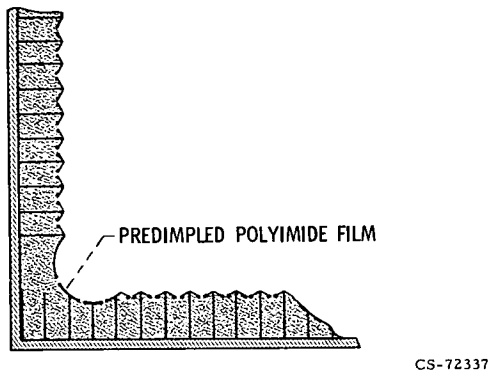

Figure III-13. - Corner joint configuration.

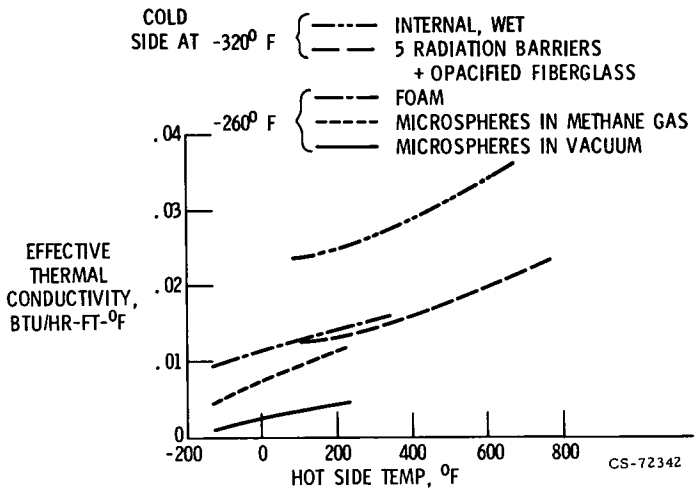

Figure III-14. - Insulation systems.

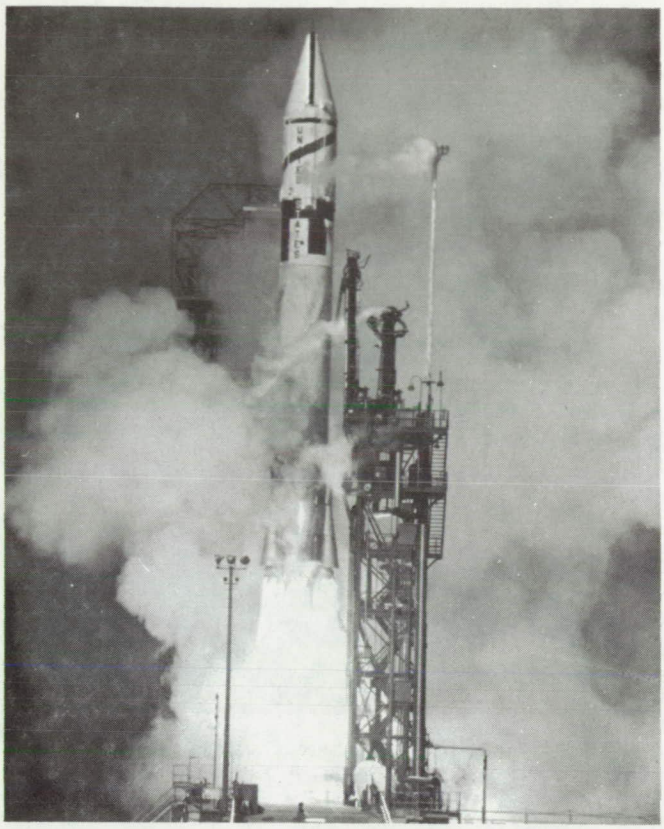

Figure III-15. - Atlas-Centaur vehicle.

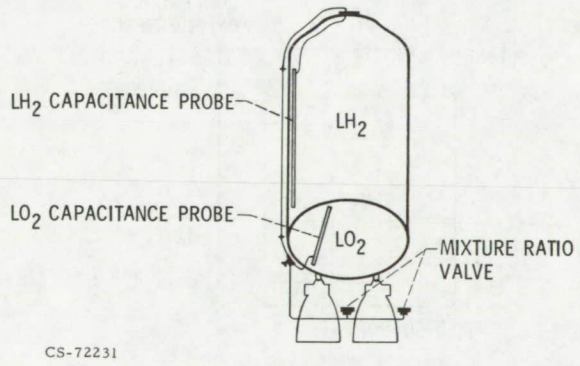

Figure III-16. - Centaur propellant utilization system.

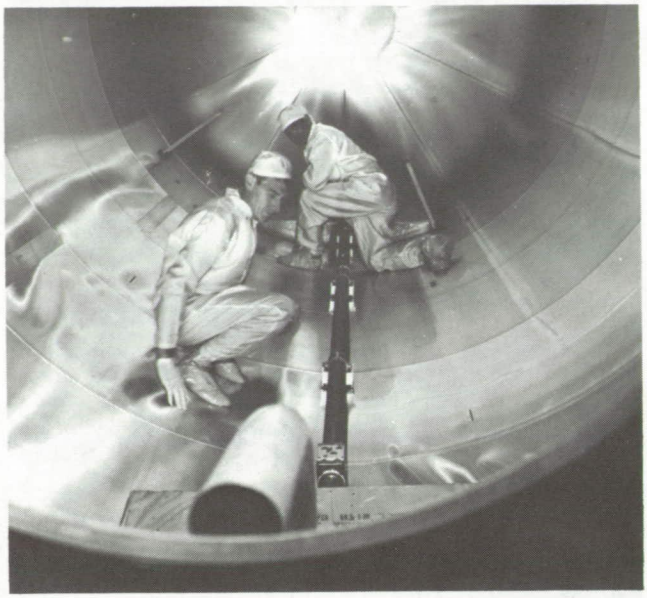

Figure III-17. - Installation of capacitance sensor.

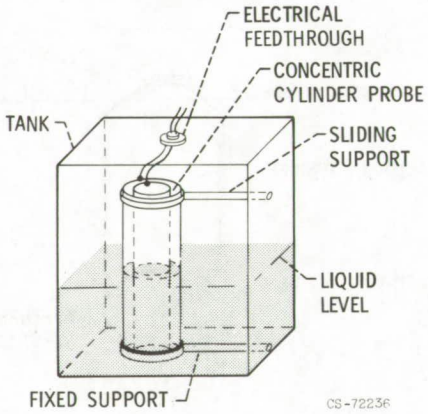

Figure III-18. - Quantity measurement using capacitance probe.

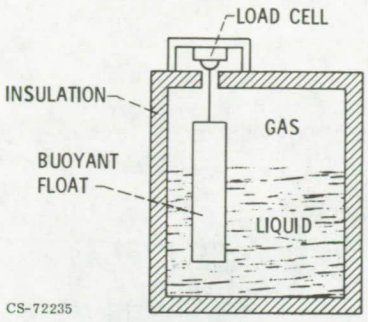

Figure III-19. - Quantity measurement using buoyant float.

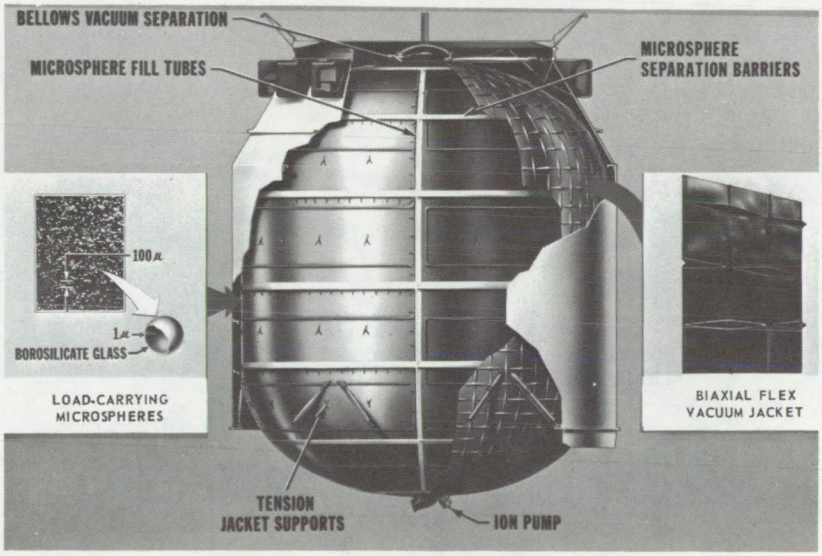

Figure III-20. - Microsphere insulation system.

Figure III-21. - Composite struts. CS-72190

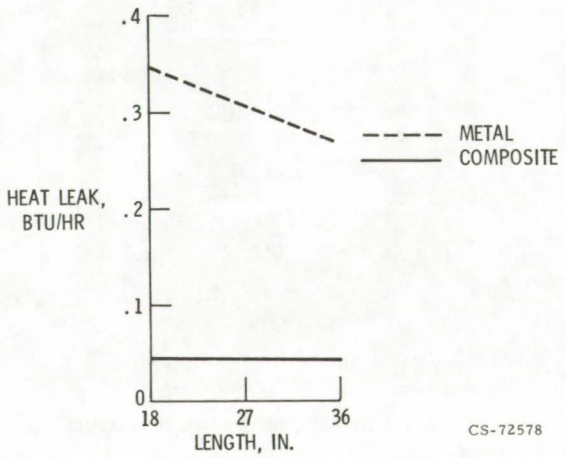

Figure III-22. - Comparison of composite and metal struts.

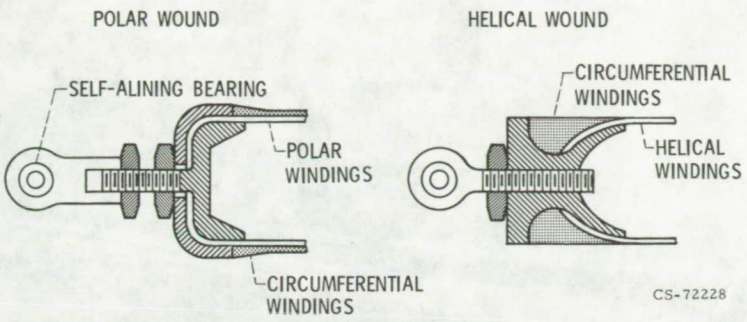

Figure III-23. - End construction of composite supports.

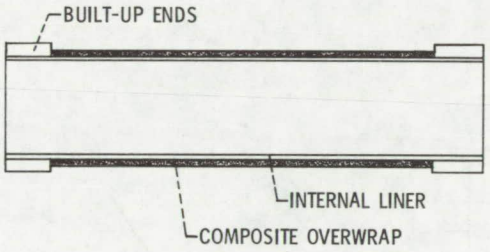

Figure III-24. - Composite lines.

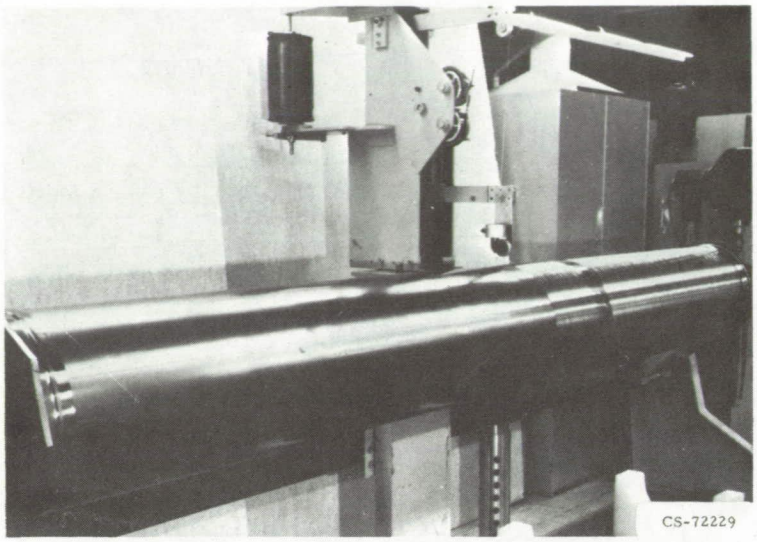

Figure III-25. - Tube being wrapped (10 ft length by 15 in. diam by 0.005 in. wall).

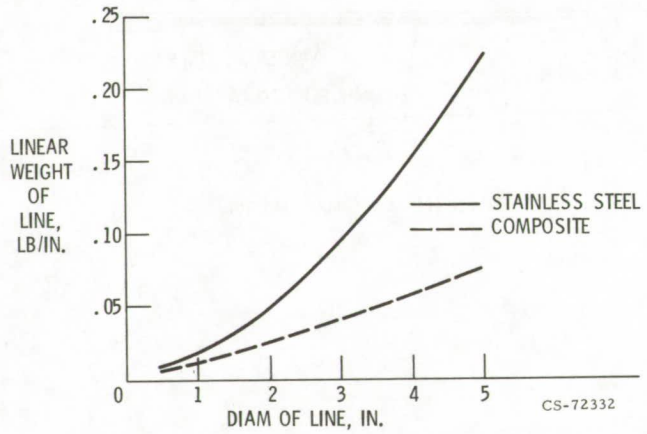

Figure III-26. - Weight comparison. Service pressure, 50 psi.

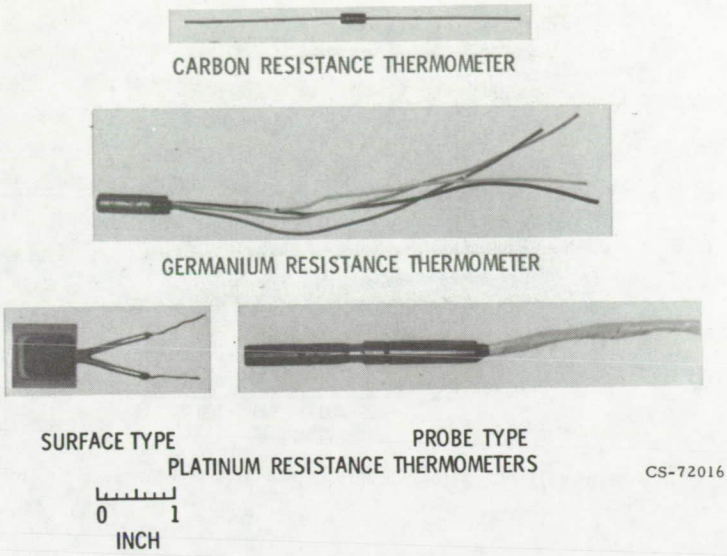

Figure III-27. - Typical resistance thermometers.

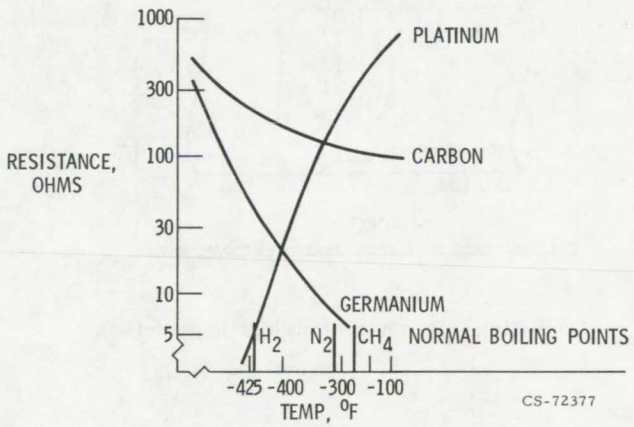

Figure III-28. - Resistance thermometers.

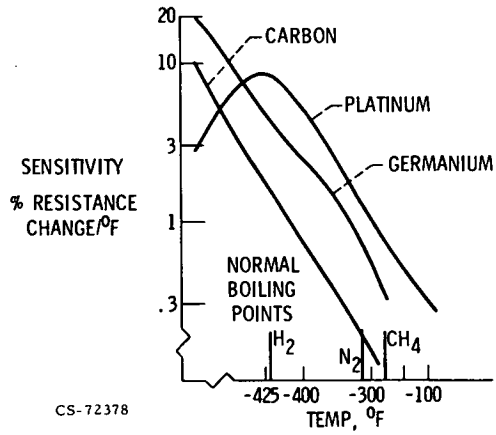

Figure III-29. - Sensitivity of resistance thermometers.

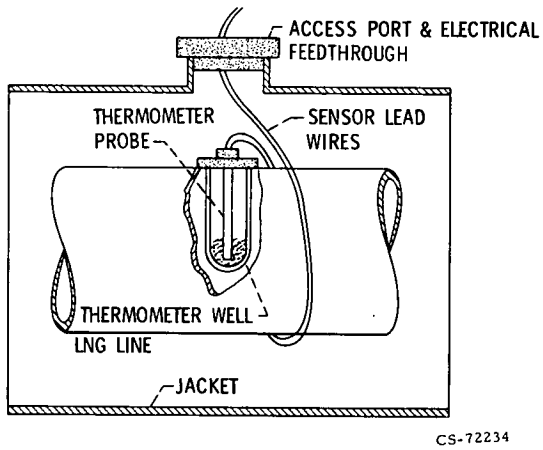

Figure III-30. - Thermometer installation in jacketed line.

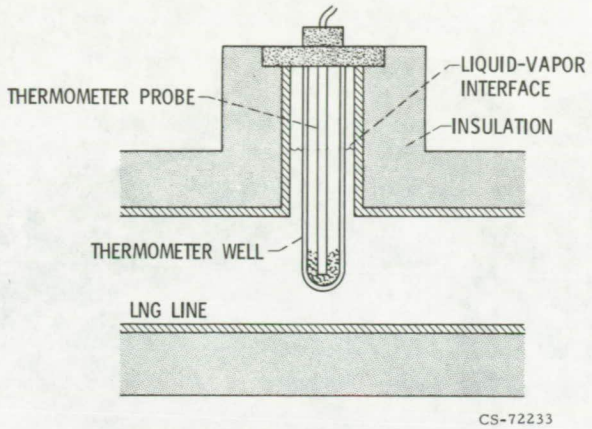

Figure III-31. - Thermometer installation in insulated line.

Figure III-32. - Two-phase flow of cryogenic fluid. Ratio of volume flow rate of vapor to total volume flow rate, 1.6 percent.

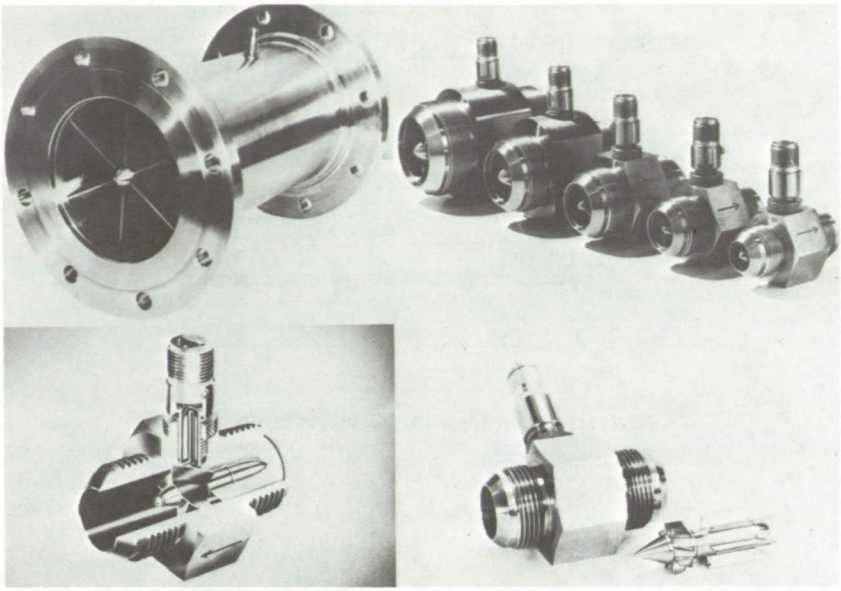

Figure III-33. - Turbine flowmeters.

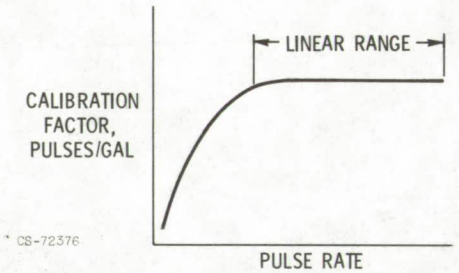

Figure III-34. - Typical calibration of turbine-type flowmeters.

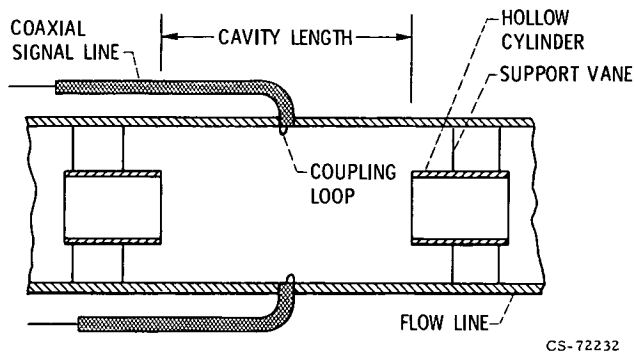

Figure III-35. - Microwave cavity for measuring density.

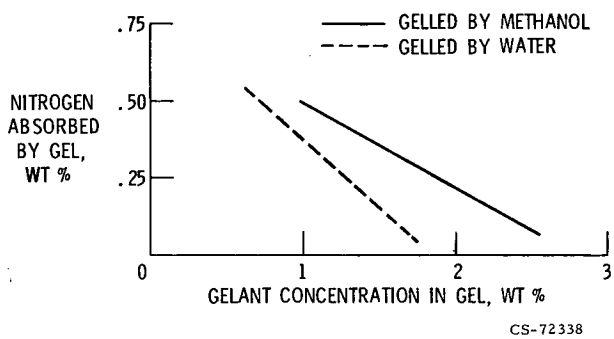

Figure III-36. - Nitrogen absorption in gelled methane at -284° F in 1 hour.

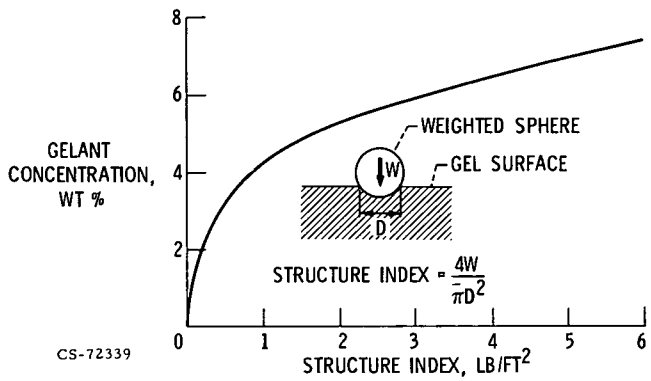

Figure III-37. - Structure index of methane gels.

IV. SAFETY

Paul M. Ordin

NASA experience in the safety of aerospace systems can be very beneficial to the gas industry, especially with regard to fuels and low-temperature systems. Liquid hydrogen and liquid oxygen are the propellants used for most space missions. These propellants (fuel and oxidizer) are stored and used as cryogenic fluids. The problems involved are similar to what we would expect with liquefied natural gas (LNG). Also, hydrogen is a flammable fluid. And the problems of fires, explosions, and detonations with hydrogen-air mixtures are again similar to what we might expect with gas-air mixtures.

A number of programs concerned with fuel safety are being conducted at NASA. An overview of these programs is shown in figure IV-1. Two major areas are being studied: LNG and compressed-gas safety and hydrogen and oxygen safety. Several hydrogen and oxygen studies will be described since we feel similar programs should be conducted for LNG.

Programs pertaining to fuels safety include the Aerospace Safety Research and Data Institute (ASRDI) safety data bank. The data bank contains a collection of technical safety information that has been reviewed and evaluated. Cryogenic fluid safety, including hydrogen and LNG, is one of the information areas. Explosion and fragmentation studies are concerned with the hazards of flammable fluids and compressed fluid storage systems. These hazards include pressure waves and fragments from exploding propellant tanks and bursting pressure vessels.

An NASA technology utilization program on LNG safety was undertaken at the request of the New York City Fire Commissioner. Information is to be provided on the safety of LNG and LNG facilities. Three NASA Centers are involved in this program: The Lewis Research Center (Cleveland), the Ames Research Center (California), and the John F. Kennedy Space Center (Florida).

The liquid and gaseous hydrogen and oxygen studies include material compatibility and safety studies, thermophysical property compilation, and accident surveys.

ASRDI SAFETY DATA BANK

The safety data bank is operated by the Aerospace Safety Research and Data Institute (ASRDI) at the Lewis Research Center. ASRDI was established in 1968 by NASA Headquarters to support NASA, its contractors, and the aerospace community with technical information and consultation on safety problems. In addition to the operation of the safety data bank, ASRDI sponsors research in various areas concerned with safety.

The information for the ASRDI safety data bank is obtained from many sources. Over 6500 citations dealing with the safety of cryogenic fluids, 2500 citations dealing with fire safety and hazards, and 600 citations dealing with the mechanics of structural failure are presently in the data bank and available for retrieval. Two hundred citations on explosions and fragmentation are being placed into the data bank.

The technique of operation, showing how the information is prepared for input into the data bank and the type of material available as output, is shown in figure IV-2.

The documents screened for input to the data bank include research reports, conference papers, journal articles, unpublished data, codes and regulations, and accident/incident reports. The documents are analyzed for their safety information. A safety-oriented abstract and special key words are prepared, the document is evaluated, pertinent figure references are identified, and a bibliography of related references is assembled. The evaluation gives the reviewer's opinion of the importance or relevance of the document's contents.

The information is then prepared for computer processing and placed on the ASRDI search tape. A specialized dictionary containing key words and specific terms for each of the document files is prepared. Typical output from the data bank includes evaluated abstracts and safety information. Additional outputs include state-of-the-art reports, handbooks, bibliographic reports, and accident/incident reports. On a regular basis we are contacted

for information on safety problems by the NASA staff, NASA contractors, universities, and industry.

In many instances, we may not have ready access to the required information, but we do work very closely with other data centers where the information would be available, such as the following:

(1) NBS Cryogenics Data Center (CDC)
(2) NASA Scientific Technical Information System (RECON)
(3) Characteristics of Materials (COMAT)
(4) National Transportation Safety Board (NTSB)
(5) FAA Maintenance Analysis Center (MAC)
(6) Highway Research Information Service (HRIS)
(7) National Highway Traffic Safety Administration (DOT-NHTSA)
(8) Defense Documentation Center (DDC)
(9) Nuclear Safety Information Center (NSIC)
(10) Toxicology Information Project (TOXLINE)
(11) ERDA Technical Information Center
(12) National Institute for Occupational Safety and Health (NIOSH)

An additional output from the data bank is a register or directory of experts in each field. These registers cover the fields of firefighting, mechanics of structural failure, aerospace safety, and two which are just being prepared for publication on hydrogen and cryogenic fluids. The experts on each register are identified with respect to their particular area of expertise. For example, the hydrogen register is subdivided into thermodynamic and transport properties, hydrogen production and liquefaction, materials of construction, engineering systems, transportation systems, instrumentation, and safety hazards.

A typical document entry is shown in figure IV-3. The numbers and letters at the top of the entry are coded to indicate such information as type of document; security classification; accession number; publication data; number of figures, tables, and references; and evaluation. The variable fields with the identifying mnemonics alongside include author; title; corporate source; journal/proceedings, including volume number, page, and year; linked descriptors (key words); major and minor subject terms; abstract; pertinent figure references and description; and a bibliography, which includes a list of references in the document. The report entitled LNG for Base Load Use describes the Brooklyn Union Gas Company LNG plant and

terminal. The safety aspects of the plant are emphasized. The author and source of the articles are presented. The linked descriptors (LKS) and major (MJS) and minor (MNS) terms are key words which indicate the technical material in the document. The reports are retrieved by using the related subject key words for the particular information required. Combinations of terms are used to restrict the document selections from the data bank to those which contain relevant information. At the Lewis Research Center the TSS/360 computer system is used for retrieval.

The search procedure for obtaining documents related to a specific safety problem is demonstrated in figure IV-4. An NASA contractor working on the Space Shuttle program was concerned with the hazards of liquid oxygen (LOX) pumping systems and wanted information on LOX pump failures.

From the Cryogenic Fluids Safety Thesaurus, appropriate key words were selected and entered into the data bank to retrieve documents that would be related to this specific subject. As indicated in the figure, 66 citations were obtained that contained information on LOX pump failures and accidents. This information was given to the NASA contractor. In addition, in an effort to reduce the initial selection of reports on LOX pump failures to the most frequent causes, the key words contamination and bearing failures were entered into the data bank. The forthcoming reports were then intersected with those identified under LOX pump failures and accidents. This procedure reduced the number of documents to 34.

The data bank is being expanded to include additional files which would have potential value to the gas industry. Safety data bank information also serves to indicate areas where study should be pursued. Explosions and fragmentation is one of these areas.

EXPLOSIONS AND FRAGMENTATION

Fuel-air mixtures resulting from spills or leaks of flammable fluids have resulted in damage and injury due to explosions. Study programs underway for a better assessment of risks from explosions include

(1) Railroad tank-car accident studies

(2) Fragment hazards survey

(3) Accidental explosions studies

(4) Pressure vessel fragment study

The railroad tank-car accident studies are concerned with risks from pressure waves and fragments from exploding fuel tanks. Populations close to storage areas or adjacent to water, rail, or highway shipping routes are exposed to such safety risks. Studies were performed to determine evacuation areas in the vicinity of these possible accident sites that would limit the risk of personal injury.

The fragment hazards survey was undertaken to assemble and analyze fragmentation data from exploding liquid propellant tanks. Attempts are being made to develop correlations of fragmentation effects with type of accident, type and quantity of propellant, and blast yield.

The blast yields of explosions involving propellants are normally expressed as TNT equivalents on the basis of a scaled overpressure or pressure impulse. The TNT equivalent is the percent by weight of TNT which would produce the same blast yield as the given weight of detonable material. Actually, there is a poor correlation between the propellant explosions data and the standard TNT curves. The studies of accidental explosions are concerned with the structure of blast waves and are aimed toward obtaining a direct evaluation of explosions without recourse to the ill-fitting TNT method.

The pressure vessel fragment study is being supported at the Naval Ordnance Laboratory. These experiments involve pressurizing vessels until they rupture. The vessels are designed to rupture at 15 000, 30 000, and 50 000 psig. We expect to obtain data on the generated blast waves and fragments.

Railway Car Accidents

A study was made of 98 railway accidents that involved spills of flammable liquid chemicals. In many of these accidents, train derailment caused puncture of the chemical tank car, spillage, and ignition of its volatile contents. A photograph of such an accident is shown in figure IV-5. Eventually, other tank cars exposed to the fire ruptured. Fragments from such accidents were thrown or rocketed hundreds of meters and then impacted in surrounding communities after causing casualties and extensive property damage.

In the majority of train accidents that involved explosions, the tank cars contained either liquefied petroleum gas (LPG) or liquid propane. Similar catastrophic results may be expected in derailments which involve bulk quantity shipments of flammable chemicals such as liquid methane and liquid hydrogen. Documented data from such accidents that occurred between 1958 and 1971 show that the tank cars exploded from 3 minutes to 48 hours after their exposure to the fire.

Data from the Railroad Tank Car Safety Research and Test Program (1971) are summarized in figure IV-6. The data show that 64 fragments impacted and came to rest at distances ranging from tens of meters to 1500 meters (4900 ft) from the origin. About 50 percent of the fragments came to rest beyond a distance of 150 meters (490 ft), and 20 percent were found beyond 300 meters (980 ft). Only a few small fragments traveled beyond 150 meters (490 ft). Thus, if there were sufficient time to evacuate the area within a 500-foot radius, the primary hazard would be from the impact of large fragments rather than from the shrapnel effects of small, high-velocity pieces.

These fragmentation data were used to develop evacuation area guidelines. The fragment range distribution was plotted as a function of the fragment travel distance (fig. IV-7). The results showed an excellent statistical fit to the log normal distribution. The equations developed were combined with estimates of average impact areas, launch angles of fragments, and numbers of people per unit area that would be exposed. (The average rural/urban population density used was 166 people/km^2 (ref. 1).) These data were used to predict the risk of a person being hit by fragments within a certain distance from a railway accident. The results of the study (ref. 2) showed that, for such accidents, an initial minimum radius of 600 meters (2000 ft) should be established for an evacuation area. This radius would limit the statistical probability of a fatality from impact of large tank-car fragments to 1 in 100 accidents. It is recognized that more work is needed to reduce the uncertainty in establishing evacuation area guidelines that would minimize danger from impact. However, the present guidelines have been adopted by the Department of Transportation (DOT) and incorporated in their recent publication (ref. 3).

Fragment Hazard Studies

Fragmentation data from exploding propellant vessels were obtained from reports of tests and accidents. These data included measurements or estimates of blast effects, fragment velocities, fragment shapes, and other parameters. The data are being reduced, and studies are underway to fit the data to various statistical functions. The goal is to develop methods that predict the characteristics of pressure waves and fragments from exploding and/or bursting tanks. Some methods have been developed which predict fragment patterns, provided the type and quantity of propellant, the type of accident, and the time of propellant mixing are known. One such method is demonstrated in figure IV-8.

In figure IV-8 the mean ranges of fragments evolved during the explosions are plotted against the blast yields (in percent) of the propellants (ref. 4). The percent yield relates the propellants reacted to the total available for reaction. For example, for event 2, 101 000 pounds of propellants were caused to mix but the results of the explosion indicated that only 1 percent of the propellants reacted. The equation $R = 314.74\ Y^{0.2775}$, where R is the mean distance and Y is blast yield, appears to fit a certain number of the events. The tests were all different, but all were made with liquid hydrogen and liquid oxygen. Events 1 and 2 were simulated Saturn-rocket-type explosions in which a diaphragm separating liquid hydrogen and oxygen was ruptured and the fluids reacted. Events 3 to 5 were spill tests of liquid hydrogen and oxygen and RP-1. The three propellants were poured from individual containers onto the ground, and the mixture was set off with a small charge. All these tests fit the curve reasonably well. Events 6 to 8 were liquid hydrogen - liquid oxygen tests in which the contents of one tank were poured into the other. The blast yields were high for these tests because of the forced mixing of the propellants before they were set off.

Considerable scatter exists among the data shown in figure IV-8, but these studies are being continued. We plan to develop methods that predict characteristics of pressure waves and fragments from exploding and/or bursting tanks or pressure vessels, as well as methods to determine the probability of the arrival of fragments and the damaging effects of fragments and pressure waves as a function of scaled distances for equivalent TNT yields. The prediction methods are to be reduced to scaled graphs, nomo-

graphs, and simple formulas that allow for an easy assessment of risks. These methods will be compiled in a state-of-the-art handbook.

Accidential Explosions

Most of the fragmentation and blast wave data are expressed as equivalent TNT yields, but the data from accidental propellant explosions differ from TNT explosions. Propellant explosions and vessel ruptures are not really point-source explosions. And the rate of energy release is usually slower than for TNT explosions. The effects of such differences are demonstrated in figure IV-9. A program was recently initiated to relate the data from propellant explosions and vessel rupture to the rate of energy deposition and the spatial extent of the deposition region. Various classes of explosions will be investigated in which the energy addition functions and the affected regions are different. These include pressure vessel failures without combustion, pressure vessel failures with prior internal explosions, and failures followed by explosions. Gaseous explosions in enclosures and unconfined vapor-cloud explosions will also be studied. It is expected that the energy addition functions and the affected regions can be determined from pressure-time histories by taking into account the volume rate of change of the explosion or combustion.

NASA LIQUEFIED-NATURAL-GAS TECHNOLOGY UTILIZATION PROGRAM

Three NASA Centers are involved in the LNG technology utilization studies to assist the New York City Fire Department (NYFD). At the Lewis Research Center, we have begun the evaluation of reports concerned with LNG safety and the compilation of an LNG bibliography. An LNG safety manual is also being compiled. After discussions with the Fire Commissioner and his staff, it was decided to prepare the LNG safety manual in two sections: one on LNG hazards and fire protection, and the other on safety engineering information. The initial section will review the approaches to LNG safety and will contain data on the thermodynamic and transport properties of LNG, methane (CH_4), and gas-air mixtures. It will also cover cryogenic hazards, fires and explosions, fire protection, firefighting personnel safety, and codes and standards.

The Ames Research Center is developing computer codes to improve understanding of the physical and chemical phenomena of LNG spills on water and land. It is hoped that a model can be developed which would be of practical benefit in reducing the explosion and/or fire hazard of LNG.

At the Kennedy Space Center, a program has been initiated to develop a risk management system for the design and operation of LNG facilities and equipment for use by the NYFD. Also, a technical analysis was recently completed of the NYFD regulations for manufacture, storage, transportation, delivery, and processing of LNG. Instructions (ref. 5) were prepared describing both the risk management system and the methods of establishing uniform requirements, criteria, and procedures by which the NYFD could implement the systems. The approach developed by NASA and an NASA contractor, Boeing Aerospace Company, was based on the management techniques developed for the NASA Apollo and Skylab programs. The suggested risk management logic is shown in figure IV-10.

This method requires the identification of hazards for each of the system activities, which include planning, design, construction, startup, and operation. The plant owner would be required to present documentation to the NYFD for the review of each phase of activity. From this documentation, the hazards associated with each phase could be identified and the requirements evaluated. The risks from these hazards would then be analyzed to reduce them to acceptable levels. The hazard risk levels include

(1) Catastrophic - loss of life; no means for corrective action

(2) Critical - major damage; counteracted by emergency action (time a factor)

(3) Controlled - counteracted

The conditions under which a hazard would be classified as catastrophic, critical, or controlled would be resolved by the NYFD. After the hazard factors have been identified, a hazard reduction procedure sequence should be applied. This sequence is a technique to design hazards out of the system.

Hazard accountability includes the preparation of reports and summaries for examination by the responsible personnel at the NYFD. The summaries would include listings of the hazards and each particular closure status, that is, whether it has been eliminated, controlled, or accepted. Each hazard would be identified by a number and a reference containing more detailed information. Initially, the data may be controlled manually, but it was sug-

gested that, with increased accumulation and system expansion, a computer-oriented program would be required to define, acquire, control, process, disseminate, and utilize the risk management system information. Project reviews would then be performed by the NYFD in meetings with the plant owners to discuss compliance with the fire department requirements.

With respect to the reduction of hazards, a number of risk analysis techniques were discussed. These include the hazard reduction sequence, fault tree analysis, and failure modes and effects studies. The hazard reduction sequence (fig. IV-11) involves designing the hazards out of the system. In the fault tree analysis approach, an evaluation is made of "an undesired event." The work is backward from the undesired event to the cause; both hardware and nonhardware (human error) causes are identified. The failure mode and effects analysis method develops a qualitative means of evaluating reliability, maintainability, and safety of design by considering potential failures and their resulting effects on the system. The analysis involves tabulation of failure modes of a component or system.

The method recommended to the NYFD is to design the hazards out of a system by using fail-safe features, redundant systems, safety devices, warning devices, and special procedures. In addition to installing facility protection systems, there are further activities relating to public safety which may have to be performed by the NYFD. These contingency plans may cover hazardous operations, disaster events, manpower and equipment programming, fire equipment availability, and manpower training.

It was emphasized that the risk management system would be of significant advantage to both the NYFD and the facility owner. With careful documentation and reviews, the NYFD would become more satisfied with the decision to permit operations. The owner of the plant would have better communications and less delay in putting his facility into operation. No doubt, a cost savings would result with a reduction in the occurrence of undesirable events, increased confidence in operation, and a more efficient work force. The NYFD is in the process of incorporating some risk management system concepts into its operating procedures.

HYDROGEN AND OXYGEN SAFETY STUDIES

Several of the NASA hydrogen and oxygen safety studies which contain information pertaining to LNG and gas safety are

(1) Accident surveys
(2) Compilation of thermophysical properties
(3) State-of-the-art reports
(4) Safety practices in industry
(5) Experimental programs concerned with materials compatibility tests and two-phase flow

Accident surveys have been performed for both hydrogen and oxygen (refs. 6 and 7). A compilation was made of the most reliable and accepted thermophysical properties of oxygen (ref. 8) and hydrogen. Over 2500 references were considered in the hydrogen review. The report, presently being published, contains descriptive material, graphs, and tables for over 50 properties of liquid and gaseous hydrogen. State-of-the-art reports have been published on oxygen instrumentation: flow, pressure, temperature, and leak detection (refs. 9 to 11).

Also, as a further help in defining safety problems in oxygen systems, contracts were let by the Lewis Research Center to three companies involved in the oxygen production and handling business to obtain a thorough and detailed study of their safety practices in the design and use of equipment in oxygen service. Specific questions concerning their oxygen safety practices were included in the contracts. These questions covered material compatibility, operational hazards, maintenance programs, systems emergencies, and accident/incident investigations.

A great deal of the material provided in these reports was considered company information and was so identified. However, the importance of sharing information with the public for increased safety was pointed out to the companies. Air Products Chemicals, Inc., recognized such a public need and released their information, which was published in four volumes (ref. 12). Such an industry-wide survey of safety and handling practices would greatly benefit the natural gas industry.

Also experiments were performed on the compatibility of nonmetallic materials in gaseous hydrogen. The experiments were designed to evaluate physical properties of materials and to characterize some of the failure

modes considered vital to the safe use of these materials in hydrogen. The materials under study are those commonly associated with hydrogen systems. The following tests have been completed: mechanical impact, flash and fire, reaction propagation, gas erosion, rapid depressurization, hydrogen permeation, pneumatic impact, notched/unnotched gaseous hydrogen tensile, and high-temperature material off-gassing and exposure.

The mechanical impact tests included Charpy impact tests at room temperature and at liquid hydrogen temperature. Flash and fire tests evaluated the tendency of heated materials to ignite in a hydrogen atmosphere when subjected to an ignition source. The reaction propagation tests evaluated the behavior of materials when they were subjected to a heat input sufficiently large to initiate a reaction. The reaction may then propagate to consume large quantities of materials. These tests were performed on specimens wrapped with an igniter wire and heated with electrical energy until the wire fused. Gas erosion tests evaluated the behavior of materials when they were subjected to high-velocity gas impingement. Such conditions could result from the opening of valves or through the development of leaks which could expose the materials to high-velocity compressed gas streams. Rapid depressurization tests evaluated the effects of depressurization in terms of some physical property change. Permeation tests evaluated the permeation of gaseous hydrogen through materials under high differential pressure.

These tests indicated that some of the materials are affected by the hydrogen environment. Additional tests are being planned. Consideration should be given to performing similar tests with materials in both LNG and CH_4.

A review of accidents and incidents with hydrogen in NASA operations was conducted to obtain an insight as to the causes of accidents. The general causal factors of these accidents are shown in figure IV-12. More than one causal factor was involved with most accidents. The major causal factors of the hydrogen accidents include

(1) Operational deficiencies in the work area, such as inadequate or sloppy work in installation, fabrication, or cleaning

(2) Procedural deficiencies based on failure to follow established procedures or failure to prepare step-by-step action

(3) Design deficiencies, which include use of inadequate component and system designs, flow, and/or stresses or omission of suitable safety

devices

(4) Planning deficiencies, which include failure to prepare test plans or to perform hazard studies such as investigating the effects of the release of hydrogen through vent or relief valves

Other factors are indicated, but the study shows that over 87 percent of the accidents were caused by not adhering to the basic safety considerations for the successful operation of any engineering system - not necessarily a liquid hydrogen system.

Data were also obtained on specific hardware failures, the effects of the release of hydrogen due to accidents, and also the results of over-the-road accidents. Such a study would be helpful for investigating the causes of LNG accidents.

The NASA safety operations have been extremely successful, probably because the overall NASA safety concept requires the identification, listing, evaluating, and resolution of all conceivable hazards. This safety concept should be considered for adoption by the gas industry.

REFERENCES

1. World-Wide Environmental Summary. I - Demographic, Soils, and Meteorological Data. SNS-NUS-932, Atomic Energy Commission, 1972.

2. Siewert, R. D.: Evacuation Areas for Transportation Accidents Involving Propellant Tank Car Pressure Bursts. Presented at the JANNAF Propulsion Meeting, New Orleans, La., Nov. 27-29, 1972.

3. Emergency Service Guides for Selected Hazardous Materials: Spills, Fire, Evacuation Areas. Dept. of Transportation, 1974.

4. Baker, W. E.; Parr, V. B.; Bessey, R. L.; and Cox, P. A.: Assembly and Analysis of Fragmentation Data for Liquid Propellant Vessels. (Southwest Research Institute; NAS3-16009.), NASA CR-134538, 1974.

5. Medkief, C. A., Jr.; Niergarth, A. W.; and Parsons, W. H.: Risk Management Technique for Design and Operation of Liquefied Natural Gas Facilities and Equipment. (Boeing Aerospace Co.; NAS10-7200.), NASA CR-139183, 1974.

6. Ordin, Paul M.: Mishaps with Oxygen in NASA Operations. Presented at the Oxygen Compressors and Pumps Sym., Atlanta, Ga., Nov. 9-11, 1971.

7. Ordin, Paul M.: Review of Hydrogen Accidents and Incidents in NASA Operations. Presented at the 9th Intersoc. Energy Conversion Eng. Conf., San Francisco, Calif., Aug. 26-30, 1974.

8. Roder, Hans M.; and Weber, Lloyd A., eds.: ASRDI Oxygen Technology Survey. Volume I: Thermophysical Properties. NASA SP-3071, 1972.

9. Mann, Douglas B.: ASRDI Oxygen Technology Survey. Volume VI: Flow Measurement Instrumentation. NASA SP-3084, 1974.

10. Sparks, Larry L.: ASRDI Oxygen Technology Survey. Volume IV: Low Temperature Measurement. NASA SP-3073, 1974.

11. Roder, Hans M.: ASRDI Oxygen Technology Survey. Volume V: Density and Liquid Level Measurement Instrumentation for Cryogenic Fluids Oxygen, Hydrogen, and Nitrogen. NASA SP-3083, 1974.

12. Lapin, Abraham: Liquid and Gaseous Oxygen Safety Review. Vols. I-IV. Air Products and Chemicals, Inc. (NASA CR-120922), 1972.

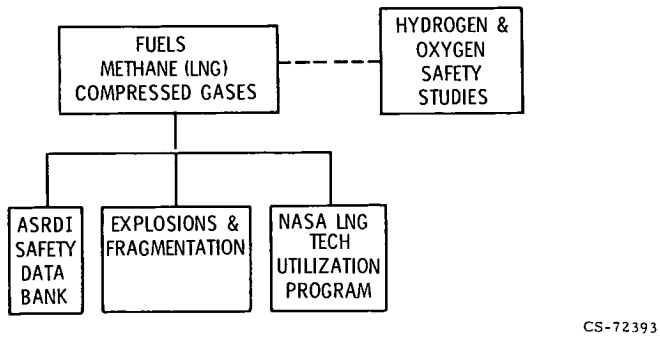

Figure IV-1. - NASA fuel safety programs.

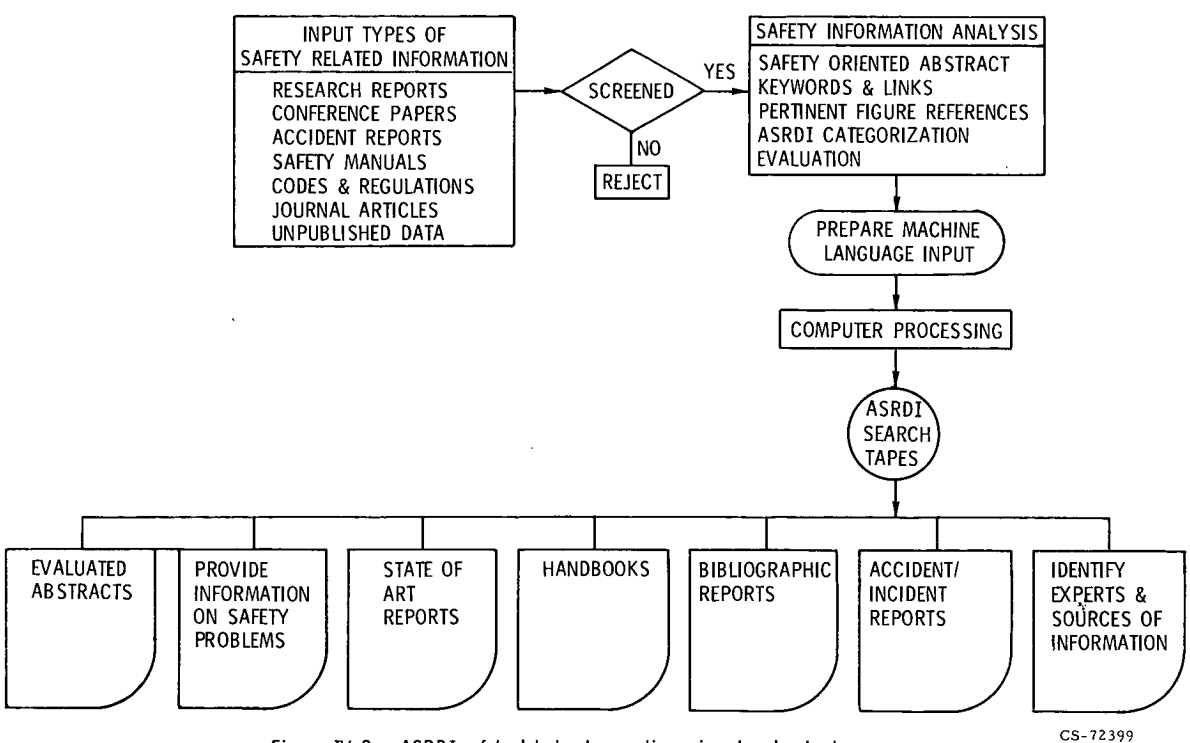

Figure IV-2. - ASRDI safety data bank operation - input and output.

```
C       867211111010975USC11111  3060073000400030000000NNNNNB04
AUT*PREUSSER,R.M.
UTL*LNG FOR BASE LOAD USE
SRC*BROOKLYN UNION GAS CO., NEW YORK
JRL*PIPE LINE IND. VOL 38, NO. 6, 26-9 (JUN 1973)
CAT*E,4,00,00//E,5,00,00//E,7,00,00
LKS*(ENGINEERING SYSTEMS, MARINE TERMINALS, BASE-LOAD PLANT, UNLOADING SYSTEMS
    DESIGN, VAPOR HANDLING SYSTEMS, STORAGE TANKS, FIRE DETECTORS, FIRE
    FIGHTING SYSTEMS, EMERGENCY PROCEDURES, SHUTDOWN, PRESSURE RELIEF, LNG)//
    (COMPONENTS, VALVES AND CONTROLS, CONTROL VALVES, SHUTOFF VALVES, PRESSURE
    RELIEF VALVES, MARINE TERMINALS, LNG)//(COMPONENTS, VESSELS, STORAGE TANKS,
    STRATIFICATION, ROLLOVER, TRANSFER OPERATIONS, PIPING, CIRCULATION, MIXING,
    MARINE TERMINALS, LNG)//(FAILURE CAUSES, PRESSURIZATION FAILURES, STORAGE
    TANKS, STRATIFICATION, ROLLOVER, TRANSFER OPERATIONS, VAPORIZATION RATES,
    EXCESSIVE PRESSURES, LNG)//(CORRECTIVE MEASURES-ACCIDENT PROBABILITY,
    COMPONENTS, STORAGE TANKS, STRATIFICATION, ROLLOVER, TRANSFER OPERATIONS,
    PIPING, CIRCULATION, MIXING, MARINE TERMINALS, LNG)
MJS*CRYOGENIC FLUID SAFETY//TRANSPORTATION//STORAGE//HANDLING
MNS*BARGES//STEAM HEATERS//COLD BLOWERS//CARBON STEEL//SEPARABLE CONNECTORS//
    ALARM SYSTEMS//PERLITE//CONCRETE
MJI*BROOKLYN UNION GAS COMPANY//DISTRIGAS CORPORATION
ABS*THIS PAPER BRIEFLY DESCRIBES THE BROOKLYN UNION GAS COMPANYS BASE-LOAD
    LNG PLANT AND TERMINAL AT GREENPOINT, N.Y. EMPHASIS IS GIVEN TO THE SAFETY
    ASPECTS OF THE PLANT, INCLUDING EMERGENCY SYSTEMS AND PROCEDURES.
```

CS-72313

Figure IV-3. - Typical document entry in ASRDI safety data bank.

SET	NO. DOCUMENTS	SUBJECT
1	123	PUMPS, PUMPING SYSTEMS, CENTAUR BOOST PUMPS
2	233	ACCIDENTS, DAMAGES
3	860	FAILURE ANALYSES
4 (2 + 3)	887	FAILURES, ACCIDENTS
5 (1 * 4)	66	PUMPS, FAILURES, ACCIDENTS
6	344	CONTAMINANTS
7	23	BEARING FAILURES
8 (6 + 7)	362	CONTAMINANTS, BEARING FAILURES
9 (5 * 8)	34	PUMPS, FAILURES, ACCIDENTS, CONTAMINANTS, BEARINGS

CS-72729

Figure IV-4. - Procedure for obtaining specific information from ASRDI safety data bank.

Figure IV-5. - Railway accident involving flammable chemicals.

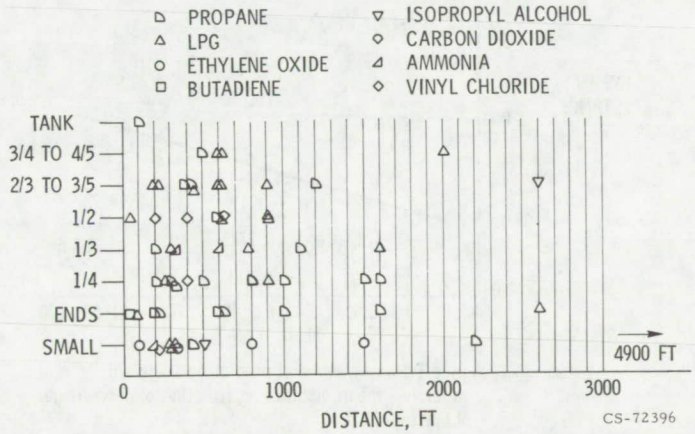

Figure IV-6. - Fragment impact distance as function of fragment size and type of flammable chemical.

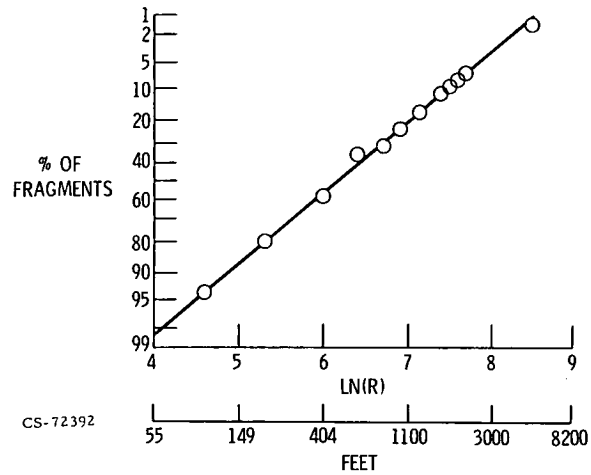

Figure IV-7. - Distribution of fragments - percentage of total fragments as function of log normal distance traveled.

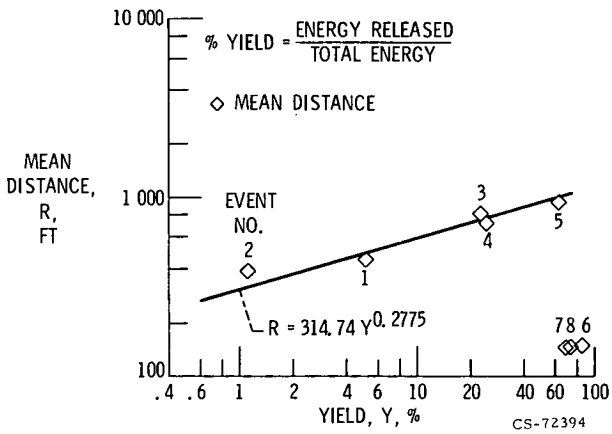

Figure IV-8. - Method of predicting fragment patterns - mean distance as function of percentage of blast yield.

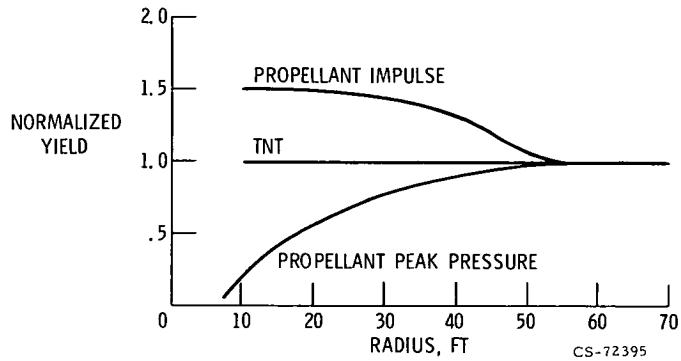

Figure IV-9. - Difference between propellant explosions and TNT explosions.

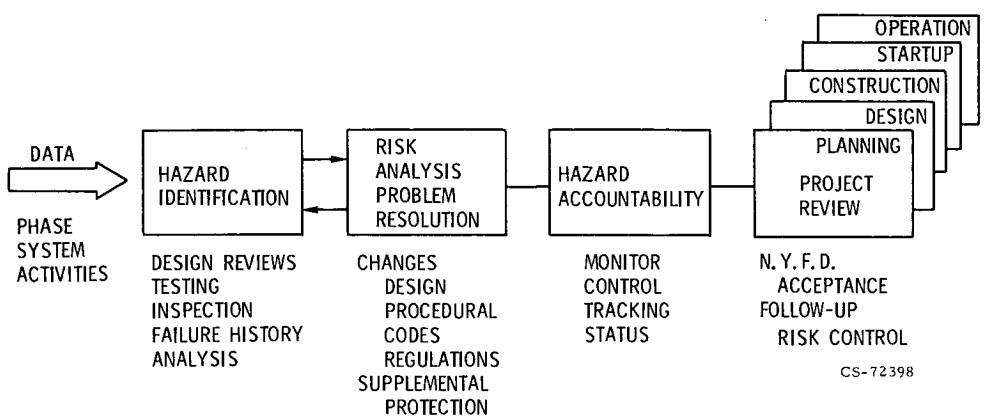

Figure IV-10. - Risk management system logic.

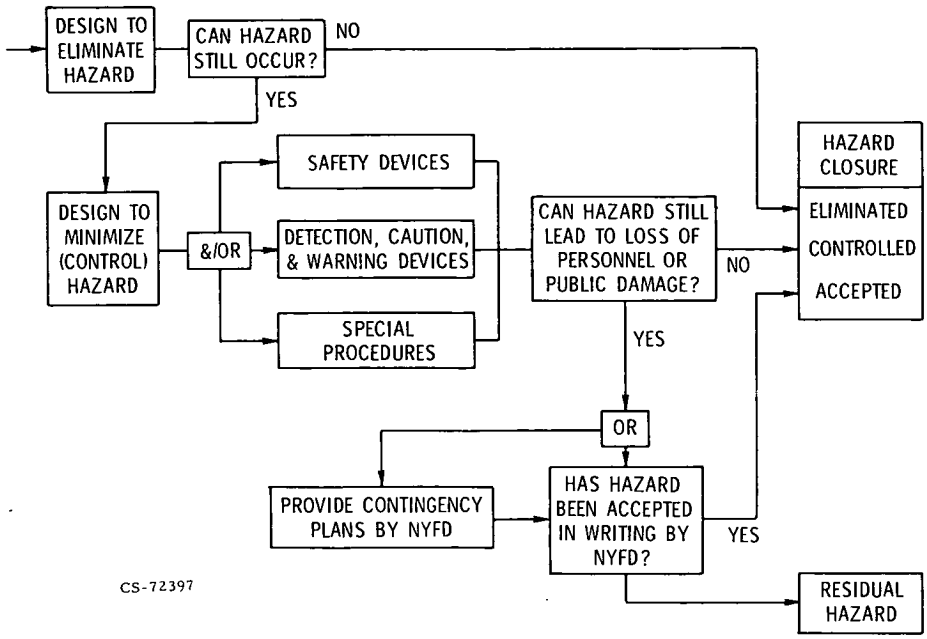

Figure IV-11. - Hazard reduction sequence.

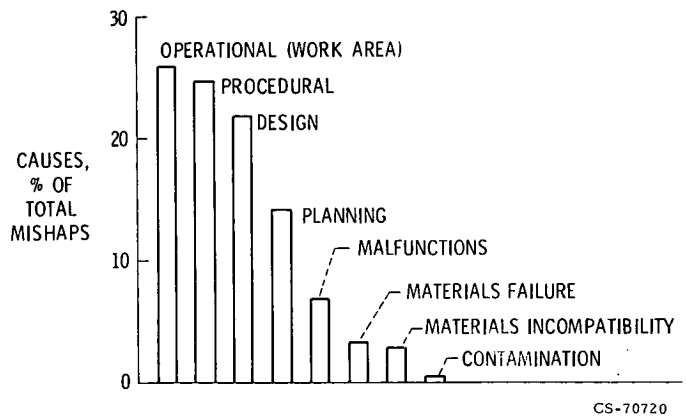

Figure IV-12. - General distribution of hydrogen accidents/ incidents.

V. TURBOMACHINERY TECHNOLOGY

Harold E. Rohlik, Harold H. Coe, James E. Crouse,
William F. Hady, Robert E. Jones, and John L. Klann

Experience at Lewis has included a large variety of gas turbine engine systems. Those applications where there have been impact and resulting benefits include aircraft jet engines, auxiliary power units for both aircraft and spacecraft, powerplants for space and ground use, heavy-duty engines as in trains or buses, gas turbines for cars, and total energy systems. The first three were NASA's responsibility and reflect aerospace experience; prime responsibility for the rest lies with other government agencies with NASA working in these areas through cooperative agreements.

Lewis study efforts have not looked directly at the concerns of the gas industry, such as drive engines for compressor stations, portable compressor units, or LNG (liquefied natural gas) powerplants. Nor has Lewis studied gas industry end-use equipment such as gas-fired industrial prime movers or heat pumps. However, much of the system analysis methodology and component technology developed can be applied in the gas industry. This discussion includes cycle analysis, compressors, turbines, system analysis, seals, bearings, and emissions.

CYCLE ANALYSIS

Most of the engine work at Lewis uses either the Brayton or the Rankine thermodynamic cycle. The Brayton, or gas, cycle is the basis for jet engines. The Rankine, or vapor, cycle is widely used in steam powerplants. Discussion here will be limited to the gas cycle. It has the potential for a lot of different uses - mainly because of its flexibility and many possible variations. Four cycle variations applicable to compressor-station drive engines are discussed.

Some older compressor stations use gas turbines that came from aircraft, that is, turbine engines based on the simple open cycle shown in figure V-1. This cycle is called simple because it has the fewest main parts: a compressor, a combustor, and a turbine. Newer compressor stations often use recuperators for better fuel economy. The recuperated open cycle is shown in figure V-2. The job of the recuperator is to take some of the potentially lost heat from the hot turbine-outlet gases and transfer it to preheat the air entering the combustor. Recuperation, however, adds to engine costs, and this must be weighed against the improved fuel economy.

Closing the gas turbine power loop, as indicated by the recuperated closed cycle shown in figure V-3, might be profitable in locations like the desert or near the sea. To close the power loop, a heater and a cooler are added. The problems of salt corrosion or particle ingestion would be restricted to the external combustion region, where they would be easier to handle. The tradeoff then is between longer times before maintenance and higher first costs.

There are some other considerations, too. Since the power loop is closed, there is a choice available for the working gas. Inert gases like helium, neon, or argon could be used. In space systems, mixtures of helium and xenon have been used. Also, the shaft power output can be controlled by varying the amount of gas within the power loop, rather than by varying the engine speed as in the open cycle. This feature could offer better part-load fuel economy. However, a gas inventory control system would be needed. Another concern is the temperature drop occurring in the heater between the combustion gas and the turbine inlet gas. This reduces the cycle efficiency. To get economy equivalent to an open cycle, therefore, the recuperator would have to be a little bigger for the closed cycle.

One way of easing the problems of the closed cycle and still retaining some of the good features, such as part-power economy, is with the semi-closed turbocharged cycle shown in figure V-4. A small turbocompressor is used to supply the combustion air. The heater, with its additional temperature drop to the turbine inlet, is no longer there. The turbocharger is a built-in gas inventory control. However, the engine controls would be more complicated than those of the fully closed cycle.

This cycle, like the closed cycle, could be run as a constant-speed engine over a large range in output. Gas transmission compressors are also

run at nearly constant speed. The combination might offer an alternative to turning units on and off with the duty cycle.

The point here is that there are a lot of possibilities and tradeoffs to be made with respect to choice of cycle. Cycle analysis is one of the first steps in evaluating the tradeoffs. Computer programs are available for all of the variations discussed. These cycle programs serve to evaluate components as far as fuel economy is concerned. However, these programs do not directly yield size or cost.

Through a series of computations with a cycle program, performance maps like those in figures V-5 and V-6 can be generated. Figure V-5 is for an unrecuperated open cycle. Specific fuel consumption is plotted against specific shaft horsepower. The solid lines show constant cycle pressure ratio, while the dashed lines show levels of turbine inlet temperature. To get low fuel consumption, high pressure ratios and high temperatures are needed. The cross-hatched area is the usual design range for aircraft turboshaft engines. Temperatures are above 2000° F, and pressure ratios are 8 or more. These engines have high specific shaft horsepower, which yields a relatively lightweight powerplant.

In comparison, figure V-6 is for a recuperated open cycle. Recuperation causes the performance lines to be closer together. To get a specific fuel consumption of about 0.4, both pressure ratio and temperature can be lower than for the unrecuperated cycle. Most gas turbines for cars are designed with a pressure ratio near 4 and a temperature of 1800° or 1900° F. Engine weight is not as important and these engines are relatively heavier than the aircraft engines (on a per hp basis). These car engines are more conservatively designed, with lower temperatures and fewer machinery stages. They are relatively less costly and are easier to maintain.

The performance maps in figures V-5 and V-6 are for essentially "rubber" engines; that is, these maps have fixed levels of component performance and each point is a potential new design. Along the lines, the size of components is changing New levels of recuperation would shift the performance lines, and those shifts would give a measure of changes in fuel consumption.

Another facet of cycle analysis is that it determines all of the required component conditions - pressures, temperatures, and flow rates. This is

the information needed to start the design of the compressor and turbine for the engine.

COMPRESSORS

Axial-Flow Compressors

The general configuration of an axial-flow compressor is shown in figure V-7. This is an eight-stage research compressor with one-half of the split casing removed. The axial configuration is naturally suited for aircraft because it has a high volume flow per frontal area and a low weight to power ratio. The axial-flow compressor has been developed into an efficient and reliable component of aircraft engines. The high efficiencies attainable with this type of compressor have and are continuing to make it a candidate for many other applications.

With present technology, attainable efficiency levels for axial-flow compressors are shown in figure V-8. The band represents well-designed machines which are aerodynamically conservative. At low pressure ratios where only one or two stages are required, efficiencies of 90 percent are being obtained with large compressors. Many stages are required to produce the higher pressure ratios, but the overall adiabatic efficiencies are still in the very respectable mid-80's. Many compressors at pipeline booster stations are operating at pressure ratios of less than 2, with efficiencies of about 80 percent. This means there is significant efficiency improvement available.

The cantilevered blades of the axial-flow compressor give the impression of being mechanically fragile; however, blade failure is quite rare in aircraft engines. The standard for major inspection is 10 000 hours, and even then blades are seldom replaced. The most common cause of blade failure is damage from foreign objects such as birds and debris from runways.

Another example of axial-flow compressor durability comes from an application closer to that of the gas industry. Electric power companies sometimes use gas turbine powered generators for peak power loads because of the relatively low costs of the units. The compressors for this application

are more conservatively designed than those for aircraft. These compressors often require no service for years.

The compressor program at Lewis is more research than development oriented; however, we do have one compressor that has been running a long time. It is a compressor for our 10- by 10-Foot Supersonic Wind Tunnel. As can be seen from figure V-9, it is very large - 20 feet in diameter. The compressor was designed at Lewis in the early 1950's. The pressure ratio is 2.4. The use of eight stages for a 2.4 pressure ratio is a very conservative design by today's standards. In fact, it was fairly conservative at that time, mainly because they wanted the compressor to work properly without reblading. The first build of the compressor did perform well. It has an efficiency in the high 80's. It has run about 10 000 hours over the last 20 years, and there never have been any blading problems.

In the past, the prime objectives of military aircraft compressors were low weight, high efficiency, and durability, with cost taking a secondary roll. To a large extent this was also true for the engines used by the airlines. By keeping the planes in the air, the airlines could spread the high capital cost over so many miles that the initial cost was not of great consequence. Times are changing though and costs are catching up with everyone. The military has to make more efficient use of their dollars for hardware, and the commercial airlines are faced with higher fuel costs and higher interest rates.

The immediate thing to do in such a situation is to cut costs within the same technology. Such a trend is appearing in the form of a reduced number of blades, as indicated by figure V-10. With a lower number of blades, the spacing between blades is wider. The individual blades in such a blade row must be longer to give approximately equivalent aerodynamic performance. This lengthens the compressor and adds weight, but the cost is lowered because blade costs are approximately dollars per piece rather than dollars per pound. This is a good trend for the gas industry because weight is not of that much concern. The trend is also in the direction of even better blade durability.

For conservatively designed machines, there appears to be a considerable reduction of cost possible through technology. One promising possibility is the use of airfoil shaped strip stock blading, which is very inexpensive. The strip stock can be coined or twisted to the desired shape and pinned or welded to the rotor hub. Another possibility is precision casting

of blades; casting technology for small parts has progressed substantially in the last decade. If one or more of the procedures are indeed developed into practical fabrication methods, the higher efficiencies offered by axial compressors could be realized in many more applications.

Another important aspect of compressor performance is range of operation. A multistage compressor performance map is shown in figure V-11, where pressure ratio is plotted against flow rate for various speed lines. The stall line generally indicates a suddenly encountered severe time-unsteady flow separation. When the stall region is entered, there is a sudden drop in efficiency. There is also considerable blade vibration; so, it is a generally undesirable region to operate in. With this restriction, the flow range of the axial-flow compressor is relatively small at the near full speed. At part speed, the range is better. Also, compressors with lower design pressure ratios have somewhat better range.

In figure V-12, the performance map of a single-stage axial compressor is shown. This compressor is near the type needed at a pipeline booster station. It was designed and tested by Pratt and Whitney under NASA contract. It yields a pressure ratio of 1.5 at a tip speed of about 1000 ft/sec. Thus, it has very high aerodynamic loading. Even so, the efficiency level is good and the flow range is quite respectable too.

The range shown in figure V-12 is adequate for stationary compressors and for aircraft engines operating near steady state. Most system operating lines basically follow the good efficiency island as speed is changed. The tough systems control and component range of performance problems for aircraft arise from sudden transients caused either by fast throttle changes or by bad inlet conditions from sudden maneuvering, gusts, etc.

One of our major research efforts is to extend the range of good operation of the axial-flow compressor. One approach that we have been using for several years is the upgrading of our design and analytical performance prediction techniques. The objective is to do a better job of predicting when and where in the blade a flow separation will occur. If problem areas can be found with analytical studies, the pressure distributions often can be adjusted by design modifications to delay the onset of separation. The ability to avoid repeated tests and hardware modifications reduces development time and cost considerably.

Other approaches to range extension come under the heading of hardware

complexities. They include variable-setting stators, flow bleed, and casing treatment. Casing treatment involves putting specially shaped cavities in the casing over the rotor tip. These approaches often are effective in improving range; however, for the most part, the hardware changes required add to the cost of the compressor. It is not likely that such additional hardware complexity would be needed for compressor-station application. The flow range obtained from conventional hardware ought to be adequate.

Centrifugal Compressors

Centrifugal compressor research at Lewis peaked in the late 40's and early 50's when they were being used in the early turbojets. After a period of strong emphasis on space systems, work resumed, but in a much smaller size range. Small compressors for space power systems were studied in the middle 60's. Also, interest in automobile and helicopter engines led to work in the 1- to 10-lb/sec flow range. Test results and design methods developed, however, are applicable to the large centifugal machines used in pipeline booster stations.

Figure V-13 shows a photograph of a 4-inch compressor designed for a space power system. This view with the shroud removed shows the impeller and the diffuser blade rows. The design is fairly sophisticated in that extensive computational flow analysis was done to establish the hardware shape. The measured efficiency from the experimental test was 82 percent, quite good for a machine of this size.

The efficiency levels now attainable with single-stage centrifugal compressors are shown in figure V-14 as a function of pressure ratio. The size effect is shown by the width of the band of efficiency. The lower edge represents the best efficiencies attainable with a 1/2-lb/sec air compressor. The corresponding size is about 4 inches in diameter at the impeller tip. The upper curve of the band represents an 8-lb/sec air compressor. This would be a compressor about 12 inches in diameter. Again we see that pipeline compressor efficiencies could be improved significantly with the use of the best design methods. New concern over the cost of energy may justify more sophisticated blades and diffusers. These, with closer running clearances, can raise efficiencies to the high 80's.

Part of the effort to get better efficiencies is made with the use of advanced computerized internal flow analyses. Most programs at present use an ideal fluid flow model for the mathematical calculations with the application of experience factors to adjust for fluid friction effects. New advances in high-speed computers, however, are making it possible to perform rigorous three-dimensional viscous flow calculations in reasonable times. Output and display of three-dimensional solutions are difficult though. One way is to show data on flow surfaces such as the blade-to-blade surface shown in figure V-15. This flow surface extends from the suction surface of the passage to the pressure surface, which is the hidden surface in the figure. In the other direction, the flow surface is some fraction of the passage height from hub to shroud. In figure V-16, velocity vectors calculated in the passage are shown on a blade-to-blade surface near the shroud. Flow is from the inlet at the left to the impeller tip on the right, as indicated by the arrows. The calculation of the viscous flow eddy near the exit represents a major breakthrough in the analysis of internal flow in turbomachinery. This program, being developed under NASA contract, is highly complex. It requires many hours of computer time for one complete solution. Current work is directed toward reducing this time by using fewer solution points in the passage without experiencing mathematical instabilities.

A little over 1 percent of our Nation's total energy usage from all fuels is used to pump natural gas. This amounts to something on the order of 1000 trillion Btu of energy per year. Saving part of this will not by itself solve the energy crisis, but it is a very large base figure to work from. Any improvement in compressor efficiency amounts to significant energy and cost savings to gas transmission companies. With the trend of fuel prices, use of the best design technology available has to be good long term economics. To help in this regard, we have a number of design and analysis computer programs available for both axial and centrifugal compressors.

TURBINES

Large turbine research at Lewis is being carried out in two major areas: very high temperature compressor-drive turbines requiring large cooling flows, and high-work low-speed turbines to drive high bypass fans. The

overall objectives of these two programs are to increase engine thrust-to-weight ratios and to reduce specific fuel consumption. High turbine temperatures along with high engine pressure ratios provide high cycle efficiencies and high thrust per pound of air. Improvements, then, lead to lower fuel consumption and lighter engines. In fan-drive turbines, work is directed toward increasing stage loading while maintaining good efficiency. Higher stage loading means fewer turbine stages and therefore lighter engines.

In the area of turbine inlet temperature, figure V-17 shows trends with time for cooled and uncooled blades. The three bands shown are for uncooled turbines, existing cooling methods now flying in engines, and advanced cooling methods that include such features as precooled cooling air. The lower band starts with the first jets that flew in the mid-40's at about 1300° F and continues to the 1800° F level with the best alloys available today. As temperatures increase beyond 1800° F, progressively more sophisticated cooling designs must be employed. They progress from simple internal convection to film cooling through holes in the blade surfaces, and then to very complex internal structures that direct and meter the flow selectively to various parts of the blades.

Turbine cooling work at Lewis began in the 40's and continued to the late 50's. At that time, our heat transfer work was directed to the cooling of rocket combustion chambers and nozzles. In those early days we did heat transfer and structural analysis on all of the cooling methods noted previously. This included a demonstration engine that was run with a turbine inlet temperature of 2500° F in 1954. We resumed turbine cooling work in the late 60's. Figure V-18 shows a turbine stator vane for a very high temperature engine. The upper photograph shows the complete vane with about 700 holes for full film cooling. The ribs on the vane insert, shown in the lower photograph, form compartments within the vane, and internal jets cause the cooling air to impinge on the inner surface of the shell. The air then flows out through the holes in the shell. Some interesting new work is being done in holes that are flared to provide better spreading over the outer blade surface. This shows promise for greatly reducing the number of holes and, therefore, the cost of these blades.

The use of cooling involves some penalties in overall engine performance. One penalty is the partial loss of working fluid to the cooling circuits. Another is an aerodynamic performance loss associated with the thick

blade profiles and the cooling air itself. The stator vane shown in figure V-18 has been tested for aerodynamic performance with and without cooling flow, with results as shown in figure V-19.

Figure V-19(a) shows the wake, in terms of pressure loss contours, of the solid vane as measured just downstream. The dashed line shows the projection of the blade trailing edge. The 96 percent efficiency indicates that 96 percent of the available pressure energy has been converted to velocity. The wake is wide and deep with loss concentrations near the ends. Figure V-19(b) shows the effect of cooling flows. These were introduced through the vane surfaces and through the inner and outer walls. The efficiency has dropped to 92 percent and the loss regions in the wake and on the inner wall are much larger. More important, however, is the deviation of the wake from the vane trailing edge projection. The vane cooling air caused the flow to separate from the blade surface. The cooling holes are being modified to reduce coolant flow in this critical area on the blade.

The other major area in our turbine research is that of stage loading in low-speed fan-drive turbines. A good measure of how critically a stage is loaded is a term we call stage work factor. This is a ratio of stage work to rotor blade speed squared. Work factor is inversely related to turbine stage number. For a particular application, a turbine with a stage work factor of 1 will have five times as many stages as a turbine rotating at the same speed but with a stage work factor of 5. Figure V-20 shows the relation between stage work factor and turbine efficiency. Low values, near 1, are associated with high aerodynamic efficiency. As the work factor increases, efficiency goes down because of increasing fluid friction losses relative to useful work output. This is the kind of curve we use in design studies.

On the curve in figure V-20 are some points experimentally determined at Lewis and under contract. The vertical dashed lines show the work factor ranges of an in-house design now being tested and two other turbines being designed. The variation in efficiency as determined to date is approximately linear from the low 90's at low stage work factors down to 85 at the very high loading indicated by the work factor of 5. Almost all turbines flying today have stage work factors between 1 and 2. Studies for future commercial aircraft, however, show that drive turbines for the high bypass fan jets of the 80's and 90's optimize out with stage work factors near 5. The dashed line on the right shows the work factor indicated for an advanced technology

subsonic transport. Use of conventional work factors would require an eight- to ten-stage fan-drive turbine rather than the four-stage designs currently being made in-house and under contract at Pratt & Whitney. The use of high work factors does involve a performance penalty as shown in figure V-20. The studies have shown, however, that in some cases the penalty is more than offset by the reduced turbine cost and weight in going to fewer stages. The influence of efficiency increases with increasing fuel costs. As these studies are updated, we may move toward more stages in the advanced transport.

This curve can also be useful in selecting turbine stage numbers for gas-line booster drives. For those low-speed requirements, first cost and maintenance or replacement costs will depend on the number of stages. The importance of high efficiency, however, would probably lead to the selection of a stage work factor between 1 and 2. This, with good aerodynamic design procedures, would provide efficiencies of about 92 percent. Current gas-line drive turbines have efficiencies near 85 percent. The previously noted numbers on gas-line pumping power can be used to examine the energy to be saved. If turbine efficiency increases from 85 to 92 percent, and compressor efficiency from 80 to 88 percent, a savings of 16 percent in fuel can be realized. For the pumping stations with turbine-driven compressors, the savings amounts to about 60 trillion Btu per year. At Cleveland's rates, that is worth about $90 million a year.

After the turbine designer has selected the number of stages for the job to be done, he progresses through the detailed aerodynamic design. This means definition of the velocity diagrams, contouring of the inner and outer walls, and finally, three-dimensional flow calculations within the blade rows to determine the final blade numbers and blade shapes. Computer programs are available for these steps, but they will not be discussed here. One program that should be mentioned, however, is the prediction of off-design performance. This prediction can be made with knowledge of interstage design velocity diagrams and hub and tip radii between blade rows. The program can generate performance maps before the complex blade channel flow calculations are made.

Figure V-21 shows calculated performance for a single-stage turbine. This is the conventional form with work per pound of air plotted against the product of airflow and speed for lines of constant speed. Contours of pres-

sure ratio and efficiency are superimposed. When compared with experimental performance, this particular map showed a maximum error of 2 percent in efficiency and only 1.3 percent in flow. This computer program was developed under contract by General Electric. Similar maps can be generated for both axial and centrifugal compressors and computer programs for both are available. After compressor and turbine maps are generated, they are used in system simulation computer programs as discussed in the next section.

SYSTEM ANALYSIS

The general idea of system analysis is to provide a systematic method for evaluating engines before fabrication of hardware is initiated or before money is committed. This logical approach is especially important for new engines or new variations. For existing engines, where there is a lot of experience, a lot of calculations are not needed to make a logical choice. The total approach for the study of new variations is shown in figure V-22. Shortcuts will be indicated for studies of existing engines. The approaches will be related to the problem of choosing compressor-station drive engines.

There are three types of computer tools used in the general process. They are shown in the rectangular boxes of figure V-22: cycle studies, system selection studies, and system performance studies. But, at the start of the study, clear problem definitions are required. Need might be defined as a more energy-conservative drive engine. Intended use could be restricted to booster stations, to main stations, or possibly to a single drive engine suitable for both. The desired goal might be a 20-percent decrease in natural gas consumed during transmission. Study limits might be the use of current state-of-the-art components and materials.

After the problem definitions are made, the analysis begins. The overall process is a continuous narrowing of choices or options. The potential cycles for a new drive engine, as discussed in the section CYCLE ANALYSIS, could include the open, closed, and semiclosed recuperated cycles. The cycle studies would be used to look at potential changes in specific fuel consumption, and some options might be dropped because of small gains. After the cycle studies, the best types of component geometry for each re-

maining engine option are selected.

The next step in figure V-22 is a system selection study with a PSOP. PSOP means Power System Optimization Program. With a PSOP, the lowest engine weight or volume or the cheapest engine to build is calculated over a range in design-point conditions. Cycle programs are used in PSOP as subprograms, and component sizing routines are added. Among these are recuperator codes, which by themselves could be helpful in retrofit studies. Compressor and turbine subprograms are also used to determine attainable efficiency and desired speed and staging.

These optimization codes can also be programmed to handle constraints. If, for example, the new drive engine must fit inside a boxcar, PSOP can be programmed to exclude those solutions which do not fit. However, PSOP is a special tool, and none of it has been published for general use. The Lewis staff has a lot of useful subprograms that can be used to assemble a PSOP for any particular application.

A system study conducted for a new compressor-station drive engine might provide results of the type indicated in figure V-23. Built-in repetitive calculations from two PSOP's, or optimization codes, generate the curves labelled engine type A and B. Engine first cost is plotted against design-point specific fuel consumption (SFC). For each type of engine, all possible solutions lie to the right and above these curves. Along the curves, therefore, are potential sets of design conditions yielding the least costly engine for each design fuel consumption. The analysis has not been done, and the relative results are unknown. But, type A might be the open cycle and type B might be the semiclosed cycle. In either case, the upswing in cost with low SFC would be mainly because of increasing recuperation.

These potential design conditions are next used as input to a system performance computer program (see fig. V-22). This step is often called an off-design study. The analytical turbomachinery performance maps are used here. In general, all component performance is described as functions of flow, temperature, pressure, and Reynolds number. For each operating condition, the performance program satisfies and balances flow, work, and speed. The output from the program in the example of figure V-23 would be engine gas consumption versus drive power available to the compressor station.

In figure V-23, engine type B has been sketched with a flat SFC charac-

teristic and type A with a sharp rise at low power. These effects are explained in figure V-24, where gas turbine operating characteristics are shown on the engine compressor map. The solid hooked lines show constant engine speed. The dashed line is the compressor stall limit. The open cycle operating point goes down and to the left on the operating line as shaft power and engine speed are decreased. It is this decrease in pressure ratio that causes the increase in fuel consumption indicated in figure V-23.

In contrast, the shaft output of the closed or semiclosed cycle can be controlled by changes in gas inventory rather than by speed. Its part-power operation is seen as a rather small region on the compressor map (fig. V-24). The operating point varies only a little with changes in ambient conditions or turbine-inlet temperature. All cycle conditions remain good and result in the relatively flat part-power curve.

Some system performance programs are directly available for general use. With one, an engine can almost be flown or driven. The cycle computer programs and the performance programs, together, could be used to evaluate existing engines. After the system studies, designers can make detailed layouts for the engines. Then, final decision points can be reached through use calculations - duty cycle, consideration of emissions, and economic impact.

A hypothetical compressor-station duty cycle is sketched at the lower left side in figure V-23. The engine gas consumption would be taken over the needed range of drive power and over some average daily use cycle. Then it would be summed as one of the operating costs. Based on experience for other similar engines, maintenance costs and the useful life of the engine would be evaluated. Finally, consideration of financing and amortization would result in an annual total cost for the drive engines.

Columns A_1, A_2, and A_3 in figure V-23 represent three potential design points on the first curve for engine type A. A_1 is shown as the least costly for engine type A. B_1 would be the least costly for type B. As a result of this type of evaluation, which might include some new engines along with some existing engines, a basis for a decision on whether to buy or build would be established.

SEALS

An approach to improving engine performance and life is through the development of new or improved sealing practices. In general, there are two main types of seals throughout the engine. They are the primary gas path seals and main shaft seals. With higher temperatures, pressures, and speeds predicted for the next generation gas turbine engine, improvement in either current sealing practices or entirely new seal concepts will be required. This discussion, however, will be limited to shaft seal concepts that have been developed for both gaseous and liquid environments.

Gas-Film Seals

By way of introduction to the first seal concept, figures V-25 and V-26 show some typical shaft seal configurations currently used in the gas turbine engine. In this seal application, the seal or seal system is designed to limit the leakage of the hot compressor discharge gas into the oil sump and bearing compartment.

Figure V-25 shows a conventional face contact seal. It consists of a primary ring made up of a metal retainer and carbon nosepiece, a piston ring or secondary seal that is used for balancing, compression springs that ensure sealing during shutdown, and the rotating seat. This design depends upon rubbing contact for sealing during rotation. Consequently, the seal is subject to continuous wear and does impose an additional horsepower requirement on the engine.

The labyrinth seal system, figure V-26, on the other hand, requires less horsepower because of the clearance between the shaft and the knife edges. It does, however, allow more leakage into the sump and this results in increased degradation and consumption of the oil. When excessive degradation or loss of oil occurs, the incidence of early bearing failures and maintenance costs both increase.

The seal concept that has been developed by Lewis, under contract, for this application is somewhat of a combination of both. It is similar to a rubbing contact seal but operates as a very close clearance labyrinth. It is called a self-acting seal concept and is shown in figure V-27. The similarity

to the rubbing contact seal is apparent, the primary ring, the piston ring, and the compression springs being common to both. Note, however, the separation or gap between the primary ring and the rotating seat. This separation is produced and maintained during rotation by a self-generating life geometry called the shrouded Rayleigh step pad.

Details of the self-acting geometry are shown in figure V-28. Starting at the inside diameter, the important features are (1) the recessed pad area (0.0005 to 0.001 in. deep), (2) the shrouds, or rails, (3) radial feed grooves, (4) a circumferential groove, and (5) the dam at the outer diameter. During rotation of the seat, the high pressure gas is dragged into the pad and is compressed as it passes over the 0.001-inch step at the end of the pad. This creates a lifting action or force that separates the primary seal ring and the rotating seat. The lift force that is generated is on the order of 1 to 2 pounds per pad, depending upon the recess pad depth and speed of the rotating seat. Balancing of the seal, by selective positioning of the piston ring and proper spring compression, allows this small generated lift force to maintain positive separation. Seals of this type are designed to operate at clearances of 0.0002 to 0.0004 inch. This clearance is less than one-tenth that associated with labyrinth seals.

The lift force generated by the pad is also strongly dependent upon the clearance. The smaller the clearance, the greater the lift force that can be generated. As a consequence, increases in the ambient pressure that would tend to reduce the clearance result in increases in the lift force that moves the primary ring away from the seat to a new operating position. During shutdown, or periods of nonrotation, the primary ring is held in contact with the seat by the compression springs ensuring positive sealing.

Performance of this seal concept, based on seal leakage, is compared to the performance of a labyrinth seal and a conventional face seal in figure V-29. These data are for $2\frac{1}{2}$-inch-diameter seals operating at 600 ft/sec and at an air temperature of 300° F. The figure indicates that the range of leakages for the currently used seals is substantially higher than that measured for the self-acting face seal. The higher leakage of the conventional rubbing contact seal is attributed to intermittent face separation caused by distortion of the rotating seat and shaft dynamics. These distortions are the result of both thermal and pressure gradients inherent in most seal applications.

Additional testing, under contract, of a 6-inch-diameter seal demon-

strated successful operation at speeds to 500 ft/sec, pressure differentials to 500 psi, and temperatures to 1000° F. Seal wear after 500 hours of testing was negligible.

The same shrouded Rayleigh step pad has also been utilized in the design of a shaft riding seal shown in figure V-30. Shown in this schematic is a shaft riding or circumferential seal consisting of two segmented rings. Each ring is made up of three segments that overlap one another as shown at the left. These segments are held together around the shaft by the garter spring. The shrouded Rayleigh step pad has been machined into the bore of the rings. For this type of seal, sealing takes place between the bore, or inner diameter, of the rings and the outer diameter of the rotating shaft. As balancing of the rings is limited, the pressure differential capability is also limited to pressures of 75 psi or less. Testing done under contract has shown that pressure differentials of 35 psi were attainable at speeds of 600 ft/sec and temperatures of 300° F. This far exceeds the speed capability of similar shaft riding seals operating at similar pressures and temperatures.

Seals using this self-acting concept are being considered for the high pressure liquid oxygen turbopump for the Space Shuttle engines. The face seal design will be used as the primary liquid oxygen seal. The segmented shaft seal design will be used as the helium buffer seal that prevents mixing of the liquid oxygen and the hot hydrogen gas driving the turbine. Favorable testing of these turbopump seals could result in their application in all future cryogenic pumping facilities.

Liquid-Film Seals

The preceding seal concepts, the face seal and the shaft riding seal, are designated gas-film riding seals. Separation of the sealing surfaces is maintained by a thin gas film. The shaft seal concepts to be discussed now are designated liquid-film seals. These concepts are used for such viscous liquids as water, hydraulic oil, and liquid metals.

The first of these, shown in figure V-31, is the helical groove seal, or viscoseal. This seal utilizes the pumping action generated within the grooves while the shaft is rotating to establish a liquid-gas interface. This schematic shows the helical grooves machined into the housing with the shaft being

smooth. The operating clearance between the housing bore and rotating shaft is based on 0.001 inch per inch of shaft diameter. The length-to-diameter ratio, for most applications, has been near 2 to 1. Experimental studies have indicated similar performance can be achieved with the grooves machined onto the shaft and the housing smooth.

The second liquid-film seal concept is the spiral-groove seal, shown in figure V-32. Spiral grooves, approximately 0.002 inch deep, are machined or chemically etched into the nonrotating nose. An orifice is drilled so that the high pressure fluid is allowed to flow into the spirals. This flow, or circulation, helps to dissipate the heat that is generated in shearing of the oil. Because of the motion of the rotating seat, the fluid is pumped outward, and the pressure increases as the fluid passes over the dam. Selective seal balancing, again, permits the small self-generated lift action to separate the sealing surfaces.

Experimental testing of these two liquid-film seal concepts in water, hydraulic oil, and liquid metals showed that acceptable leakages were maintained at temperatures of 250^{o} F and pressure differentials to 200 psi. The maximum rotative speed achieved during these tests was 10 000 rpm. The horsepower requirements for these liquid-film seals are greater than for the gas-film seals.

These two liquid-film concepts are currently being considered for use in the Space Shuttle hydraulic pumps. In this application, we are attempting to prevent leakage of the hydraulic fluid out of the pump and into areas under vacuum within the vehicle. Fluid vaporization and subsequent deposition on any electrical parts could be detrimental.

The preceding seal concepts, both the gaseous- and liquid-film concepts, have been developed primarily to meet particular needs of aeronautical and space applications. However, there is no reason why they cannot also be used for an industrial gas compressor. Figure V-33 shows schematically the high pressure oil buffer seal that is, for the most part, current practice in the industry. Figure V-34 is representative of the costly and complex oil lubrication system consisting of pumps, separators, and plumbing required for this type of seal.

In the seal system shown in figure V-33, high pressure oil is introduced between the bushing seals and allowed to flow along the shaft in both directions. Oil flow toward the journal bearing is returned to the reservoir. Oil

flow toward the compressor, however, mixes with the high pressure gas and must pass into a separator, if either the gas or the oil is to be salvaged.

A simplified seal system that utilizes some advanced seal concepts is shown in figure V-35. Here, the self-acting face seal provides sealing of the high pressure compressor gas. The pumping action of the viscoseal, at the left, restricts the flow of oil from the journal bearing toward the compressor. During periods of shutdown or nonrotation, when it is desirable to maintain system pressure, the face seal closes down because of selective balancing and makes a positive seal.

Another seal system, shown in figure V-36, that would also reduce the complexity of the high pressure oil buffer system utilizes some of the other advanced seal concepts that were presented. On the left, a spiral-groove face seal in combination with the viscoseal prevents flow of oil from the journal bearing toward the compressor. On the right, the majority of the gas flow through the labyrinth is returned to the compressor at a reduced pressure. This reduced pressure permits the use of the segmented circumferential seal and minimizes leakage out the vent. Positive sealing at shutdown is accomplished both by the segmented seal and the spiral groove.

From a conceptual point of view it appears that the use of these advanced seal concepts is feasible for an industrial gas compressor. The two seal systems shown, however, have not been analyzed and are, therefore, not to be considered as working designs. If after in-depth analysis and evaluation seal systems using these advanced concepts prove sound, the choice is that of the potential user. Based on high initial installation costs, maintenance costs, and complexity of the current high pressure oil buffer system, serious consideration should be given to the use of these advanced seal concepts in the compressor as well as in the gas turbine engine driving the compressor.

BEARINGS

There are four areas of bearing technology that will be discussed. These are flexible rotor balancing, fixed-geometry fluid-film bearings, foil bearings, and rolling-element bearings.

Flexible Rotor Balancing

A shaft, or rotor, is usually designed to be rigid, that is, not to bend as the speed or rotation is increased to the operating speed. A mass unbalance in the system, however, can cause the shaft to vibrate very badly at certain speeds. So, the system is usually balanced at a relatively low speed using a normal two-plane balance technique as indicated in figure V-37. This is a sketch of a rotor with an unbalance at the center. With balance planes at the ends, weights added on the opposite side, as indicated, would balance the system satisfactorily.

However, there are a number of reasons, such as a long distance between supporting bearings, that could cause a rotor to be flexible. A flexible shaft will bend as the rotative speed is increased to the operating speed. Flexible rotors are used in powerplant steam turbines and in an advanced technology helicopter turbine engines. This bending can result in considerable damage.

With a flexible rotor, normal two-plane balancing is no longer adequate, as illustrated in figure V-38, which shows a flexible rotor in the first bending mode. (The bending is slightly exaggerated.) If the rotor had been balanced in two planes, as before, the balance weights would no longer help, but would be detrimental. The reason is that, as the shaft speed approaches the critical speed (the speed at which bending occurs), the centrifugal force from the unbalanced mass causes the shaft to bend, and the centifugal force from the balance weights cause it to bend even farther.

A technique developed for balancing flexible rotors is called multiple-plane balancing. The technique requires that proximity probes be used to measure the radial movement of the rotor and that several balance planes be chosen where weights can be added or removed, as indicated in figure V-39. This is a sketch of a rotor with five locations for the proximity probes and four balance planes. A trial weight is added at the first balance plane. The shaft is rotated and data are taken. The trial weight is then moved to the next balance plane and the process is repeated until this is done for all the balance planes. All of this information is then input to a computer program. The program, by determining the influence that the trial weight has on the rotor excursions, computes where to add or remove weight and how much.

The results of using this program on a special test rotor are shown in

figure V-40, which is a plot of rotor amplitude against rotor speed for the probe station that registered the largest amplitude. Note the rapid rise in amplitude of the unbalanced rotor as the speed approached the first bending critical speed. After a first balancing run was made and the weight removed as calculated, the rotor was operated again. After the first balance, the rotor was able to pass through the first critical speed with a reduced rotor amplitude, but the amplitude again increased as the rotor approached a second bending critical speed. After a second balancing run was made, the rotor amplitude was greatly reduced at the first critical speed, but still was large at the second critical speed. After a third balancing run, the rotor was actually able to pass through and operate above the second bending critical speed. Depending on the amount of unbalance, one balancing run is normally required for each bending critical speed.

The advantages of multiple-plane balancing are (1) it allows operation above the first bending critical speed; (2) it allows balancing in the field, as the proximity probes can be brought to the machine; (3) it allows a relaxation of balance-related tolerances (for example, shaft concentricity and straightness); and (4) it can result in significant cost savings. When a study was made that applied this technique to a 1500-horsepower advanced turbine engine, the projected cost savings amounted to a least $500 per engine, or a total of $3,000,000 over the life of the program.

Fixed-Geometry Fluid-Film Bearings

Often, the first choice in bearings when machinery is designed is the familiar hydrodynamic fluid-film bearing, sometimes called a journal bearing. A typical plain journal bearing is shown in figure V-41. As the shaft rotates, a wedge-shaped film of fluid is created that separates the surfaces and supports the load. The clearance between the shaft and the bearing is shown exaggerated for clarity. In actual use, these clearances are quite small (on the order of 0.001 inch per inch of diameter).

These bearings are inexpensive and usually last a very long time. However, there can be problems. First, there can be a very large power loss in these bearings as the sliding velocity increases. And second, if the bearings are lightly loaded, they can become unstable at higher speeds with what is

known as half-frequency whirl. This is where the shaft orbits around in the bearing at about one-half the shaft speed. Whirl can cause large shaft excursions and result in appreciable damage to the bearing.

If power loss is a problem, a rolling-element bearing will probably be used. If stability is a problem, a tilting-pad-type bearing, such as shown in figure V-42, can be used. This is a three-pad bearing with each pad able to "tilt" or pivot about a fixed point. A converging wedge of fluid is formed at each pad. This provides a restoring force and the bearing operation remains stable. However, these bearings are somewhat complex and are usually fairly expensive.

Therefore, several less-expensive fixed-geometry bearing concepts were tested for stability. The results for three of them are shown in figure V-43, which is a plot of whirl onset speed against radial clearance of the bearing. Since whirl onset speed denotes the onset of instability, stable operation of the bearing occurs in the area below each curve. Unstable operation would then be in the areas above each curve.

For a centrally lobed bearing, shown in figure V-44, stability is lost rapidly as the clearance is increased. The bearing is called lobed because the radii are slightly larger than the shaft and offset. It is called centrally lobed because the minimum fluid-film thickness, with the shaft centered in the bearing, is at the center of the sector. This forms a converging film for half of each sector.

A somewhat better design, as indicated by the larger area of stable operation in figure V-43, is the familiar Rayleigh step bearing shown in figure V-45. This version has three pads and each pad has a feed groove, a step region, and a ridge region.

As shown by the top curve in figure V-43, the tilted-lobe bearing, shown in figure V-46, demonstrated the best stability over the clearance range tested. Again, it is called lobed, as the radii of the bearing are offset. It is called tilted because the minimum film thickness is other than at the center. This design is called wholly converging because that minimum film occurs at the trailing edge of each sector.

The importance of these special bearings can be summarized as follows: (1) they allow stable operation; (2) they are less complicated than the tilting-pad bearing; and (3) they can be inexpensive. So, if whirl is a possible problem, perhaps it can be solved with an inexpensive fixed-geometry bearing.

Foil Bearings

Gas bearings are sometimes used to eliminate seals or the complexity of a lubrication system. This is accomplished by utilizing the ambient or process gas in the bearing itself. In this way, a separate oil system is not required, and a seal between the bearing and the process gas is unnecessary. However, gas bearings are usually rather expensive; they require tight tolerances and must operate in a very clean atmosphere.

A recent concept, however, called a foil bearing, is far less expensive. This concept has been developed for use on small machinery. The foil bearing is a gas bearing made of thin flexible strips of metal as the bearing surfaces. These bearings are self-acting; that is, they generate their own pressure. They can support about 25 psi maximum load at atmospheric pressure. There are three designs that will be discussed.

The tension foil bearing is shown in figure V-47. This bearing is formed from one continuous strip of foil. The strip is wound around the mounting pins and then pulled tight with the tension device, thus forming in this case, a three-section bearing. The work on this bearing was done at Ampex under NASA sponsorship. It has been applied to a NASA 10-kilowatt power system as a backup bearing.

A second concept is the overlapping cantilevered foil bearing, also called a leaf foil bearing, shown in figure V-48. Each leaf foil is attached to the retainer ring and the foils overlap. The clearance is exaggerated for clarity. This design was developed by Garrett-AiResearch and is being used on a small Brayton cycle space power system. It has also been used on air cycle machines, for example, for cabin cooling air for the DC-10 and the 727.

There are several other foil bearing designs available. One of them, called a bump foil, is being developed by Mechanical Technology Inc. for use in an automotive gas turbine.

In summary, the advantages of foil bearings are (1) they are less expensive than standard machined gas bearings; (2) they are more forgiving of dirt particles and can, therefore, be used in a "less clean" atmosphere; (3) they operate stably and, therefore, allow high-speed operation; and (4) they can eliminate the complexity of a lubrication system.

Rolling-Element Bearings

The ball bearing and the roller bearing have very low power loss, and that is a very large advantage over other types of bearings. That is one of the main reasons rolling-element bearings are used in aircraft turbine engines. As an example of a rolling-element bearing, a typical ball bearing is shown in figure V-49. This is an angular-contact split-inner-race bearing.

The operating life of rolling-element bearings is limited only by material fatigue if the bearing is properly designed and lubricated. The term "material fatigue" can be defined as a cyclic stress phenomenon where repeated loading and unloading cause a crack to initiate in the material. This crack propagates to the surface, material breaks off, and a fatigue spall forms as shown on an inner race in figure V-50. The bearing can still run for a while, but with much noise and vibration.

Many factors influence the fatigue life of rolling-element bearings. Identification of some of these factors has resulted in a dramatic improvement in fatigue life in recent years, as shown by figure V-51. Plotted is the history of fatigue life improvement over the last 30 years. The history starts in the 1940's, when standard formulas were first presented that could successfully correlate predicted fatigue lives with the actual test results. The bearing steel at that time was air melted. These standards were accepted by the Anti-Friction Bearing Manufacturers Association (AFBMA) and are still in use today. The values of fatigue life predicted by these formulas are often called the AFBMA values. On this chart, then, the AFBMA values are the base values and have a relative life of 1.

In the 1950's, as the bearing material gradually improved, the resulting fatigue lives became longer than the AFBMA values. By 1962, after the process known as CEVM (consumable electrode vacuum melt) was established, fatigue lives were increased to five times the AFBMA value. The aircraft industry, today, uses this life improvement factor of 5 in their calculations.

Research during the 1960's showed all the items listed in figure V-51 to be important influences on fatigue life. In general, the better the control of hardness of the balls and races, the longer the life. Better surface finishes tended to result in longer lives. Different lubricants could change the results of fatigue tests. It was long ago noted that forged races lasted longer than

races made from a tube of material, the difference being fiber orientation. In 1968, full-scale bearings were made utilizing all the latest technology available. These 120-millimeter-bore bearings, which were the size and type shown in figure V-49, were tested at 12 000 rpm. The fatigue lives obtained were 13 times the AFBMA value.

With a requirement for higher speed bearings being recognized, plans were made to test full-scale bearings again starting in 1974. These bearings have all the latest technology but are being tested at a higher speed. This time it is 25 000 rpm. The only significant difference, besides the test speed, is that these latest bearings were made with a VIMVAR (vacuum induction melt, vacuum arc remelt) material process. The tests, being run at 425° F, are not complete, but early indications are that the fatigue lives are going to be 80 to 100 times the AFBMA value.

In summary, rolling-element bearings have low power loss; and improved material, design, and manufacturing techniques have dramatically increased bearing life and reliability. It now appears that very long lives are possible. A rolling-element bearing may, with care in design and manufacturing, last as long as needed and provide a noticeable savings in friction power loss.

EMISSIONS

The Environmental Protection Agency is presently preparing a set of standards to regulate the level of pollutant emissions from stationary gas turbine engines. These standards are expected to be formally published near the end of 1975. The standards as presently conceived are shown in the following table together with the pollutant levels from natural gas fueled stationary gas turbine engines in the 1000 shaft horsepower size and in the 9000 to 20 000 shaft horsepower range. At present, only two pollutants are regulated. These are the oxides of nitrogen NO and NO_2, commonly referred to as NO_x, and carbon monoxide, CO. The proposed standard values are given in parts per million by volume and are referenced to an oxygen concentration in the exhaust of 15 percent. The engine pollutant values given in the table were obtained from reference 1 and have been adjusted to an oxygen level of 15 percent. All of the engines tested in reference 1 had a higher

POLLUTANT	ENGINE EMISSIONS, PPMV		EPA STANDARD, PPMV
	1000 HP	9 000-20 000 HP	
NO_x	~45	46-130	55
CO	40-60	5-50	90

level of oxygen in their exhaust than the 15 percent level required by the EPA standard. Thus, since less fuel was consumed than allowed for by the standard, the rule requires that less NO_x be present in the exhaust. Some of the engines tested complied with the standard, but most did not, and some form of NO_x emission control must be applied.

As far as carbon monoxide emissions are concerned, all of the engines tested complied with the EPA standard. This is not a surprising result. The combustion efficiency of gas turbine engines is virtually 100 percent at all power levels except for those at or near engine idle. Therefore, no emission control techniques for carbon monoxide emissions are required.

The NO_x emissions from these engines, as mentioned previously, do have to be controlled. The NO_x is formed in the hottest portion of the combustion zone. There, small quantities of nitrogen in the air react with oxygen to produce the NO and NO_2. There are many factors that affect the rate of formation of NO_x in combustors, but the most important parameter is the local flame temperature within the primary zone of the combustor.

Figure V-52 illustrates the strong dependance of NO_x concentration on the local flame temperature. The curve shown is calculated from a chemical kinetics computer program for realistic values of combustor operating conditions. The assumed operating conditions were an inlet total pressure of $5\frac{1}{2}$ atmospheres, an inlet-air temperature of 620° F, and a residence time of 2 milliseconds for the gases in the hottest portion of the flame zone. Values of NO_x computed at chemical equilibrium would be up to two orders of magnitude greater than the values shown. Note that changes in the local flame temperature of as little as 100° F can significantly affect the level of NO_x emissions.

The localized flame temperature can be reduced in several ways. The use of a diluent can significantly affect flame temperature. Both water and steam injection have been used in the past to lower flame temperature. These diluents act to absorb heat of combustion with resulting reduction in the maximum level of temperature that can be reached. Water, of course, is more effective than steam as additional heat is removed just to vaporize the water. The use of these two diluents has been well documented, and the NO_x standards can be met by this technique. The application of this "wet control" technique is at present the only way to meet the EPA standard. The disadvantage of this approach is that the water must be demineralized to prevent the buildup of boiler scale deposits within the engine. The amount of water used varies with the degree of NO_x reduction required, and water flow rates up to an amount equal to the fuel flow rate have been reported. Typical data indicate that a 55 percent reduction in NO_x is possible at a water-fuel ratio of 1/2.

Exhaust gas recirculation is another technique that can be used to dilute the combustion air. This technique is probably more applicable to fully recuperated gas turbine engine applications, as the recirculated gases must be cooled to near ambient temperature levels before recompression.

The most desirable approach to NO_x emission control would be a "dry control", which is a control achieved by modification of the combustion chamber. The technique proposed here is the use of premixed fuel and air. Figure V-53 shows a schematic representation of two different fuel injection techniques. The conventional fuel injector injects natural gas fuel into the combustor as a spray or a jet from a nozzle. Combustion air is admitted through the swirler surrounding the nozzle and through air admission holes in the combustor. Fuel injected in this manner produces a wide distribution of local fuel-air ratios in the primary burning zone. By contrast, the premixed fuel injector has virtually complete uniformity of fuel-air composition in the primary zone. This is achieved by intimately mixing the fuel and the primary combustion air prior to injection into the combustor.

Figure V-54 illustrates how NO_x emission levels can be lowered by use of premixed fuel injection techniques. This figure shows the relative rates of NO_x formation for both conventional and premixed injection as functions of the mean fuel-air equivalence ratio. The equivalence ratio is defined as the ratio of the local fuel-air ratio to the fuel-air ratio for stoichiometric com-

bustion. The two curves illustrate the differences between the rates of NO_x formation for premixed and conventional fuel injection. At values of the equivalence ratio below 0.8, substantial reductions in NO_x are achievable. However, with conventional injection, variation in mean equivalence ratio in the primary zone will have only a slight effect on NO_x formation. This is due to the wide distribution in local fuel-air ratios produced by conventional fuel injection techniques.

Figure V-55 shows results of premixed combustion tests using propane fuel compared to a perfectly stirred reactor prediction for propane and natural gas. The oxides of nitrogen concentration in parts per million are shown plotted against the mean fuel-air equivalence ratio. The data and the theory for propane fuel are in very good agreement except at the highest values of equivalence ratio. These tests have not been done using natural gas fuel so the theoretical prediction will be used to illustrate the point. Note that at constant equivalence ratio, less NO_x is produced with natural gas than with propane. This is a flame temperature effect. Natural gas has a lower flame temperature than propane and significantly less NO_x is produced at the same equivalence ratio. Also shown in this figure is the NO_x level required to meet the EPA standard of 55 ppm. These experiments indicate that, if the primary zone was operated near or below an equivalence ratio of 0.8, then the NO_x standard could be achieved. This approach would require a redesign of the front end of existing gas turbine engine combustion chambers and, as such, would not be available on future engines for some time. It is, however, our belief that the EPA standard can be achieved by a dry control technique such as this premixed combustor approach.

In summary, it appears that water injection will probably be used to control NO_x emissions for the near term, but we feel that future engines incorporating premixed fuel injection can be made available and that compliance with EPA standards can be achieved.

CONCLUDING REMARKS

The material presented herein describes the analytical tools and experimental data bases that can be used in the definition of gas turbine engine systems for natural gas transmission. The steps of cycle studies, component

selection, off-design system studies, and then some considerations in the design of the bearings, seals, and combustor have been examined. Use of these computer programs and design approaches can result in sizeable fuel savings in natural gas systems.

REFERENCE

1. Dietzmann, Harry E.; and Springer, Karl J.: Exhaust Emissions from Piston and Gas Turbine Engines Used in Natural Gas Transmission. AR-923 Southwest Research Institute, San Antonio, Texas, January 1974.

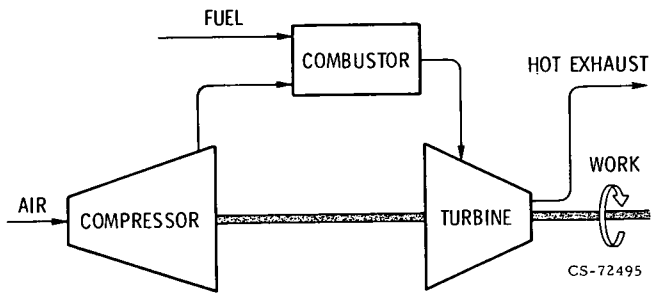

Figure V-1. - Simple open cycle.

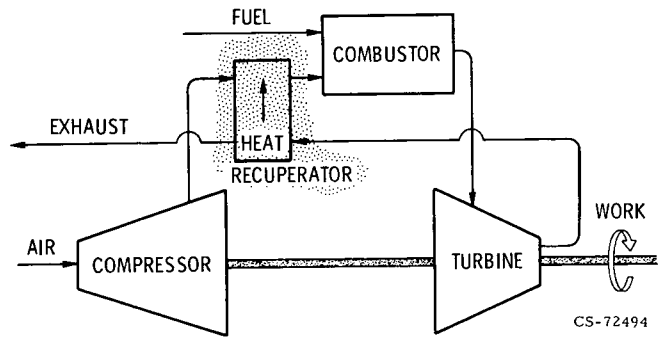

Figure V-2. - Recuperated open cycle.

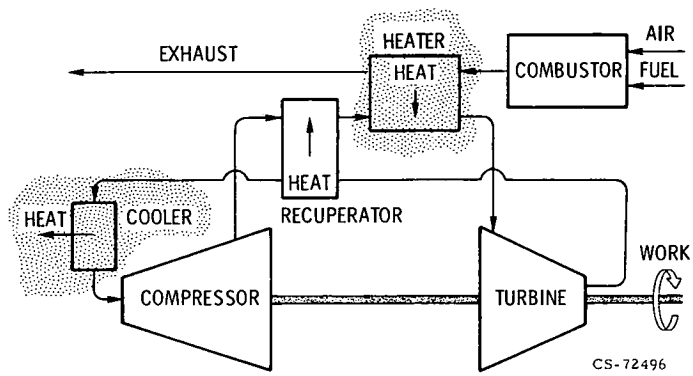

Figure V-3. - Recuperated closed cycle.

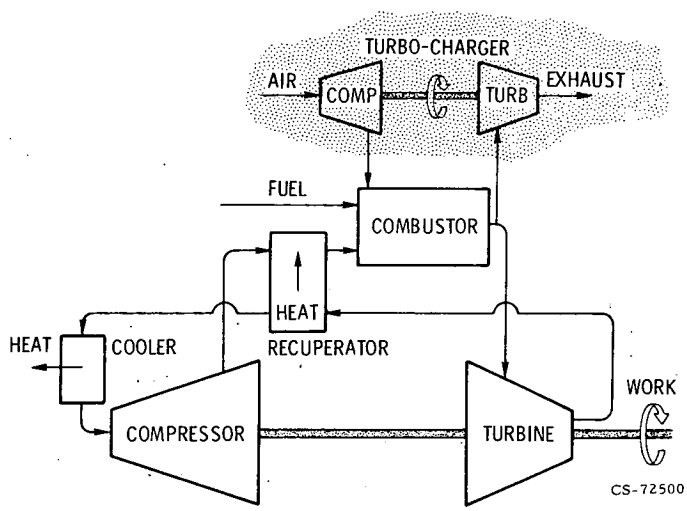

Figure V-4. - Semiclosed recuperated cycle.

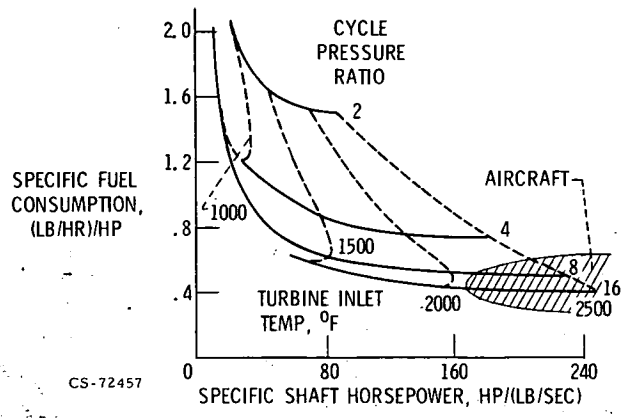

Figure V-5. - Unrecuperated open Brayton cycle performance.

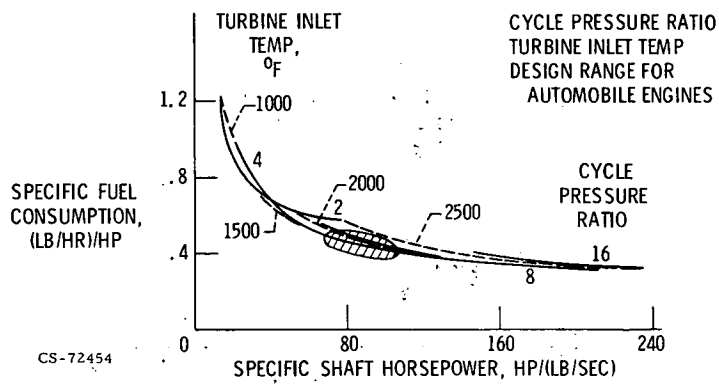

Figure V-6. - Recuperated open Brayton cycle performance.

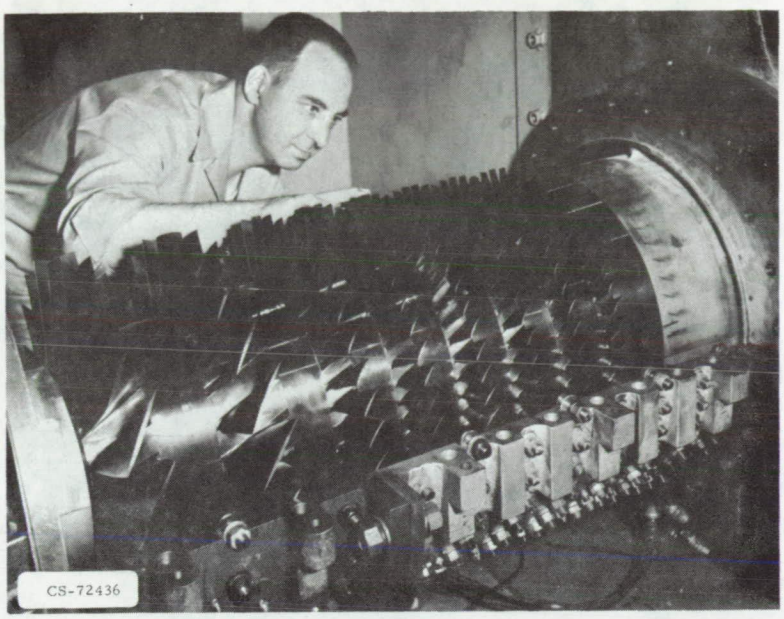

Figure V-7. - Axial-flow research compressor. Peak efficiency, 87.5 percent.

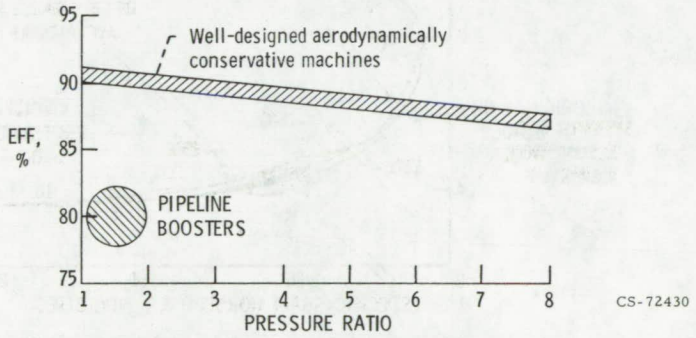

Figure V-8. - Maximum efficiencies of axial compressors.

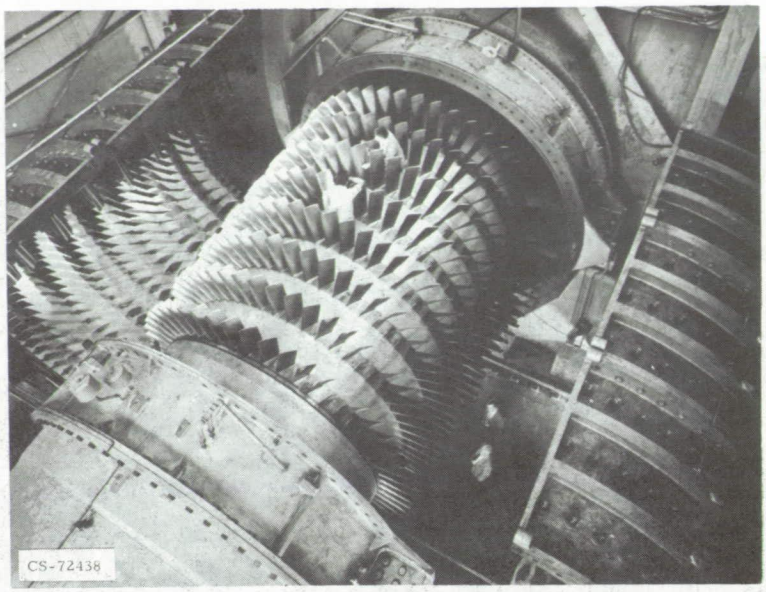

Figure V-9. - 20-Foot-diameter compressor. Peak efficiency, 90 percent.

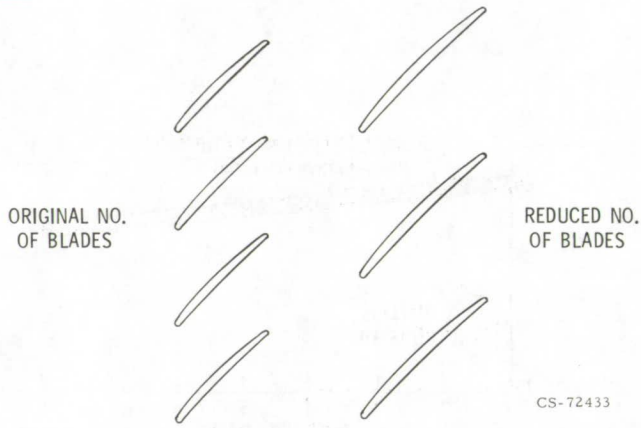

Figure V-10. - Blade comparison for cost reduction.

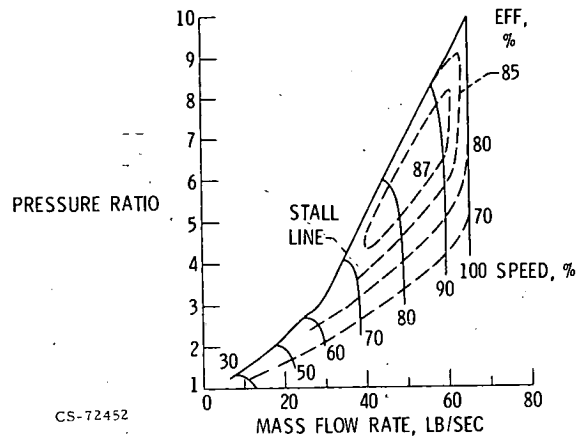

Figure V-11. - Axial compressor performance map.

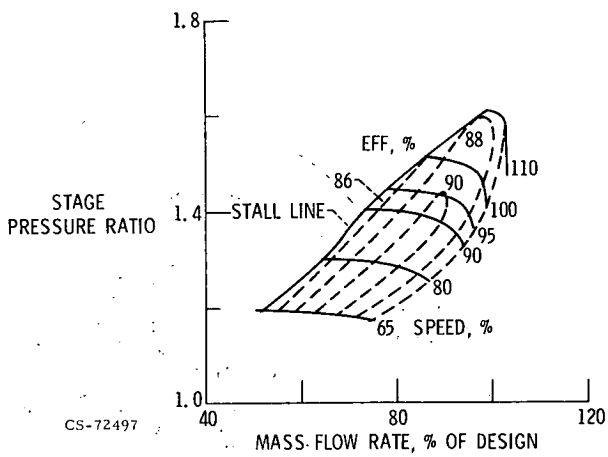

Figure V-12. - Single-stage axial compressor performance.

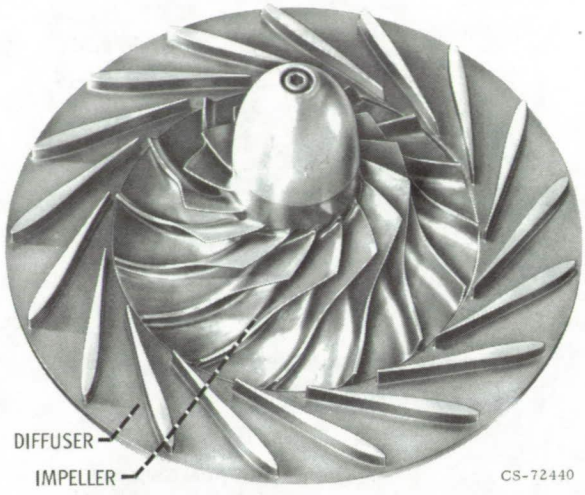

Figure V-13. - Centrifugal compressor.

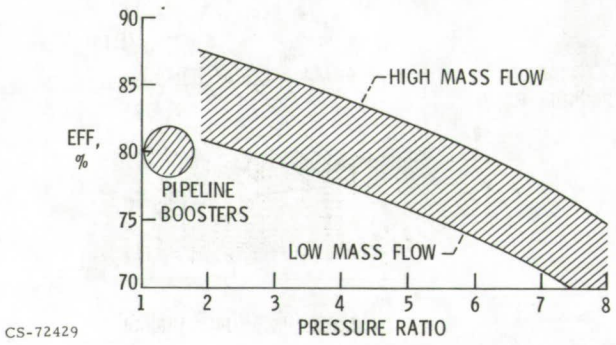

Figure V-14. - Maximum efficiencies of centrifugal compressors.

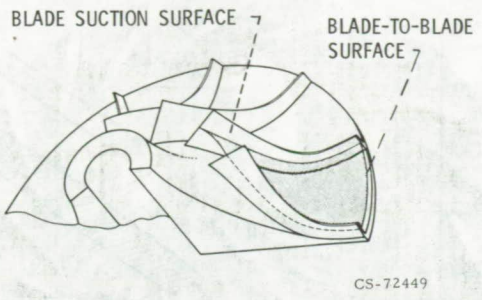

Figure V-15. - Centrifugal compressor blade-to-blade surface.

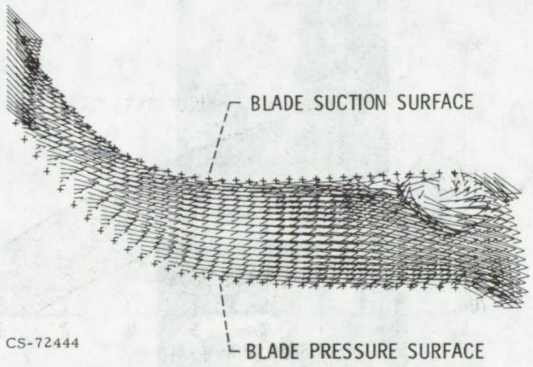

Figure V-16. - Computer velocity vector plot on blade-to-blade surface.

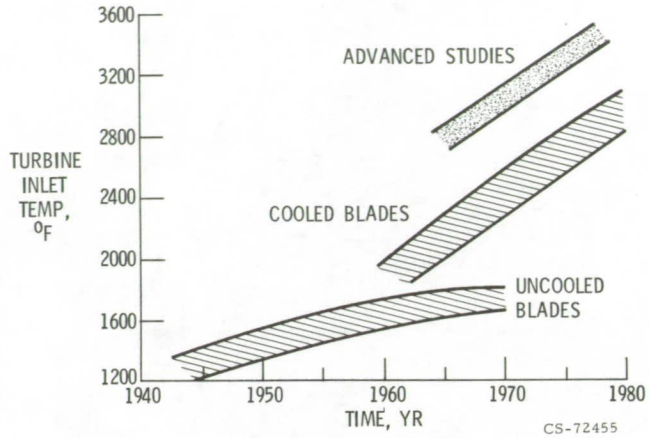

Figure V-17. - Turbine temperature trends.

VANE

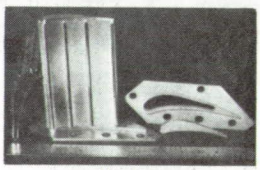

INSERT CS-72437

Figure V-18. - Cooled turbine vane.

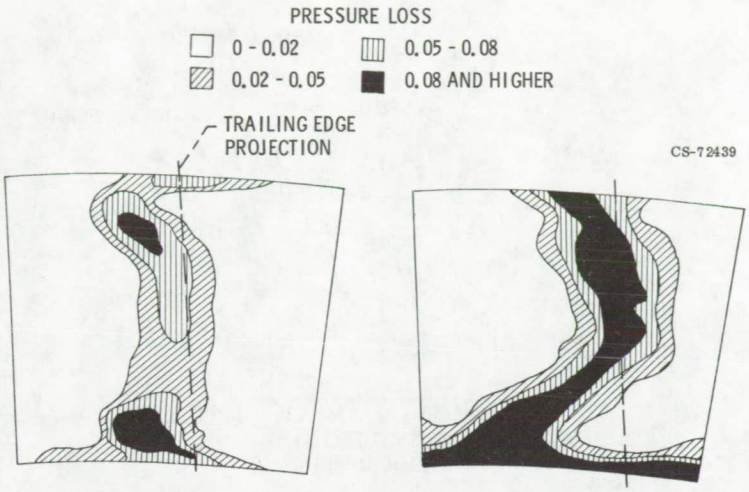

(a) Solid vane; efficiency, 0.96. (b) Cooled vane; efficiency, 0.92.

Figure V-19. - Vane exit surveys.

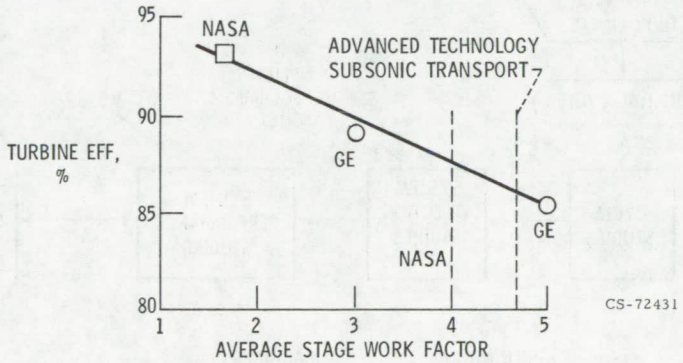

Figure V-20. - Multistage turbine efficiencies.

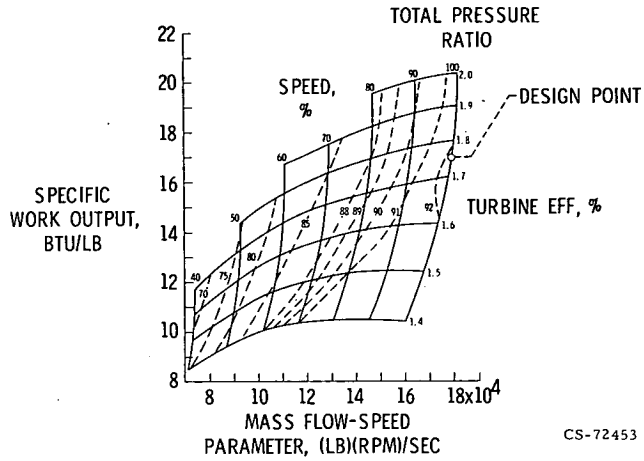

Figure V-21. - Turbine performance map.

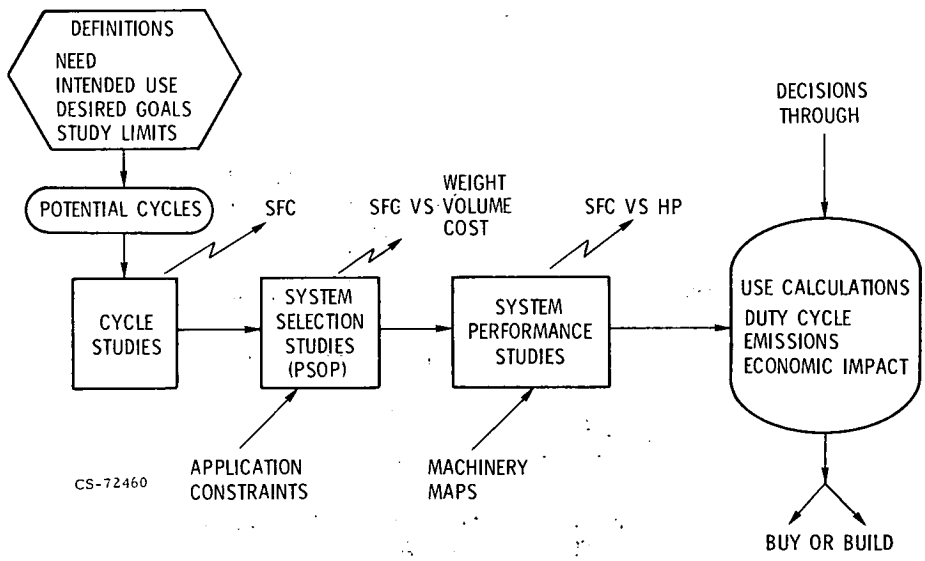

Figure V-22. - Generalized system study approach.

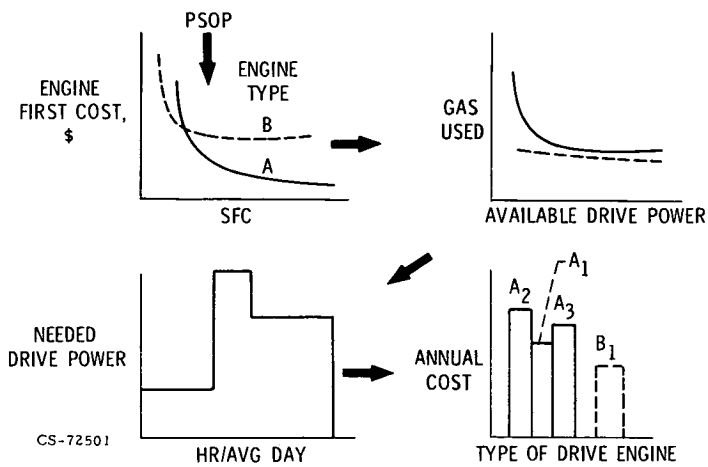

Figure V-23. - System study for new compressor station drive engines.

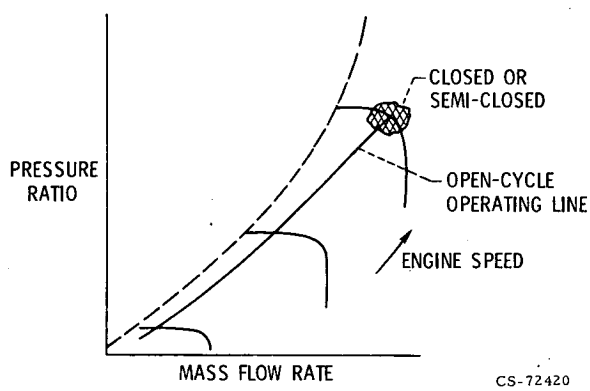

Figure V-24. - Gas turbine operating characteristics on engine compressor map.

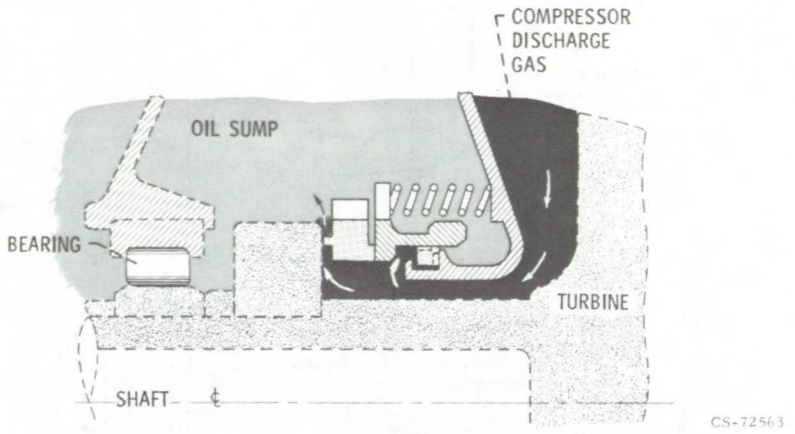

Figure V-25. - Face contact seal (main shaft seal application).

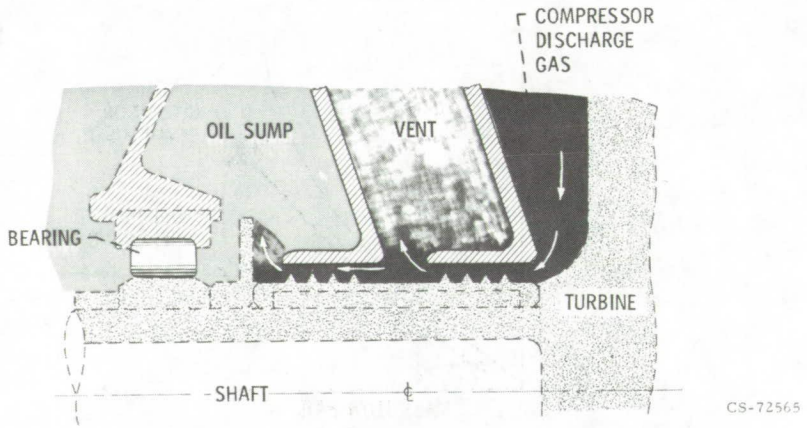

Figure V-26. - Labyrinth seal (main shaft seal application).

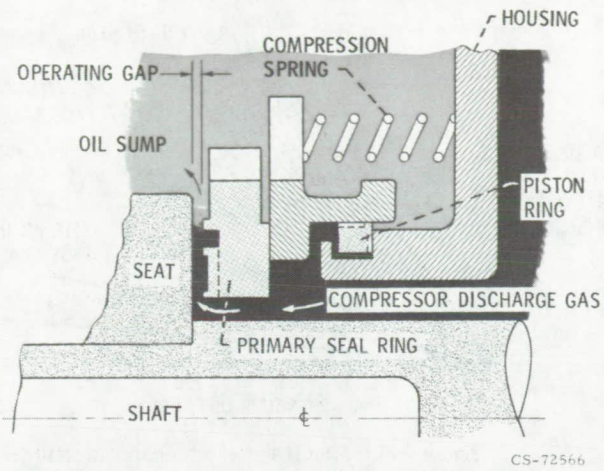

Figure V-27. - Self-acting face seal showing shrouded Rayleigh step-pad design.

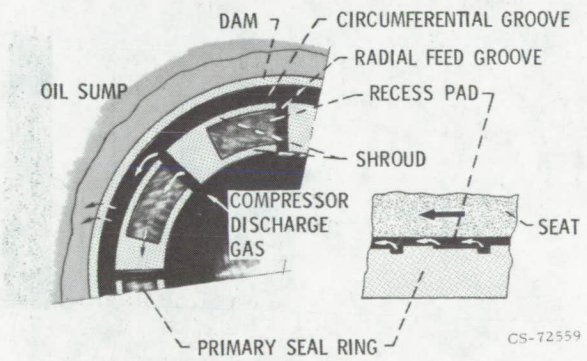

Figure V-28. - Shrouded Rayleigh step pad.

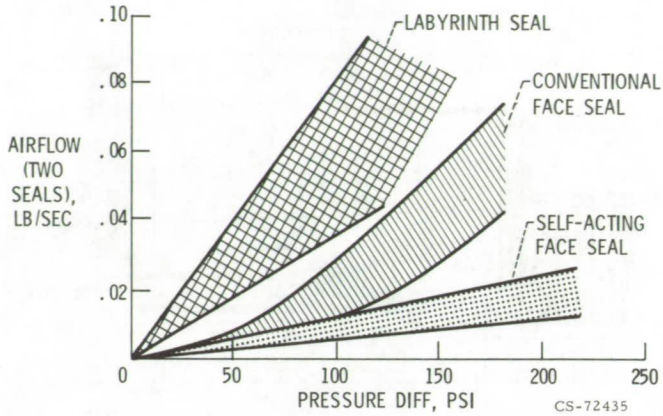

Figure V-29. - Main shaft seal performance in small gas turbine eninge.

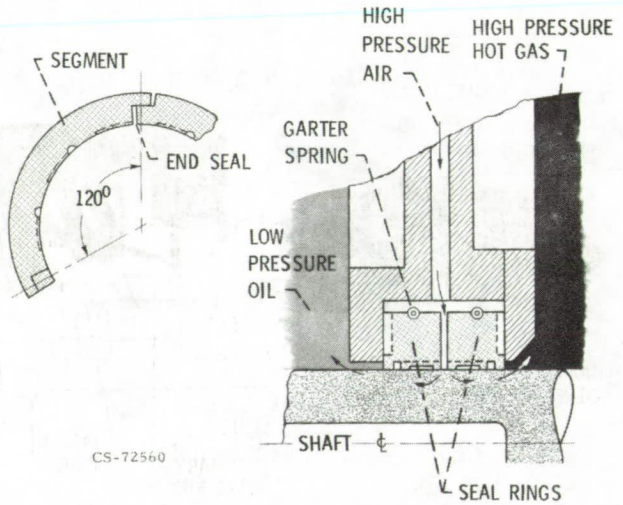

Figure V-30. - Self-acting circumferential seal (segmented ring design).

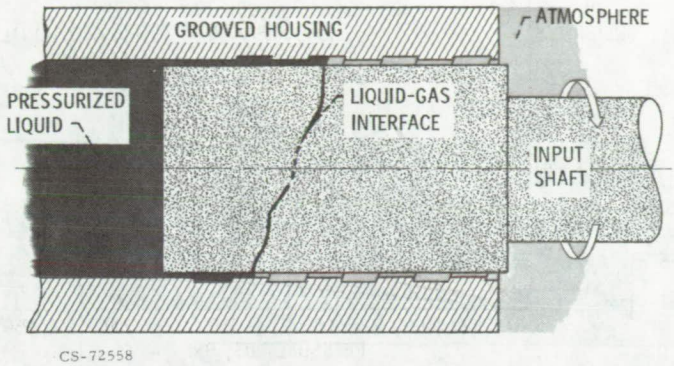

Figure V-31. - Helical-groove liquid-film seal or viscoseal.

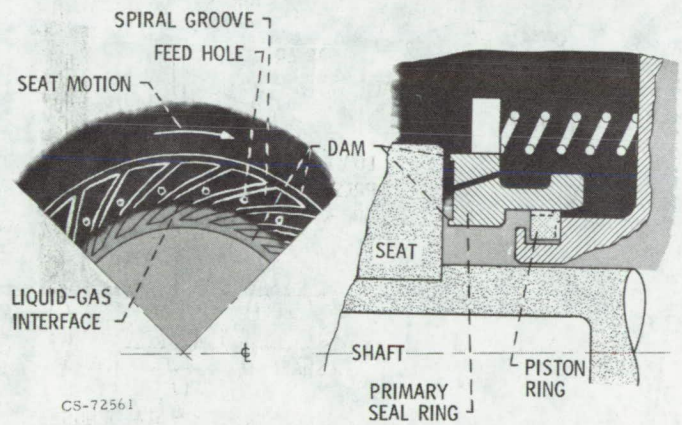

Figure V-32. - Spiral-groove liquid-film seal.

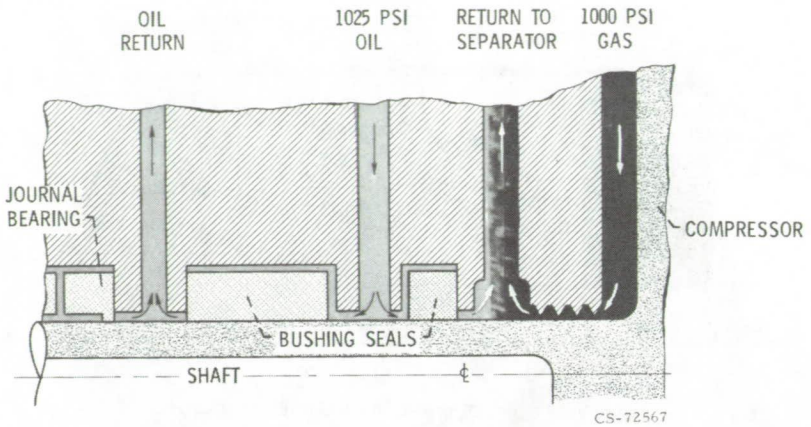

Figure V-33. - Liquid buffer seal-current practice (industrial compressor application).

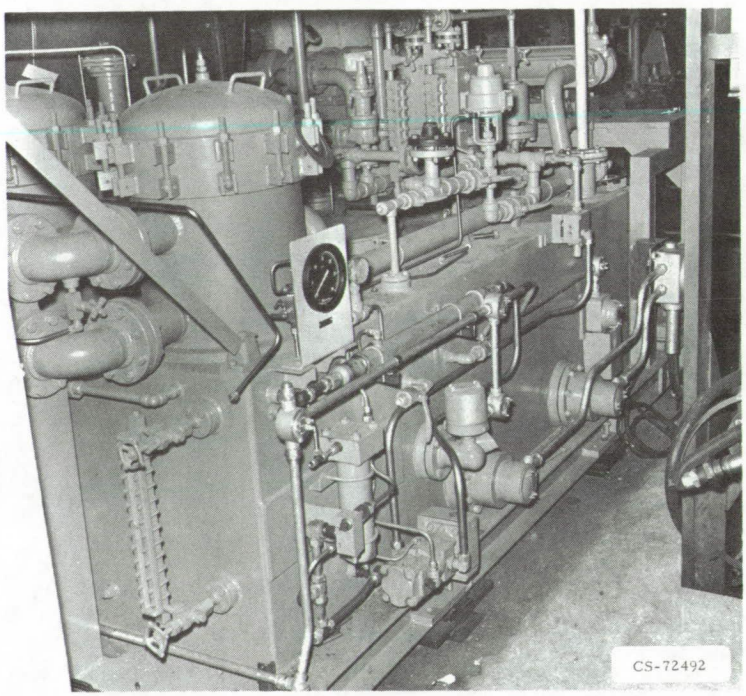

Figure V-34. - Lubrication and seal oil system.

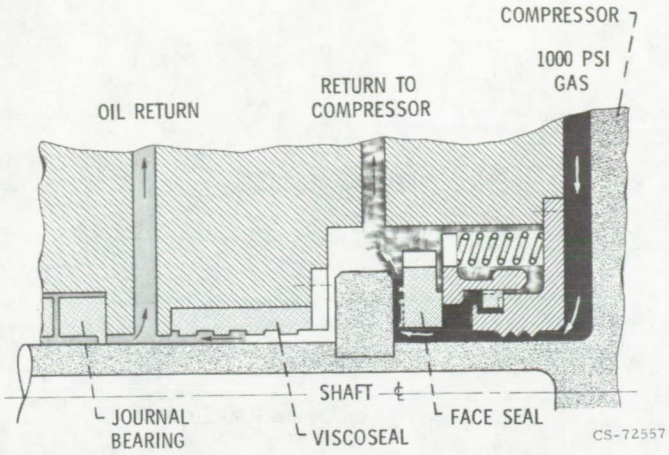

Figure V-35. - Advanced seal concept 1 (industrial compressor application).

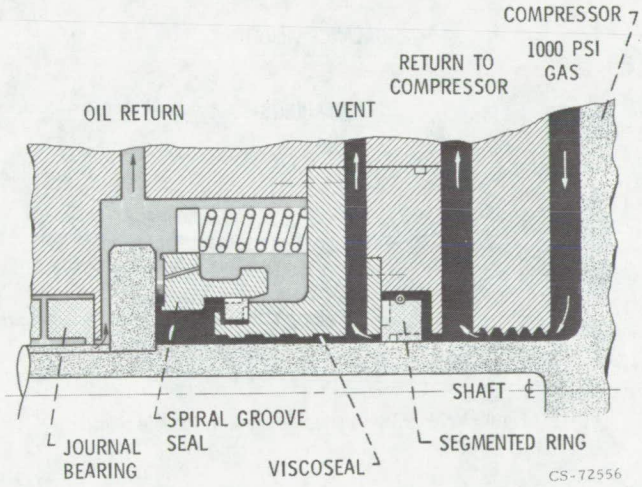

Figure V-36. - Advanced seal concept 2 (industrial compressor application).

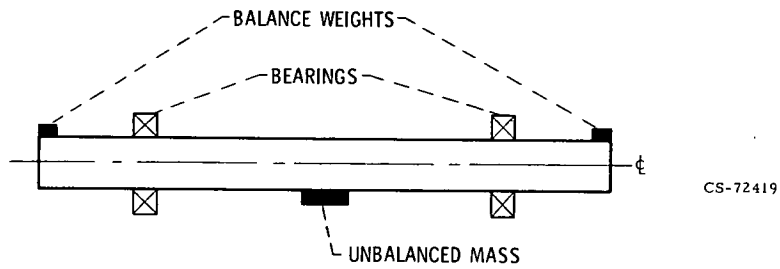

Figure V-37. - Two-plane balance with rigid rotor.

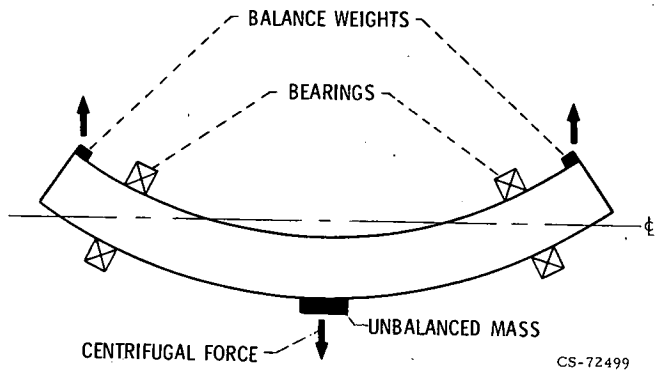

Figure V-38. - Two-plane balance with flexible rotor.

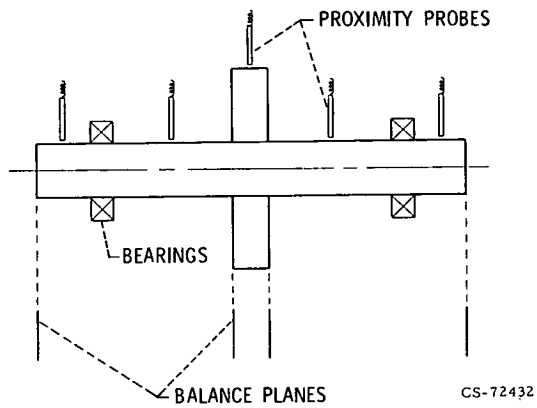

Figure V-39. - Multiple-plane balance technique.

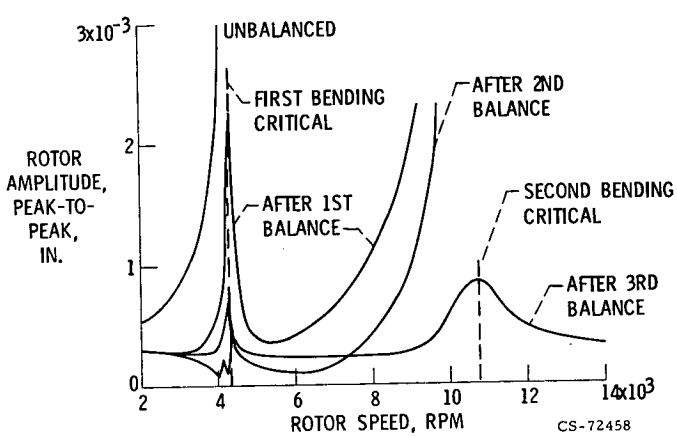

Figure V-40. - Results of multiple-plane balancing.

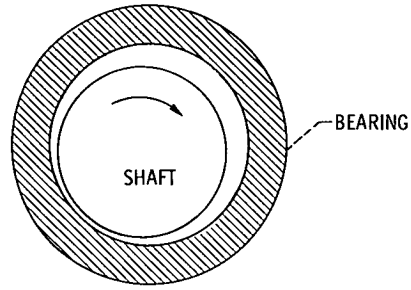

Figure V-41. - Plain journal bearing. CS-72418

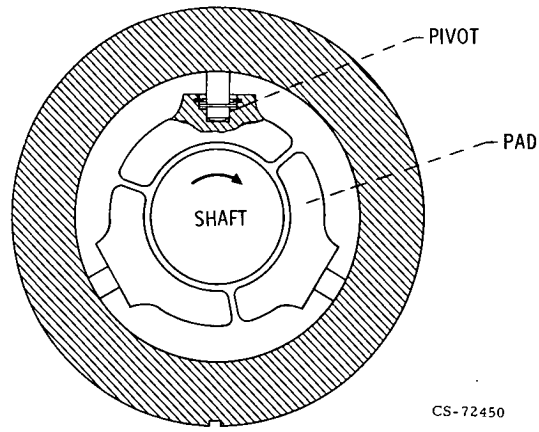

Figure V-42. - Tilting-pad bearing.

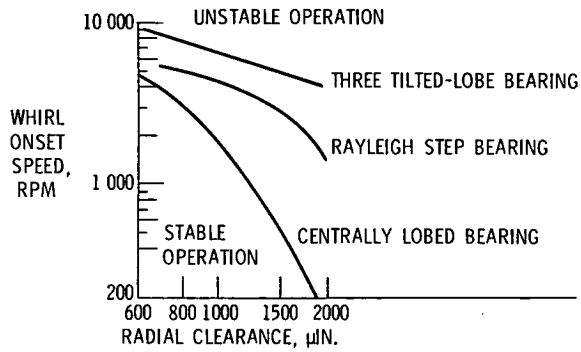

Figure V-43. - Stability of fixed geometry bearings.

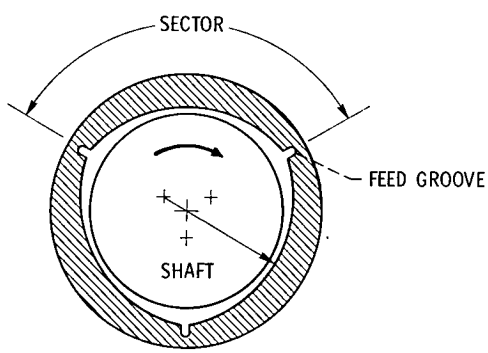

Figure V-44. - Centrally lobed bearing.

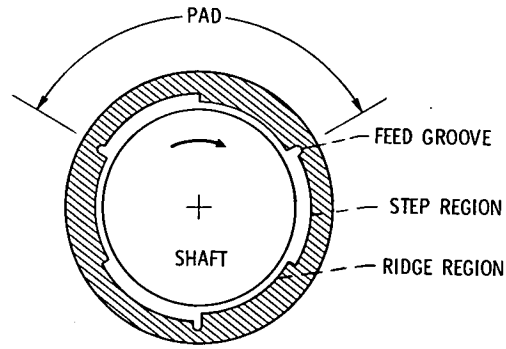

Figure V-45. - Rayleigh step bearing.

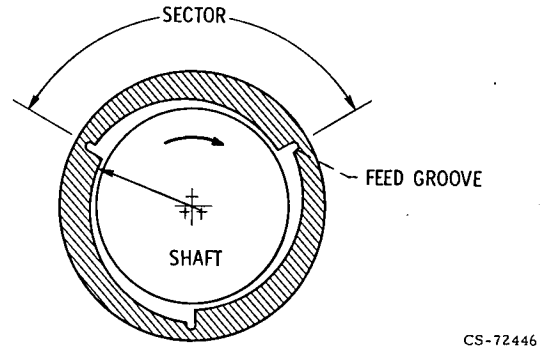

Figure V-46. - Three tilted-lobe bearing (wholly converging).

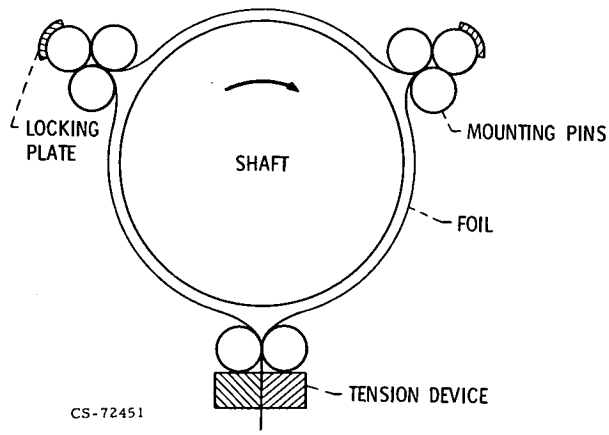

Figure V-47. - Tension foil bearing.

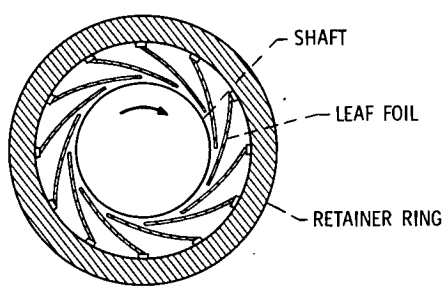

Figure V-48. - Leaf foil bearing.

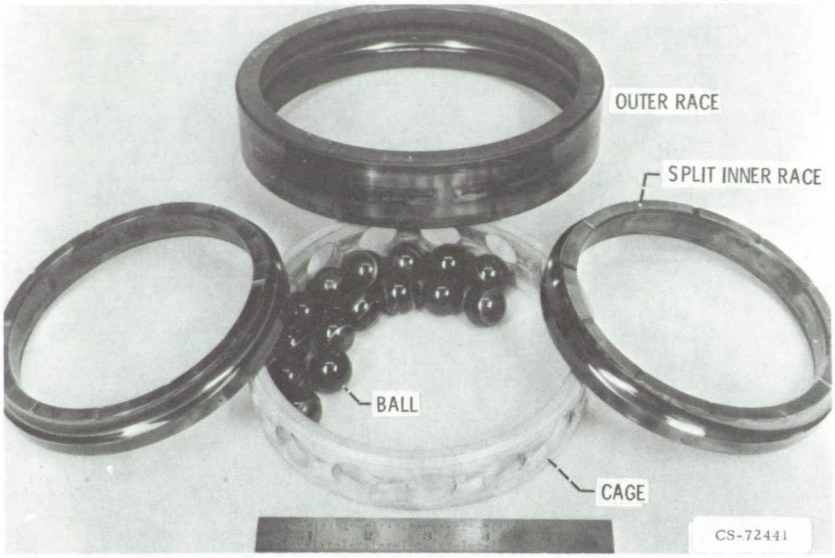

Figure V-49. - Angular-contact ball bearing.

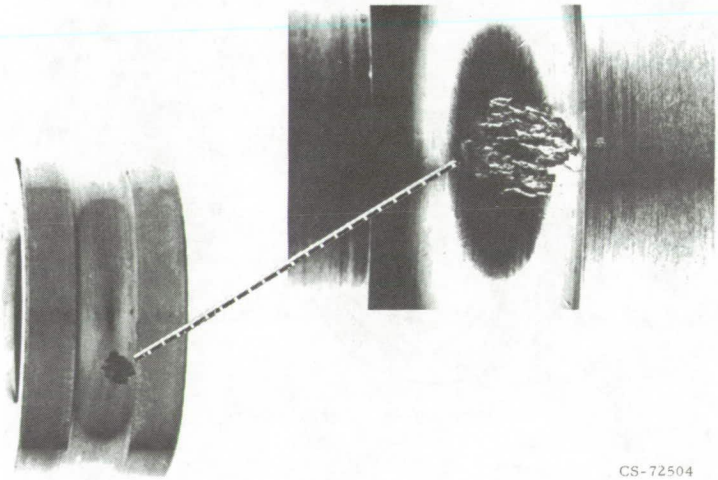

Figure V-50. - Typical fatigue spall.

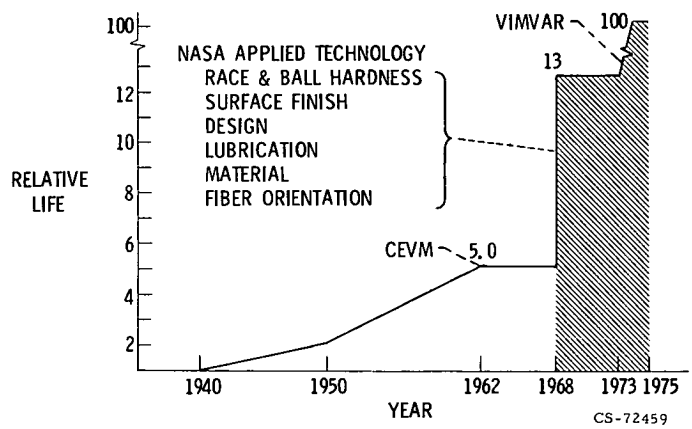

Figure V-51. - Rolling-element bearing history.

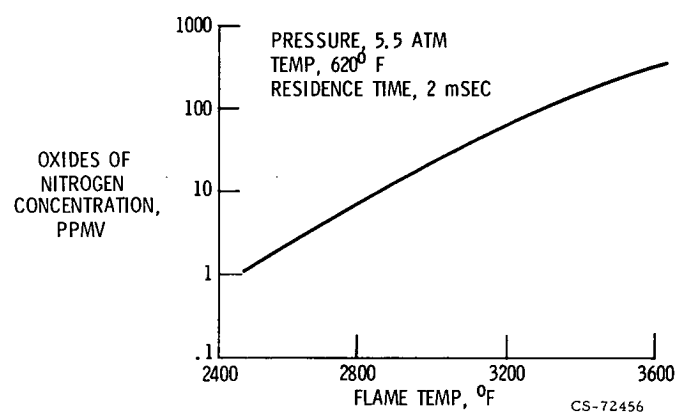

Figure V-52. - Effect of flame temperature on NO_x emissions.

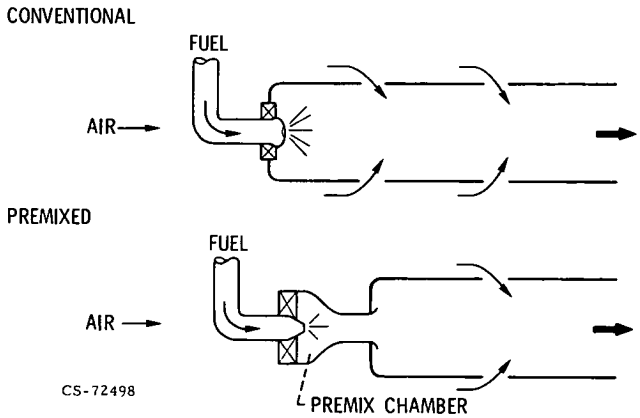

Figure V-53. - Fuel injection types.

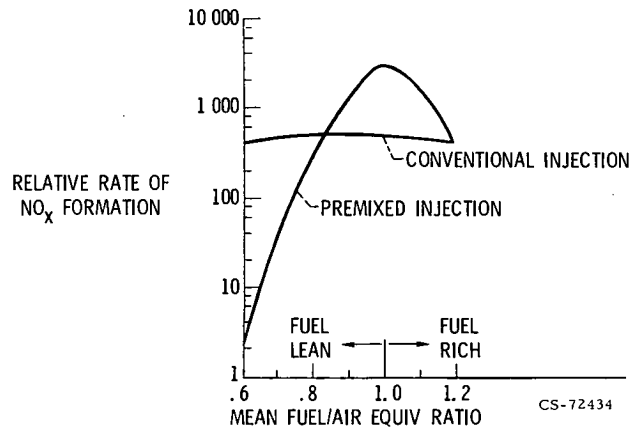

Figure V-54. - Effect of premixing on NO_x formation rate.

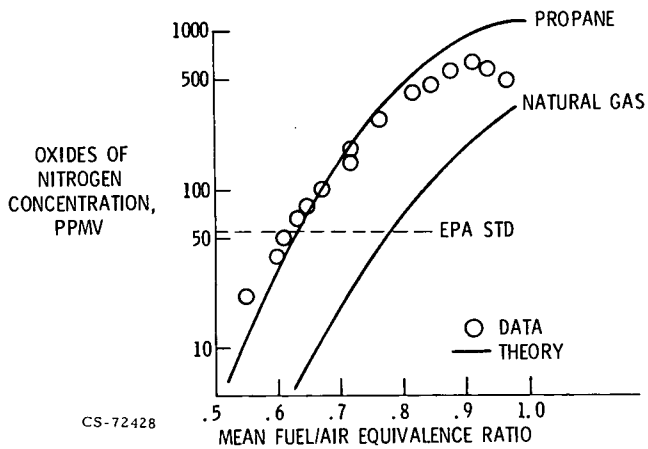

Figure V-55. - NO_x emissions with premixed combustion.

Page intentionally left blank

Page intentionally left blank

VI. FLUID PROPERTIES, FLUID FLOW, AND HEAT TRANSFER

Lester D. Nichols, Vernon H. Gray, Robert C. Hendricks, and Paul T. Kerwin

NASA has developed technologies in the broad disciplines of fluid property evaluation, heat transfer, and fluid flow which can be used in the gas industry. Appropriate aspects of these broad disciplines are discussed from the point of view of specific applications of interest to the gas industry. Information is presented which is not only useful, but also new and unique.

Fluid property values are frequently required by the gas industry. Data on the viscosity and phase equilibria of multihydrocarbon mixtures are needed for improved natural gas recovery and reservoir control. Flow measurements of such mixtures can be made more accurately with better fluid property data. Designing compressors and pipeline systems used in the transportation of such mixtures requires data on fluid properties. Computer programs developed at the Lewis Research Center to calculate the physical properties of fluids are particularly versatile and unique. They are constantly updated to include the latest information.

Fluid properties are also needed to evaluate closed thermodynamic cycles, such as liquefied-natural-gas refrigerators or heat pumps. Our capability in the fluid property evaluation area can be demonstrated by relating it to cycle performance evaluation and component design. We use a Joule-Thomson liquefier as an illustrative example. Some examples are given of the use of our programs in supplying the required property information.

In many cases, a thermodynamic cycle uses fluids whose thermodynamic states lie near the critical point. In this region, much care must be taken in designing components and in evaluating properties. Our research into heat-transfer and fluid-flow mechanisms in the near-critical region has produced significant results.

Also, many components are designed to operate with high-pressure liquids. When these liquids expand to lower pressures, they may become partially vaporized. This is called two-phase flow. Many times the resulting mass flows reach a maximum value, and further reduction in pressure does not increase the mass flow. This situation also occurs with gases and is called choking. We have measured choking in two-phase flow.

The thermodynamic properties of the combustion products must be known, not only to design the necessary components but also to calculate the resulting pollutants. Also, if different fuels (such as synthetic natural gas or hydrogen) or different combustors (such as surface combustors) are used, a versatile computer program including transport properties and chemical kinetics is required. NASA has developed such a computer program that is presently being used by hundreds of organizations both in the United States and abroad.

Heat exchangers are extremely important in all aspects of the energy industry. NASA has developed heat exchangers for a variety of applications. Some of them, for example, high-temperature metal and ceramic recuperators and regenerators and very-high-temperature drilled-core storage heaters, may be of particular interest to the gas industry. These heat exchangers can be used to improve heat recovery in industrial processes as well as in residential uses. The technology of very-high-temperature drilled-core heat exchangers may be applicable to the design of components used in the manufacture of synthetic natural gas.

Extremely compact, dynamically stable vaporizers have been developed that deliver very pure vapor after one pass of the fluid through the boiler. There are two types of these boilers - single tube and rotating. This boiler technology should be applicable to the liquefied-natural-gas industry, as well as to any thermodynamic cycle which requires a fluid to be vaporized.

Our heat-pipe technology might be helpful in Arctic transmission problems, process heat recovery, and many other applications which require the versatility of heat pipes.

FLUID PROPERTIES COMPUTER PROGRAMS

Designing much of the equipment used by the gas industry requires a

knowledge of thermodynamic and transport properties. Because property information is so important, there are many sources of such material available to the engineer. There are tables available to read or company computer programs to read the tables for you and give you the answer quickly. However, there is much more that the engineer needs to know in order to design equipment. The right kind of program and a high-speed computer with large data storage capacity can supply this information to him. The important characteristics of such a program are as follows:

(1) The data must include all real fluid properties over the entire range of interest of pressure, temperature, and density. Tables found in handbooks usually provide only saturation properties and gas-phase properties. There is recent interest in high-pressure data, which are not available on many of the company computer programs. If they are available, the data are usually limited to some specific applications and would not be useful to the entire industry.

(2) In order to be most useful, the program should use self-consistent equations to describe the pressure-volume-temperature (PVT) surface which are continuous over the entire region of interest. A program may be thought of as merely an assembly of tables which can be searched or a collection of curve fits for different regions. These types of programs would not be too useful in comparing different working fluids. Later an example is given wherein the Joule-Thomson coefficient is calculated for several different working fluids by using the reduced properties.

(3) The program must be easy for the engineer to use. This means the program must be available, versatile in its ability to accept different types of input data, and accurate, and it must not require a large amount of computer time or storage.

(4) The program should always be current and reproduce measured data. As new data become available, they should be included. This is especially important for those designing equipment to operate near the thermodynamic critical point because of the extreme sensitivity of the properties to slight changes in temperature and pressure in this region.

NASA has developed such programs. They are available to the gas industry, and the information used in creating them is well documented. These computer programs have been given the names GASP for Gas Program, WASP for Water and Steam Program, and HELP for Helium Liquid

Program. GASP handles 10 fluids: parahydrogen, helium (above 6 K), methane, neon, nitrogen, carbon monoxide, oxygen, fluorine, argon, and carbon dioxide. WASP handles the properties of water and steam, and HELP returns properties for helium both above and below 6 K.

The programs accept as input any two of pressure, temperature, or density. In addition, pressure and either entropy or enthalpy are also accepted as input variables, which is a highly desirable flexibility for cycle analysis. The properties available in any combination as output include temperature, density, pressure, entropy, enthalpy, specific heats, sonic velocity, viscosity, thermal conductivity, and surface tension (where applicable). For those having need of other derived thermodynamic properties, we also provide the partial derivatives $(\partial P/\partial \rho)_T$ and $(\partial P/\partial T)_\rho$. The subprograms are modular in structure so that the user can choose only those subroutines that are necessary to his calculations.

A typical computer operating time for determining cryogenic properties from GASP is 6 msec. Units can be metric, English, SI, or those of the user's choosing. WASP faithfully reproduces the International Skeleton Tables and the ASME Steam Tables, and GASP and HELP closely correspond to National Bureau of Standards data. The parameter ranges are slightly different for each fluid. In general, they are from the triple point to 500 atm, which includes the dense-gas and critical regions. Dissociation is not included.

The GASP-WASP-HELP programs are continually being updated as new information becomes available. As such they have become an integral part of the NBS-NASA thermophysical properties program.

Many times the designer needs to know how properties vary in a certain region as some of the design variables change. An aid to the designer in helping him visualize such changes is the ability to plot diagrams of the properties of the fluids we have been discussing. A particularly useful plot is the temperature-entropy diagram. The temperature-entropy diagram for methane shown in figure VI-1 was drawn by our computer program. As you can see, the diagram looks much like the diagram for water and steam. Shown are the saturation vapor and saturated liquid curves, lines of constant pressure, lines of constant enthalpy, lines of constant density, and - in the two-phase region - lines of constant quality. Now, if there is a particular region where the engineer requires a more detailed visualization, for

example, the rectangular region near the critical point, the program can draw the diagram on an enlarged scale. The scaling parameters will be proportional to the size of the box, and so the boxed region will be stretched in the horizontal and vertical directions to fill the page. This enlargement is shown in figure VI-2. With this capability, much of the engineer's experience and insight can be readily used in designing a component. Not only that, but the computer can then calculate the performance of the component. (Now anyone can draw a temperature-entropy diagram and use a magnifying glass to blow it up, but by using a computer program it can be done to the desired accuracy in a matter of minutes.)

CYCLE PERFORMANCE AND COMPONENT DESIGN

In general, property information can be used to evaluate the performance of thermodynamic cycles. A familiar illustrative cycle is the liquefaction of a fluid, for example, methane. Liquefaction can be accomplished by the use of a Joule-Thomson expansion valve. While this is not the most efficient cycle, it is useful in relating much of our capability in fluid properties evaluation to your needs. Shown in figure VI-3 is a schematic diagram of the components which make up the Joule-Thomson liquefier. The gas to be liquefied is compressed isothermally to the desired pressure. It then passes through a heat exchanger, where it is cooled to a lower temperature. The fluid expands through the Joule-Thomson valve. During the expansion, some of the gas condenses and collects at the bottom of the tank. The remaining gas, which is still cold, then passes through the heat exchanger, where it cools the gas coming from the compressor and becomes heated to approximately room temperature.

This cycle can be idealized and represented as a temperature-entropy diagram (fig. VI-4). Shown are the saturated vapor curve, the saturated liquid curve, and the critical point (at the peak). The gas to be liquefied is shown at state point 1 and is first compressed isothermally to state point 2. The process of cooling in the heat exchanger to state point 3 is idealized as a constant-pressure cooling process. The expansion through the Joule-Thomson valve is idealized as a constant-enthalpy process, and the fluid emerges at state point 4, which is in the two-phase region. The liquid,

represented by state point 4a, is separated from the vapor, represented by state point 4b, and the vapor is passed through the heat exchanger again. There it is warmed in a constant-pressure heating process to the initial starting point. Enough gas to compensate for the amount which was liquefied is brought into the compressor and the process is repeated again.

It is apparent that, if the properties are known at each of the state points, the ideal cycle performance can be calculated. In order for the Joule-Thomson expansion valve to be designed properly, the conditions upstream of the valve (at state point 3) must be selected so that, when the gas expands, the fluid temperature decreases. This design can be made for any fluid if the Joule-Thomson coefficient is known.

There is a curve in the pressure-temperature plane where the Joule-Thomson coefficient changes sign. This curve is called the "inversion curve" and separates the conditions which give cooling from those that do not. Such a curve exists for every fluid. However, with our computer programs it is possible to plot all fluids very nearly onto one curve, as shown in figure VI-5. Instead of pressure and temperature, we have plotted the data for the reduced temperature and the reduced pressure T_R and P_R. These results show good agreement for such a wide variety of fluids. The maximum amount of cooling occurs when conditions at state point 3 are selected to fall on the inversion curve. In this way the appropriate pressure and temperature for state point 3 can be selected for any working fluid.

However, many times a mixture is being liquefied. If proper mixing rules were known, it would be possible to use them to calculate the critical properties of the mixture from the single-component property data. Then the actual temperature and pressure required to liquefy the mixture could be set. Again, this could be done through calculation, without having to mix the components each time. Or, consider a situation where you want to design a refrigerator to operate at a certain temperature and pressure. From this curve the best reduced temperature and pressure for cycle performance could be determined. Then by using the mixing rules, a mixture could be created which would have the proper critical properties. It would be a case of creating the best refrigerant for a given pressure and temperature, rather than the best pressure and temperature for a given refrigerant.

Near-Critical Heat Transfer

The computer programs developed at NASA contain transport properties, such as thermal conductivity, as well as thermodynamic properties. Transport properties are also being constantly updated so as to include the best available data. These data would be required in determining the size of a heat exchanger such as the one described for use in the liquefier.

Notice that in figure VI-3 the curve representing the constant-pressure, heat-exchanger process can come quite close to the thermocritical point. In the region near this point, properties are very sensitive to small changes in either pressure or temperature. As an example the thermal conductivity of methane as a function of density for selected temperatures is shown in figure VI-6. At 205 K, which is a temperature away from the critical temperature, thermal conductivity increases smoothly with density. But, at 190.8 K, which is very close to the critical point, conductivity is not a uniformly increasing function of temperature but is nearly 14 times larger than the conductivity at 205 K. As a matter of fact, conductivity becomes infinite exactly at the critical point. This rapid variation in thermal conductivity, as well as variations in other transport properties, must be accounted for in the design of heat exchangers and other cycle components which must operate near the critical region.

Unfortunately, rapid variations in all the properties around the critical point combine to make forced-convection, heat-transfer calculations as well as conduction heat-transfer calculations extremely difficult to handle. The following peculiarities have been experimentally observed for forced-convection, heat transfer in the thermocritical (or near-critical) region:

(1) Heat flux in conventional heat transfer is proportional to the temperature difference between the fluid and the wall. The proportionality constant is called the heat-transfer coefficient and usually is not a function of the heat flux or the temperature difference. However, near the critical point that is not true. The heat-transfer coefficient is shown as a function of the fluid (in this case, carbon dioxide near the critical point) temperature with heat flux as a parameter in figure VI-7. Near the critical temperature the coefficient varies rapidly. This variation ultimately must be traced back to the variation in fluid properties. However, there is a heat flux for

which the coefficient is a maximum and one where the coefficient is a minimum.

(2) Behavior similar to that in the two-phase region is also observed. The surface temperature of a tube with heated (in this case) hydrogen flowing through it as a function of distance down the tube is shown in figure VI-8. The curves for both ambient-temperature gas and low-temperature gas are similar and are monotonically increasing - which is characteristic of turbulent flow. However, this is not true for the supercritical or subcritical flow. In this case, there is a maximum temperature, which means a minimum heat-transfer coefficient.

(3) Property variations can introduce natural convection effects into a forced-convection, heat-transfer problem that would not be expected with fluids away from the critical point. In figure VI-9 the upward velocity parallel to a heated flat plate at various distances away from the plate is shown. The wall is at a higher temperature than the fluid. Both a gas and a liquid are represented on the lower curve, which shows the familiar power-law profile that monotonically approaches zero from its free-stream value. However, near the critical point, there is a peak in the velocity profile near the wall. Again, because of rapid density variations, in this case with temperature, the natural convection force can add a buoyant force to the pressure force, and the fluid gets pushed up faster in this region.

(4) As you might suspect, in the near-critical region there can also be large momentum pressure drops and, maybe somewhat more surprisingly, almost negligible friction pressure drops compared to the momentum values.

(5) Oscillations in pressure can be expected at frequencies from 1/2 hertz to 8000 hertz. These low-frequency oscillations are system dependent. (System-dependent oscillations are discussed further in connection with boilers.) The high-frequency oscillations can occur as the result of the heat-transfer process itself. These oscillations must be considered because of the possibility of damage to equipment, even though they enhance heat transfer.

(6) The conventional correlations used in other regions fail to predict heat-transfer and pressure drop in the thermocritical region.
Some engineering techniques have been developed at NASA for near-critical heat transfer. However, mostly we have acquired the art of operating in

that region. The complexity of the engineering techniques really depends on the specific application and is much beyond the scope of this paper.

Two-Phase Choked Flow

The heat-transfer technology developed at NASA is useful in the design of heat exchangers, where the fluid is usually flowing in constant-area tubes or pipes. However, there are other components of thermodynamic cycles and fluid-flow devices where the flow is not in a constant-area tube or pipe, for example, flow through a flowmetering nozzle or orifice or flow through the seals around rotating shafts. Such flow situations have been studied extensively for gases. However, for high-pressure liquids some care must be taken. Let us take the example of flow through a converging-diverging nozzle. When the downstream pressure is sufficiently low, the nozzle is choked, that is, further decrease in the backpressure will not increase the flow rate. Thus, the flow rate is at a maximum. A nozzle used this way makes an excellent flow-measuring device, since the flow depends only upon upstream properties, that is, those in the stagnation chamber. Again, for gases, coefficients are available for the effects of geometry - whether you are using a nozzle, an orifice, or even a slit. The nozzle can then be corrected for use with various gases.

As a result of careful experiments we have been able to find a correlation that is accurate for four quite different fluids: oxygen, nitrogen, parahydrogen, and methane. This correlation is shown in figure VI-10 for oxygen and nitrogen. There is a characteristic mass flow rate per unit nozzle area which can be defined for each fluid in terms of its properties at the thermocritical point. This characteristic flow rate, which we call G^*, plays a role similar to the product of density and speed of sound for perfect gases. We have plotted the maximum flow per unit nozzle area G divided by G^* for the particular fluid being measured as a function of the reduced pressure. There are two separate curves for two different reduced temperatures. The essential point to be learned is that both nitrogen and oxygen fall on the same curves for the same reduced temperature. We believe this is true for all the fluids we have studied. With these curves it is possible to calculate flow rates for any choked two-phase flow in terms of the

upstream (or stagnation) temperature and pressure and the fluid properties.

Two-phase, choked-flow experiments have been performed with nitrogen in sharp-edged orifices and slits as well as in nozzles. We have compared the data to various theories in the literature and modified them to take advantage of our ability to compute thermophysical properties accurately over a wide range of parameters. This work has resulted in some insights into two-phase choked flow phenomena:

(1) Testing the four fluids shows quite conclusively that two-phase choked flow for all these fluids can be evaluated by using the characteristic mass flow parameter G*. Data both above and below the critical temperature are in very good agreement. Likewise the pressure data are in good agreement, even though simple models cannot properly predict the behavior below the critical temperature. With this data the mass flow through a nozzle for any fluid can be measured in terms of its upstream (or stagnation) properties.

(2) The shape of the opening is very important in determining the mass flow rate. While the flow rate through a slit is similar to that through a nozzle, it is significantly different for an orifice. Thus, while an average discharge coefficient may be adequate for a slit, it is not adequate for an orifice. Thus, although different geometries must be calibrated, the reduced properties and characteristic mass flow parameter approach can still be used to determine the flow rates for different fluids.

(3) The data suggest that thermodynamic nonequilibrium does exist in the expansion phase-change mechanism. The flow-rate data are sensitive to geometry. However, for engineering estimates of the flow rate below the critical temperature the nonequilibrium isentropic model works quite well - about 15 percent high over the whole range. Above the critical temperature the equilibrium model appears to be applicable.

In summary, these results should be very significant for workers in the gas industry since they deal with mixtures of high-pressure fluids. For single-component fluids and mixtures, such as liquefied natural gas, if the flow normalizing parameter G* is known, choked flow rates can be predicted from our data and the associated simple models. Much time and money can be saved by employing these experimentally determined facts.

COMBUSTION PRODUCTS COMPUTER PROGRAM

Another aspect of the use of methane is combustion. Figure VI-11 shows our version of a burner which converts a mixture of air and methane into a more complicated mixture of hydrocarbons, oxides, and even free radicals. In designing a burner to provide a certain amount of heating, it is necessary to know the extent of the reaction which occurs between the fuel and the oxidant. The further the reaction proceeds, the more heat will be released. The extent of the reaction also determines the concentrations of the various possible combustion products. They are listed at the top of the figure for this particularly simple fuel. You can imagine the complexity if more elements (such as sulfur) were included. There are equations which can be solved to tell you the concentrations of the products. First, no elements can be destroyed in this chemical reaction, so they must be conserved. (Here we cite only four elements for simplicity.) Second, all the energy that comes into the burner from the fuel must appear in the combustion products. Third, there is an equation which specifies the pressure at which burning takes place. Finally, there are constants which describe each particular chemical reaction that could possibly take place. The only thing remaining to do is to solve all these equations simultaneously for the unknown concentration of each possible product. The solution gives the concentrations and, hence, the extent of the reaction. From there the engineer can design his burner.

A very general computer program (COSMIC code LEW 11997) has been developed here at Lewis for solving such problems with even more complicated fuels and oxidants. The program calculates chemical equilibrium composition and mixture properties. In this computer program the gases are assumed to be ideal. The program can handle fuels and oxidants constructed from 15 different chemical elements. There are 600 different products of combustion whose data are stored in the computer. Any given combustor can be designed by considering any 150 of them. The program also includes both solid and liquid condensed phases and ionization. It is quite versatile. A number of different input states can be used to specify the initial known conditions for the combustor:

P,T P,H P,S V,T V,U V,S

where P is pressure, T is temperature, H is enthalpy, S is entropy, V is volume, and U is internal energy. If any one of these six input states are known, the program will compute the reaction products. Another very important feature of this program is that it is well documented and readily available through the Computer Software Management and Information Center, "COSMIC," at the University of Georgia. Literally hundreds of organizations are using this program, both here in the United States and abroad.

Under certain conditions there may not be sufficient time for a reaction to go to completion. In this case, the kinetics of the reaction, or rate at which it occurs, must be included. There is such a capability in this program. This is important when calculating pollution products and combustion, as well as in rocketry, detonations, shocks, atmospheric reactions, and cycle analysis.

Finally, just as in the case of the single-component fluids, it is important to know the transport properties, such as thermal conductivity, for the design of equipment used in combustion systems. This program also provides the transport properties for the mixtures of combustion products.

In summary, the program provides the engineer with a very powerful tool which can compute the concentrations of combustion products, transport properties, and reaction kinetics for a multiplicity of chemical elements.

HIGH-TEMPERATURE HEAT-EXCHANGER TECHNOLOGY

Metal Recuperators

NASA has been involved in the development of high-temperature, gas-turbine-system, heat exchangers since the early 1960's. Initially, this work was conducted as part of the space power systems programs. More recently, it has broadened to include energy-related applications.

The recuperator is the component of a gas turbine system which transfers heat from the turbine discharge gas to the compressor discharge gas - thus increasing system efficiency. The recuperator is a critical component because it operates at peak system pressure and within several hundred

degrees of peak system temperature. Recently, the trend has been toward higher temperatures and higher performance because of higher fuel costs and concern with energy conservation. For any gas turbine system, fuel consumption is reduced as system temperature and recuperation increase.

Our work in high-temperature recuperator technology applies to a number of systems of interest to the gas industry. These systems include space power, automotive, and the generation of electricity - which span a broad range of power levels.

Gas transmission, electric power generation (base and peak loads), refrigeration, and gasifier heat recovery require or would benefit from the use of high-temperature recuperators. There are presently almost 400 gas turbine units in gas transmission service along the pipelines. Also a number of electric utilities use natural-gas-fired turbines for base-load and peak power generation. Gas-fired refrigeration systems - including both the small units for railroad car refrigeration and the larger units for liquefied-natural-gas tankers - require high-temperature heat exchangers. And, finally, efficient heat recovery is a key to economical coal gasification.

Heat-exchanger operating conditions and performance requirements are a function of system trade-offs that depend on the application. However, in any application the heat exchanger must transfer heat from the hot to the cold fluid with no mixing or leakage from the high- to the low-pressure side. Any leakage results in reduced system efficiency.

Because of the wide range of applications, heat exchangers are built in a variety of materials, core geometries, and flow configurations. In general, heat exchangers are described by the flow arrangement and type of heat-transfer surface. Figure VI-12 illustrates plate-fin construction, while figure VI-13 shows the tubular geometry. Plate-fin and tubular cores are the most commonly used types of heat-transfer surfaces in recuperators. In these cores the flow arrangement is termed crossflow, that is, the fluid streams flow at right angles.

In a plate-fin case the two streams are separated by plates, and heat is transferred by conduction through the fins. The hot and cold streams flow in adjacent passages. A large number of fin types are available. The offsets, perforations, or louvers are added to improve heat-transfer performance.

In a tubular crossflow core, one fluid flows inside the tubes, and the

other fluid flows normal to the tube bundle. Again, a large variety of plain and finned cores are available.

A crossflow configuration is fairly simple. No elaborate manifolding is required since the streams do not share entrance and exit faces. But performance is limited. Flowing the streams at right angles is not an efficient heat-transfer arrangement.

The most efficient heat-transfer arrangement is counterflow - where the fluids flow in parallel but opposite directions. For most gas-to-gas recuperator applications a counterflow, plate-fin core results in minimum volume, weight, and cost. This construction is typical of many aircraft and industrial heat exchangers.

A plate-fin counterflow recuperator (fig. VI-14) consists of three sections: the counterflow core, where most of the heat transfer occurs and the two end sections, which are necessary for directing the streams into and out of the core. Counterflow heat exchangers require end sections because the fluids share an inlet and outlet face at each end of the unit. For illustration, these end sections are shown separated from the core.

Low-pressure (hot) gas from the turbine enters at the hot end and turns in the end section into the counterflow core. It is cooled as it passes through the core. At the cold end, it is turned again and discharged. The high-pressure compressor discharge enters at the cold end. It is turned into the core, where it is heated. At the hot end, it is turned again and discharged. Some heat transfer does occur in the end sections; but if design care is not taken, they can represent a good fraction of overall heat-exchanger volume and weight.

A plate-fin recuperator is built up by alternately stacking plates and fins to the desired height. Figure VI-15 shows adjacent low-pressure and high-pressure passages with their respective flow streams. The ends are built up as an integral part of the core. The sides of the passages are sealed by what are called header bars. In the end sections opposite faces are sealed - thus permitting proper fluid access to a passage.

For any heat exchanger that undergoes thermal cycling from ambient to temperatures in the range of 1000^{o} F, fatigue cracking is a major factor in limiting life. When we began our power system technology in the early 1960's, we relied on state-of-the-art aircraft heat exchangers. Unfortunately, we learned that these did not meet our needs. Startup cycling

resulted in fatigue cracks and working fluid leakage. Present-day industrial recuperators are also limited in temperature and cyclic life.

Metal sections with sharp transitions from thick to thin material are critical from the standpoint of thermal fatigue. In a plate-fin core the header-bar-to-plate joints have this large mass difference. The sketch on the left in figure VI-16 illustrates conventional construction. In a startup transient the thinner plates and fins heat up much more rapidly than the header bars, resulting in severe thermal stresses. Failure eventually occurs in a plate, resulting in bypass leakage from the high- to the low-pressure stream, or in the joint between bars, resulting in leakage from the system.

An approach to solving this problem is reducing material thickness, particularly in the header bars. One of a number of concepts that have been considered is shown on the right in figure VI-16. This approach should be well suited for use in systems with rapid startup transients, such as automotive gas turbines, or systems that undergo frequent cycling, such as utility peaking systems. This alternate approach uses channeled header bars, which have less mass and more resilience than solid bars. The width is retained for accurate stacking and placement. A channeled-bar recuperator is being developed for use in a Brayton demonstration system. Peak recuperator temperature is 1340^{o} F.

Ceramic Recuperators

As another approach to advanced high-temperature heat exchangers, we are considering the use of ceramic materials. This work draws from the materials technology program to develop ceramic turbomachinery and combustors.

Ceramics have a number of distinct advantages over metals. They have high strength at elevated temperatures, and because of their low thermal expansion are resistant to thermal fatigue failures. They are lower in weight than comparable metal units because of their lower density - which is important in mobile applications. Glass ceramics are fairly inexpensive and are produced in highly automated processes giving them a potential for low cost. And finally, the raw materials are readily available in this country.

Domestic technology has focused primarily on ceramic regenerators for automotive and truck gas turbines. A regenerator, or "heat wheel," is a rotating-disk heat exchanger (fig. VI-17). It requires some sort of external drive system for rotation. The disk is alternately heated and cooled as it rotates through the turbine exhaust and compressor discharge gases. The streams are counterflow. No elaborate manifolds or end sections are required. Fluid streams are separated by a system of rubbing seals. A regenerator always has a certain amount of carryover and seal leakage that can be minimized but not avoided.

Figure VI-18 shows a ceramic regenerator disk with an enlargement of the heat-transfer matrix. The disk is made up of tiny glass tubes stacked and bonded to form the matrix. During heat treatment the tubes deform slightly into a honeycomb shape.

Recently, work has begun on ceramic recuperator technology. As part of our automotive gas turbine effort, Lewis is conducting a small program to demonstrate the feasibility of fabricating ceramic recuperators. A number of modules have been built in several flow configurations. Figure VI-19 is a recuperator module consisting of the same tubular matrix as the regenerator. This unit is only a 6-inch cube, but it does demonstrate the fabrication technology required for a full-size heat exchanger.

Ceramic recuperator technology is in its infancy. Much remains to be done before a ceramic recuperator can be integrated into an engine. A better understanding of these brittle materials is required. Such matrix properties as leakage, pressure containment capability, and thermal fatigue characteristics are presently being evaluated.

In summary, ceramics are preferred over metals for use in heat exchangers because they can be used at higher temperatures and are cheaper. But it will take a decade for the ceramics technology to develop. A regenerator has two advantages over a recuperator: (1) it does not require elaborate manifolding and end sections, and (2) the flow reversal tends to reduce fouling problems. However, as the technology develops, a ceramic recuperator should replace the regenerator (1) because it needs no drive system, (2) it has no rubbing seals that need maintenance and replacement, and (3) there is no built-in leakage or carryover to degrade performance.

High-Temperature Storage Heaters

In order to test supersonic and hypersonic aircraft in wind tunnels, it is necessary to have a source of high-pressure, high-temperature air. One technique is to add heat to solids until they are heated to a very high temperature and then to pass air over the solids rapidly, which in turn heats the air for short-time testing. This technique can also be used to transfer heat from a high-temperature gas to a cold gas by alternately flowing the hot and cold gases across the solids. The use of ceramic solids whose melting point is extremely high makes it possible to heat air to temperatures in excess of 4000° F.

Such a heat-storage device is shown in figure VI-20. This is a sketch of a heater built at Lewis. It uses graphite as the storage material. Energy is supplied from electrical induction heaters to heat the graphite. Carbon felt and bricks insulate the heat-storage elements from the pressure vessel. Nitrogen is passed over the graphite and becomes heated. Then oxygen is added to provide a mixture of oxygen and nitrogen with the same proportions as air. The oxygen cannot be heated directly by the graphite because the graphite would burn. However, a heater using yttria-stabilized zirconia was built, to heat air directly, at the Ames Research Center. Zirconia will not oxidize, so this heater can also store heat that results from burning fuel. If gas temperatures of only 3000° F are required, the cheaper alumina or magnesia ceramics can be used instead of the more expensive zirconia.

In developing such a heat-storage device, an important decision is what shape to make the graphite. One could use spherical bricks, called "pebbles," which is attractive because of their simplicity and ease of manufacture. However, the point-contact loading of pebbles leads to their deformation at high temperature. Also, rubbing at the point contact creates dust.

These difficulties can be bypassed by using a drilled-core geometry as shown in figure VI-21. The cylindrical slab has holes "drilled" in it for the gas to flow through. The heater is made up of a stack of these elements. In order to aline the holes, hexagonal keys and mating key ways are machined into the core. With this design, it is possible to heat the bed to greater depths without compaction and to minimize creation of dust. One

other advantage is the low-pressure-drop characteristic compared to pebble beds. The maximum pressure drop that is allowable is the amount required to lift the bricks, the so-called flotation limit. The drilled-core bricks offer a higher mass flux and longer testing time at the same mass flow when compared to spherical bricks.

The operating characteristics of the graphite and zirconia heaters are compared in the following table:

	TYPE OF CORE	
	ZIRCONIA	GRAPHITE
WORKING FLUID	AIR	NITROGEN
BLOWDOWN TIME, MIN	1/2	2 - 3
MAXIMUM TEMPERATURE, ^{o}F (K)	4200 (2600)	4500 (2780)
MAXIMUM PRESSURE, PSIA (N/CM^2)	500 (340)	1000 (700)
TECHNIQUE TO MAKE HOLES	CASTING	DRILLING

Once-Through Boilers

The once-through boiler, which was developed for space electric power generation systems, may have advantages for terrestrial uses because of its compactness and therefore its low cost. In figure VI-22, an older design of a conventional coal-fired boiler is compared with an advanced once-through boiler. The once-through boiler (fig. VI-22(b)) is a tube-in-shell counterflow heat exchanger. The shell contains the heating fluid, generally a liquid. Boiling occurs in the central tube (or tubes). The small once-through boiler shown at the upper right is drawn to the same scale as the conventional boiler and transfers the same amoung of heat. The volume of the once-through boiler is about 1/1000th of the conventional boiler volume. However, in order to boil liquefied natural gas, for example, we would need probably a combustion heat exchanger for heating the boiler heating fluid. That equipment is not shown here.

The conventional boiler uses gravity to separate the vapor from the liquid, and it recirculates any unvaporized liquid. The once-through boiler

does neither of these. It is designed to convert liquid into dry, superheated vapor in one pass. Without the use of gravity and recirculation, several heat-transfer and instability problems arise. The following discussion of these problems and several solutions to them, including new boiler concepts that have been tested at Lewis, are taken from reference 1.

In figure VI-23, two representative flow patterns that can occur in once-through boiler tubes are shown. On the left, a high-heat-flux case is illustrated. When the heat flux through the tube wall is too high, film boiling occurs almost immediately. This creates a vapor blanket on the wall with most of the liquid flowing in the center of the tube, a very inefficient mode of boiling. The heat-transfer coefficient drops to a low value in the region of film boiling, and only slowly recovers as the convective velocity of the vapor increases. At some point the coefficient starts dropping again when the wall becomes totally dry and the liquid is in a mist flow.

A lower heat flux (right side of fig. VI-23) results in good wet-wall boiling with the vapor gradually congregating in the center of the tube. There can be an intermediate region of undesirable slug flow, as shown. The heat-transfer coefficient is generally very high until the boiling crisis is reached, at which point the wet-wall region breaks up into largely a dry-wall region. The coefficient abruptly decreases almost to the level of a gas coefficient, and thereafter inefficient vaporization of the dispersed liquid mist in the vapor flow occurs.

Several boiler-tube insert devices have been tested at Lewis. These devices were designed to solve some of the heat-transfer problems encountered with boiling in hollow tubes. Some of these devices are shown in figure VI-24. Performance improved when twisted tapes, helical vanes, or wire coils were inserted into the boiler tubes. These inserts all caused the flow to rotate and to centrifuge the liquid from the two-phase mixture onto the outer, heated wall of the tube. In this manner the wet-wall region was maintained much farther along the tube. Inlet-region central plugs, shown at the bottom of the figure, were found to help in breaking up the slug-flow regime.

Another method of centrifuging the liquid to the wall in a single-tube boiler was by using blade-type helical flow inducers (fig. VI-25). Stationary rotor elements obtained from turbine-type flowmeters were used to spin the flow and throw the liquid droplets to the electrically heated tube wall. Sev-

eral of these nonrotating rotor elements were axially positioned on a central wire. These blade-type helical flow inducers (or swirlers) have an advantage over continuous helical wire inserts in that their pressure drop is less.

Although these various inserts improved heat transfer and vapor generation, additional measures were required to overcome various flow instabilities in once-through boilers.

The first type of instability to be recognized is shown in figure VI-26. This is the flow-excursion instability, which results from improper matching of the pump to the boiler. Here, pressure drop ΔP is plotted against boiler-fluid flow rate. Typical curves are shown for all-liquid flow and for all-vapor flow. The S-shaped transition curve between them is the curve along which a boiler must operate. The system is unstable if the operating point is in the negative-slope portion of the boiler curve, where the slope of the supply-system (pump) curve is less steep than the slope of the boiler curve. In this case, the operating point will jump to one of the other two points of intersection. This excursion instability can be avoided by increasing the system pressure drop to steepen the pump curve, as shown by the stable-supply-system curve.

Another mode of instability, that of boiler and feed-system coupling, can occur when the dynamic flow resistances produce, instantaneously, this form of instability. However, such a dynamic instability produces oscillations rather than excursions. There are other instabilities also, which are not discussed here. The solutions, generally, are to restrict the flow at the boiler inlet by the addition of pressure-drop devices such as nozzles or venturis.

We investigated a novel boiler-inlet stabilizing device that has important advantages over a simple inlet nozzle. This concept is the vortex-chamber inlet (fig. VI-27). A cylindrical vortex chamber, shown on the right, has an outlet tube, shown on the left, containing a venturi nozzle which discharges into the boiler tube. The cylindrical vortex chamber has both a central and a tangential inlet feed tube, shown approaching from the top. With the tangential inlet feed tube in use, as shown by the arrow, a free vortex generates in the cylinder. Rotative velocity increases as flow approaches the center. Increased velocity is accompanied by a decrease in static pressure. Ultimately the vapor pressure of the fluid is reached and a small central core of vapor is created. Figure VI-28 shows this inlet de-

vice made of transparent material with hot water flowing through it.

In figure VI-28(a), a small-diameter vortex filament (or core) of vapor can barely be seen at the vortex chamber centerline. With increased flow and increased velocities (fig. VI-28(b)), the core has increased in diameter and has extended into the venturi nozzle, where cavitation bubble formation and collapse are superimposed on the vortex flow. In figures VI-28 (c) and (d), progressively more flow creates progressively more cavitation, appearing as a dark cloud of vapor bubbles in the nozzle. A helical flow pattern persists through the nozzle and a thin annulus of clear liquid is dispersed along the inside wall of the nozzle.

The tangential inlet feed creates a nozzle pressure drop that is 10 to 20 times as much as with the central feed, which produces straight axial flow. Thus, the nozzle pressure-drop characteristics can be drastically altered by externally valving the proportions of axial and tangential flows into the vortex chamber. This is useful for achieving control and stability. This function is roughly equivalent to that of a nozzle with some kind of a mechanically variable throat diameter. In this way, the control advantages of a fluidic valve can be added to the other requirements of a good boiler-inlet device, namely, a sharp, stable liquid-vapor interface and the liquid phase in helical flow along the heat-transfer wall.

Lewis has successfully tested, with water, a once-through tube-in-shell boiler design that incorporates a simple venturi nozzle at the inlet, followed by a short tapered central plug, with a helical wire coil extending the full length of the plug and boiler tube. Figure VI-29 gives performance data for this boiler in terms of exit-vapor quality as a function of the boiler heated length. For this case, boiling-fluid-inlet temperature was high and flashing, or sudden initiation of vapor, occurred in the inlet venturi. Flow oscillations were less than ±5 percent. Vapor superheat was observed as exit vapor qualities of over 100 percent. In comparison, a plain hollow-tube boiler had a maximum achievable exit quality of only about 80 percent because of the onset of dry-wall boiling at about 60 percent of length. The hollow-tube boiler also had severe flow oscillations. The pressure drop of the boiler with inserts, however, was several times as large as that with the hollow tube. A similar design, tested with potassium as the working fluid and lithium as the heating fluid, achieved stable flow with exit vapor superheats of over 400° F above the saturation temperature level.

Finally, a once-through boiler that uses the concept of rotating the whole boiler to achieve vapor-liquid separation (fig. VI-30) was successfully tested. Here, the liquid enters at the bottom of the device through a hollow shaft. It passes through a regulating valve and then sprays out to the cylindrical walls, which are the heated surface. There it forms an annulus of liquid. The liquid passes up into the heated zone to replace the liquid that has boiled off. At the liquid-vapor interface, vapor leaves the liquid and flows toward the center of rotation and then out the top of the boiler.

The top of the rotating cylinder, which is 4 inches in diameter and 2 inches in vertical height, is a transparent window. A high-speed motion picture camera was mounted above it, looking down into the cylinder. Film C-253, which is available from the Lewis Research Center on request, shows boiling activity inside the cylinder for several different operating conditions.

At a low heating rate of 0.9 kW and a centrifugal acceleration of 100 gravities (or g's), individual bubbles, as well as chains of bubbles, moved across the liquid annulus in a radial direction toward the liquid-vapor interface. There the bubbles broke, and the vapor flowed to the center of rotation and out of the boiler. Sometimes bubble clusters welled up at the interface and formed domes that later broke up into droplets which were thrown back into the liquid annulus as the vapor escaped.

At a high heating rate of 24 kW, the annulus was foamy and opaque at 100 g's, but at 400 g's the fluid had alternating clear and bubbly areas, with a more distinct interface. This heat flux was about 30 percent higher than the maximum, or so-called "burnout," heat flux at 1 g and 1-atm pressure. In one test at 400 g's, twice the normal earth-gravity burnout heat flux was exceeded with the boiling remaining stable.

At an intermediate heating rate of 4.5 kW, the same amount of heat was transferred and the same amount of vapor was generated at 25 g's as at 400 g's. However, at 25 g's, the bubble activity was intense and the interface was very turbulent, while at 400 g's the annulus was mostly clear liquid and the interface was a thin sharp line. There were very few bubbles at 400 g's, indicating that most of the vapor must originate at the interface by direct evaporation.

The rotating boiler has several advantages. It creates a stable liquid-vapor interface and is insensitive to earth gravity or orientation. It is a low-pressure-drop device with high heat flux. Also it produces high-

quality vapor; in all our tests the exit vapor quality was always above 99 percent.

Heat Pipes

There are some heat-transfer situations where large amounts of heat must be moved with a small temperature difference. The thermal conductivity of even the best conducting metals may be too low, but a pumped heat-transfer loop may be too complex and expensive. In this case, a heat pipe might be just the answer.

Heat pipes, like once-through boilers, are heat-transfer systems where the working fluid operates in the two-phase region. An example of a heat pipe that is familiar to everyone is the steam heating system that was used in many buildings some years ago. In this case the heat was carried from the furnace as steam and given to the room by condensation in the radiators. The condensed water returned to the furnace in pipes by gravity.

Figure VI-31 shows a heat-pipe which does not need gravity. It is a closed container consisting of a capillary wick structure and a small amount of vaporizable fluid. This heat pipe also employs a boiler-condensing cycle in which the capillary wick pumps the condensate to the evaporator. The vapor pressure drop between the evaporator and the condenser is very small. Therefore, the boiling-condensing cycle is essentially an isothermal process. The temperature losses between the heat source and the vapor, and between the vapor and the heat sink, can be made small by proper design. As a result, one feature of the heat pipe is that it can be designed to transport heat between the heat source and the heat sink with very small temperature losses. Although the heat pipe behaves like a structure of very high conductance, it possesses heat-transfer limitations by certain principles of fluid mechanics.

Figure VI-32 shows the limiting range of operation for heat pipes as the operating temperature increases. The region 1-2 is called the sonic limit. In order to transport the heat with low-vapor-pressure fluid, a high velocity is required. This velocity is limited by the sonic velocity at the evaporator exit. Region 2-3 is the entrainment limit. Here a high dynamic head of vapor shears fluid from wicks and grooves. The wicking limit is region 3-4,

where the maximum capillary pressure differential available for pumping is reached. Region 4-5 is the boiling limit, where the temperature gradient across the fluid in the grooves and wicks causes a vapor lock and limits the flow rate.

The advantage of a heat pipe is mainly centered on its ability to transfer large amounts of heat with little temperature difference. The heat-transfer capability of a heat pipe can be 10 to 100 times that of other heat-transfer methods. A particularly impressive comparison can be made between using lithium in a high-temperature heat pipe and using copper to conduct the same amount of heat. Even though copper is one of the best conducting materials, the effective conductivity of a lithium heat pipe is thousands of times greater than that of copper.

An example of NASA heat pipe use is shown in figure VI-33. It shows three heat pipes which are used on the Communications Technology Satellite (CTS). The three heat pipes are mounted to a panel which serves as a radiator to eject the heat given up by the fluid when it condenses. The evaporator section takes heat from the power processing system and the traveling wave tube. This tube is part of the transmitter which will send television signals from the orbiting CTS back to the earth. The entire CTS spacecraft with the heat-pipe radiator is shown in figure VI-34. This picture was taken while the spacecraft was being tested here at Lewis.

The Lewis Research Center has an extensive heat-pipe test program underway. This includes pipes in the temperature range from 80° F to over 2000° F, which is of interest to the gas industry. The program is aimed at improving reliability, life, and performance and at decreasing the manufacturing cost.

Pipes in the low-temperature range (80° to 500° F) have methanol, water, Freon, or ammonia as the working fluid and are made of stainless steel or aluminum. Pipes of this type may lend themselves to use in exchangers for waste heat recovery in heating and ventilating. Internal corrosion can cause the generation of noncondensable gas, with performance deterioration and decreased life. The effectiveness of various fabrication, cleaning, filling, and closing procedures and material combinations in relieving this problem and in lowering cost are being studied.

Pipes containing alkali liquid metals with various stainless steel and superalloy wicks and enclosures are being procured. These will be tested

in atmospheres containing air and combustion products at temperatures to 2100^{o} F. The effect of various material combinations and atmospheres on the internal and external corrosion will be studied. The pipes with improved performance and life resulting from these studies may prove adaptable to use in high-temperature gas heat exchangers and plant processing equipment.

CONCLUDING REMARKS

The technology developed by NASA in the fields of fluid property evaluation, heat transfer, and fluid flow should be of use to the gas industry. Our computer programs are available to you and can be used to calculate thermophysical properties for 10 gases. Computer graphics software are available to plot these properties directly from the computer. We have illustrated ways in which this capability can be used to evaluate cycle performance. Components which use fluids in the near-critical region can be difficult to design because of the peculiarities in the heat transfer in this region. We have given you some insights into these peculiarities and warned you to watch for others. Our two-phase choked flow data can be used for mass flow measurements for many fluids and might be useful in the design of components which carry high-pressure liquids. We have indicated how the data might be useful even for mixtures of liquids.

The properties of chemically reacting mixtures can also be evaluated by computer programs developed at Lewis. These programs are versatile and also include rate equations and transport properties.

Our heat-transfer technology is directed toward reliable, compact, high-temperature metal recuperators and higher-temperature ceramic recuperators. Still higher temperatures can be achieved by drilled-core brick heat exchangers. Technology for fluids in the two-phase region led to the development of several different types of compact, stable boilers which provide high-quality vapor with a single pass through the heat exchanger. The ongoing heat-pipe program should improve the reliability, lengthen the life, and reduce the cost of these devices under conditions of interest to the gas industry.

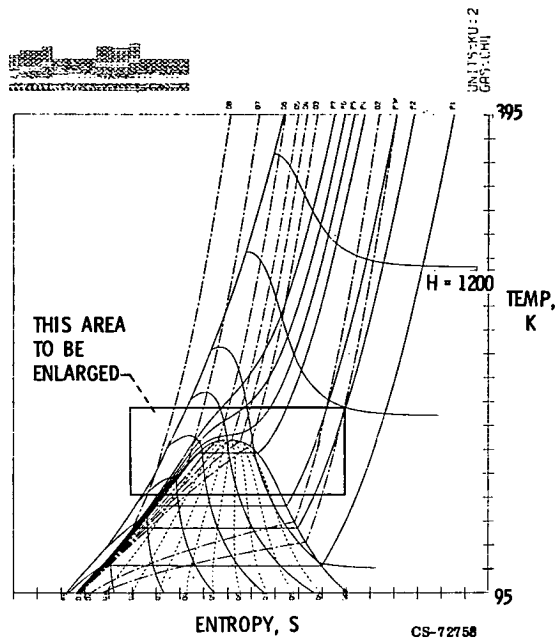

Figure VI-1. - Computer-generated temperature-entropy diagram.

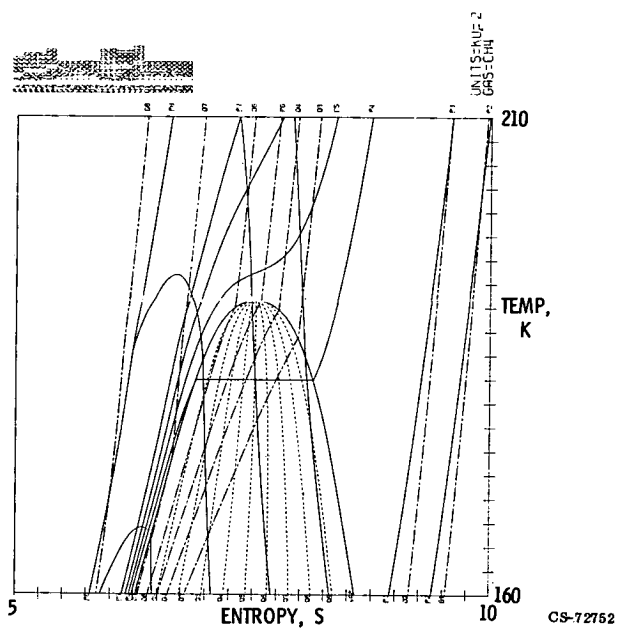

Figure VI-2. - Enlarged portion of temperature-entropy diagram shown in figure VI-1.

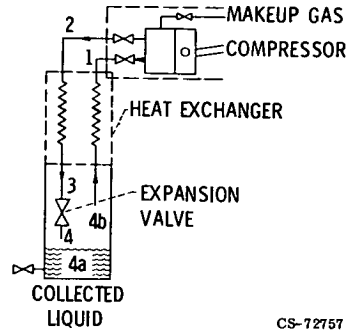

Figure VI-3. - Joule-Thomson liquefier.

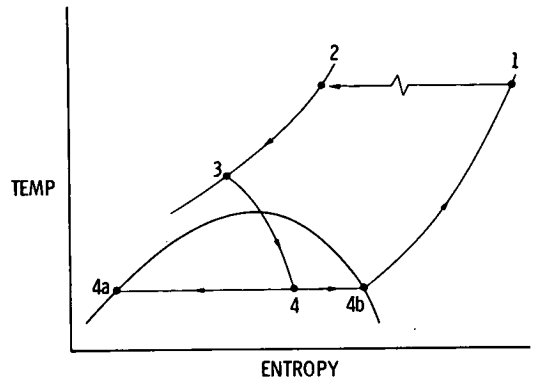

Figure VI-4. - Temperature-entropy diagram for Joule-Thomson liquefier.

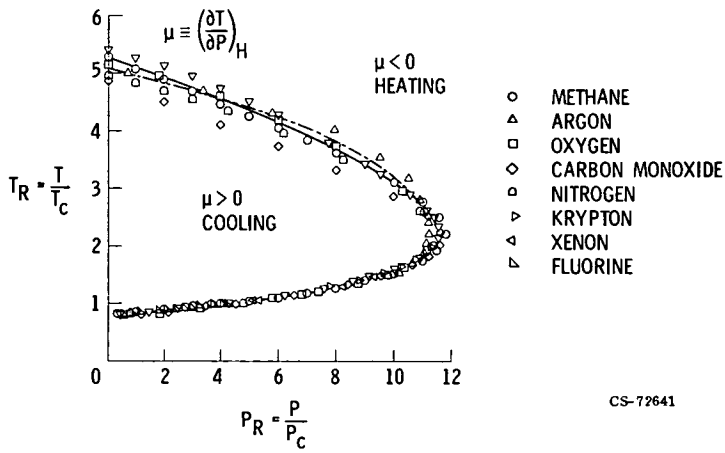

Figure VI-5. - Generalized reduced Joule-Thomson inversion curve.

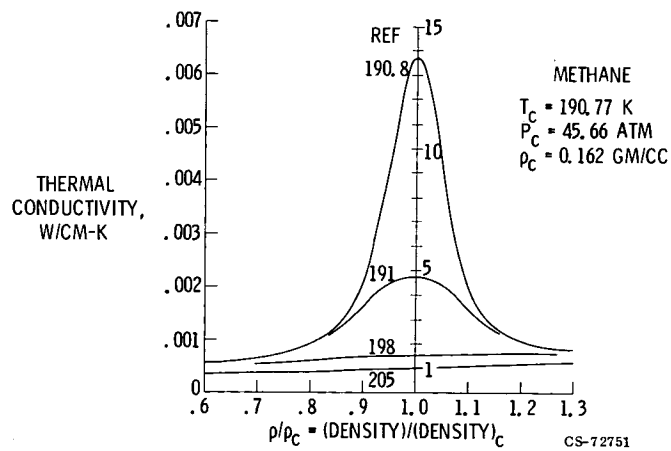

Figure VI-6. - Anomalous thermal conductivity of methane.

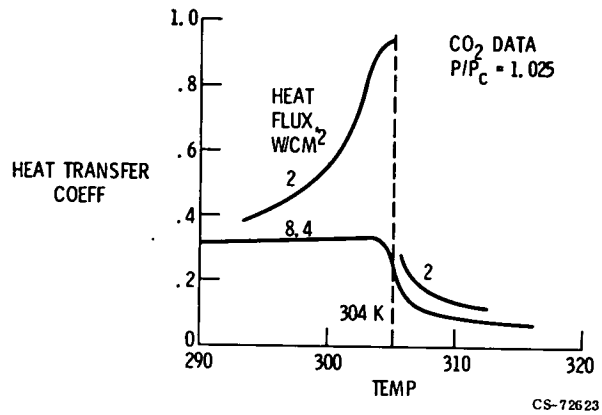

Figure VI-7. - Anomalous heat transfer of carbon dioxide.

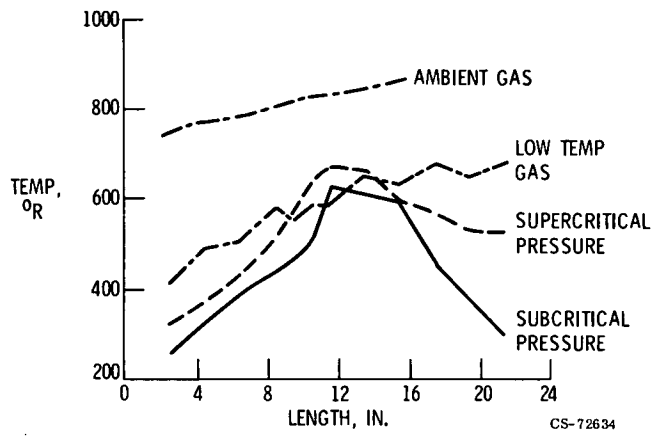

Figure VI-8. - Surface temperature distribution of heated tube as function of tube length.

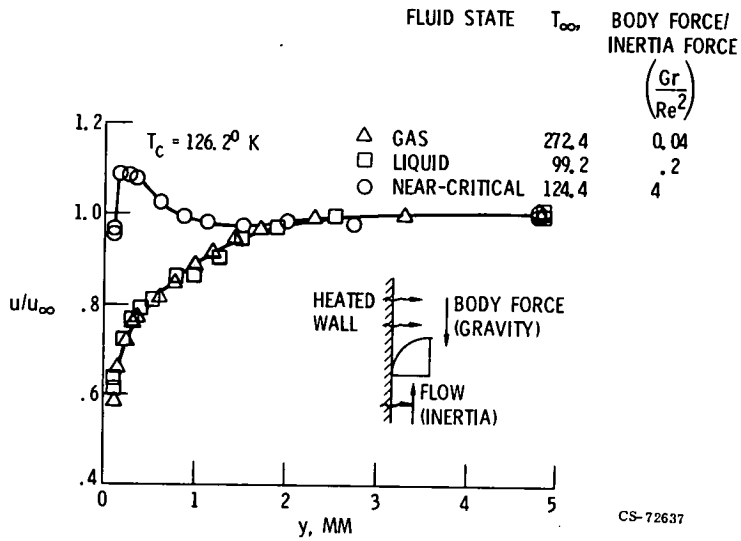

Figure VI-9. - Comparison of velocity profiles for a gas, a liquid, and a fluid near the critical point.

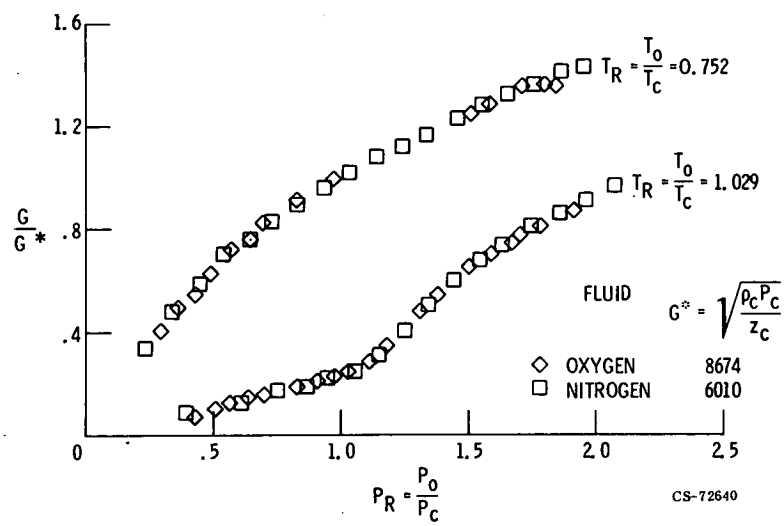

Figure VI-10. - Normalized choked flow of oxygen and nitrogen for two reduced temperatures.

NASA
C8-37856

$C(g), C(s), C_2(g), C_3(g), H(g), O(g)$
$CH(g), CH_2(g), CH_3(g), CH_4(g)$
$C_2H_2(g), C_2H_4(g), H_2(g), O_2(g), N_2(g)$
$CO(g), CO_2(g), H_2O(g), OH(g), HCO$

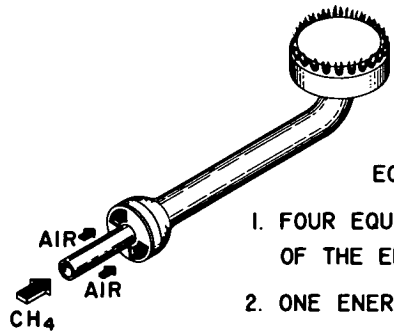

EQUATIONS TO BE SOLVED:

1. FOUR EQUATIONS FOR MASS CONSERVATION OF THE ELEMENTS (C, H, O, N)
2. ONE ENERGY CONSERVATION EQUATION
3. ONE EQUATION SPECIFYING PRESSURE
4. SIXTEEN EQUILIBRIUM CONSTANT EQUATIONS

Figure VI-11. - Air-methane burner and combustion process.

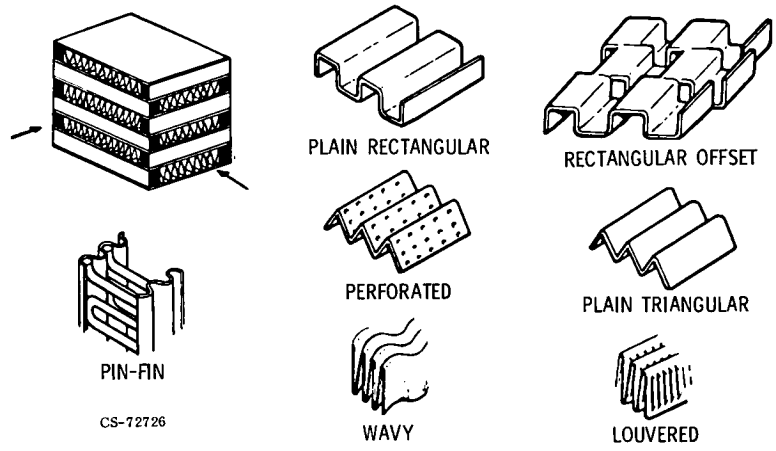

Figure VI-12. - Plate-fin extended surface geometries for heat exchangers.

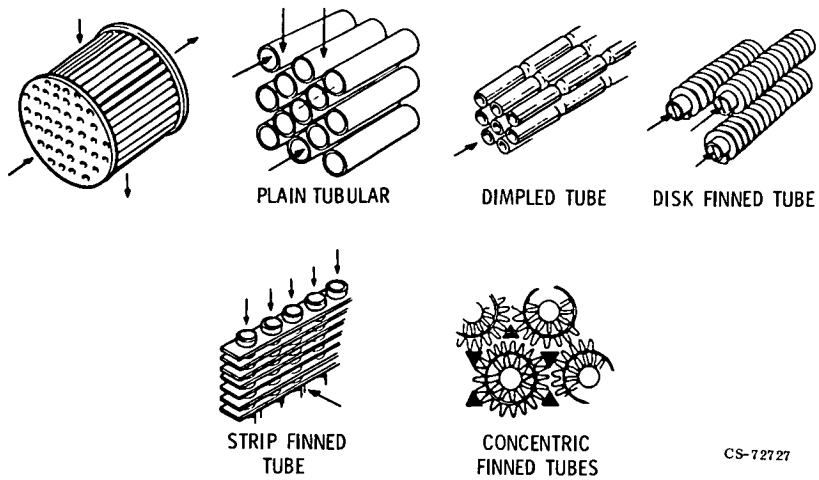

Figure VI-13. - Tubular and extended-surface tubular geometries for heat exchangers.

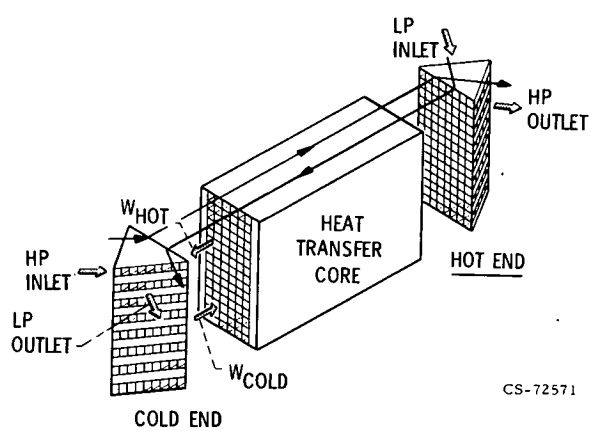

Figure VI-14. - Plate-fin counterflow recuperator with triangular end sections.

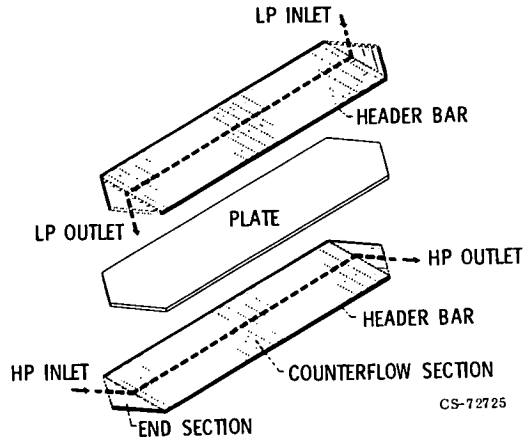

Figure VI-15. - Details of plate-fin recuperator with triangular end sections.

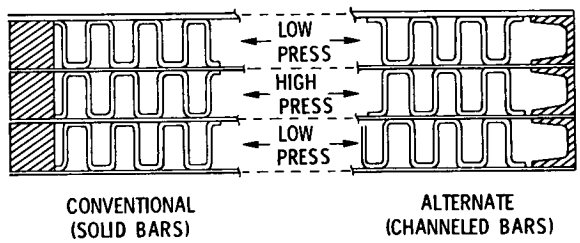

Figure VI-16. - Plate-fin core construction.

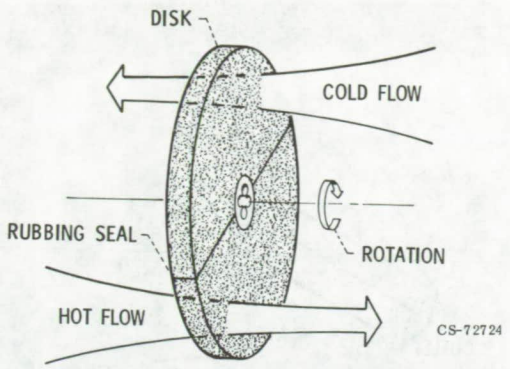

Figure VI-17. - Regenerator flow schematic.

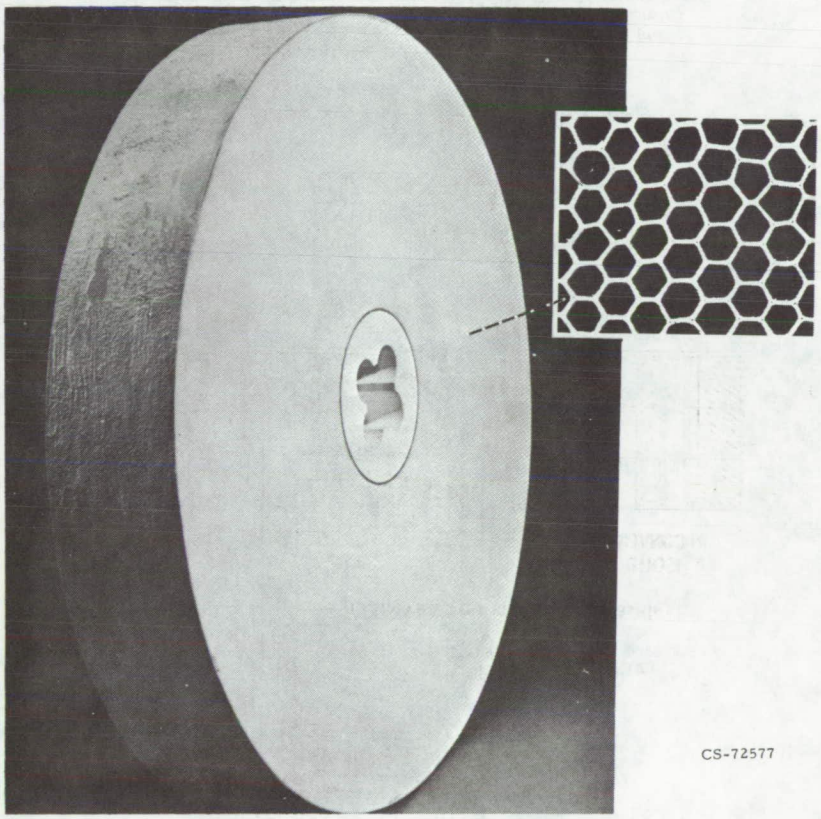

Figure VI-18. - Ceramic regenerator disk.

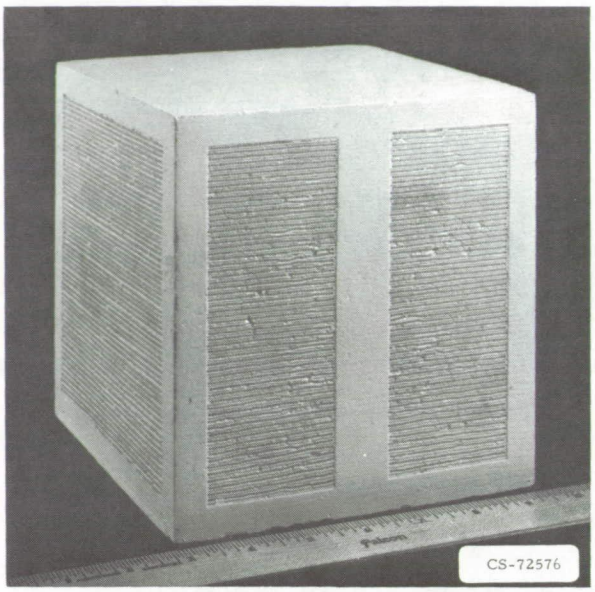

Figure VI-19. - Ceramic recuperator.

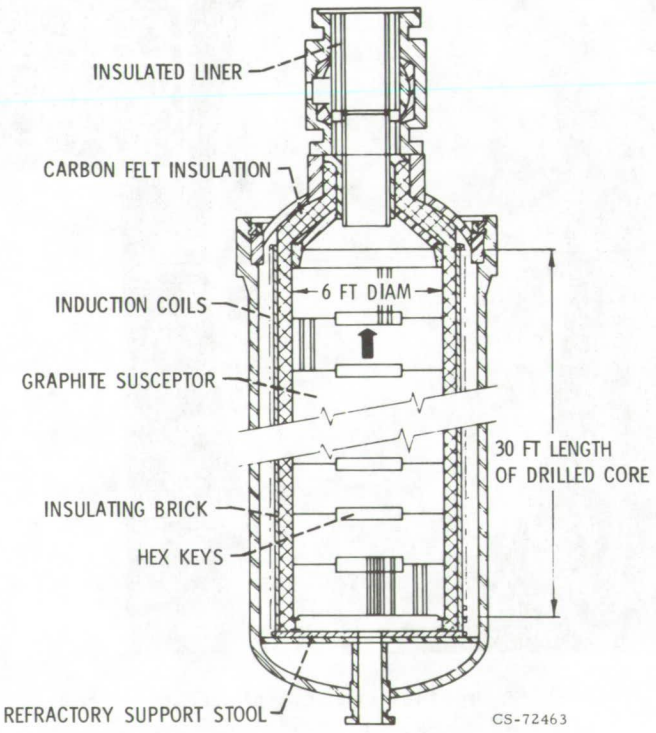

Figure VI-20. - High-temperature (4500° F) nitrogen heater.

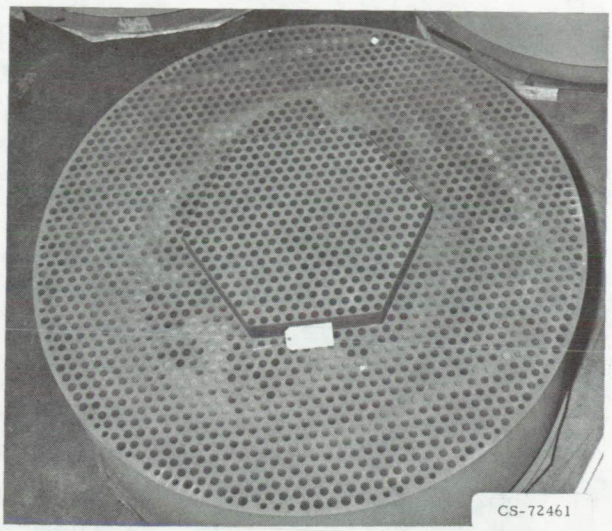

Figure VI-21. - Typical graphite drilled-core section.

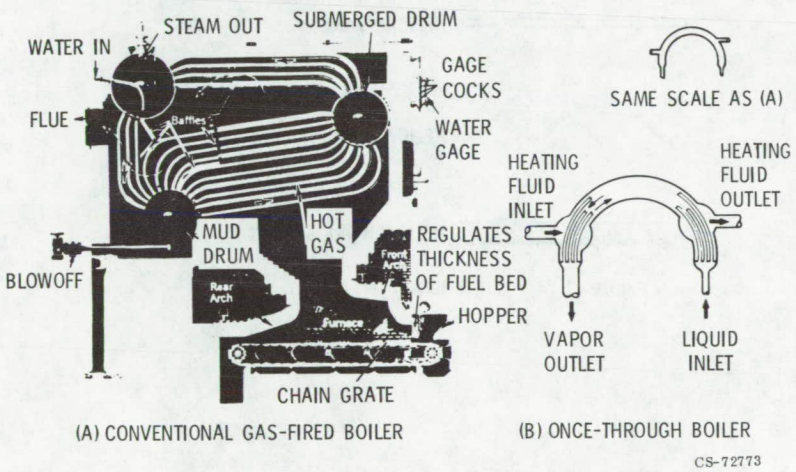

Figure VI-22. - Comparison of conventional and space boilers.

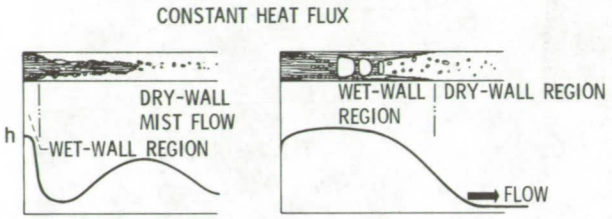

Figure VI-23. - Two-phase-flow models representative of once-through boiler tubes.

CS-72635

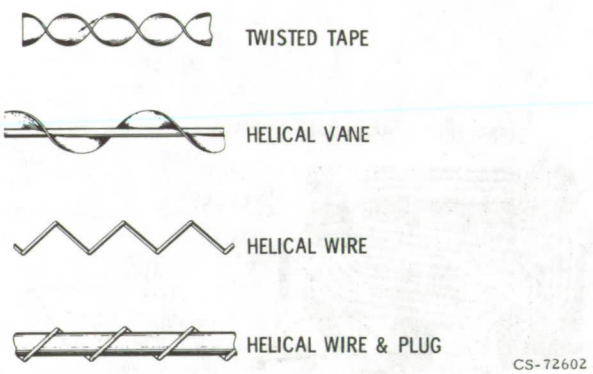

Figure VI-24. - Boiler-tube insert devices.

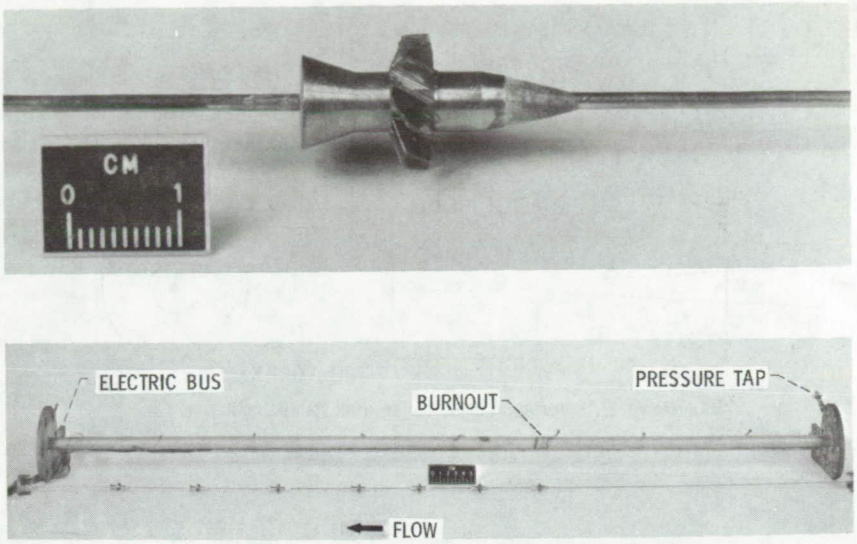

Figure VI-25. - Blade-type helical flow inducers (swirlers). CS-72597

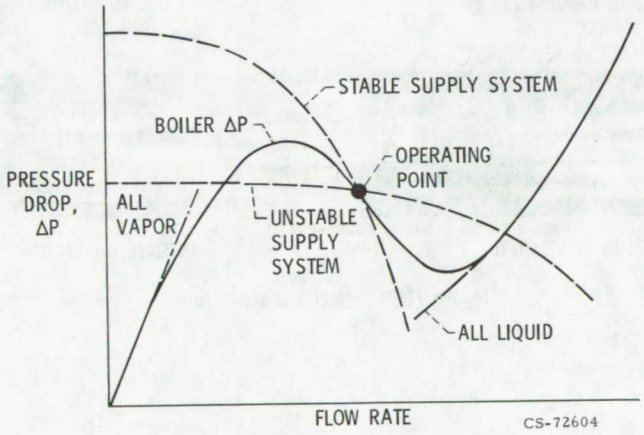

Figure VI-26. - Boiling-film flow-excursion instability.

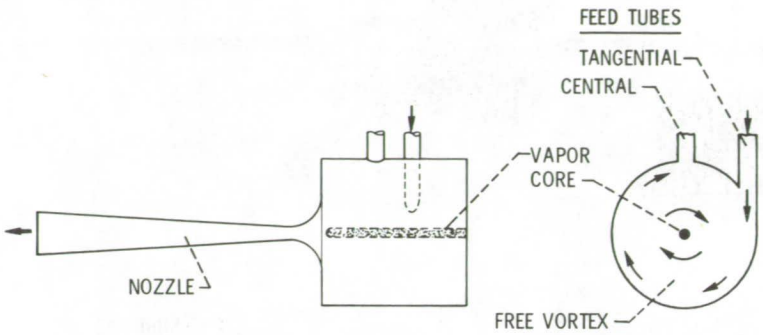

CS-72772

Figure VI-27. - Vortex chamber boiler-inlet stabilizing device.

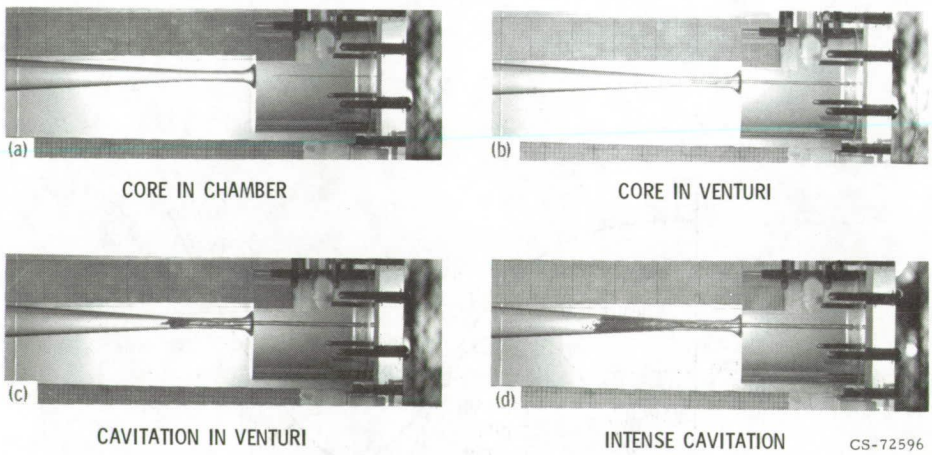

CS-72596

Figure VI-28. - Vortex chamber inlet.

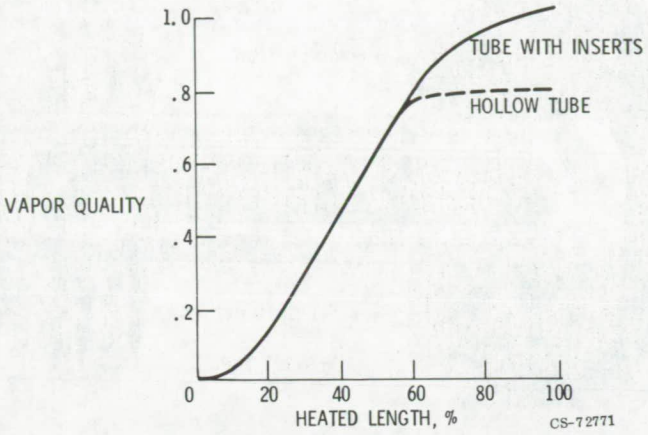

Figure VI-29. - Comparison of water boiler performance between tube with helical wire insert and hollow tube.

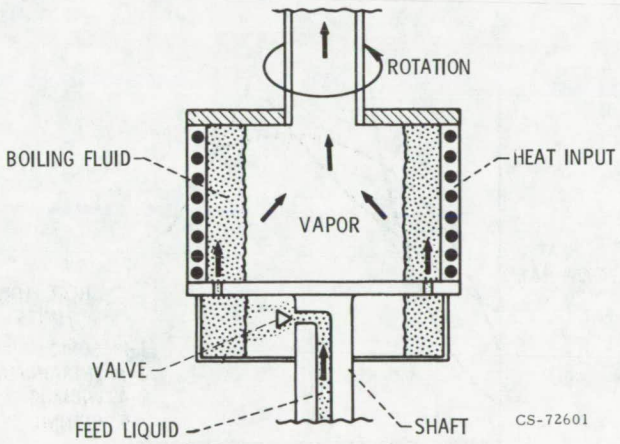

Figure VI-30. - Rotating once-through boiler.

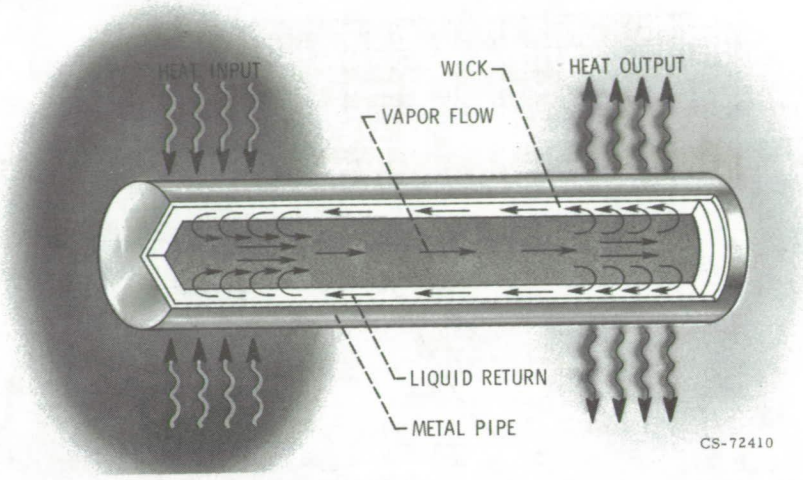

Figure VI-31. - Heat-pipe operation.

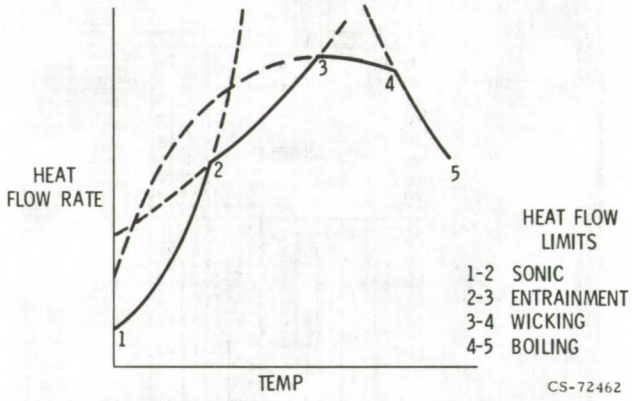

Figure VI-32. - Limiting range of heat-pipe operation.

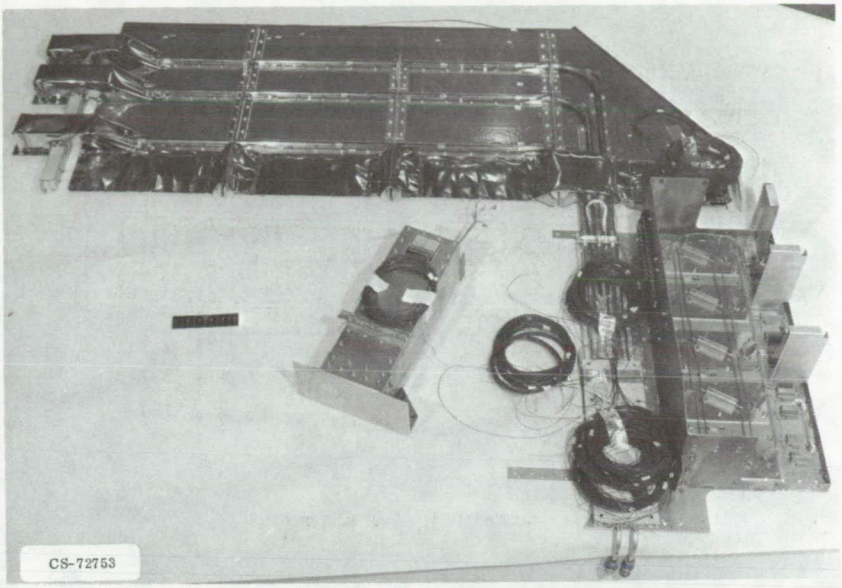

Figure VI-33. - Example of heat-pipe application - CTS spacecraft.

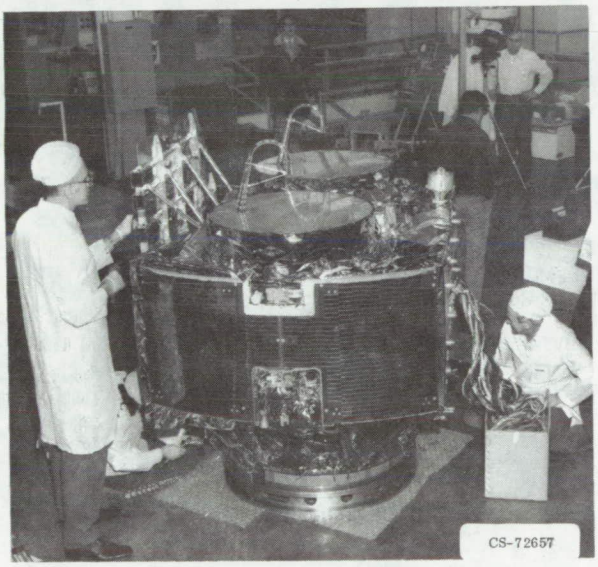

Figure VI-34. - CTS spacecraft.

Page intentionally left blank

Page intentionally left blank

VII. NASA INFORMATION

Jeffrey T. Hamilton*

Current national problems, such as those in energy and environmental pollution, pose a challenge to the transfer and use of aerospace technology. In response to this challenge, NASA has learned much about the problem-solving environment which gives impetus to the transfer process and about how this process can be made easier through an organized and planned effort.

In this presentation, this problem-solving environment is explored and some insight is provided into the structure and operation of NASA's Technology Utilization Program. Finally, the elements and operation of the information system that provide basic documentation and systematic access to the results of NASA's research and development are reviewed.

PERSPECTIVE

Faced with a continuing shortage of its natural gas supply, the Nation's largest city, as well as many other cities and the utility companies serving them, has chosen to use a significant advancement in technology to meet the problem. Four firms in the New York Metropolitan Area (Brooklyn Union, Consolidated Edison, Distrigas, and Texas Eastern) have developed or are in the process of developing ways to handle imported liquefied natural gas (LNG). Liquefied natural gas, because of its storability characteristics, offers great flexibility in use. This use has been promoted by the technological developments emanating from space research and requirements.

For instance, cryogenic transfer methods developed for the space nuclear program were used by Chicago Bridge and Iron to design piping sys-

*Director, Technology Utilization Office, NASA Headquarters, Washington, D.C. 20645.

tems at most large LNG import terminals in the United States. These terminals include the 3 billion cubic foot Distrigas facility in Massachusetts, the 6 billion cubic foot Algonquin facility in Rhode Island, and the 5 billion cubic foot Consolidated System in Maryland.

In addition, the insulations developed by Rockwell International and McDonnell-Douglas for the Saturn S-II and S-IVB stages are being used in new LNG facilities and ships. Of perhaps greatest importance in the development of the LNG technology was that NASA had provided a major market for advanced cryogenic equipment and systems developments like high performance, multilayer insulation. Such insulation is now used extensively in both ground and flight cryogenics storage tanks, railroad dewars, tanks, and pipelines. NASA's requirements created a significant market and development stimulus for materials like single and double aluminized Mylar, which is now available for most LNG systems. Similarly, NASA's requirements in large measure stimulated the development of the cryogenic liquefaction, handling, and storage industry. When the space program began, liquefiers, storage facilities, transportation, transfer lines, valves, seals, burst disks, flow control devices, liquid level sensors, pumps, and even simple connectors for low temperature use were not widely available nor of adequate quality to meet the needs of the space program. NASA was forced to adapt and modify existing industrial gas equipment as the mission requirements called for increased use of liquid hydrogen, oxygen, nitrogen, and helium. The cryogenic industry was thus moved an order of magnitude ahead.

People in the gas industry recognize that the technology of liquefaction and cryogenics is moving rapidly both as a means of storing natural gas and as a means of transporting needed additional supplies. And, if you are in the New York Metropolitan Area you know about the citizens concern for their environment and safety. The tragic fire in an LNG storage tank on Staten Island in 1973 which killed 40 people dramatically highlighted the need for increased attention to this problem (see fig. VII-1).

In the wake of the Staten Island disaster, New York City Fire Commissioner John O'Hagan asked the NASA Technology Utilization Office for assistance since NASA and New York City had already cooperated successfully in a number of other efforts where aerospace technology was adapted to solve problems in the public sector. A meeting was set up in New York City

to review NASA's experience relevant to the Fire Departmen's problems. As a result, projects related to LNG safety were begun at various NASA Centers with periodic review meetings conducted in New York City. The projects include the following:

(1) A risk management system is being developed for all phases of design, construction, operation, and maintenance of LNG and other technologically advanced facilities. Emphasis is placed on hazards identification, control, and elimination. The program is based on the launch experience gained at NASA's Kennedy Space Center in the management of risk situations including man-rating, facilities certification, and hazard identification.

(2) An LNG safety manual is being prepared. There is at present no total compilation of LNG safety information. This program is a follow-on to such widely respected NASA-prepared compilation efforts as the Hydrogen Safety Manual developed at NASA's Lewis Research Center.

(3) Engineers at the Kennedy Center are completing a prototype risk management technique for the New York City Fire Department to use for following LNG plant development and operations. This technique was designed for assessing and minimizing the risks at hazardous facilities such as LNG plants, nuclear power plants, and naphtha plants. The technique is presented in the form of an instructional document to guide the user in operating the risk management system. Also, it will provide a means of identifying risks and developing risk analysis techniques as well as a followup reporting system. Another portion of the Kennedy Space Center effort was a technical analysis of the New York City Fire Deparment's regulations for the manufacture, storage, transportation, delivery, and processing of LNG. This analysis led to recommended changes in the regulations, many of which were accepted by the Fire Department. The New York Fire Department is now in the process of incorporating the risk management system into its operating procedures. They are also evaluating its incorporation into the new computerized Fire Department Management Information System now in the planning stage.

As this example has shown, the technology from the space program continued to be applied to the needs of the gas industry - even to assisting in the community acceptance of a new but necessary technical innovation. Generally, the most effective sources for obtaining technological information in a form which would be best suited to the needs of a particular group

or organization are the professional societies, industrial design codes, and published technical information. For example, NASA's concern for minimizing the weight of flight systems has led to the extensive use of high-strength materials such as the stainless steels and aluminum alloys. The performance of these materials is sensitive to the presence of flaws. To define this sensitivity, researchers at the Lewis Research Center developed the "plane strain fracture toughness test." Now, for the first time, engineers can quantitatively determine the weakening influence of flaws in selected structural materials. Early dissemination of information on the plane strain fracture toughness test was primarily accomplished through ASTM and special technical publications.

Different adoption patterns for fracture mechanics are now appearing. Producers of primary metals, such as Alcoa, have found a growing number of customers demanding guaranteed minimum toughness values for the materials they purchase. Also, in response to similar demands, U.S. Steel conducted a program to determine plane strain fracture toughness of at least eleven commonly used steels. They have also established a working group at their Monroeville (Pa.) facility to evaluate and develop pipeline materials using this technique. The importance of these adoption patterns can be appreciated by those familiar with transmission pipeline construction and operations. Once a crack is started in a pressurized pipeline, it can race along the wall of the pipeline for miles completely unaffected by the pressure being relieved in its wake.

TECHNOLOGY UTILIZATION PROGRAM

Because the Space Act of 1958 challenged NASA to disseminate its research and development widely (fig. VII-2), NASA recognized that the rather informal process of natural diffusion could be enhanced and accelerated by having an organized program. To this end, NASA established the Technology Utilization Program in 1962. The program's structure is as follows:

(1) Industrial applications - "Encourage adaptation and use of NASA technologies in industry":

Publications

Regional centers
Commercialization/user markets

(2) Technology applications - "Apply NASA capabilities and know-how to public problems":
Application teams
Application demonstration projects
State and local government/minority business

(3) Technology transfer and impact studies - "Understand technology transfer and the benefits of aerospace technology":
Case studies
Economic analysis

The Technology Utilization Program's real value is its organized effort to improve the access to the technology emanating from the Nation's research and development effort in aeronautics and space. The Program is especially helpful to those organizations like the New York City Fire Department who would not otherwise have ready access to such information.

The NASA Tech Brief is probably the most widely known technical innovation announcement medium. It is a technical description of an innovation with straightforward explanations of basic concepts and principles. They are often republished in the industrial press (fig. VII-3) in addition to direct dissemination. The Tech Brief reader can obtain more detailed information from a Technical Support Package (TSP). The TSP, which includes test data, drawings, and specifications, is available by contacting the NASA Technology Utilization Officer whose address is provided in the Tech Brief. While aerospace innovations often need to be modified for new applications, the record indicates that strong industrial interest and considerable technology transfer are stimulated by Tech Briefs and TSPs.

As an example, one NASA Tech Brief (fig. VII-4) describes a method for tapping into pressurized pipes without shutting down the system. The method is being used by a major oil company in refinery maintenance operations. The company reports savings in repair time and manpower as well as hazard reduction. Another Brief announced a new high-strength nickel-base alloy (fig. VII-5) that was developed at Lewis Research Center. This relatively low cost alloy has high strength at elevated temperatures, high impact resistance, long service life, and is readily castable. Finally, another Brief (fig. VII-6) describing a high-speed shaft seal generated about

500 inquiries from industry for additional technical information. Several firms are adopting the seal for their own use, and at least one firm is attempting to develop the seal commercially for gas pipeline compressors.

The NASA Industrial Applications Center Program, another major element in the NASA effort to transfer technology, was established in 1963 to foster the transfer of NASA technology to the nonaerospace community, principally the private sector. The transfer function is carried out by Industrial Applications Centers, which are operated under contract to NASA with the assistance of the NASA Technology Utilization Offices at NASA facilities. Five of the Industrial Applications Centers are university operated, and one is operated by a state government organization on a matching-fund basis with NASA.

These Industrial Applications Centers use the computerized NASA technology base as a primary source of technological information to provide individual retrospective and current awareness data searches to industrial clients for a fee which covers the costs of the service. These searches are, for the most part, prepared for a client in response to a specific technical question or specific research and development requirements.

The computerized NASA technology base is a product of NASA's Scientific and Technical Information System. The primary function of NASA's Scientific and Technical Information System is to assemble the results of worldwide aerospace-related research and development activities. It summarizes, indexes, and stores this wealth of knowledge. It helps individuals find and benefit from the particular parts of this mass of technical literature that are most likely to help them solve their problems. The NASA information bank now contains well over a million documents, and thousands more are added to it every month. These government, industry, research institute, and university reports, journal articles, and reviews contain the detailed findings of NASA personnel, contractors, subcontractors, and grant holders. Along with these items, the information bank regularly receives new technical literature and specialized reports, such as project records, patents, etc., from other U.S. Government agencies, laboratories and institutions supported by private industry, and other major sources of aerospace-related knowledge throughout the world.

In response to industrial needs and requirements for access to a total capability for technology information and transfer, the Industrial Applica-

tions Centers also have available a wide variety of other data bases (fig. VII-7) such as Chemical Abstracts, Engineering Index, and American Society of Metals.

Of particular interest, a series of special in-depth bibliographies in the energy field have been prepared under the sponsorship of the Energy Research and Development Administration and NASA (Lewis Research Center, in particular) by the energy information service at the Industrial Applications Center at the University of New Mexico. These include the following:

Heat pipe technology[1]
Solar thermal energy[1]
Hydrogen energy[1]
Remote sensing technology[1]
Wind energy utilization[1]
Deep coal technology
Gas turbine power generation
Energy storage technology
Magnetohydrodynamics (MHD)
Surface transportation propulsion
Geothermal power technology
Electric power transmission
Coal to clean fuel
Waste heat utilization
Geothermal energy

Examples of the subheadings for deep coal technology and gas turbine power generation are as follows:

Deep coal technology:

Overview documents
Mine systems
Mining mechanics
Mining methods
Coal getting equipment and techniques
Electrical and communication systems
Underground transportation
Excavations

[1]Published.

Support systems
Related techniques
Manpower
Safety and health
General information
International coal industry and examples of operating mines

Gas turbine power generation:
Overview documents
Turbine operation
Turbine problem areas
Types and applications
Gas turbine fuels
Gas turbine components
Subassembly components
Waste heat
Related topics
Recent patents

These data bases, which are updated regularly, are available for search from the Industrial Applications Center at the University of New Mexico or through the nearest Industrial Applications Center. We believe that they represent the most comprehensive set of reference material produced for users of energy information.

Although industrial clients served by the centers in 1974 increased 26 percent to over 4000 and fees paid by clients exceed $960,000, the information services provided by the Industrial Applications Centers, though fundamental to the technology transfer process, are also augmented by NASA Center technical and scientific skills to provide user groups with a better understanding of the application and utility of technology to their specific needs - be it problem solving or new product development.

One example of a NASA Center cooperative effort with an Industrial Applications Center is the trans-Alaskan pipeline. At first glance, the heat pipes used in Skylab would seem to have little bearing on the Alaskan pipeline environmental controversy. Yet, the Skylab heat pipes contributed significantly to solving an Alaskan pipeline environmental problem. Although the principles of heat pipe operation were demonstrated during World

War II, there was little concentrated research and development until the space program required a reliable device with highly effective thermal conductivity. Heat pipes are used routinely in spacecraft to provide cooling for electronic packages so that environmental control can be maintained aboard satellites.

The NASA Industrial Applications Center at the University of New Mexico established a heat pipe program to collect, organize, and disseminate technical information. The center publishes a continuing bibliography in the field and conducts short courses on heat pipes. Engineers from Alyeska, the trans-Alaskan pipeline consortium, have attended the short courses and otherwise used NASA information as well as other heat-pipe information gathered by the center. In addition, scientists at NASA's Goddard Space Flight Center worked directly with Alyeska in the heat-pipe design. The NASA Industrial Applications Center at the University of Southern California was also involved in this effort. It provided technology services to Mechanics Research Corporation which was selected by the Department of the Interior to review the design and monitor startup construction of the pipeline.

The pipeline will be supported above the Arctic tundra by piles with internal heat pipes extending many feet into the permafrost (fig. VII-8). Operating as a thermal diode, the heat pipes will help freeze the soil to full depth in the fall when air temperatures are low. During this time, the heat pipes will absorb heat from the ground and more it upward into the atmosphere. In the summer, the heat pipes will be inactive and the permafrost will thaw only near the surface. If a solid mass of permafrost is maintained around each supporting pile, the shifting of the soil will be reduced and pipeline settling will be avoided. Without this thermal protection, the uncontrolled freezing and thawing of the soil could stress the crude oil line to the point of rupture. Protecting the tundra environment by keeping the permafrost frozen was a significant consideration in passing the pipeline bill.

McDonnell-Douglas Corporation, under contract to Alyeska, will produce the heat pipes for this vast project which spans 798 miles from the oil field at Prudhoe Bay on the Arctic coast of Alaska to the marine tank ship terminal at Valdez, the ice-free port in the south-central part of the state. The heat pipes (trade name, Cryo-Anchor Stabilizers), which were devel-

oped using NASA technology, are 2 and 3 inches in diameter and range in length from 30 to 60 feet. Some 110,000 units are being built at the Tulsa (Oklahoma) Plant of McDonnell-Douglas for delivery beginning in January 1975.

Another example provides additional insight into the operations of the Industrial Applications Centers. Recommendations for improving the reliability of electromagnetic coils, supplied by the Industrial Applications Center at Indiana University and the Lewis Research Center, enabled the Duncan Electric Company to increase the life expectancy of its manufacturing process equipment by nearly 1400 percent (fig. VII-9). The firm indicates that, with a modest expenditure for assistance from the Industrial Applications Center, the first year savings are likely to approach $150,000.

Space flight could never have been achieved without computer technology. NASA pioneered in the development of highly complex computer programs in such areas as information storage and retrieval, reliability assurance, inventory control, and structural analysis. Since these programs have wide application in industry, NASA established a special nonprofit center called COSMIC at the University of Georgia to make all of these programs available to U.S. industry at very nominal prices. COSMIC, or the Computer Software Management and Information Center, collects all of the computer programs NASA develops (as well as some of the best programs developed by the Department of Defense and other government agencies), verifies that they operate properly, and then adds them to their inventory of software available for immediate use by industry. A program's price, which depends on its size and complexity, generally ranges from $500 to $1000. Program documentation is available separately so that a prospective purchaser may fully evaluate the software and ensure that it will meet his needs; this usually costs less than $25. To announce the availability of each program, COSMIC prepares an abstract which is published in a catalogue of NASA software called the Computer Program Abstracts Journal. The CPA Journal contains abstracts of the more than 1500 computer programs in COSMIC's inventory.

One very popular software package, called NASTRAN, has been used by hundreds of firms ranging in size from General Motors to one-man consulting organizations. NASTRAN is used to perform all types of structural

analyses and is reported to have affected hundreds of millions of dollars of industrial production.

There are also programs available from COSMIC which are specifically applicable to energy research and development and properties. One frequently requested program, developed by the DOD, is used to analyze or calculate sizing parameters/and stresses within complex piping systems. Two NASA programs for calculating the thermodynamic properties of fluids in operating systems have also found wide use. One program recently acquired through an international software exchange with Canada, which simulates line voltages and currents in radial electrical power distributions systems, is now available. Another, called Multiwick, is used to analyze a wide varity of heat pipe designs such as those described in the Alyeska pipeline example. Furthermore, there are programs to simulate the performance of nickel-cadmium batteries, analyze and monitor electrical power system performance, design electric transformers, and analyze thermal safety aspects of gas-cooled nuclear power plants.

COSMIC also has a number of less technical programs, such as those to monitor and improve the performance of an entire process installation. Whatever business a firm is in, if it uses a computer, there is likely to be a program in COSMIC's inventory which could improve efficiency, help solve a problem, or satisfy a software need.

To summarize, the Industrial Application Centers' products and services are as follows:

Technology information services:

- Current awareness
- Retrospective search
- Abstract analysis
- Documents/photographs

Technology consulting services:

- Problem identification
- Suggested solutions

Technology conferences/seminars

SCIENTIFIC AND TECHNICAL INFORMATION SYSTEM

The NASA information system has the mission of providing scientific and technical information support to NASA itself, the aerospace community, and to the Technology Utilization Program. The preceding section outlined the various publication mechanisms and documentation services provided by the Technology Utilization Program to promote access to aerospace technology. These mechanisms and services, however, finally depend on the systematic efforts that have been made to acquire, store, and retrieve the documentation of the aerospace R&D experience.

The sources of documents for the NASA STI system are shown in figure VII-10. On the left, input by NASA, NASA contractors, and NASA grantees is shown. NASA research centers submit reports of their inhouse research and development. NASA contracts and grants require that copies of each technical report be submitted for processing into the data base. As shown in the second segment, documents also are received from government agencies other than NASA. These include the Department of Defense, Department of Commerce, Energy Research and Development Administration, and the Department of Transportation, among others. The third group of sources comprises the industrial community, academic institutions, and private research establishments as they publish reports of research and development not supported by government contract. The fourth group, which is that of foreign exchanges, consists of some 300 agreements between NASA and foreign sources located in 60 different countries.

Figure VII-11 shows the proportions of documents in the data base obtained from various sources: 20 percent were received from DOD and its contractors, 22 percent from NASA and its contractors, 7 percent from ERDA (formerly AEC) and its contractors, 14 percent from other domestic organizations, 14 percent from USSR and the Soviet Bloc, and 23 percent from other foreign sources. Note also that the documents in foreign languages amount to approximately 14 percent of the total. It should be noted that this breakdown includes the International Aerospace Abstracts accessions from the open literature of journals, books, and conference papers.

The processing flow in STI operations is shown in figure VII-12. After a document has been acquired, it goes through the input processing operation which consists of duplicate checking, subject evaluation, cataloging,

indexing, and abstracting. Processing is then split into two paths, the handling of the bibliographic data and the handling of the document itself. In the first path, the input data are keyed into the computer (direct online keypunching to disk storage). As shown on the chart, the data base is then used to prepare the announcement journals Scientific and Technical Aerospace Reports (STAR), Computer Program Abstracts (CPA), the indexes to International Aerospace Abstracts (IAA), and the current awareness service SCAN (Selected Current Aerospace Notices). The computer also operates on the data base to produce the NASA continuing bibliographies, indexes, and chronologies, and supports the RECON literature searches at the NASA Centers.

Processing the document involves sorting, microfilming, distributing microfiche copies to qualified requesters, and then storing the documents.

Figure VII-13 illustrates the dissemination pattern for NASA information. The announcement media are SCAN, IAA, and STAR. While SCAN is primarily an internal announcement tool, IAA and STAR are widely available in libraries across the country and both journals can be purchased from the Government Printing Office. Each document citation in these media includes a notice of where the document itself may be obtained.

NASA publications and sponsored documents are also available at a large number of public, university, and other libraries. The most nearly complete collections, however, are available at the public libraries (usually the central ones) in the following cities:

California: Los Angeles, San Diego
Colorado: Denver
Connecticut: Hartford
Delaware: Wilmington Institute Free Library
Maryland: Enoch Pratt Free Library, Baltimore
Massachusetts: Boston
Michigan: Detroit
Minnesota: St. Paul, Minneapolis
Missouri: Kansas City, St. Louis
New Jersey: Trenton
New York: New York, Brooklyn, Buffalo, Rochester
Ohio: Cleveland, Cincinnati, Dayton, Toledo, Akron
Oklahoma: Oklahoma City
Tennessee: Memphis
Texas: Fort Worth, Dallas
Washington: Seattle
Wisconsin: Milwaukee

In addition, NASA's technical documents and bibliographies are deposited in 11 special libraries. Each library listed below is prepared to furnish to the general public services of personal reference, interlibrary loads, photocopies, and help in obtaining personal copies of NASA documents by microfiche if requested. These special libraries are located as follows:

California: University of California Library, Berkeley

Colorado: University of Colorado Libraries, Boulder

District of Columbia: Library of Congress

Georgia: Georgia Institute of Technology, Atlanta

Illinois: The John Crerar Library, Chicago

Massachusetts: Massachusetts Institute of Technology, Cambridge

Missouri: Linda Hall Library, Kansas City

New York: Columbia University, New York

Pennsylvania: Carnegie Library of Pittsburgh

Texas: Southern Methodist University, Dallas

Washington: University of Washington Library, Seattle

Finally, primary and secondary distribution provide for document availability within NASA, the aerospace community, and at the depository libraries. It is the "search service," however, offered by the following Industrial Application Centers that provides the industrial community with computer access to the information bank in specific and selective ways tailored to their clients' particular interests:

Aerospace Research Applications Center (ARAC)
Indiana University
400 E. 7th Street
Bloomington, Indiana 47401

Dr. Robert D. Shriner, Director
Phone: (812) 337-7833

Technology Application Center (TAC)
The University of New Mexico
Alburquerque, New Mexico 87131

Computer Software Management & Information
Center (COSMIC)
Suite 112, Barrow Hall
The University of Georgia
Athens, Georgia 30601

Thomas W. Quigley, Jr., Director
Phone: (404) 542-3265

Knowledge Availability Systems Center (KASC)
University of Pittsburgh
Pittsburth, Pennsylvania 15260

Edmond Howie, Associate Director
Phone: (412) 624-5212

New England Research Application Center (NERAC)
Mansfield Professional Park, Box U-41N
The University of Connecticut
Storrs, Connecticut 06268

Dr. Daniel U. Wilde, Director
Phone: (203) 486-4533

North Carolina Science and Technology
Research Center (NC/STRC)
P.O. Box 12235
Research Triangle Park, North Carolina 27709

Peter J. Chenery, Director
Phone: (919) 549-8291

Western Research Application Center (WESRAC)
University of Southern California
809 West 34th Street
Los Angeles, California 90007

Radford King, Director
Phone: (213) 746-6132

Figure VII-1. - LNG storage tank fire.

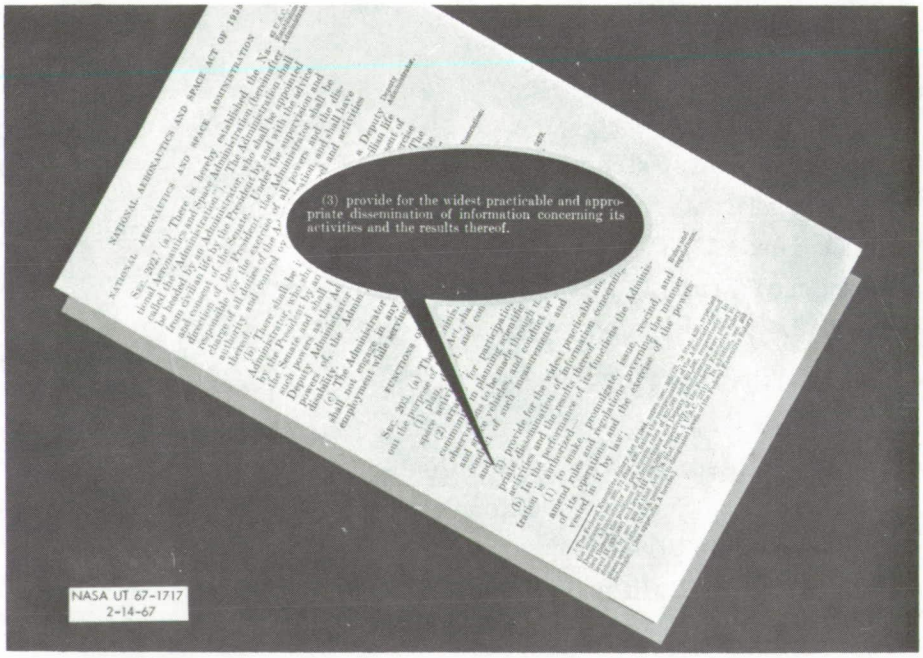

Figure VII-2. - National Aeronautics and Space Act of 1958.

Figure VII-3. - Industrial press.

July 1972

B72-10385

NASA TECH BRIEF

Lewis Research Center

NASA Tech Briefs announce new technology derived from the U.S. space program. They are issued to encourage commercial application. Tech Briefs are available on a subscription basis from the National Technical Information Service, Springfield, Virginia 22151. Requests for individual copies or questions relating to the Tech Brief program may be directed to the Technology Utilization Office, NASA, Code KT, Washington, D.C. 20546.

Noncontaminating Technique for Making Holes in Existing Process Systems

A technique has been developed for making cleanly-contoured holes in assembled process systems without introducing chips or other contaminants into the system. Such holes are often required for instrumentation ports, bypass lines, sampling station lines, and system observation holes. This technique uses portable equipment and does not require dismantling the system.

Normally, making access holes in process piping involves removing sections of the system. The holes are drilled, and the section cleaned and reinstalled in the system. Since this method involves disassembly and reassembly, the system must usually be retested for leaks.

In this new technique, a blind pilot hole is drilled part way through the piping or vessel wall, the system is pressurized with an inert gas to a pressure of approximately 7.5 to 13-cm of water (3 to 5 inches), the hole is completed by heating with a welder to melt the remaining wall material, and the molten metal is pushed outward by the pressure in the system.

The blind pilot hole is drilled with a hand-held electric drill to within 0.127 to 0.152-cm (0.050 to 0.060 inch) of the inner wall. This remaining metal thickness was chosen as the minimum allowable as a safety factor to prevent breaking through the pipe wall during the drilling process. The pilot hole is then flat-bottomed with either an end mill or a bottoming drill. The pilot hole is then countersunk with a ball-type rotary file to form an area for the metal to flow into during the melting process. A cross-sectioned drawing of a typical blind pilot hole is shown in Figure 1. Holes up to 0.635-cm (0.250-inch) diameter have been made with a 0.95-cm (3/8-inch) diameter pilot hole and a 1.59-cm (5/8-inch) diameter rotary file as the countersink.

The hole is completed by pressurizing the closed-loop system to 12.7 -cm (5 inches) of water and melting through the remaining metal thickness with a welding machine. The completed hole is usually small initially, and can be increased in size by additional melting (aftermelt). For the aftermelt phase, internal pressure is maintained at one inch of water to keep the metal flowing toward the outside of the pipe. Figure 2 is a photograph of the cross section of a hole in 0.25-inch thick Inconel tube. As can be seen from the photo, all the metal from the bottom of the pilot hole flowed to the countersunk area. There was no buildup of metal on the inside of the tube, and no contaminants were found inside the test section.

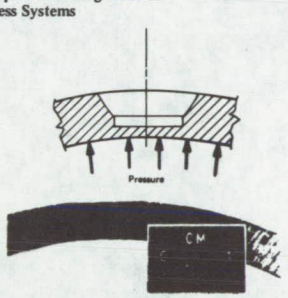

On pipes having wall thickness around 0.127 to 0.152 cm (0.050 to 0.060 inch), no pilot hole is drilled and no aftermelt is performed. The hole size is determined by the pressure on the inside of the pipe during the melting phase. A pressure of 5-cm (2 inches) of water results in about a 1.27-cm (½-inch) diameter hole. A pressure of 7.5 cm (3 inches) of water results in about a 0.95-cm (3/8-inch) diameter hole. For these thin-walled pipes,

(continued overleaf)

Figure VII-4. - Sample NASA Tech Brief.

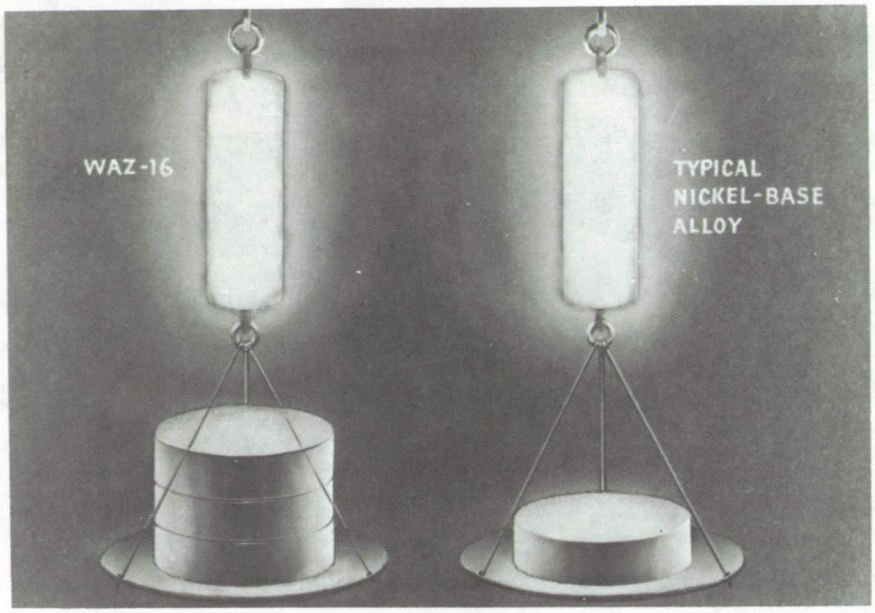

Figure VII-5. - High-strength nickel-base alloy (WAZ-16) three times stronger at 2200° F than strongest cast nickel-base alloy and costs one-third less.

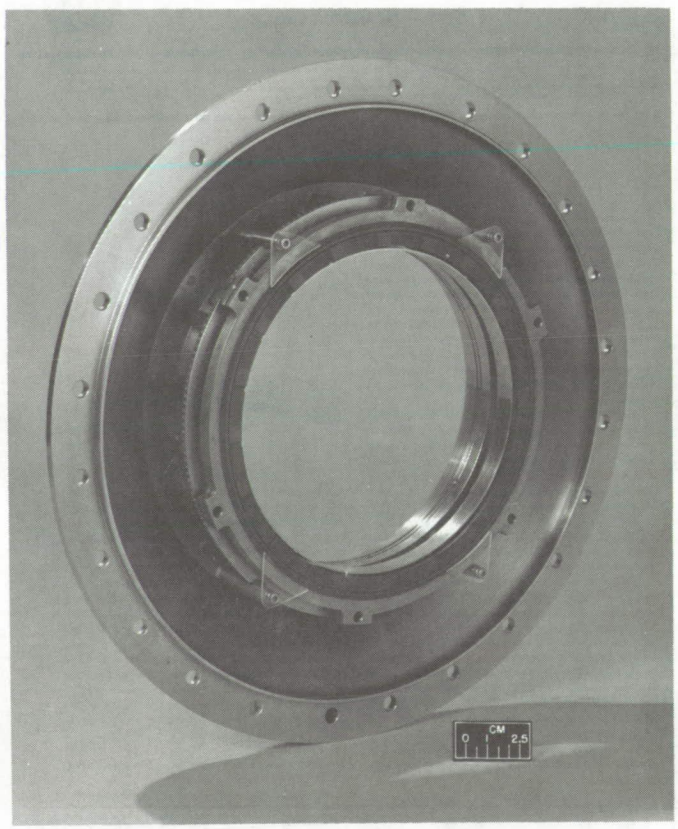

Figure VII-6. - High-speed, self-acting, face-contact shaft seal.

IAC DATA BASES

- NASA STI FILE (1,000,000)
- GOVT. REPORTS ANNOUNCEMENTS (GRA) - (292,000)
- ENGINEERING INDEX (EI) - (300,000)
- EDUCATIONAL RESOURCES INFORMATION CENTER (ERIC) - (189,000)
- CHEMICAL ABSTRACTS CONDENSATES (CAC) - (200,000)
- AMERICAN SOCIETY FOR METALS (ASM) - (200,000)
- OTHER DATA BASES - (3,400,000)

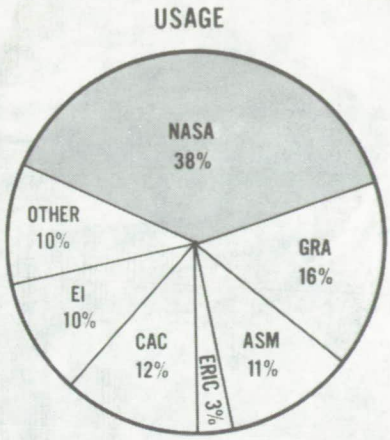

NASA HQ N74-6199
10-21-74

Figure VII-7. - Industrial Application Centers' data bases.

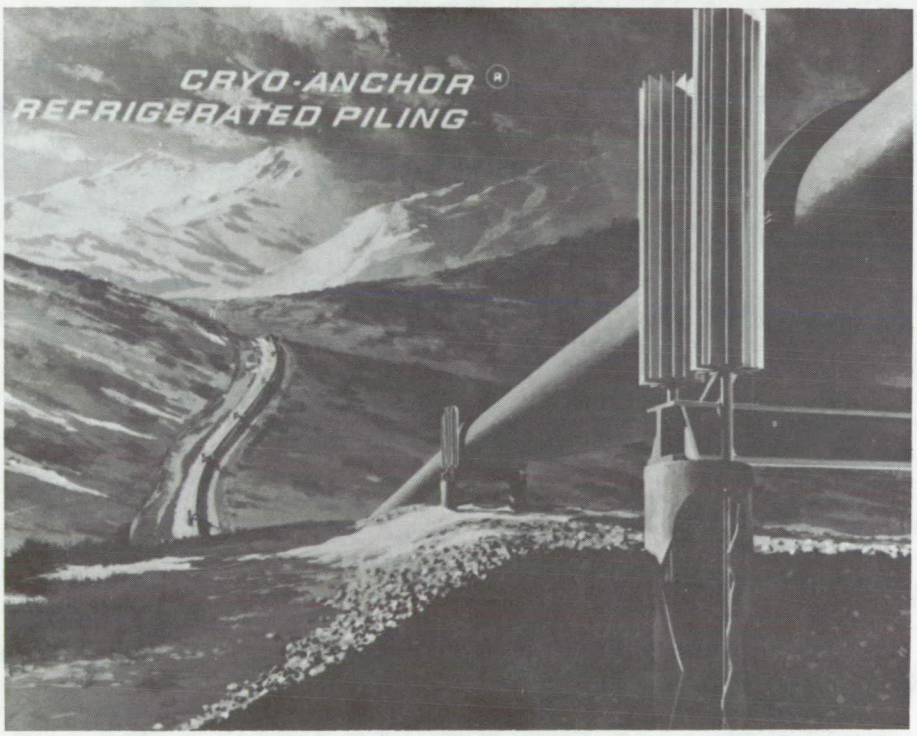

Figure VII-8. - Heat pipes used on trans-Alaskan pipeline.

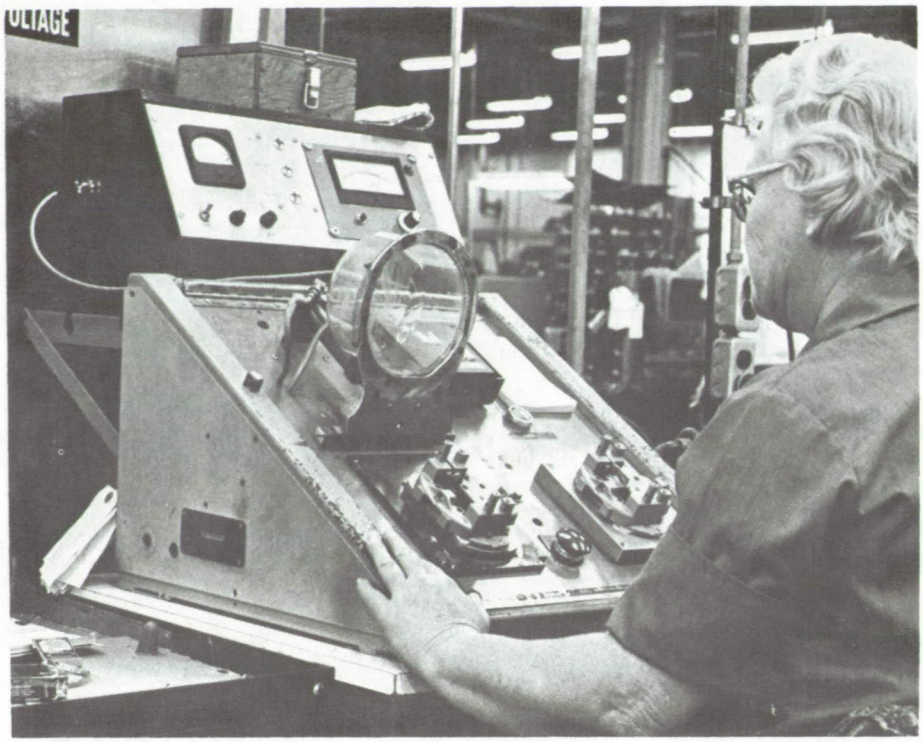

Figure VII-9. - NASA technology and manufacturing processes.

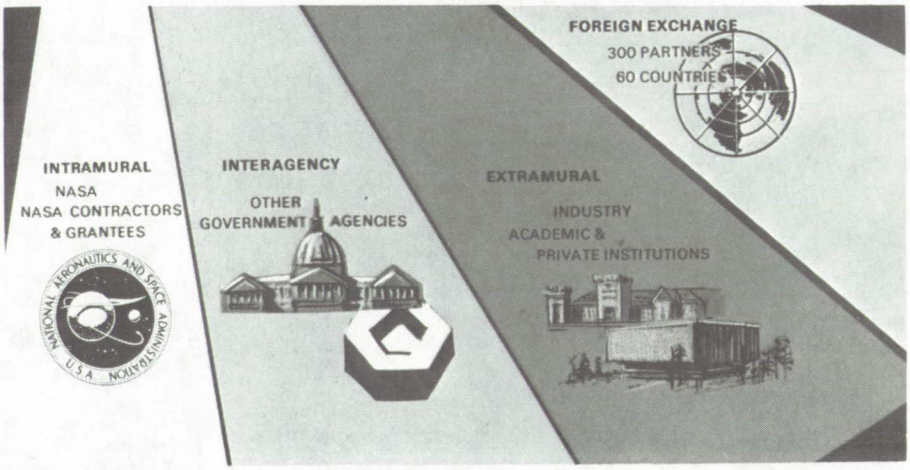

Figure VII-10. - Sources of NASA scientific and technical information.

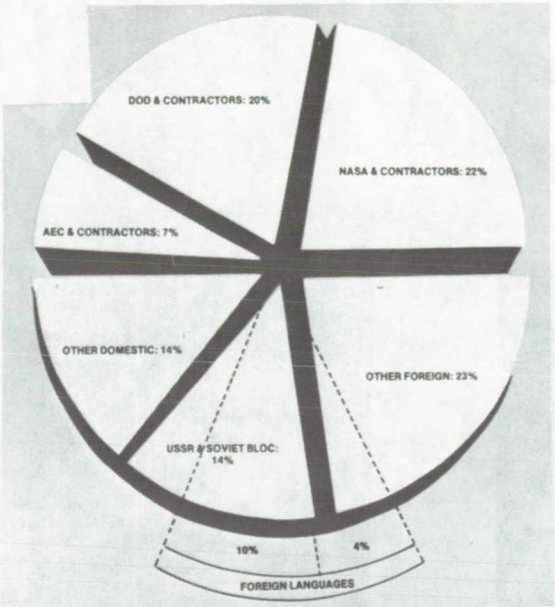

Figure VII-11. - Origin of documents.

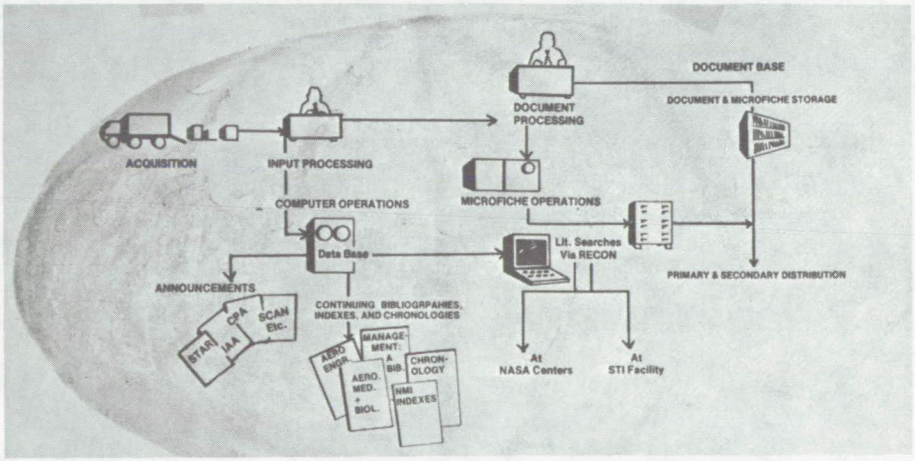

Figure VII-12. - Processing flow in Scientific and Technical Information System.

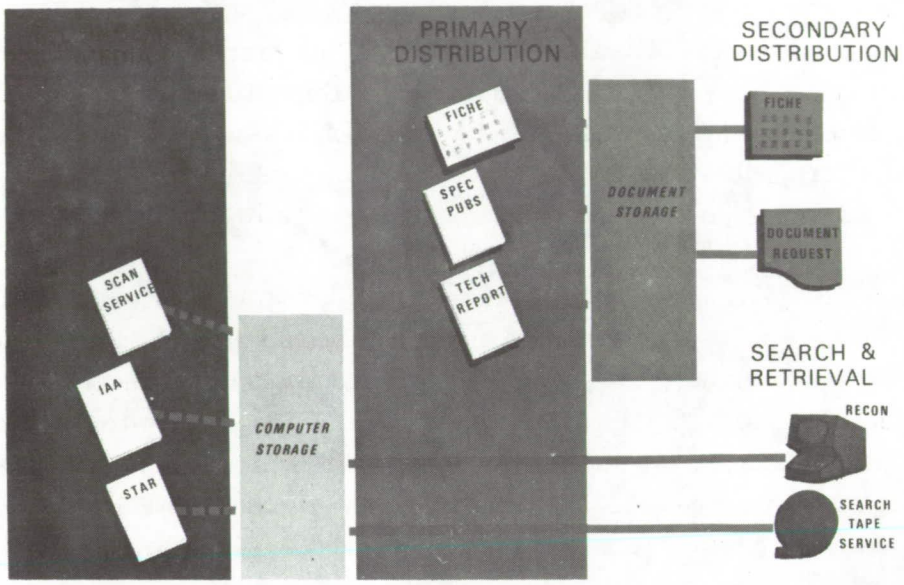

Figure VII-13. - Dissemination of information.

VIII. INSTRUMENTATION AND MEASUREMENT

Norman C. Wenger, Lloyd N. Krause, and William C. Nieberding

Present efforts in many areas of research, manufacturing, and distribution are impeded by the inability to make certain critical measurements. In some cases the measurements can be made but at a much reduced speed or accuracy from that desired. In some cases the cost may be prohibitive. In other cases, the measurements cannot be made at all with existing technology.

NASA has instrumentation and measurement programs covering virtually all areas of aerospace technology. Program emphasis is on increased capability, performance, and economy. Three main topics from NASA's instrumentation program will be discussed herein: the custody transfer of gases; instruments for the testing and monitoring of machinery - specifically large industrial gas turbines; and data handling and control. The instrumentation technology that is presented is embodied in either actual working hardware or in instrumentation being constructed.

CUSTODY TRANSFER OF GASES

A gas flow metering device that has been receiving recent interest is the sonic nozzle. The sonic nozzle has been used in the aerospace field for over a decade and in the last few years it is finding applications in the metering of natural gases both in the United States and in Europe. One of its advantages is that it can serve as a prover or working standard for calibrating meters at the operating pressure of the meter. It is not limited to operation at only 1 atmosphere pressure like the commonly used bell-type prover. This eliminates extrapolation uncertainties because the meter can be calibrated at the exact conditions of intended use.

Figure VIII-1 shows a cross section of a sonic nozzle. It is called a

sonic nozzle because sonic velocity exists at the throat. These nozzles are also called critical flow or choked nozzles. The upstream diameter is generally about four times the diameter of the throat. The bellmouth entrance is usually circular arc in shape and is followed by a diffuser section that reduces the pressure drop needed to produce sonic flow at the throat. With a diffuser, sonic velocity can be achieved in the throat with a pressure drop across the nozzle as small as 10 percent. When the nozzle is operating sonically, the mass flow rate can be expressed as shown by the equation in figure 1 where $\dot{m}$ is the mass flow rate, C_D is the discharge coefficient, and A is the throat area. The term φ depends on the gas being metered and is a function of the specific heat ratio and the gas constant. For a perfect gas φ is a constant. For a real gas φ not only depends on the gas being metered but also is a function of both pressure and temperature. The last terms in the equation in figure VIII-1 show that the flow is directly proportional to upstream pressure and inversely proportional to the square root of the temperature.

To use the sonic nozzle as a proving device, it is placed in series with the meter to be calibrated. The meter is usually placed upstream of the nozzle to avoid any effects of the high-speed flow that are generated in the nozzle throat. If the meter being calibrated is a volume flow rate meter, the density at the test meter must be known to convert $\dot{m}$ into volume flow rate. This requires measuring the pressure and temperature at the test meter location.

One of the features of the sonic nozzle is that it is quite immune to damage compared to other types of flow meters. It has no moving parts and nothing protrudes into the gas stream. Also, there are no sharp edges which can possibly erode.

Another feature is that the flow is directly proportional to the upstream pressure. This gives the device good rangeability and the linear variation of flow with pressure is valuable when using the nozzle in a flow control system. It is generally simple to measure the upstream pressure accurately since the velocity in the upstream section is usually low enough so that a simple pipe tap is sufficient. The nozzle is also unaffected by downstream disturbances such as pumps or other pressure fluctuations. Such fluctuations cannot propagate through the sonic flow plane at the nozzle throat.

Another feature of the sonic nozzle is the ability to predict or compute

the flow without performing a calibration. Three factors are involved in the prediction. Two of them are in the discharge coefficient. The main one involves the low velocity flow in the boundary layer along the wall in the curved portion of the nozzle. This low velocity region can cause the discharge coefficient to be as much as a few percent below unity. The second factor comes from changes in the velocity profile across the throat plane caused by the inertia of the gas going through the curved bellmouth. This effect is usually less than 1 percent.

Figure VIII-2 shows how accurately the discharge coefficient can be predicted. The coefficient is plotted against Reynolds number which is a nondimensional index of the flow. The data in figure VIII-2 are for a small sonic nozzle that was calibrated under real gas conditions with pressures ranging up to 1500 psi. The black dots are experimental data points, and the curve labeled "Measured" is a mean curve which has been drawn through the points. The calculated curve is for the case where the nozzle boundary layer is assumed to be turbulent. From the difference between the measured and calculated curves, it can be seen that the discharge coefficient can be predicted to within about 1/4 percent without resorting to a calibration.

The third factor in predicting the flow rate involves the calculation of the quantity φ. For a gas such as methane or natural gas, φ can deviate from the ideal by a considerable amount as shown in figure VIII-3. The deviation of φ from the ideal, in percent, is plotted for methane and for one natural gas mixture at two temperatures and at pressures up to 100 atmospheres. The dashed line is for methane and the solid line is for the gas mixture which is about 93 percent methane. The difference between methane and the gas mixture at the end of the 100° F curves is 0.2 percent and at the end of the 0° F curves it is 0.5 percent, so that if inaccuracies less than 1/2 percent are desired, properties for gas mixtures must be used. A correlation based on 19 different natural gas mixtures has been developed at Lewis so that φ can be determined for most natural gases of interest. It is estimated that the inaccuracy of this determination is about 1/4 percent which is the same as the inaccuracy for the discharge coefficient. Based on the work that has been done on sonic nozzles, it appears that they are a good choice as a prover to calibrate natural gas meters at line pressures of intended use to an inaccuracy approaching 1/4 percent.

TESTING AND MONITORING OF MACHINERY

Instrumentation techniques that apply to aircraft jet engines will apply in many cases to large industrial gas turbines such as the one shown in figure VIII-4. In this section, five different measurement categories that have direct application to machinery testing and monitoring will be discussed.

High Gas Temperature Measurement

The hot gas sections of the engine are at the exit of the combustor and at the inlet and downstream of the turbine. Here temperatures can range from 1000^{o} F behind the turbine to as high as 2500^{o} F at the outlet of the combustor. Some future engines are planned which will have turbine inlet temperature between 3000^{o} and 4000^{o} F. Measurement of gas temperature in these regions is required to determine engine performance and to verify that the combustor generates the required temperature profile as well as temperature level.

Traditionally, thermocouples have been used to make these gas temperature measurements because of their low cost, ease of use, and because they can easily be fabricated into small probes. As shown in the following table Chromel-Alumel is the usual choice for the thermocouple wire for

TEMPERATURE RANGE, ^{o}F	TECHNIQUE
<2000	CHROMEL-ALUMEL THERMOCOUPLES
2000-3000	PLATINUM ALLOY THERMOCOUPLES
>3000	IRIDIUM ALLOY THERMOCOUPLES COOLED INFERENTIAL PROBES OPTICAL RADIATION METHODS

temperatures up to 2000° F. Other parts of the temperature probe are made of stainless steel or Inconel.

Between 2000° and 3000° F, noble metal thermocouples such as platinum alloys are used. Whenever possible, in this higher temperature range, most of the probe supporting the thermocouple wire is incased in a water-cooled shell to reduce the amount of noble metal materials required for the probe structure. Above 3000° F, iridium alloy thermocouples are used. Other techniques which have been used to a limited extent above the range of the platinum thermocouple include cooled inferential probes and remote sensing techniques such as optical radiation methods.

Two thermocouple probe designs that have been used extensively in jet engine testing are shown in figure VIII-5. Both designs can use either Chromel-Alumel or platinum thermocouples, so they both can be used up to 3000° F. The simplest design is the bare wire with its junction in the middle of the wire. Normally such a thermocouple when placed in a hot gas stream will indicate a temperature lower than the stream total temperature because of three errors or three types of heat loss. First, the junction can lose heat by thermal conduction along the wires to the cooler support. This conduction loss can usually be made negligible by exposing enough length of thermocouple wire to the hot gas. Secondly, the thermocouple junction indicates a temperature lower than total temperature because the gas cannot be stagnated perfectly. This effect can be determined by flow calibration, and, for the bare wire design is about a half percent effect in a combustor application. The third error or heat loss is due to the junction losing heat by radiation to the normally cooler surroundings. For example, in a combustion gas at 3000° F, a 30-mil-diameter bare wire thermocouple has a radiation error of 200° F or about 7 percent. When using designs such as the bare wire, these errors must be accounted for in order to get good accuracy.

In the shielded design, radiation error is eliminated by using shielding so that the thermocouple junction does not radiate to cooler surroundings but only radiates to the shields which have been heated by the hot gas. The gas is aspirated through the shields and past the junction. There are small holes in the inner shield below the thermocouple junction to allow the gas to flow past the junction. This design indicates very close to gas temperature. Of course, for a 3000° F design the shields have to be constructed of plati-

num alloy tubing which is the main factor in cost of the shielded probe.

Even with the extensive use of noble metals at the higher temperatures, thermocouples are still the overwhelming choice for the measurement of high gas temperature. They are low in cost compared to other methods, they are easy to use, and they can easily be built into probes.

Gas Flow Measurement

Historically, gas flow mapping has been done in engines by the insertion of a probe to measure the total and static pressures from which velocity is computed. If instantaneous flow velocity or turbulence is of interest, a fast responding pressure probe or a hot wire anemometer is used. These probes are either fixed multielement rakes or survey probes which are traversed through the region of interest to obtain the flow map.

Probes, however, can generate several problems. For instance, the probe causes flow blockage. This blockage becomes extremely severe at transonic Mach numbers where a small percentage of blockage will reflect in large changes in flow conditions. Also, these probes cannot be used in critical locations such as between the rotating blades in compressor stages.

The most significant advance in recent years for detailed flow mapping is a device called the laser Doppler velocimeter. Because it is a remote-sensing laser based technique, it does not have the problems associated with immersion probes.

Figure VIII-6 shows a very simple diagram of a laser Doppler velocimeter being used to measure the flow velocity at a point in a pipe. A beam of laser light of known frequency is sent into the pipe through a window in the pipe wall. Small amounts of this light are scattered in all directions by particles which happen to be in the stream, or which are put there for this purpose. It is assumed that the particles are sufficiently small so that they move at the flow velocity. An optics system collects a portion of the scattered light and focuses it on a light detector. The detector converts the scattered light signal into an electronic signal which is sent to the signal processor which in turn generates an output proportional to the difference in frequency between the known laser light and the collected scattered light. All that must be known to calculate the particle or flow velocity and the

location of the spot which is being sensed is this difference frequency and the geometry of the optics system.

The entire flow field can be mapped by scanning the laser beam over the region of interest. In mapping the flow field in a moving region an additional problem is present. For example when mapping between rotating blades, it must be determined just which blade is in view, when each data point is taken, and where the point is located between the blades. This results in the need for timing and synchronization between the data taking and the machine rotation. A minicomputer is shown in figure VIII-6 which performs these as well as the data reduction and display functions.

The following is a summary of the major features of laser Doppler velocimetry. First, it is used for flow velocity mapping in difficult areas in machinery. Second, it needs no calibration because the flow velocity is directly proportional to the measured frequency difference between the incident and scattered laser light. Third, it is a point measurement. Fourth, it is a noncontacting optical technique; thus, no probes are required which might cause flow blockage. Fifth, it is capable of mapping within the rotating blade rows, but, of course, this raises the complexity of the data system. And last, but not least, it is an expensive system.

A laser Doppler velocimeter is not a replacement for probes in general, because it is too complex and expensive. Its application is warranted when the environment is not suitable for probes.

Mechanical Integrity of Machine Parts

Two areas where Lewis has done instrumentation research aimed at protecting the mechanical integrity of machine parts are holography for vibration mode determination and turbine wheel crack detection.

The holographic technique is more specifically called time average holography. It is a method for obtaining a picture or hologram, using laser light, showing the vibration mode stress concentration patterns at any chosen vibration excitation frequency. The blade, wheel, or whatever part is being investigated is mounted on a small shaker or vibration exciter to obtain these holograms.

The purpose of these holograms is to find the stress concentrations so

that optimum strain gage locations can be selected for monitoring that part during maching operation. Other uses for the hologram are to find complex vibration modes that are not analytically predicted, and to detect flaws.

Figure VIII-7 shows a turbine wheel from a small jet engine. This wheel was mounted on a shaker to obtain the subsequent holograms. Figure VIII-8 shows a time average hologram of the wheel excited at its center at 3975 Hz. Note the bright circle around the hub of the wheel. This bright region represents the locus of points of zero displacement. Counting the interference fringes toward the center of the hub or out onto the blades allows computation of the relative displacement of any point on the wheel. The areas of maximum stress are determined from this pattern. Since the hologram identifies the maximum stress locations for this particular mode, strain gage locations can be optimized for later monitoring during operation of the machine. Other holograms are then required for other modes. The circular pattern shown is a vibration mode that is analytically predictable.

Figure VIII-9 shows a hologram of the same wheel, excited the same way but at 3065 Hz. Note that the bright region traverses the hub of the wheel, out onto the blade roots, back through the hub, and then back out to the blade roots. It forms an elliptical pattern which is not predicted analytically and illustrates one of the major advantages of the holographic technique.

Another hologram (fig. VIII-10) taken at an excitation frequency of 4265 Hz shows an almost regular pattern with six-sided symmetry. As shown, many modes are possible in a complex wheel such as this. Some modes are predictable and some not.

A second area of research at Lewis for protecting the mechanical integrity of machine parts is turbine wheel crack detection during operation. In many turbine wheels, cracks are a major problem. These cracks are usually induced as a result of temperature cycling of the highly stressed wheels. The cracks can occur almost anywhere on the wheel but they are most likely to occur at stress concentrations such as at the blade root region where the blade attaches to the wheel. If the fatigue crack propagates far enough, the wheel will fail catastrophically.

Lewis is developing a sensor and electronic system that monitors a suspected area on the wheel for cracks while the turbine is in operation. One of the benefits from this system is the prevention of some of the unneeded

overhauls of the machine. With the monitor, cracks can be detected when they are starting and thus overhauls for inspecting turbine wheels can be performed only when necessary rather than after some fixed number of hours of operation.

Figure VIII-11 shows a turbine wheel from a helicopter engine. A fatigue crack normally starts to propagate from the blade root region onto the wheel. This is a very typical spot for cracks to develop because of the high stress concentrations. Figure VIII-12 shows an enlargement of this region with a further enlargement in the inset showing a crack which is about 0.1 inch in length. This size crack is about the smallest that is detectable with the present crack detection system.

Figure VIII-13 shows a line drawing of a segment of a turbine wheel. A crack is shown emanating from one of the blade roots. The crack sensor consists of a coil of wire excited electrically at a high frequency. This induces a flow of eddy currents in the turbine wheel region adjacent to the sensor. A crack produces a discontinuity in the electrical conductance of the material. As the discontinuity passes the sensor which is fixed to a stationary part of the machine, the impedance of the sensor is momentarily perturbed. This perturbation then produces an output from the electronic system which is a function of the size of the crack. Thus the system functions as a crack detector and to some extent as a crack length monitor.

Since the sensor must be in the high temperature turbine, it must be constructed of materials capable of withstanding this environment.

Turbine Blade Temperature Measurement

To increase the performance of the entire gas turbine, it is desirable to increase both the turbine inlet temperature and pressure. The ultimate limit is not how high the gas temperature and pressure can be raised, but rather how high a temperature the turbine will withstand. Presently, uncooled turbine blades can withstand inlet gas temperatures of up to about 1800° F. Beyond this, blade cooling must be used. In order to evaluate and monitor blade cooling techniques, blade temperature must be measured.

In turbine engine testing at Lewis the blade temperature is measured using two different techniques. Sheathed thermocouples are used for making

point measurements, and temperature profile measurements are obtained using a scanning infrared pyrometer which was developed at Lewis.

For making point temperature measurements Chromel-Alumel sheathed thermocouples are used (fig. VIII-14). Each thermocouple wire is surrounded by a magnesium oxide insulator which is covered with an Inconel sheath with an outside diameter of 10 mils. Both legs of the thermocouple are placed in a 12-mil-deep groove which is cut into the blade surface. The groove is covered with a 2-mil-thick strip of metal which is welded in place. Many tests using this type of construction and materials have been performed and this technique has been found to be very reliable.

The main limitation with this method is that the number of measurements that can be made is rather limited. Each measurement requires a separate set of thermocouple wires and an additional groove in the blade. Structural considerations limit the number of grooves that can be cut into one blade. Furthermore, newer higher performance turbines use very thin-walled blades. Figure VIII-14, which is drawn to scale, shows a 50-mil-thick blade wall. The groove depth represents 25 percent of the wall thickness so that the thermocouple is probably giving a poor measurement of the blade temperature.

To overcome these limitations, a scanning infrared pyrometer has been developed (fig. VIII-15). The device measures the amount of infrared energy coming from the hot blade, and from this energy measurement the blade temperature is computed. The pyrometer actually looks at a single spot on the blade at any instant of time. The spot size is about 20 mils in diameter. Some of the energy that is radiated by this spot is collected by a lens and imaged onto the end of an optical fiber which is contained in a water-cooled probe. At the other end of the optical fiber the infrared energy is converted into an electrical signal which is indicative of temperature. The result is exhibited on a display device in real time.

As the turbine wheel rotates, the spot scans along the blades producing a display of blade temperature versus circumference around the turbine wheel at a given radius. To scan other radii of the blades, the radial scan actuator moves the cooled probe in a step-wise manner until the entire surface is mapped.

Figure VIII-16 shows a typical display of blade temperature as a function of angular position. The blades shown have midchord regions which

are a little above 1300° F and trailing edges which have temperatures in the vicinity of 1600° F. Notice how the indicated temperature drops rapidly as the scanned spot passes from the trailing edge of one blade to the midchord region of the following blade. Notice also that, for the configuration shown, the optical system is unable to "see" the leading edge of the blades since the leading edge is always shielded by the previous blade. This illustrates one of the limitations of this technique; that is, you must have optical access to all points of interest. When faced with a configuration like the one illustrated, thermocouples are used on the leading edges and the pyrometer is used for the remainder of the blade.

Data Acquisition from Rotating Parts

One of the main problems in obtaining measurements on rotating components, such as thermocouple temperature measurements on turbine wheels, is getting the sensor signals across the rotating-stationary interface. In a typical development application, there can be as many as 60 to 100 such signals.

Three common techniques used for data acquisition from rotating components are discussed here. The first, one that has been used for many years, is the slip ring. Slip rings work well in many applications but they have some very severe attendant problems including maintenance, cooling, lubrication, sliding contact and wear, and the generation of electrical noise that deteriorates the signals from the sensors. Of course, the main advantage of slip rings is that they provide a direct connection to the sensor wires and thus require no on-shaft electronic signal conditioning.

The second type of data acquisition system for use with rotating components is radio telemetry; that is, sending data signals from the rotating component by means of radio transmission. There are advantages to this technique. First, there are no sliding contacts so that most of the problems associated with slip rings are gone. Second, the telemetry system can be located almost anywhere. This is of paramount importance if sensors are required on the high speed, or outer spool of a multispool machine. In this case the end of the shaft is not accessible for locating slip rings or other

conventional data systems. Telemetry, in this case, may be the only solution.

Telemetry has some disadvantages. In order to operate the telemetry system, electrical power must be available on the shaft or coupled to the shaft to run the system. An additional disadvantage of telemetry is its present high cost which now runs to several thousand dollars per channel.

A compromise solution to slip rings and telemetry is the rotary transformer which has been adopted for many of the applications at Lewis. Commercially available rotary transformers require access to the end of the shaft and they require powered electronics on the shaft rotating with the shaft. This technique, however, has several distinct advantages. There are no sliding contacts such as in slip rings. The maintenance problems are eliminated. The problem of coupling electrical power onto the shaft to operate the electronics is solved since the same transformer assembly is used to couple the power onto the shaft and to couple the conditioned sensor signals off the shaft.

Figure VIII-17 shows the latest version of the rotary shaft data system that was developed at Lewis. It consists of a metal cylinder which rotates on the end of the shaft of the machine. Inside the cylinder are stacked typically six to ten small circular printed circuit boards on which commerically available integrated circuits are mounted. These circuits form the power supply, the multiplexer, the signal conditioner and, in some cases, the digitizer for the sensor signals.

A multiple pin connector is located on one end of the cylinder for providing connections from the sensor wires to the electronics. This end is toward the machine. On the other end of the cylinder, the rotary transformer is attached through a combination flexible coupling and electrical connector. The cable shown connects the transformer stator to the stationary data acquisition system.

The particular system shown in figure VIII-17 multiplexes and signal conditions the signals from 64 dynamic strain gages. Systems like this have been operated successfully for a few hundred hours at speeds up to 18 000 rpm.

DATA HANDLING AND CONTROL

Modern instrumentation systems have the ability to generate large amounts of data so that elaborate data acquisition systems are often required. In addition, these instrument systems also require many complex and specially sequenced input signals for such purposes as range changing and calibration.

Up to now some of these functions such as range changing and calibration were either performed manually, generally at a considerable cost in manpower, or they were performed automatically with a minicomputer. However, even the smallest minicomputer systems available were often far too powerful and too costly to service a single instrument or small group of instruments. Typical minicomputer costs today are $10,000 to $50,000 for a complete system. If a large number of instruments have to be controlled simultaneously, then the minicomputer operated on shared basis among the various instruments is an ideal solution. However, in most cases the minicomputer is too costly for a single or small group of instruments.

Within the last year or two a new type of computer known as the microprocessor has been receiving wide attention (fig. VIII-18). The microprocessor is a complete computer. The central processor unit, which is the light colored chip on the printed circuit board shown in the foreground, performs the arithmetic operations such as adding, subtracting, and comparing two numbers. In order to make it operate, additional components are necessary such as a memory, buffer registers, and a power supply. The entire unit shown presently sells for about $1500. The microprocessor is the least powerful and least expensive member of the computer family.

Lewis is using microprocessors to automate several of its instrument systems. A typical example is a pollution monitoring system. Figure VIII-19 shows a typical monitoring system that is <u>not</u> microprocessor controlled. It consists of a collection of commercially available instruments for measuring carbon dioxide, carbon monoxide, nitrous oxides, and total hydrocarbons. Several such systems are in use at Lewis for measuring the exhaust gas concentrations from turbine engines, both to monitor their performance and to determine if they comply with EPA standards. These systems are expensive to operate in terms of the manpower required. Period-

ically, such as every few hours, all of the instruments are calibrated by passing calibration gases of known composition through the system. This procedure is time consuming and expensive.

Figure VIII-20 shows a simple block diagram of a microprocessor controlled pollution monitoring system that is being developed at Lewis. The only human operation that is required is to turn the system on and off; the microprocessor does the rest. The entire sequence after turn-on, such as calibration and zero setting on the instruments, is accomplished by software stored in the microprocessor memory. The microprocessor also takes the data from each instrument, puts it in the right format, and stores it until the main computer, in this case, is ready for it. Provision for some on line real time display of the results is also being made so that the operator need not wait for the large computer to reduce all of the data to see what the results look like.

This is only one example of how microprocessors can be used as an integral part of modern instrumentation systems.

CONCLUDING REMARKS

The instrumentation and measurement techniques just described were developed for and are being used in turbomachinery research and development. It is clear, however, that they all have a much more general applicability.

BIBLIOGRAPHY

Custody Transfer of Gases

Johnson, R. C.: Calculations of the Flow of Natural Gas Through Critical-Flow Nozzles. J. Basic Eng., Trans. ASME, vol. 92, no. 3, Sept. 1970, pp. 580-589.

Johnson, Robert C.: A Set of FORTRAN IV Routines Used to Calculate the Mass Flow Rate of Natural Gas Through Nozzles. NASA TM X-2240, 1971.

Johnson, Robert C.: Real-Gas Effects in the Flow of Methane and Natural Gas Through Critical-Flow Nozzles. NASA TM X-52994, 1971.

Johnson, Robert C.: Real-Gas Effects in Flow Metering. Presented at ISA 1st Symposium on Flow - Its Measurement and Control in Science and Industry, Pittsburgh, Pa., May 1971.

Johnson, Robert C.: Tables of Critical-Flow Functions and Thermodynamic Properties for Methane and Computational Procedures for Both Methane and Natural Gas. NASA SP-3074, 1972.

Peignelin, M. G.: Calibration of High Pressure Gas Meters with Sonic Nozzles. J. Instit. Meas. and Control, vol. 5, no. 11, Nov. 1972, pp. 440-446.

Schroyer, Harry R.: Sonic Nozzles for Gas Meter Calibration, Part 1. Pipeline and Gas J., vol. 200, no. 11, Sept. 1973, pp. 31-32.

Schroyer, Harry R.: Sonic Nozzles for Gas Meter Calibration, Part 2. Pipeline and Gas J., vol. 200, no. 13, Nov. 1973, pp. 64, 66, 68, 84.

Szaniszlo, Andrew J.: Experimental and Analytical Sonic Nozzle Discharge Coefficients for Reynolds Numbers Up to 8×10^6. NASA TN D-7848, 1975.

Testing and Monitoring of Machinery

High gas temperature measurement

Glawe, George E.; Simmons, Frederick S.; and Stickney, Truman M.: Radiation and Recovery Corrections and Time Constants of Several Chromel-Alumel Thermocouple Probes in High-Temperature, High-Velocity Gas Streams. NACA TN 3766, 1956.

Krause, Lloyd N.; Glawe, George E.; and Johnson, Robert C.: Heat-Transfer Devices for Determining the Temperature of Flowing Gases. Temperature: Its Measurement and Control in Science and Industry, C. M. Herzfeld, ed., Volume 3, Part 2, Reinhold Pub. Corp., 1962, pp. 587-593.

Moeller, C. Eugene: NASA Contributions to Development of Special-Purpose Thermocouples. NASA SP-5050, 1968.

Moffat, Robert J.: Gas Temperature Measurement. Temperature: Its Measurement and Control in Science and Industry, C. M. Herzfeld, ed., Volume 3, Part 2, Reinhold Pub. Corp., 1962, pp. 553-571.

Scadron, Marvin D.; and Warshawsky, Isidore: Experimental Determination of Time Constants and Nusselt Numbers for Bare-Wire Thermocouples in High-Velocity Air Streams and Analytic Approximation of Conduction and Radiation Errors. NACA TN 2599, 1952.

Stickney, Truman M.: Recovery and Time-Response Characteristics of Six Thermocouple Probes in Subsonic and Supersonic Flow. NACA TN 3455, 1955.

Gas flow measurement

Maxwell, Barry R.: Particle Flow in Blade Passages of Turbomachinery with Application to Laser-Doppler Velocimetry. (Bucknell Univ.; NASA Grant NGR-39-027-002.) NASA CR-134543, 1974.

Maxwell, Barry R.: Particle Flow in Turbomachinery with Application to Laser-Doppler Velocimetry. AIAA J., vol. 12, no. 10, Oct. 1974, pp. 1297-1298.

Maxwell, Barry R.: Particle Flow within a Transonic Compressor Rotor Passage with Application to Laser-Doppler Velocimetry. (Bucknell Univ.; NASA Grant NGR-39-027-003.) NASA CR-134718, 1975.

Seasholtz, R. G.: Laser Doppler Velocimeter Measurements in a Turbine Stator Cascade Facility. NASA TM X-71524, 1974.

Thompson, H. D.; and Stevenson, W. H.: Proceedings of the Second International Workshop on Laser Velocimetry, Volume 1. Purdue University Engineering Experiment Station, Bulletin No. 144, March 1974.

Trolinger, J. D.; Bogdonoff, S. M.; and Smith, J. A.: Laser Instrumentation for Flow Field Diagnostics. AGARD-AG-186, Advisory Group for Aerospace Research and Development, 1974.

Mechanical integrity of machine parts

Barranger, John P.: Flight Monitor for Jet Engine Disk Cracks and the Use of Critical Length Criterion of Fracture Mechanics. NASA TN D-7483, 1973.

Camatini, Ezio, ed.: Optical and Acoustical Holography. Plenum Press, 1972.

Collier, Robert J.; Burckhardt, Christoph B.; and Lin, Lawrence H.: Optical Holography. Academic Press, 1971.

Turbine blade temperature measurement

Buchele, Donald R.; and Lesco, Daniel J.: Pyrometer for Measurement of Surface Temperature Distribution on a Rotating Turbine Blade. Instrumentation for Airbreathing Propulsion. A. E. Fuhs and M. Kingery, eds., The MIT Press, 1974, pp. 347-354.

Crowl, Robert J.; and Gladden, Herbert J.: Methods and Procedures for Evaluating, Forming, and Installing Small-Diameter Sheathed Thermocouple Wire and Sheathed Thermocouples. NASA TM X-2377, 1971.

Holanda, Raymond; Glawe, George E.; and Krause, Lloyd N.: Miniature Sheathed Thermocouples for Turbine Blade Temperature Measurement. NASA TN D-7671, 1974.

Pollack, Frank G.: Advances in Measuring Techniques for Turbine Cooling Test Rigs: Status Report. Instrumentation for Airbreathing Propulsion. A. E. Fuhs and M. Kingery, eds., The MIT Press, 1974, pp. 371-386.

Data acquisition from rotating parts

Lesco, Daniel J.; Sturman, John C.; and Nieberding, William C.: Rotating Shaft-Mounted Microelectronic Data System. NASA TN D-5678, 1970.

Lesco, Daniel J.; Sturman, John C.; and Nieberding, William C.: On-the-Shaft Data Systems for Rotating Engine Components. Instrumentation for Airbreathing Propulsion. A. E. Fuhs and M. Kingery, eds., The MIT Press, 1974, pp. 131-140.

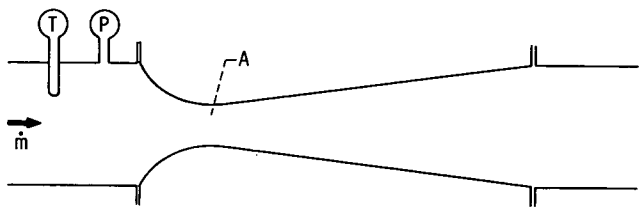

$$\dot{m} = C_D \times A \times \varphi \times (P/\sqrt{T})$$

CS-72345

Figure VIII-1. - Sonic nozzle for gas meter calibration (proving).

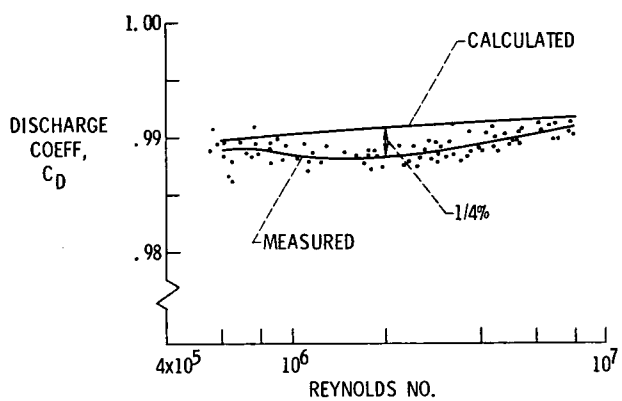

CS-72344

Figure VIII-2. - Sonic nozzle discharge coefficient.

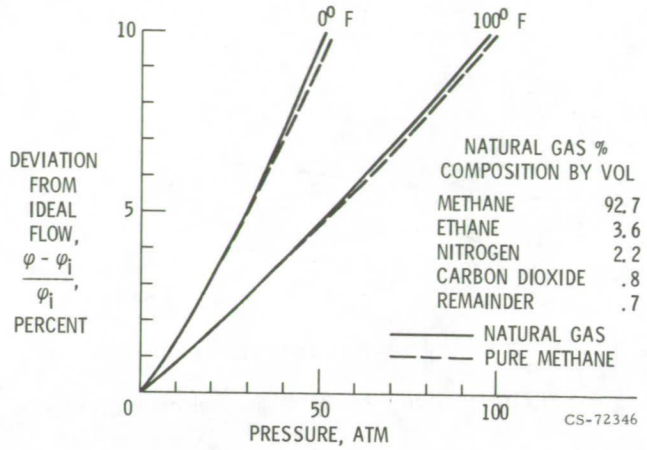

Figure VIII-3. - Sonic nozzle real gas effects.

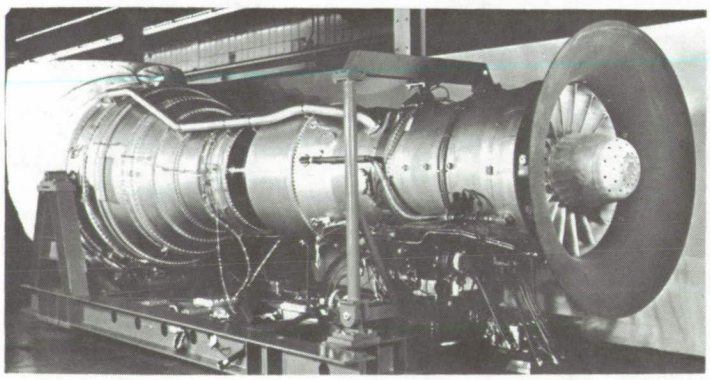

CS-72210

Figure VIII-4. - Industrial gas turbine.

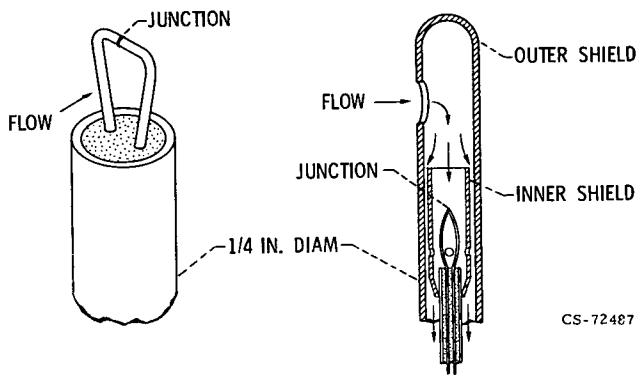

(a) Bare wire thermocouple. (b) Shielded thermocouple.

Figure VIII-5. - Thermocouple probes.

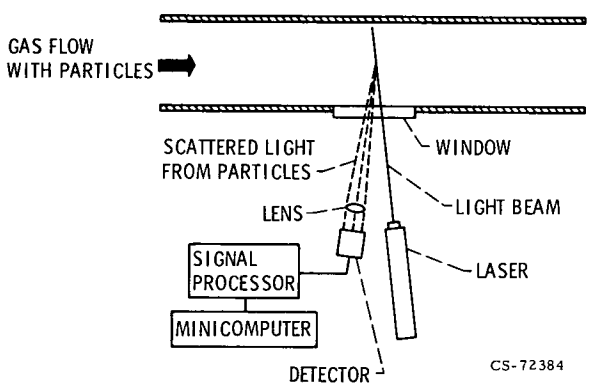

Figure VIII-6. - Laser Doppler velocimeter.

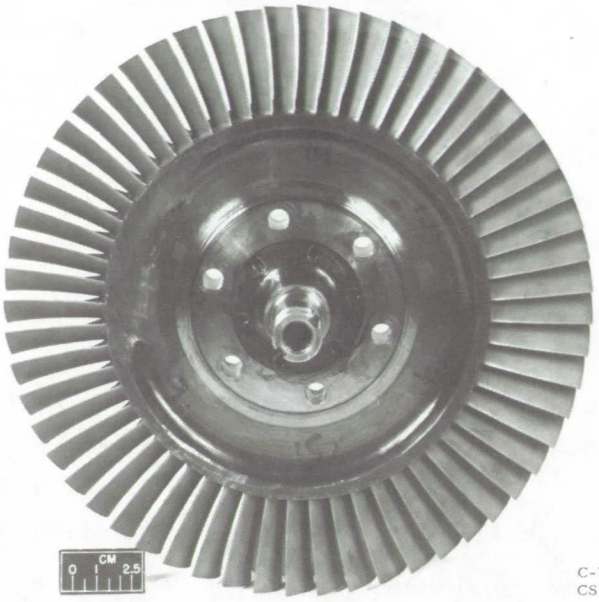

Figure VIII-7. - Turbine wheel from small jet engine.

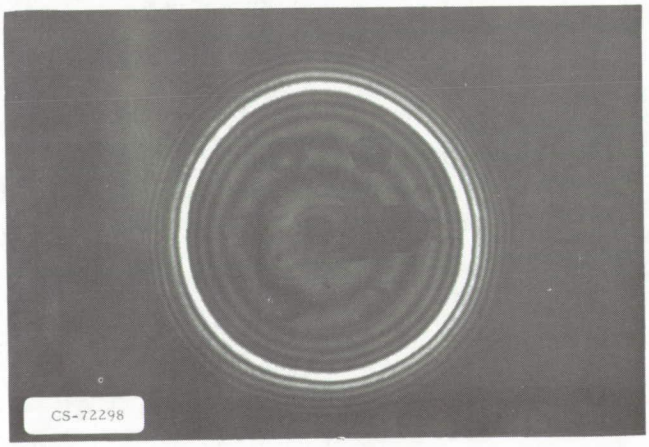

Figure VIII-8. - Time average hologram of turbine wheel at 3975 Hz.

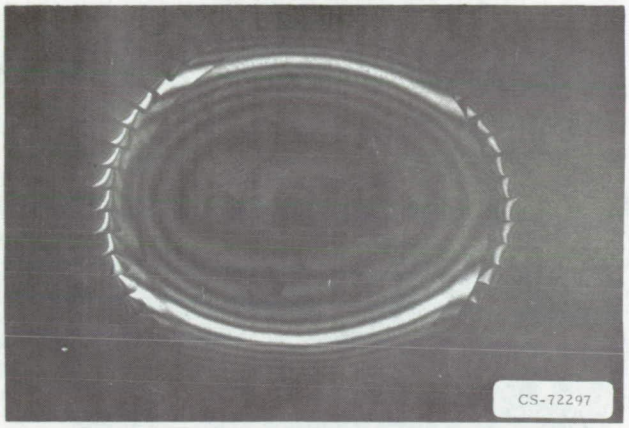

Figure VIII-9. - Time average hologram of turbine wheel at 3065 Hz.

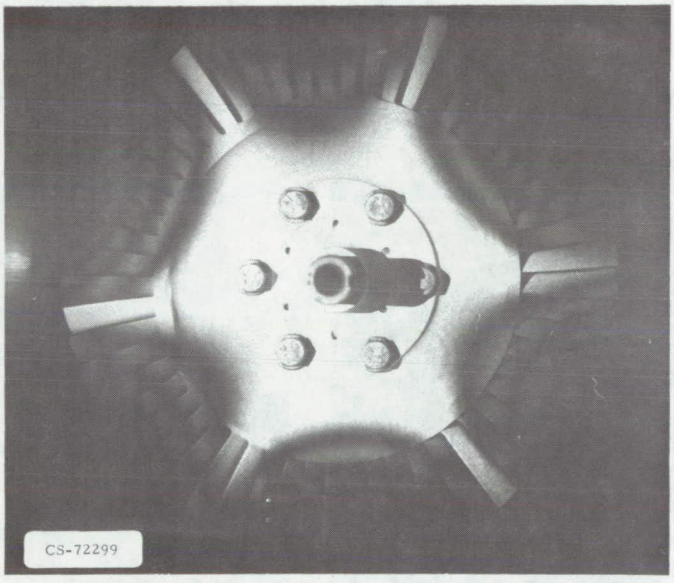

Figure VIII-10. - Time average hologram of turbine wheel at 4265 Hz.

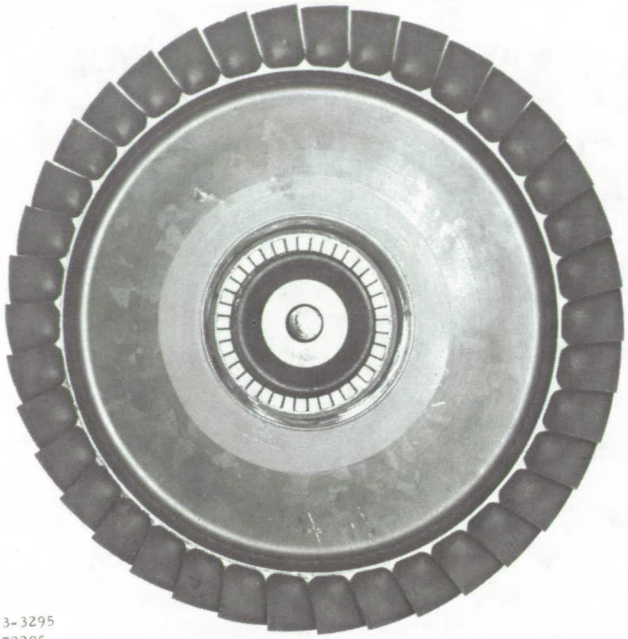

C-73-3295
CS-72295

Figure VIII-11. - Turbine wheel from helicopter engine.

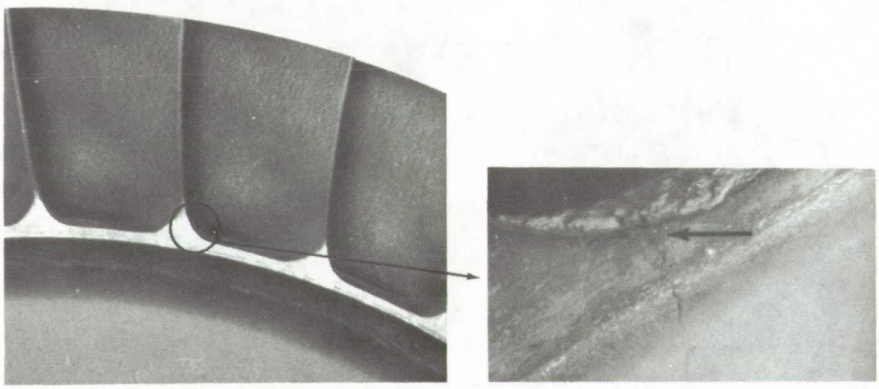

Figure VIII-12. - Enlargement of blade root region.

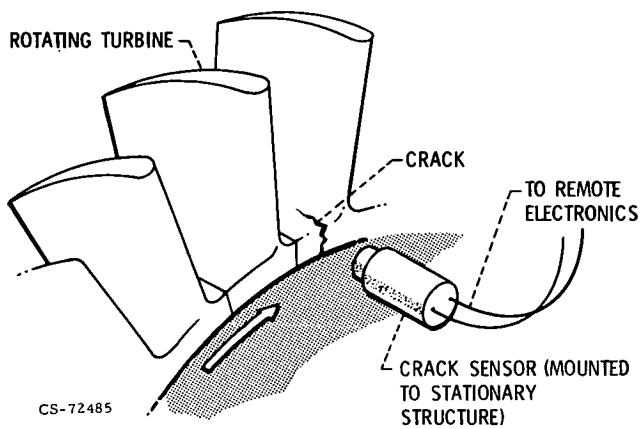

Figure VIII-13. - Turbine wheel crack detection.

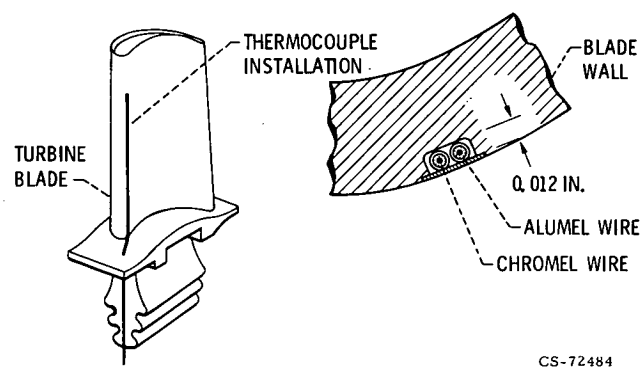

Figure VIII-14. - Turbine blade temperature measurement with thermocouples.

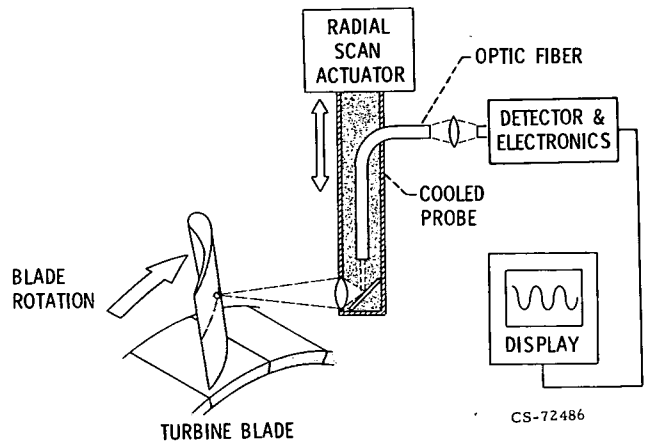

Figure VIII-15. - Scanning infrared pyrometer.

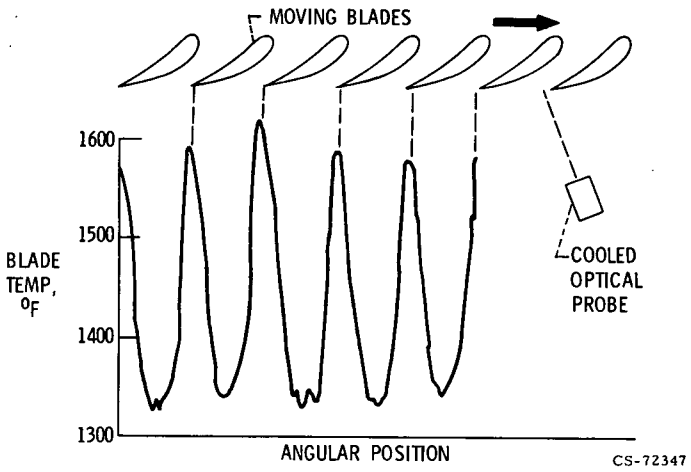

Figure VIII-16. - Turbine blade temperature display.

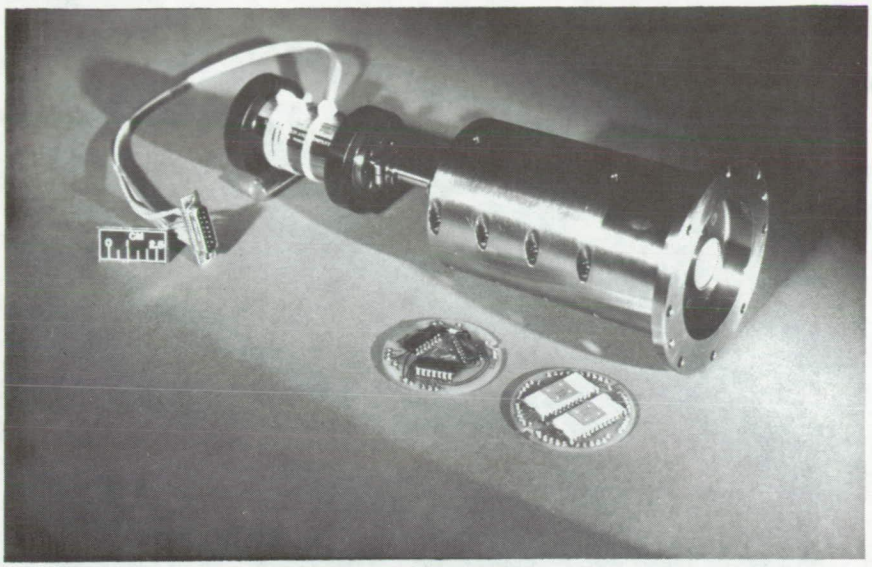

Figure VIII-17. - Shaft data system.

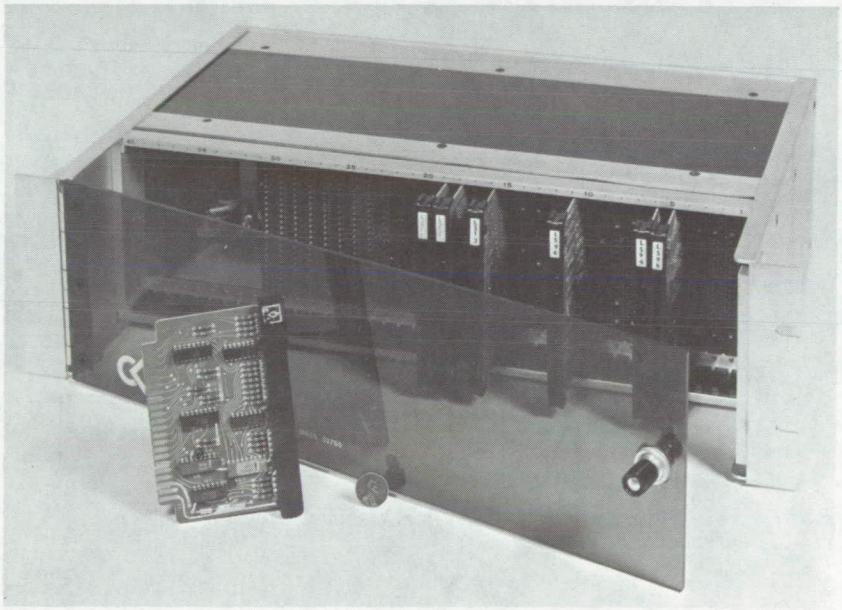

Figure VIII-18. - Microprocessor.

C-75-641
CS-72209

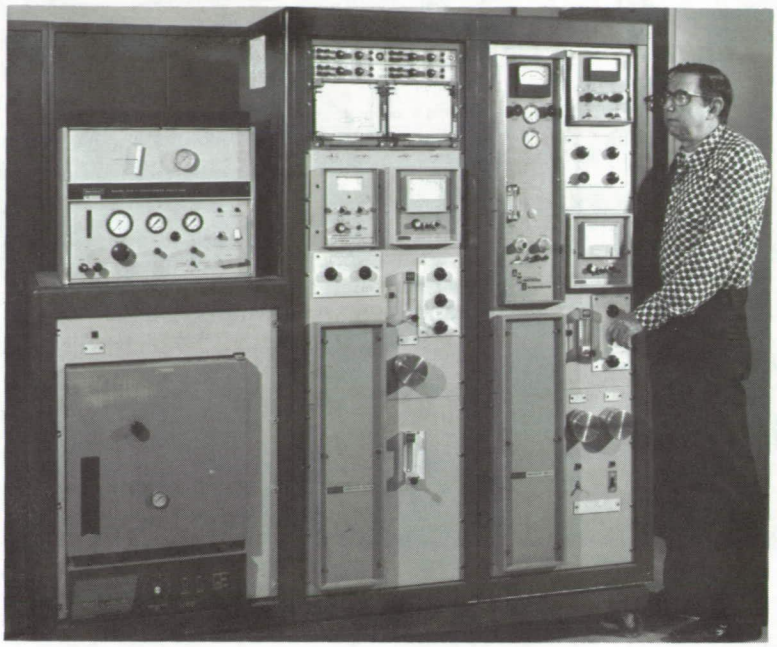

C-75-840 CS-72503

Figure VIII-19. - Pollution monitor.

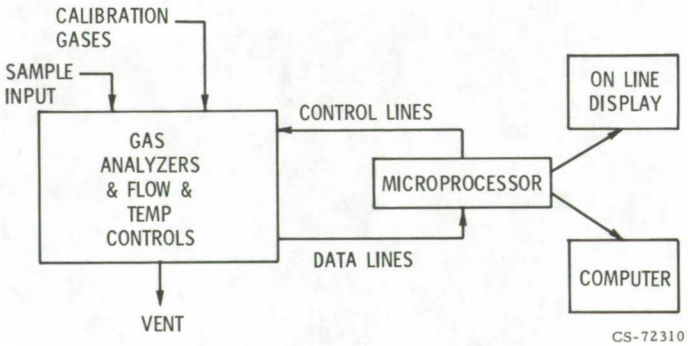

Figure VIII-20. - Microprocessor controlled pollution monitor.

IX. MATERIALS AND LIFE PREDICTION

John C. Freche, Salvatore J. Grisaffe, Gary R. Halford,
Richard H. Kemp, and John L. Shannon, Jr.

Much of the materials research conducted at NASA for aerospace propulsion should have potential applicability in a number of areas in the gas industry. Table IX-1 shows potential areas of relevancy. In the center column of this table are listed the major materials research areas to be covered. Shown in the left column are some typical aerospace applications toward which each of these work areas is directed. In the right column are indicated some potential applications to the gas industry.

The scope of the material to be covered is as follows: In the area of fracture mechanics, methods have been developed for determining fracture toughness and crack growth in metals subjected to aggressive environments. In the field of composite tank technology a new structural concept for pressure vessels is described. Advanced materials discussed include superalloys, directionally solidified eutectics, and high-temperature polymer matrix composites as well as a new, low-cost, powder-metallurgy processing technique. The area of corrosion and environmental protection deals with coatings and cladding protection and the effect of hydrogen on high-temperature alloy properties. Finally, in the area of life prediction the effect of fatigue-creep interaction on life is explored and new methods of predicting fatigue life and longtime creep-rupture life in advance of service are described.

FRACTURE MECHANICS

The problem of structural failure due to the catastrophic propagation of cracks or crack-like flaws at stresses well below the yield strength of the

structural material has been pervasive in man's attempt to build integrity and reliability into his engineering products. It is a problem that afflicts all types of engineering structures, sometimes with tragic consequences. One of the more celebrated examples, locally, is shown in figure IX-1. Terrible havoc was wrought by the failure of a liquid-natural-gas (LNG) storage tank, and subsequent gas explosion, in Cleveland, Ohio, in the fall of 1944.

This LNG installation was the first of its type in the country. The technology was not available at the time of its design to unmask the impropriety of using the constructional material and weldments that were later held responsible for the failure. With today's advanced structural mechanics and materials technology, such failures are far less likely to happen.

It is our intention to bring into view common problems for which our research may give remedy and, beyond that, opportunity. In the area of common problems, figure IX-2 presents an aerospace counterpart to the LNG storage tank failure. This is the wreckage of a 260-inch-diameter, solid-propellant rocket motor case which failed during hydrotesting at less than one-half of its design strength. The failure originated at a small crack-like defect in the heat-affected zone of a repair weld (fig. IX-3). It measured about 0.1 inch wide by less than 1.5 inches long. This tiny flaw removed less than 0.02 percent of the load-carrying cross section of the motor case wall in the plane of the flaw but cut the expected load-carrying capacity in half. It did its damage by concentrating stress in the vicinity of its boundary. Unfortunately, the material was not tough enough to relieve this stress concentration by plastic deformation. Consequently, the crack, once started, ran freely through the vessel, feeding on the stored elastic energy in the wall of the large structure itself.

The NASA Lewis Research Center has pioneered in the development of engineering fracture mechanics to deal with the vexing behavior of metals when they contain cracks or crack-like flaws and in the prevention of structural failure through the propagation of those flaws. Our initial involvement was in the development of test methods that permitted the rational selection of steels and working stresses for the Polaris missile motor case. Thereby, an end was put to a continuous series of failures that had by that time become a national emergency. Since that time, our work has been directed at the development of a quantitative measure of fracture toughness that is useful directly in design and proof testing. We have also devised test

methods for qualitative toughness indications that are useful as screening tools in alloy development, selection, and quality control.

The key to brittle fracture control in structures lies not only in understanding the weakening effect of cracks on metals and those factors which influence this weakening effect, but also in translating this understanding into the types of tests and structural mechanics that will be useful to the metal producer and the structural designer. Obviously, any meaningful evaluation of fracture resistance has to employ specimens actually containing cracks or crack-like flaws. Two such specimens which have been standardized by the American Society for Testing and Materials (ASTM) for such purposes are shown in figure IX-4. The essential features of these specimens are that they contain natural cracks (at the tips of their slots) and that the crack-tip stress field for each has been carefully analyzed in terms of a single mathematical quantity called the stress intensity factor. This quantity enables us to translate the results of laboratory tests on specimens such as these into useful approximations of the load-carrying capability of structures. The basis of this procedure can be explained with the help of figure IX-5.

The slot shown represents a crack. Attention is focused on the conditions in the immediate vicinity of the crack tip, where the fracture process begins. The complete stress field at the crack tip has been defined by the expressions shown in the figure. It is seen from these expressions that the complete crack-tip stress field can be characterized by a single parameter, K_I, which is called the "stress intensity factor." As the load on a structure is increased, the crack-tip stress intensity increases. The basic assumption that is made in fracture mechanics is that when K_I reaches a critical value, designated K_{Ic} and called the "fracture toughness," unstable crack propagation ensues. The practical significance of this development is that by determining K_{Ic} in the laboratory from specimens of the type shown in figure IX-4, structural performance can be estimated.

Figure IX-6 illustrates the application of this concept to an assessment of the fracture toughness of thick-walled, centrifugally cast, 21-6-9 stainless-steel pipe. This pipe comprises the high-pressure liquid hydrogen transfer system at NASA's Space Shuttle Main Engine Ground Test Facility in Santa Suzana, California. The system is made up of 10-foot segments of pipe which are gas metal-arc (GMA) welded in the field using 308L filler.

Cracks have been observed in the base metal adjacent to the welds, and concern has developed for the structural integrity of the system. Plane-strain fracture toughness tests were performed in liquid hydrogen at the Lewis Research Center with ASTM standard fracture toughness specimens which were removed from the pipe wall as shown in the inset to figure IX-6. Cracks were located variously in the weld metal (as shown in the figure), the fusion zone, the weld heat-affected zone, and the base metal. The most brittle area was the narrow fusion zone adjacent to the weld metal. By using its measured fracture toughness K_{Ic} of 68 ksi-in.$^{1/2}$, the relation between pipe internal pressure and crack depth was developed. For a given crack depth, expressed as a percentage of pipe wall thickness, pipe internal pressure exceeding that represented by the curve would cause catastrophic failure. These results show a very substantial reduction in pressure capability with increasing flaw depth compared to the unflawed burst capability, which exceeds 120 ksi. At the maximum expected operating pressure, a long crack slightly greater than 40 percent of the wall thickness would be required to cause failure. While this is a substantial-size flaw, it is not beyond imagination and could be difficult, if not impossible, to detect. For example, the pipe could contain a crack of supercritical size located on the inner bore, where the stresses are highest. Such a crack would very likely escape detection by state-of-the-art nondestructive testing methods - especially if it were in a residual compression field associated with the weld.

In order to ensure that such elusive defects do not exist, we will resort to a proof pressurization of the system using liquid hydrogen at a pressure 25 percent above the operating pressure. If the system survives the proof pressurization, we can be sure that cracks no deeper than about 33 percent of the wall thickness exist, or else the system would have failed during proofing. The approximate 10 percent difference in critical crack depth at the proof and operating pressures represents allowable growth during service and is considered adequate for the intended use of the system.

The technology base, or methodology, underlying fracture mechanics analyses of this type has been developed, in large part, at the Lewis Research Center over the past 15 years. Our work has been in close cooperation with users in government and industry through ASTM Committee E-24 on the Fracture Testing of Metals. The technology developed has

served as the basis of the ASTM Standard Method of Test for Determining the Fracture Toughness of Metallic Materials.

COMPOSITE TANK TECHNOLOGY

An entirely different structural approach which has the potential for avoiding catastrophic failure such as can occur in metals is composite tank technology. Composite tanks or pressure vessels also offer such advantages as weight savings and improved cost effectiveness. The Lewis Research Center has been investigating composite tanks for a number of aerospace applications. Figure IX-7 indicates the types of construction that can be used.

A section of a conventional all-metal tank is shown in the upper left corner for comparison purposes, indicating the circumferential and axial loads that result from internal pressure. Because in a cylindrical tank the stresses in the axial direction are only one-half those in the circumferential direction, the strength of the material is used very inefficiently in the axial direction. In order to improve the material utilization efficiency, circumferential or hoop fiber windings can be added to the exterior of the tank, as shown in the upper right corner. These windings are held in place with an epoxy matrix material. The metal liner is now operating in a 1:1 stress field, as compared to the inefficient 2:1 stress field in the all-metal case. The weight of the tank can be still further reduced by decreasing the metal liner thickness and adding axially wrapped fibers, as shown in the lower portion of the figure. The metal liner is still being used in an efficient 1:1 stress field, but more of the load is being taken by the fiber in both directions.

Figures IX-8 and IX-9 show two large tanks with glass fiber wrapping: one 120 inches in diameter, and another 260 inches in diameter. The liners in these two cases were elastomers. Figure IX-8 shows how the fiber passes from the reels to the tank in the winding process. Although the fiber used for these tanks was glass, other fibers (such as Kevlar and graphite) have also been used. Of these fibers, Kevlar has been outstanding in providing a minimum-weight tank that at the same time is cost effective. The strength of the Kevlar fiber is approximately 350 000 psi. The winding

resin is generally an epoxy polymer.

The advantages of composite tanks having metal liners over all-metal vessels are lower weight, lower cost, and greater safety. The weights of a Kevlar-fiber-wrapped tank, a glass-fiber-wrapped tank, and an all-steel tank are compared in figure IX-10. The wrapped tanks were wrapped only in the circumferential direction, as might be the case for reaction vessels used in synthetic gas production from coal. The steel tank weighed 2000 pounds for a given pressure and volume. For the same pressure and volume, the glass-wrapped tank weighed 1840 pounds, and the Kevlar-wrapped tank weighed 1370 pounds. This represents a weight savings of approximately 32 percent for the Kevlar-wrapped tank.

With respect to cost effectiveness, table IX-2 shows that fabrication from steel costs approximately $3.00 per pound, which forms the basis for comparison. A steel liner circumferentially overwrapped with glass in an epoxy matrix still results in a $3.00-per-pound fabrication cost. However, because the glass-wrapped tank is lighter than the all-metal tank, the total cost is 92 percent of the cost of the all-metal tank. For a steel liner circumferentially overwrapped with Kevlar fiber in an epoxy matrix, the cost per pound is higher - $5.00. However, because of the very high strength-to-weight ratio of the Kevlar fiber, the tank can be made considerably lighter, and the total cost is only 81 percent of the cost of the all-metal tank.

From a safety point of view, the overwrapped composite tank offers a large advantage. When an all-metal tank fails because of excessive internal pressure, it generally produces sharp fragments that are propelled outward at very high velocities. This situation creates a very hazardous condition to those in the vicinity of such a tank, in addition to the damage that may be done to adjacent facilities. For overwrapped tanks, a different type of failure mode is obtained, as shown in figure IX-11. The external view of a failed tank indicates that no shrapnel has been generated. When this tank was sectioned, as shown on the right, it was evident that the liner had failed but had been completely contained by the overwrapping.

All the factors discussed suggest that the advances made in composite tank technology may provide an alternative to all-metal pressure vessels where the particular circumstances of the installation indicate that such a course of action would be advantageous. We believe that there is a possible

application of the composite tank concept to the construction of the large reaction tanks required for the production of synthetic gas from coal. The tanks for this purpose are under very high pressure and are very heavy if made of all-metal construction. The composite tanks would be much lighter, would be cost effective, and would also be safer than all-metal tanks.

NEW MATERIALS

Extensive research is underway at the Lewis Research Center to develop new materials for aerospace applications. These materials may be broadly categorized as metallic systems, ceramics, and polymers.

As a major part of our materials effort, we are attempting to increase the capability of materials for aircraft gas turbine blades so that turbine engines can operate at higher cycle temperatures and achieve higher efficiencies. This technology should be directly applicable to low-Btu, ground, power conversion systems. Figure IX-12 shows the use-temperature ranking of the most advanced materials for turbine blade application. The comparison is for the stress levels encountered in aircraft gas turbine engine blades. The cross-hatched region above each bar indicates the potential growth we envision in use temperature for each material class.

Of these classes of materials, only the conventional nickel-base superalloys are in use as blades today. Directionally solidified eutectics and oxide-dispersion-strengthened superalloys are under intensive development and will probably see use as blades in the next few years. Refractory metal wire reinforced superalloys and ceramics must be considered as being in a relatively early stage of their research and development cycle. Considerably more time is required before they can satisfactorily be applied to gas turbine engine blades.

Ceramics are included in this comparison of potential blade materials. This permits a convenient comparison with the metal systems. We recognize that ceramics will find application first in stationary turbine vanes, which operate at lower stresses than rotating blades. But we do believe that ceramics will eventually find use as turbine blades as well.

Metallic Materials

The directionally solidified eutectics are a very recent and unique development. Figure IX-13 is a scanning electron micrograph of a directionally solidified eutectic superalloy. The matrix of this alloy has been etched away so that the rod-like morphology of the second phase is visible. This phase is the primary high-temperature strengthening phase and is continuous along the length of the sample, thereby further contributing to alloy strength. The directionality of the second phase has been produced by progressively solidifying the molten alloy in one direction.

Figure IX-14 illustrates the structure of one of the most advanced directionally solidified eutectic alloys known to date. The continuous reinforcing phase is the delta or Ni_3Cb phase. This alloy is called gamma/gamma prime + delta and has been successfully cast into a turbine blade, as shown on the right side of the figure. This alloy is currently undergoing extensive development aimed at qualifying it as an aircraft gas turbine blade material with a use-temperature capability of 1900° F. Although the use-temperature potential of directionally solidified eutectics is shown in figure IX-12 to be 1950° F, it should be emphasized that this is based upon known systems. We believe there is considerable potential for uncovering newer eutectic compositions with higher melting points which will further increase the use-temperature capability of this class of materials.

The refractory metal wire reinforced superalloys look promising for the temperature range 2100° to 2300° F (fig. IX-12). Refractory metal wires, such as tungsten, which have a melting point greater than 5000° F, are inserted into conventional superalloy matrices. In order to make these materials viable for gas turbine use, economical methods of fabricating the wire reinforced superalloys must still be developed, thermal fatigue problems solved, and methods found to minimize reactions between the wire and the matrix during long-term service at high temperatures.

Ceramic Materials

Our ceramics development efforts are focused in two areas: monolithic ceramics for higher temperature gas turbine applications and fibrous

ceramics for lightweight heat shields to protect the Space Shuttle Orbiter on atmospheric reentry. It appears that some commonality exists with the materials needed for gasifiers. Figure IX-15 shows a schematic cross section of a gasifier. Local temperatures can range from 1600° to 3000° F at pressures to 100 atmospheres. The environment can be locally oxidizing or reducing. Some gasifier concepts involve monolithic or castable ceramic liners which are exposed to hot, corrosive gases and erosive particles. For thermal efficiency, these high-density ceramics are backed by low-conductivity fibrous ceramic insulation. Both are contained in metal-walled vessels. While the gasifier service conditions have some similarity to gas turbine environments, total gasifier life requirements are more than 10 times greater than those for aircraft engines. In both cases it is very important to select the right materials.

In our work dealing with gas turbine applications of ceramics, we are concentrating on the development of stator vanes of monolithic silicon carbide (SiC) and silicon nitride (Si_3N_4). As shown in table IX-3, these were the materials that exhibited the most potential in screening tests using high-velocity (2200° F) combustion gases and short heating cycles. Both materials survived 120 cycles, at which point the tests were stopped. Other potential candidates suffered early failures. For example, zirconium diboride (ZrB_2) plus additives failed because of excessive oxidation, and most of the oxides failed because of thermal shock or as a result of inadequate strength. Figure IX-16 shows the post-test condition of some of these materials. There is evidence of material loss from the ZrB_2 specimen, but SiC and Si_3N_4 show little surface distress. More recently, simulated airfoils of these materials have survived 100, 1-hour test cycles at 2200° F in sonic combustion gases. However, the SiC did develop a fracture in the holder - a reminder that these materials are brittle and that significant advances in component design, composition, manufacturing technology, proof testing, and nondestructive evaluation will be needed before practical feasibility for engine service is demonstrated. In this regard, efforts are being directed toward improving ceramic/metal attachment for blades and vanes. In addition, three-dimensional finite element design approaches are being used to circumvent the brittleness problem. Continued efforts are also being directed toward minimizing the effect of foreign object impact by modifying bulk composition as well as by surface impregnation. And we are trying to

increase the strength of parts produced by low-cost processes.

Another application for which we are developing ceramics is nonablative reentry-vehicle heat shields. The primary candidate for a lightweight heat shield for the Space Shuttle Orbiter is an ultra-low-density rigidized silica fiber material. As shown in figure IX-17, tiles of this material will be bonded to the Orbiter's aluminum structure and are expected to survive 100 missions with minimum refurbishment. Made up of a network of very fine fibers, these tiles will weight only 9 lb/ft^3. On reentry they will normally operate with a coated-surface temperature of 2200° F. Only 2 to 3 inches below the surface, the bond to the aluminum skin never exceeds 200° to 400° F. This represents very good thermal insulation.

For low-cost internal insulation of the Shuttle and advanced reentry vehicles, the potential of some commercial oxide fiber products is being examined. We are currently trying to establish time-temperature use limits by checking the insulative stability of such materials after various high-temperature exposures. Stability is primarily reflected by constant density. As the insulation collapses and sinters, its density increases and thermal conductivity increases. Figure IX-18 shows some results of 25-hour tests at 2200° and 2550° F. An impure silica-based material exhibited a density decrease at 2200° F but increased in density at 2550° F. A clay-based material suffered density increases at both temperatures. This behavior can be traced to the fact that two mechanisms are at work: volatilization of impurities, which lowers density but degrades the fibers; and shrinkage, which increases density and thus degrades insulation ability. These processes will also be at work on insulation which is needed to maintain high gasification thermal efficiency. Thus, some ceramics developed for aerospace applications may also be of use for insulating the hot parts of gasifiers.

High-Temperature Polymer Matrix Resins

A promising material system for the cooler outer tank walls of gasifiers is fiber-reinforced, polymer matrix composites. This application may require higher temperature polymer matrices than are currently used in such systems. It is appropriate to first touch on the limitations of epoxy matrix materials being used today. The epoxy matrices have been used

extensively because of their availability and ease of processing; however, they have certain drawbacks, one of which is indicated in figure IX-19. The continuous use temperature of epoxy is approximately 275° F. For many composite applications in aerospace work, a matrix resin is needed that has a much higher temperature capability. We have been looking at polyimides and polyphenylquinoxalines (PPQ) to extend the use temperature to 600° F. The figure indicates that we are indeed approaching this goal with both these materials. Another problem with epoxy resins is the effect of moisture on strength as a function of temperature (fig. IX-20). The strength of epoxy, even when provision is made to prevent moisture from being absorbed, falls off to approximately 78 percent of the room-temperature strength at 350° F. When the composite is allowed to absorb moisture, the entire strength curve is severely depressed. On the other hand, the polyimide resin composite maintains its strength to at least 550° F and is not affected by moisture.

Although the advanced resins do indeed have much better high-temperature properties, there are certain limitations that seriously affect their use. For example, the conventional condensation polyimides employ toxic, high-boiling-point solvents that are difficult to work with, such as dimethyl formamide. Shelf life is a problem because of continuing reactions that occur in the partially polymerized materials in the solvent. As a result, quality control is also a problem. In addition, the condensation resins are difficult to process because of the high-boiling-point solvents and the fact that water which is generated internally in the polymerization process leaves voids in the cured composite. These voids are responsible for premature oxidative degradation and hence loss in strength.

At the Lewis Research Center, new techniques have been found to improve the processability and properties of the polyimides. These involve using a relatively new addition reaction process for polymerization that eliminates the evolution of water. A further improvement in this addition reaction approach is illustrated in figure IX-21. We call this the polymerization of monomeric reactant (PMR) approach. The monomers are dissolved in a relatively nontoxic, low-boiling-point solvent and coated directly onto the fibers, as shown, without any prior polymerization taking place. The solvent is driven off with heat lamps, the resulting "prepreg" is cut into the necessary plies, and the plies are stacked and cured in a mold. All polymerization occurs in situ on the fiber. Variations of the process are

easily accommodated by changing the monomers or the quantities of the respective monomers in the solution to permit curing by an autoclave process instead of using the laminating mold shown in the figure. This would permit making many more types of products. We have also done some work to show that the polyimides can be used as the matrix resin for composite tanks, which would increase their use temperature.

The advantages of the PMR approach are that it permits "tailor-making", has fewer fabrication steps, costs less, is safer, and improves performance. It is easy to change the monomers and their proportions in the solution phase to permit tailor-making of the resin so as to obtain different resin properties. The solution of the monomers is easily accomplished just prior to coating the fibers, which reduces the number of fabrication steps and the cost. The low-boiling-point, relatively nontoxic solvent that is used increases the safety of the process, and the properties of composites using the PMR resins are improved when compared to conventional polyimides. Their improved flexural strength is indicated in figure IX-22. Here the flexural strengths of composites made from graphite fiber and either the PMR resin or a conventional condensation polyimide are compared. The properties shown are for composite specimens that were exposed to 600° F for 600 hours and then tested at 600° F. The PMR polyimide composite is twice as strong.

Because of the ease of processability of the PMR polyimide composites, their good strength properties, and their resistance to moisture, it is conceivable that they may replace epoxies to some extent at the lower temperatures. Epoxies would normally be used as the composite matrix material at these temperatures.

PREALLOYED POWDER PROCESSING

Normally, the achievement of higher strength materials is incompatible with simultaneously achieving lower cost in fabrication. However, the PMR technique for making new higher strength polymers is a potentially low-cost process. Another departure from the norm is the prealloyed powder process for producing advanced disk alloys. This new, potentially low-cost, manufacturing technique, which was pioneered to a great extent at the Lewis

Research Center, is illustrated schematically in figure IX-23. An alloy of any given composition is vacuum melted. When the melt is poured, inert gas jets are directed at the molten metal and cause it to atomize. The atomized metal droplets solidify rapidly into powders that are collected and sized. The powders are then compacted by extrusion or hot pressing, and the resulting compact can be subjected to any desired heat treatment. The rapid solidification of the atomized metal droplets results in an extremely fine grain size and a homogeneous structure without segregation. This may be seen in figure IX-24, which compares the microstructures of the NASA-TRW VI-A alloy in the conventional cast form and in the powder product form.

Figure IX-25 illustrates the results of applying the prealloyed powder technique to the VI-A alloy. It shows the substantial strength gains possible when the prealloyed powder process is applied to a highly alloyed normally cast material. The tensile properties of the alloy are compared in the prealloyed powder product form and the cast form as a function of temperature. The prealloyed powder product has an ultimate tensile strength of 274.5 ksi, about twice that of the cast version. Above 1500° F, the curves cross and the prealloyed powder product is weaker. This weakness is also reflected in an abnormally high elongation of 300 percent at 2000° F. This is indicative of superplasticity and results from the fine grain size of the powder product. In nickel alloys, grain boundaries are stronger than the matrix at low temperatures and weaker than the matrix at high temperatures. The superplastic nature of the powder product at high temperatures allows the material to be formed isothermally by application of relatively low loads, into any desired shape, such as a disk. The powder product can be used at the lower temperatures at which it affords such marked strength advantages and which is precisely the temperature region of interest for turbine disks.

In addition to the mechanical property improvements that are possible with this process, significant economies can be realized as well. An excellent example of the weight savings that can be realized by using this process is shown in figure IX-26. Shown are the key stages in making a commonly used, commercial, engine turbine disk. The conventional forging process requires a starting billet of 360 lb. Approximately 162 lb of material are then machined from the billet to produce the preform, which is a simple rectilinear shape that is required for adequate inspection by current non-

destructive sonic inspection techniques. However, if the preform were initially made by the prealloyed powder process, the 162 lb of raw material could be saved. In addition, the powder preform method would require that only 53 lb be machined off the preform to produce the final disk. This may be compared to a total of 215 lb of material that would have to be machined off in the conventional forging process. These savings are estimated to be worth approximately $2000 per disk and could reduce the cost of the finished disk from about $10 000 to $8000 - or 20 percent.

We are now applying this process in the development of advanced disk alloys to take advantage of their superior strength at intermediate temperatures - 1000° to 1200° F - the actual temperatures where turbine disks must operate. Figure IX-27 illustrates the strength advantage of a recently developed NASA prealloyed powder alloy, IIB-7, over a widely used forged alloy. At room temperature and at 1200° F, IIB-7 is 25 to 35 percent stronger than the forged alloy. This is extremely important, since the higher the ultimate tensile strength, the greater the burst strength of the turbine disk. Although IIB-7 is somewhat less ductile than the forged alloy, these levels of ductility are considered quite adequate.

The prealloyed powder process would appear to have much to offer the gas industry. It affords potential advantages with respect to achieving both higher strength and lower cost disk alloys for application to low-Btu, ground power conversion systems.

PROTECTION AGAINST ENVIRONMENTAL EFFECTS

Once new materials are made into components, they must perform in real service environments. NASA has conducted research into the environmental effects of oxidation and hot corrosion, nonoxidizing environments, and hydrogen. Oxidation and hot corrosion resistance is becoming a major life-controlling factor of turbine alloys. Such attack will also be a prime cause of metal component failure in gasifiers. The nonoxidizing environment work is primarily related to closed-cycle Brayton power systems that use helium as a working fluid. These studies could also be useful in research on gas-cooled reactors and gas-turbine ground power systems.

Oxidation and Hot Corrosion

In establishing the usefulness of an aerospace material, a prime step is to evaluate its resistance to the actual end-use environment. For example, in the case of gas-turbine materials, such evaluation falls into three stages. First, fundamental studies are conducted on laboratory specimens under carefully controlled temperature conditions. These tests give insight as to the extent and mechanisms of oxidation and hot corrosion attack. Figure IX-28 shows a sonic combustion gas test apparatus which uses simulated airfoils and introduces the additional factors of combustion gas chemistry, specimen geometry, high gas velocity, and thermal transients. Finally, the ultimate determination of a material's usefulness is made in the turbine section of an engine (fig. IX-29). Such an evaluation process generally leads to the conclusion that for most current turbine alloys, too much surface attack would occur in 5000 to 10 000 hours of actual engine operation even at maximum material temperatures of only 1600° to 1800° F. For the conceptual advanced engines operating in the 1900° to 2000° F range, current materials would have much shorter lives. Our studies to improve the high-temperature environmental resistance of turbine materials are concentrated on alloying and coating. Figure IX-30 shows that, after 300 hours at 2000° F, a typical nickel alloy (B-1900) currently used at 1600° to 1800° F as a turbine blade material, loses considerable weight. In effect, useful load-bearing material is lost. Uncoated blades of this or any other alloy would not last long in engine service at 2000° F. Adding only 0.5-percent silicon gives this alloy improved resistance to oxide spalling, and thus metal consumption is reduced. In fact, the improvement is about equal to that conferred by a commercial aluminide coating.

Presently, such aluminide coatings protect the external surfaces of most large, jet engine. turbine blades and vanes. They extend life and reduce repair costs. These commercial coatings, however, are not stable enough for higher temperature service. Nor are they alone adequate for use in gas turbines that ingest salt-laden air or use fuels with high levels of corrosive impurities. An example of this is shown in figure IX-31, which displays the results of 200 hours of accelerated hot corrosion tests for two coatings. The tests were accelerated by adding only 5 ppm sea salt, which contains alkali metal chlorides and sulfates. Coal contains from 1 to 4 per-

cent sulfur and much larger amounts of alkali metals, chlorine, etc. Thus, coal-combustion gas corrosion would be even more severe. A commercial coating failed, and the underlying alloy was extensively attacked. A recently patented Lewis coating was essentially unaffected after the same exposure. This coating combines a fail-safe inner layer of a ductile, oxidation-resistant Ni-Cr-Al alloy overlayed with a pure aluminide layer. The excellent hot corrosion resistance of the NASA coating suggests that it may also offer extended life for metal gasifier components.

Hydrogen

In the future, hydrogen may find wider use in producing high-Btu, pipeline-quality synthetic natural gas. Hydrogen may also find wider use as a fuel. NASA has conducted considerable research on materials compatibility with hydrogen in support of hydrogen-fueled rockets such as the Centaur and the Space Shuttle. Hydrogen can embrittle structural metals by three basic mechanisms:

(1) Reaction, in which new harmful constituents are formed, such as hydrogen bubbles in steel or copper, methane in steel, and hydrides in titanium

(2) Dissolution in alloys, such as atomic hydrogen dissolved in steel or nickel alloys

(3) Interaction with surfaces, such as hydrogen with steel or nickel alloys

Figure IX-32 illustrates typical losses in ductility after exposure to hydrogen at temperatures of 700^{o} to 1300^{o} F for cold-rolled Inconel 718. Ductility after static hydrogen exposure (H in solution) is compared with ductility after exposure to air on the left of the figure. Static hydrogen exposure lessens ductility. After 33 cycles in hydrogen, additional ductility losses occur. Suitable heat treating schedules can be developed to change the alloy microstructure and thus reduce hydrogen embrittlement, as shown on the right of the figure. However, hydrogen's harmful effects on ductility have not been entirely eliminated by these heat treatments. This must be considered in design to assure long-life and high-reliability structures.

In regard to long-life considerations, continued high-temperature expo-

sure to hydrogen also has a further degrading effect on material ductility, as shown in figure IX-33. After a 1000-hour hydrogen exposure at 1200° F, the cast nickel alloy U-700 shows an elongation decrease that is small but perceptible compared to elongation after a similar exposure in air. For more ductile wrought alloys, such as the nickel-base Hastelloy X and the iron-base A-286 alloy, the decrease in ductility after hydrogen exposure is more dramatic. Such materials may be candidates for use in gasifiers and other hydrogen systems. Thus, the NASA technology base in hydrogen-resistant materials may be of help to system designers in their initial materials selection efforts.

Application of Fracture Mechanics to Environmental Problems

Fracture-mechanics-type specimens and fracture mechanics concepts are now widely used to examine, in a quantitative way, material resistance to crack growth in aggressive environments. Work of this nature that may be of particular interest to the gas industry is being done at the NASA Ames Research Center in California. Until recently, the greatest part of their work has been on structural aerospace materials in either simulated service environments or in model environments that incorporate one or more salient features of the service environment. Figure IX-34 is representative of the form most of their data takes. The influence of three different environments on the stress corrosion cracking response of a high-strength, low-alloy steel (AISI 4130) is described as the crack growth rate against crack-front stress intensity. The two curves, one for a gaseous hydrogen environment, the other for gaseous hydrogen sulfide, were developed by using a fracture mechanics specimen of a type whose basic design was developed by Dr. E. J. Ripling of Materials Research Laboratory, Inc., and which uses a stress intensity calibration done at the Lewis Research Center. The specimen is loaded to a high initial stress intensity by mechanically propping open the crack. As the crack grows during exposure to the environment, the stress intensity for this specimen type decreases until crack growth is essentially arrested. In this way, by monitoring the crack progress with time, the full relation of crack growth rate to stress intensity can be determined from a single laboratory specimen.

Two parts of the curve are especially important in characterizing the aggressiveness of the environment: they are the so-called "plateau velocity," where the crack growth rate is nearly independent of crack-front stress intensity at intermediate stress intensity values; and the apparent "threshold" value of stress intensity, where the crack velocity drops to zero. Ostensibly, at stress intensities below the threshold value, crack growth will never take place.

From the data shown here, it can be seen that both hydrogen and hydrogen sulfide are extremely aggressive environments for this high-strength material. The curve for the molcecular hydrogen environment, considering both the plateau velocity (which is high, about a half a mil per second) and the threshold stress intensity (about 27 ksi-in.$^{1/2}$) classifies hydrogen-induced cracking as "severe" even at the low pressure of this test (45 mm Hg). We know from a considerable amount of other data that if the hydrogen pressure is increased, the plateau velocity is increased nearly proportionally and the threshold is reduced.

Comparing the hydrogen sulfide data with the hydrogen data shows the extreme threat to high-strength steels that develops when the service environment contains some hydrogen sulfide. The plateau velocity is raised by three orders of magnitude (to greater than 0.1 in./sec), and the threshold stress intensity is reduced by a factor of 2. The point included in the figure for dissociated hydrogen gives us a clue to the behavior of the alloy in hydrogen sulfide. It appears that hydrogen sulfide naturally dissociates at the steel surface to produce atomic hydrogen, which is responsible for crack growth in the steel. The dissociation takes place at a much higher rate than the natural dissociation of molecular hydrogen at the steel surface.

With an increased emphasis in government research on energy-related matters, the Ames Research Center is working to determine whether the stress corrosion phenomena studied in aerospace materials might be important, technology-limiting factors in various energy processes. Environments of pure hydrogen and environments containing mixtures of hydrogen and hydrogen sulfide are foreseeable for various energy systems. For example, many people within and outside of NASA speak of a future economy which uses hydrogen as a secondary fuel and as a secondary energy-storage medium. This hydrogen economy will involve the storage and transport of large quantities of gaseous hydrogen in much the same manner as is now

done with natural gas. For this reason, NASA has begun to look at the behavior of plain carbon steels similar to pipeline-grade steels in order to determine if hydrogen-induced cracking similar to that observed in high-strength steels can occur in these low-strength materials. Preliminary results at 1 atmosphere of gaseous hydrogen indicate that some degradation does occur, especially under low-cycle stress variations such as might be caused by line pressure fluctuations.

Figure IX-35 shows some preliminary results from a study to determine the possible threat to coal gasifier pressure vessels from gas mixtures containing hydrogen and hydrogen sulfide. Our work in this area is very preliminary, and we have not yet exposed fracture-mechanics-type specimens. However, this representation shows that substantial damage can be expected Simple tensile specimens were exposed for 100, 200, and 400 hours at 986^{o} F to 500-psi hydrogen. A specimen was also exposed to the same high temperature in the absence of hydrogen. The hydrogen exposure reduces both the room-temperature strength and total elongation, and this effect increases with increasing exposure time. These data were obtained for exposure temperatures higher than normal gasifier temperatures; however, our results show similar behavior at lower temperatures and longer times. Based on our experience with other materials and environments, degradations in tensile properties, of the type shown here, strongly indicate that significant cracking may be anticipated for precracked, fracture-mechanics-type specimens. Moreover, based on our experience with high-strength steels in hydrogen sulfide environments, we may anticipate that embrittlement will be even more severe in $H_2 + H_2S$ gas mixtures. These factors will be studied as our programs progress.

LIFE PREDICTION

An important consideration for the designer of structures is the need to predict life in advance of service and do so accurately. Many factors are involved and there can be interacting effects. The problem of predicting life must take into account the phenomena of creep, oxidation, low-cycle fatigue, and creep-fatigue interaction.

Creep Rupture

Creep rupture is an important mode of failure that can restrict the useful lifetime of structural equipment operating at high temperatures. When a stress is applied to a material at high temperatures, thermally activated processes produce a time-dependent creep strain in the direction of the applied stress. If the stress is held long enough, the material will slowly stretch and eventually rupture. These stresses can be well below the yield strength of the material.

In order to prevent catastrophic rupture of turbine blades, pressure vessels, boiler tubes, and piping components that must operate for decades at high temperatures, it is necessary to keep the pressure stresses below the creep-rupture strength of the material. Seldom is it practical to conduct laboratory creep-rupture tests that are as long as the intended application. It is therefore necessary to extrapolate behavior that is measured in shorter time intervals. This is particularly true for new alloys that are currently being developed. Time-temperature parameters are used in the process of making such extrapolations.

Since 1953, the Lewis Research Center has been at the active forefront of research in the area of creep-rupture life extrapolation. We have developed a number of different time-temperature parameters during that time. Other organizations have also developed parameters for the same purpose. Several of the most commonly used parameters are the Larson-Miller, Manson-Haferd, and Orr-Sherby-Dorn. The Larson-Miller parameter is probably the most familiar of them all, partly because of its simplicity, but also because it was one of the first parameters ever to be proposed. Although the Manson-Haferd and the Orr-Sherby-Dorn parameters are not as familiar, they are used a great deal. Each of these parametric approaches utilizes the following generalized equation form:

$$f(S) = \log(t) + A \log(t) f(T) + f(T)$$

The idea behind the use of a parameter to extrapolate to longer times is as follows. Short-time, creep-rupture data are generated over a range of temperatures and stresses. These results are used to determine the constants in the specific equation chosen. Once the constants are known,

the equation is used to calculate the longer rupture times of interest. However, once a parameter is chosen for use, the form of the equation is fixed and the mathematical form is, in effect, dictating how the material should behave. Although most materials conform to this expected behavior in a general sense, there are deviations of practical significance. In order to overcome the rigidness of the conventional time-temperature parameters, the use of a more flexible approach, which is appropriately called the "Minimum Commitment Approach" was proposed at Lewis. In essence, the short-time data are used not only to determine the constants of an equation, but also to determine the mathematical form. Typically, the equation form would not be a conventional appearing one, but instead would be appropriate to material behavior at specific values of time and stress. Thus, short-time data are used to establish the parametric form that best describes the material behavior. The computer program MEGA has been written to handle the application of this new Minimum Commitment Approach.

The question arises, however, is this added complexity worth the effort? Does MEGA give more accurate predictions than the simpler conventional parameters? In attempting to answer this question, we participated in an extensive evaluation study. MEGA and a number of the most commonly used parameters were applied to 21 sets of creep-rupture data in an ASTM program involving many laboratories. In every case, MEGA and the other parameters were fit to a consistent set of short-time results. Long-time life was then predicted from the short-time fit and checked against available long-time data. Although not the best in every instance, MEGA gave good predictions more consistently than any of the other parameters.

The application of MEGA to the extrapolation of short-time data to longer times for 316 stainless steel is shown in figure IX-36. Stress is plotted against time to rupture at four test temperatures for times to 1000 hours. The question to be answered was, what would the curves extrapolate to in the life range of 1000 to 20 000 hours? In the short-time range, the functions for stress f(S) and temperature f(T) were determined by MEGA. Once known, these functions were used to calculate rupture curves beyond 1000 hours. The comparison of this extrapolation with actual data is shown in figure IX-37. Agreement between predicted and observed lives is excellent.

A more direct comparison of this approach with predictions is shown in figure IX-38, where observed life is plotted against predicted life. Shown

are three sets of predictions; by MEGA and by the Orr-Sherby-Dorn and Larson-Miller parameters. The symbols lying closest to the central 45^{o} line indicate the most accurate predictions. Clearly, MEGA gives the best predictions, with lives generally being predicted within a factor of 1.5 on life. The other two approaches were successful to within a factor of 2.0.

An important point can be made by drawing the following analogy. Extrapolation by time-temperature parameters could be likened to shooting at a target with a rifle. Obviously, the rifle must be held rigidly for best results. However, if it is always held in the same orientation without regard for how far away the target is or without regard to wind and other perturbing effects, the bulls-eye will not be hit as often as it would be if these factors were accounted for. The analogy here is that the Minimum Commitment Approach samples the perturbing effects that are evident in the short-time results and builds in the necessary corrections for the long-time extrapolation.

It should be emphasized that if the sampling is too limited, that is, if there are very few short-time data, erroneous corrections might be applied. Hence, it is essential that a reasonably sufficient size sample be available before the Minimum Commitment Approach is applied for long-time, creep-rupture extrapolation. This requirement, however, is not asking too much when large, expensive equipment must be designed to operate efficiently and safely for extremely long periods of time. In these cases, the most accurate time-temperature parameter is an absolute must.

We feel that the Minimum Commitment Approach has much to offer for predicting the ultra-long-time, creep-rupture life required in many applications in the gas industry.

Oxidation Effects

Research efforts directed toward creep-rupture life prediction have been underway for many years. However, the point is just now being reached where sufficient understanding of alloy oxidation has been obtained to attempt to predict material loss due to oxidation. Our initial work has been on nickel-chromium alloys such as Ni-40Cr. These alloys react with oxygen to form chromium oxide scales, which results in a partial consump-

tion of the alloy. Also, some of the oxide scale can vaporize, thus increasing metal consumption.

So far, a mathematical model for this kind of oxidation attack has been developed, and experimental data have been obtained to 1000 hours (fig. IX-39). With this base, it is now possible to extrapolate oxidation attack out to longer times, as indicated by the dashed line. As longer time data are obtained, the accuracy of the model can be checked and its extrapolation ability evaluated.

Our eventual goal is to give the designer an added tool to account for oxidation behavior in predicting life. With a limit on allowable metal consumption and a required component life, we are trying to provide a framework in which he can at least make a "first cut" at material suitability.

Low-Cycle Fatigue

Our involvement in the area of low-cycle fatigue life prediction began over 20 years ago with Manson's formalization of the basic plastic strain law of fatigue. Since that time, we have maintained a continuing interest and an ever increasing activity in this area of research. Primary emphasis has been placed on the development of practical life-prediction approaches.

In 1964, the Universal Slopes Equation was introduced. An important aspect of this contribution is that the low-cycle fatigue curve can be estimated from a knowledge of the tensile properties of the material at the temperature of interest. This represents pure fatigue behavior without any influences of creep or oxidation effects. The equation has had a significant impact and is widely used throughout a number of industries for preliminary design of high-performance structures.

Creep-Fatigue Interaction

Some of the most crucial low-cycle fatigue design problems are encountered at high operating temperatures, where time-dependent creep may be an overriding consideration. As a first approximation of the detrimental effects of creep, the 10 Percent Rule was introduced in 1966. This simple

rule of thumb assumes that the maximum detrimental effect of creep is to reduce the fatigue life to only 10 percent of what it would have been without creep. The 10 Percent Rule has proven to be a very helpful and widely used tool for estimating the low-cycle fatigue behavior of materials that will operate at high temperatures for long times.

We have also devoted considerable effort toward the development of the time and cycle fraction concept because such an approach offered a quantitative rationale for assessing the individually damaging aspects of creep and fatigue. Satisfactory results have been achieved in the laboratory, and in fact, the approach has been adopted by the American Society of Mechanical Engineers (ASME) Nuclear Pressure Vessel and Piping Code Case 1592 for high-temperature design. Nevertheless, there are practical limitations on the accuracy involved in the application of this approach to structural problems. Because of these limitations, we have sought alternatives. An attractive approach which we call Strainrange Partitioning accounts for the interaction effects of creep and fatigue damage. Strainrange Partitioning characterizes high-temperature, low-cycle fatigue and can effectively be used to correlate and predict fatigue life under conditions where creep effects are present.

Figure IX-40 illustrates how Strainrange Partitioning characterizes high-temperature, low-cycle fatigue behavior. A series of four fatigue curves are shown in which the range of strain, or width of the hysteresis loop, is plotted against the number of cycles to failure. The greater the strain range, the fewer the number of cycles to failure. Everyone at some time or another has taken a wire or paper clip and bent it back and forth until it broke into two pieces. The more severely it was bent, the greater the strain range, and the fewer bends it took to produce fracture.

An explanation of what is meant by the name Strainrange Partitioning is in order. At high temperatures, two distinctly different types of permanent deformation can take place in metals. These are commonly classified as creep, which is time dependent, and plasticity, which is not a function of time. The concept of Strainrange Partitioning is based on the separation, or partitioning, of a strain into these more basic components. Rapid straining is associated with plasticity, and slow straining is assocated with creep. High-temperature fatigue life depends strongly upon how these two types of strain reverse each other within a cycle.

Four curves are shown because high-temperature creep enters into a cycle in four limiting ways. First of all, if no creep is involved, the upper curve applies and we have a pure fatigue situation. An example of this type of behavior is high-frequency vibration, in which there is insufficient time for creep to occur. When creep is introduced into the compressive portion of a cycle, the fatigue life is reduced typically as shown. Certain cyclic thermal strains are equivalent to this type of cycle. When creep occurs in both tension and compression, there is an additional, although slight, reduction in life. Low-frequency loading produces such a cycle. The most severe cycle typically involves creep in only the tensile portion of the cycle. A pressure vessel that is cyclically pressurized at high temperatures, as well as some special types of thermal strain cycle, falls into this category.

Simple laboratory tests can be used to generate data from which these curves can be constructed. Two of the most important features of these curves are their relative insensitivity to test temperature and the fact that the curves represent bounds on cyclic life. Any conceivable strain cycle is a simple combination of these four basic components, and the cyclic life of the cycle will lie between the bounding curves. It is possible to characterize, with a single set of curves, the entire high-temperature, low-cycle fatigue resistance of a material. Of course, the problem still must be solved as to how much of each component strain is present in a given cycle, that is, how the strains are partitioned. We are working on a variety of experimental and analytical techniques to accomplish this end.

To date, we have been able to evaluate Strainrange Partitioning in the laboratory with a dozen high-temperature alloys. The degree of accuracy to which our new approach can calculate cyclic lives is indicated in figure IX-41. Observed cycles to failure agree with the predicted cycles to failure to within a factor of 2. We consider such agreement to be exceptionally good and significantly superior to the agreement that other approaches can achieve. For example, factors of 5 or even 10 on life are not at all uncommon when other methods are used. We are actively pursuing the application of Strainrange Partitioning to the prediction of the high-temperature, low-cycle fatigue lives of a number of important aerospace structures. With additional refinements, we expect the approach to be of great value to designers faced with the difficult problem of assessing the cyclic lives of structures operating in high-temperature environments.

TABLE IX-1. - NASA MATERIALS RESEARCH RELEVANT TO GAS INDUSTRY

AEROSPACE APPLICATIONS	RESEARCH AREAS	POTENTIAL GAS INDUSTRY APPLICATIONS
STRUCTURAL COMPONENT DESIGN	FRACTURE MECHANICS	PRESSURIZED SYSTEMS ALLOY SELECTION
CRYOGENIC TANKAGE AIRCRAFT STRUCTURES	COMPOSITE TANK TECHNOLOGY	LARGE REACTION CHAMBERS
TURBINES ROCKETS	NEW MATERIALS	GROUND POWER TURBINES, GAS MANUFACTURING SYSTEMS
HOT TURBINE COMPONENTS PROTECTION	CORROSION & ENVIRONMENTAL PROTECTION	COAL GASIFICATION SYSTEMS, PIPING SYSTEMS
TURBINE DISKS, BLADES, VANES	LIFE PREDICTION TECHNIQUES	TURBINES & GASIFIERS

CS-72315

TABLE IX-2. - POTENTIAL OF COMPOSITES FOR LOWER TANK COSTS

MATERIAL	FABRICATED COST, $/LB	RELATIVE TANK COST (COMPARED TO STEEL), %
STEEL	3.00	100
GLASS/EPOXY	3.00	92
KEVLAR/EPOXY	5.00	81

CS-72320

TABLE IX-3. - COMPARISON OF CERAMICS IN CYCLIC SCREENING TESTS

[Sonic gas-stream temperature, 2200° F; heatup time, 3 min; exposure time, 5 min.]

MATERIAL	CYCLES EXPOSED	RESULT
SiC	120	NO OXIDATION, NO THERMAL CRACKS
Si_3N_4	120	NO OXIDATION, NO THERMAL CRACKS
ZrB_2 + ADDITIVES	36	OXIDATION ATTACK
SiC + ADDITIVES	8	THERMAL SHOCK FAILURE
MOST OXIDES	1-3	THERMAL SHOCK OR MECHANICAL FAILURE

CS-72409

Figure IX-1. - Liquid-natural-gas storage tank failure. (Photograph by Cleveland Plain Dealer.)

Figure IX-2. - Catastrophic failure of 260-inch-diameter motor case.

CS-52447

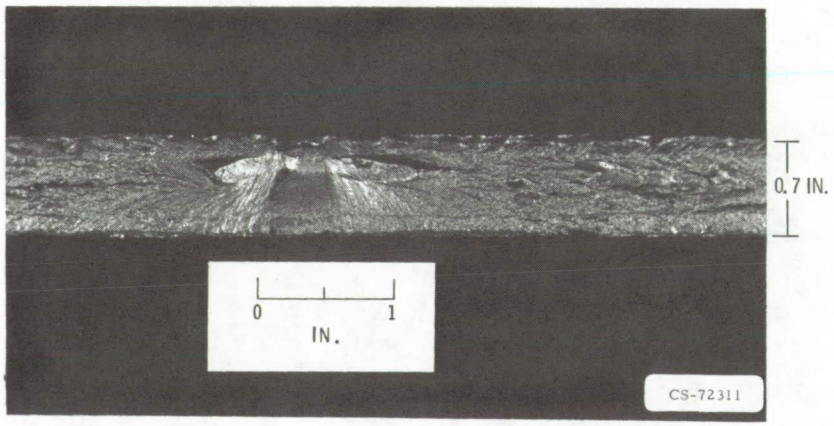

Figure IX-3. - Flaw at which fracture initiated in 260-inch-diameter motor case.

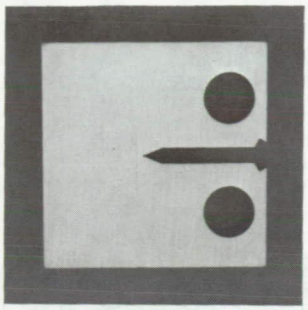

COMPACT TENSION TYPE

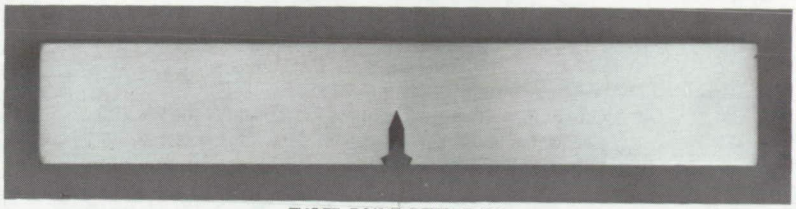

THREE-POINT BEND TYPE

CS-72033

Figure IX-4. - Standard plane-strain fracture toughness test sepcimens.

$$\sigma_x = \frac{K_I}{(2\pi r)^{1/2}} \cos\frac{\theta}{2}\left(1 - \sin\frac{\theta}{2}\sin\frac{3\theta}{2}\right) + \ldots$$

$$\sigma_y = \frac{K_I}{(2\pi r)^{1/2}} \cos\frac{\theta}{2}\left(1 + \sin\frac{\theta}{2}\sin\frac{3\theta}{2}\right) + \ldots$$

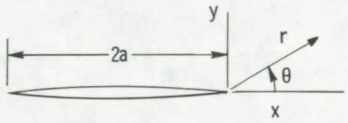

$$\sigma_z = \nu(\sigma_x + \sigma_y)$$

$$\tau_{xy} = \frac{K_I}{(2\pi r)^{1/2}} \sin\frac{\theta}{2}\cos\frac{\theta}{2}\cos\frac{3\theta}{2} + \ldots$$

$$\tau_{xz} = 0$$

$$\tau_{yz} = 0$$

K_I IS THE "STRESS INTENSITY FACTOR"

K_{Ic} IS THE "FRACTURE TOUGHNESS"

CS-72252

Figure IX-5. - Plane-strain elastic stress field in vicinity of crack tip.

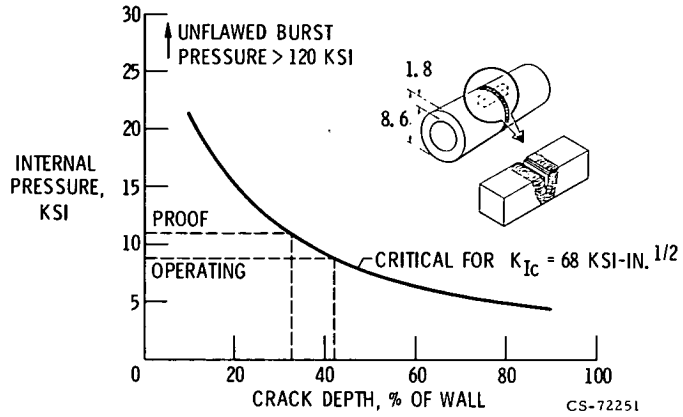

Figure IX-6. - Fracture toughness assessment of thick-walled pipe for liquid hydrogen transfer. Centrifugally cast 21-6-9 stainless steel pipe; 308L welds.

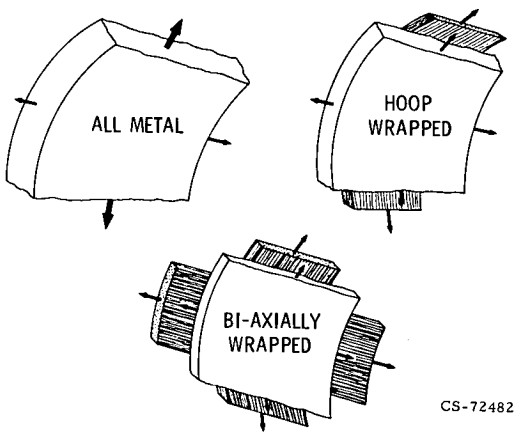

Figure IX-7. - Types of pressure vessel.

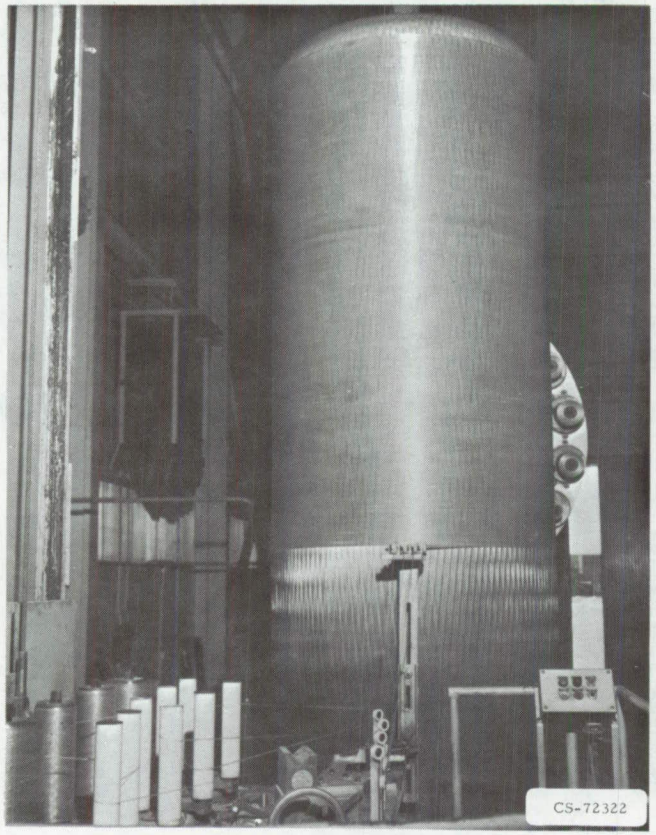

Figure IX-8. - Composite tank 120 inches in diameter.

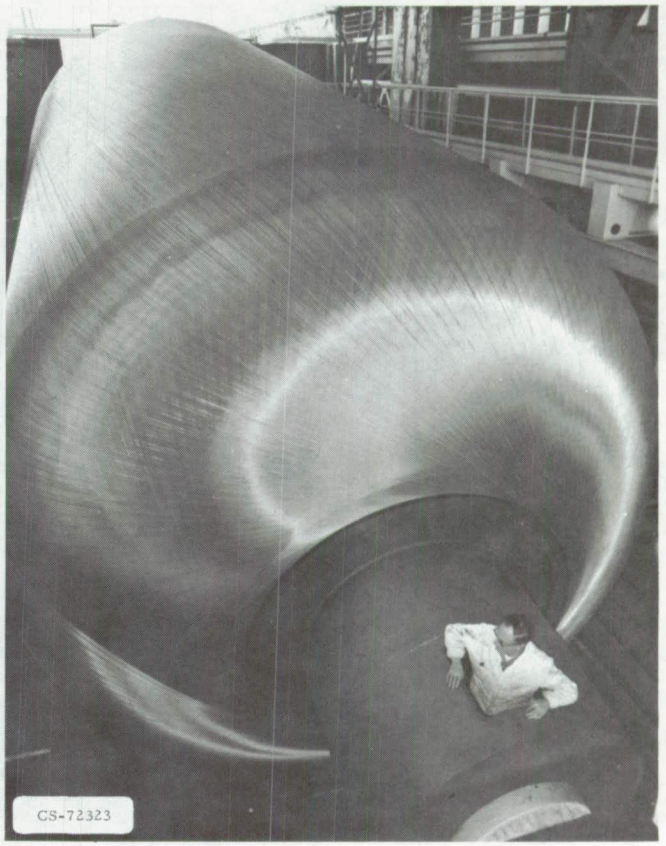

Figure IX-9. - Composite tank 260 inches in diameter.

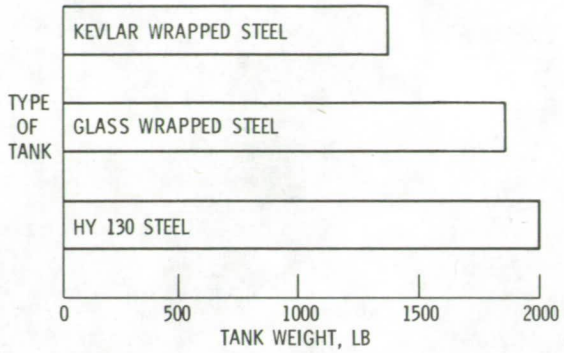

CS-72478

Figure IX-10. - Weight advantage of composite tanks compared to an all-steel tank.

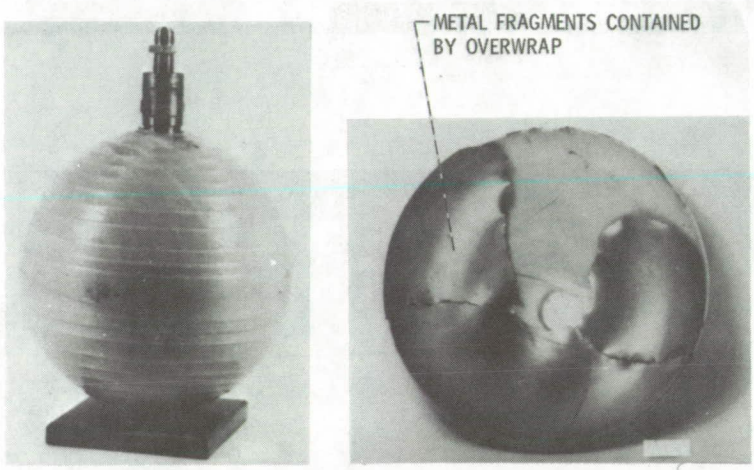

CS-72321

Figure IX-11. - Composite pressure vessel failure.

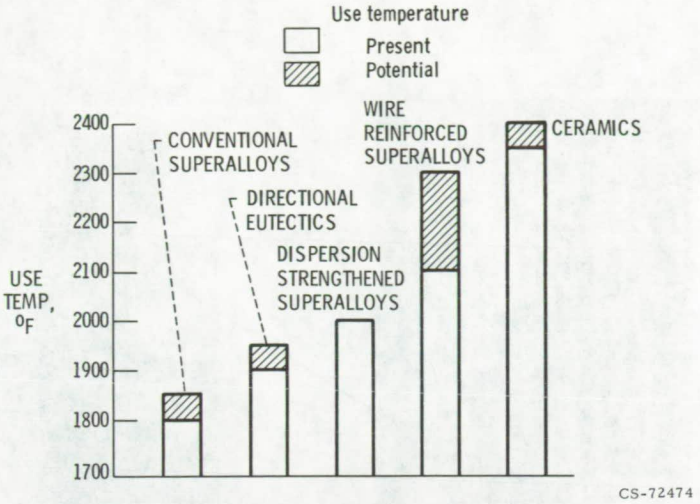

Figure IX-12. - Use-temperature potential of turbine blade materials.

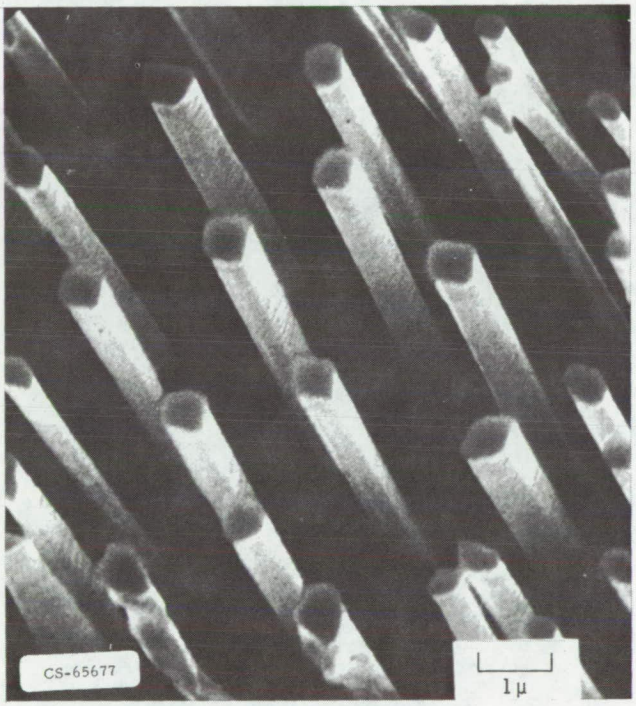

Figure IX-13. - Scanning electron micrograph of cobalt-base directionally solidified eutectic alloy.

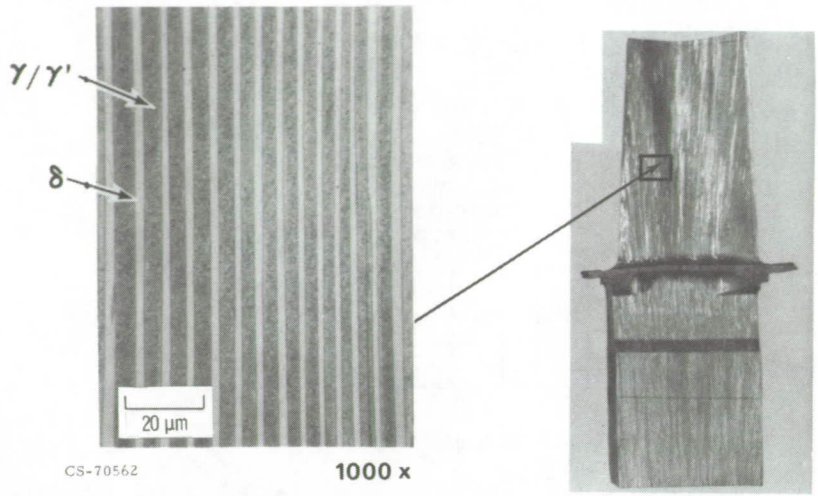

Figure IX-14. - Turbine blade of $\gamma/\gamma' + \delta$ directionally solidified eutectic alloy.

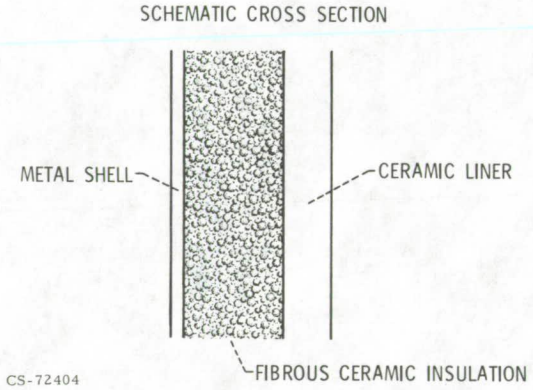

Figure IX-15. - Schematic cross section of gasifier concept using ceramic liner and insulation.

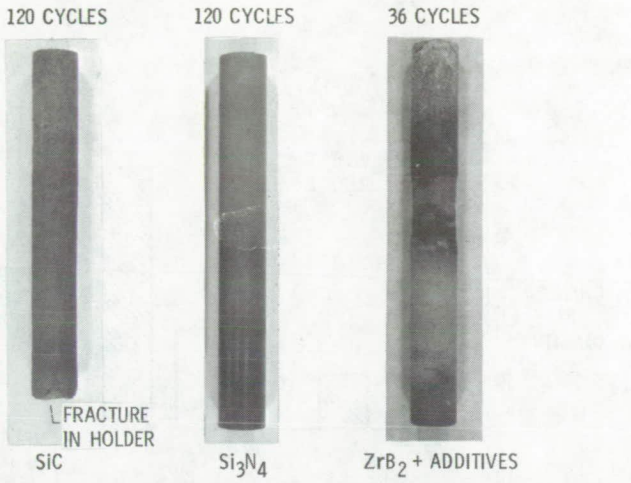

Figure IX-16. - Post-test appearance of ceramics. Sonic gas-stream temperature, 2200° F; exposure time, 5 min.

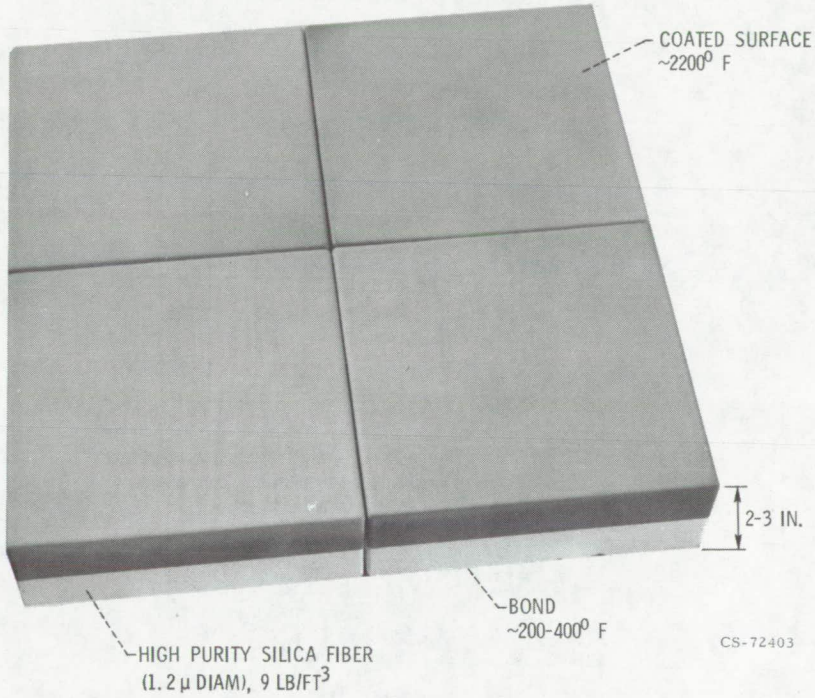

Figure IX-17. - Space Shuttle heat-shield candidate.

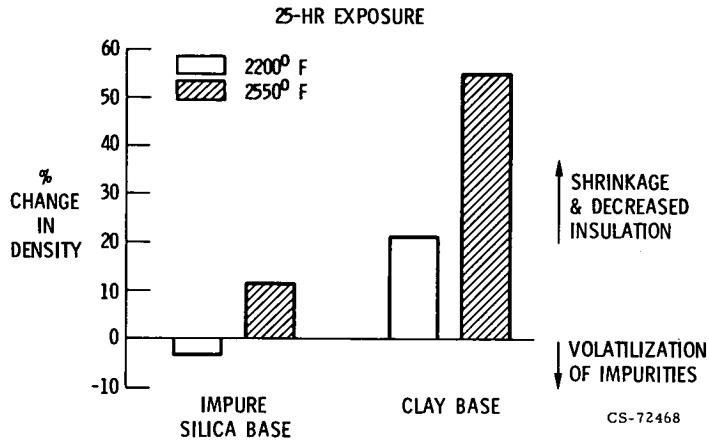

Figure IX-18. - Evaluation of commercial insulation materials. Exposure time, 25 hr.

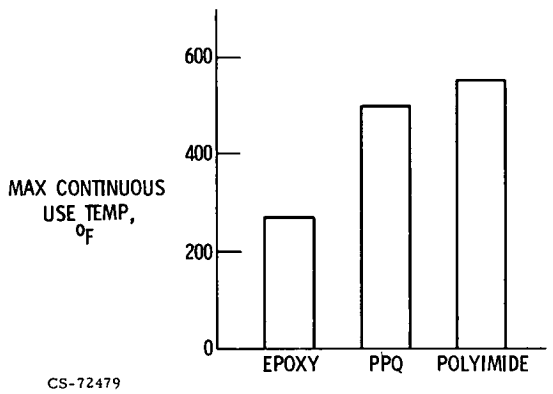

Figure IX-19. - Maximum use temperature of advanced polymers for composite matrices, as compared to epoxy.

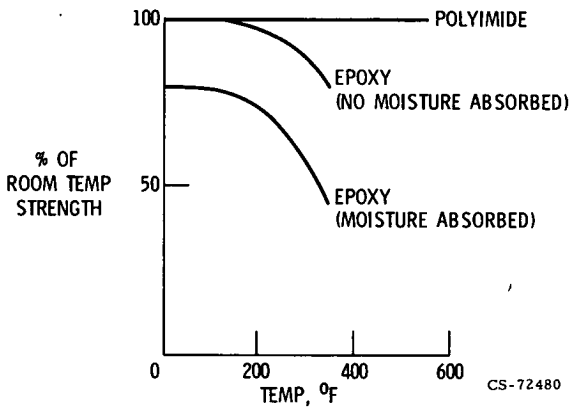

Figure IX-20. - Strength of advanced polymers for composite matrices, as compared to epoxy.

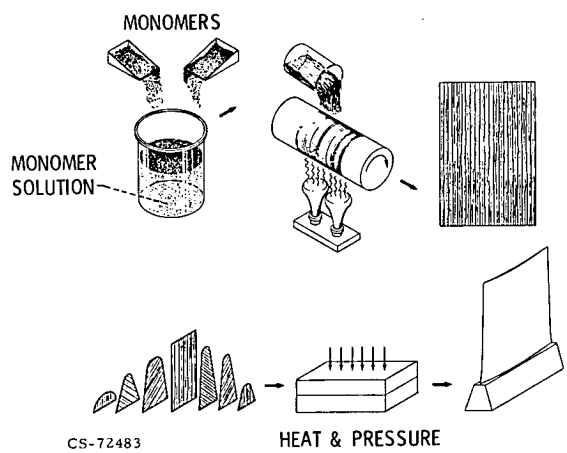

Figure IX-21. - High-temperature polymer process - polymerization of monomeric reactant (PMR) - developed at Lewis Research Center.

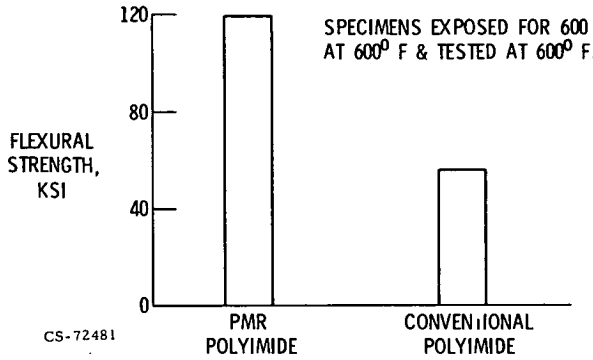

Figure IX-22. - Flexural strength of PMR composites as compared to conventional polyimides.

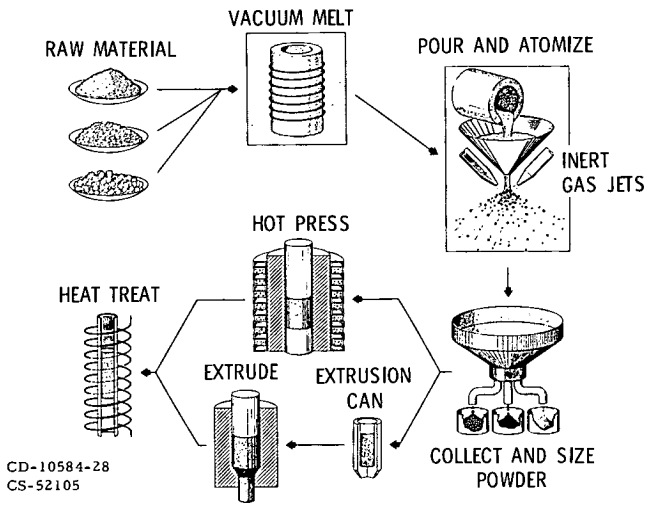

Figure IX-23. - Prealloyed powder processing method.

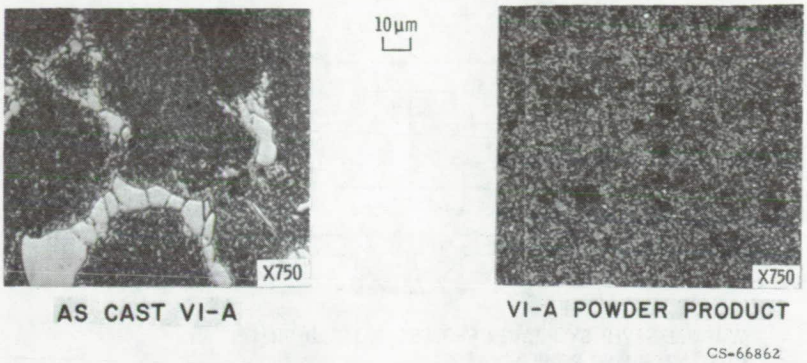

Figure IX-24. - Microstructures of NASA-TRW VI-A alloy prepared by casting and prealloyed powder processing.

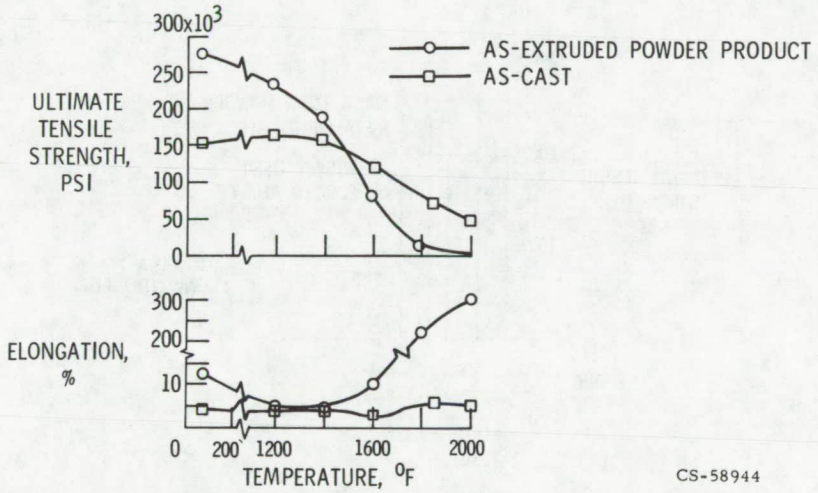

Figure IX-25. - Comparison of tensile properties of NASA-TRW VI-A alloy prepared by casting and prealloyed powder processing.

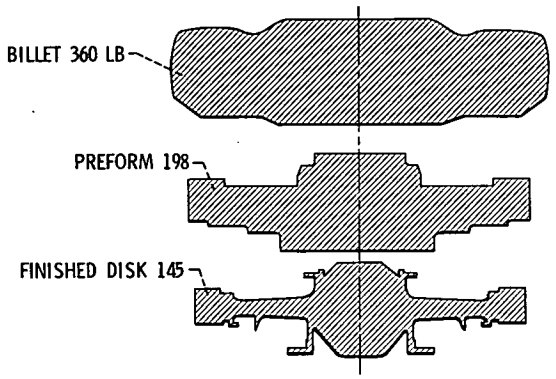

MATERIAL SAVED BY POWDER PROCESS	162 LB OR 45%
TOTAL MACHINING REQUIRED	
BY POWDER PROCESS	53 LB OR 27%
BY FORGING PROCESS	215 LB OR 60%

CS-72316

Figure IX-26. - Weight savings with prealloyed power processing, as compared to forging.

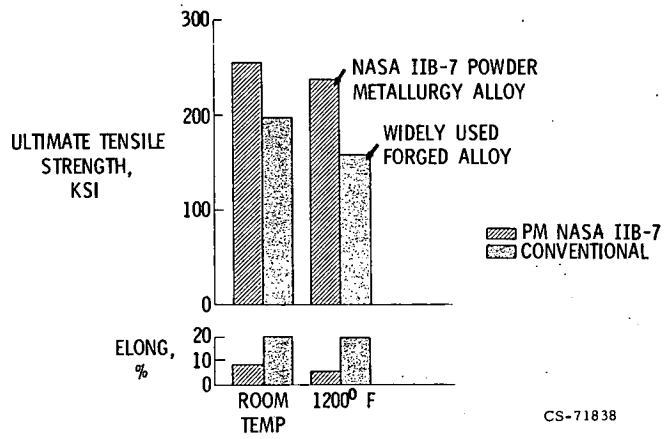

Figure IX-27. - Strength of turbine disk alloy prepared by prealloyed powder processing, as compared to a forged alloy.

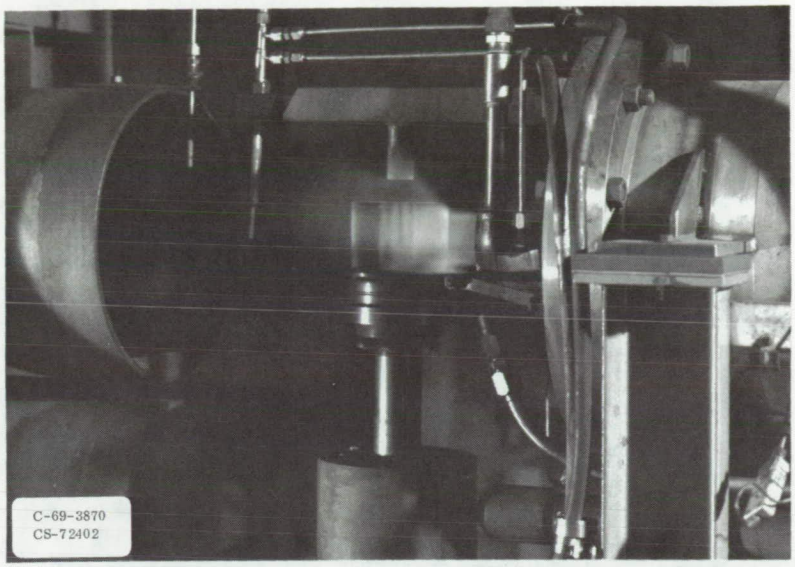

Figure IX-28. - Simulated environmental testing of resistance to oxidation and hot corrosion.

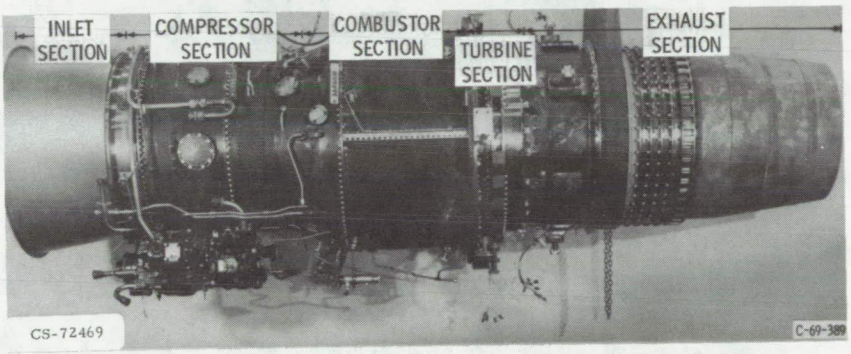

Figure IX-29. - Typical turbine used in actual environmental testing of blades.

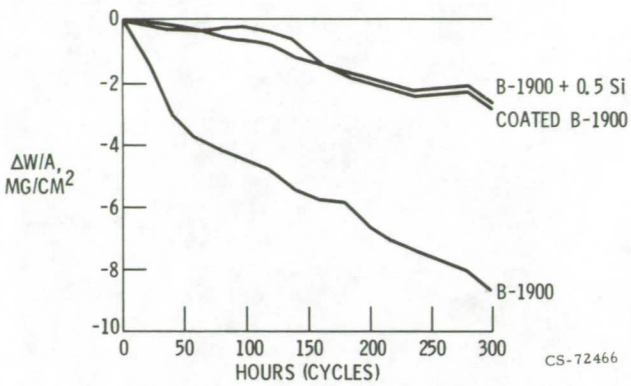

Figure IX-30. - Effect of silicon addition on Mach 1, 2000° F oxidation of nickel alloy B-1900.

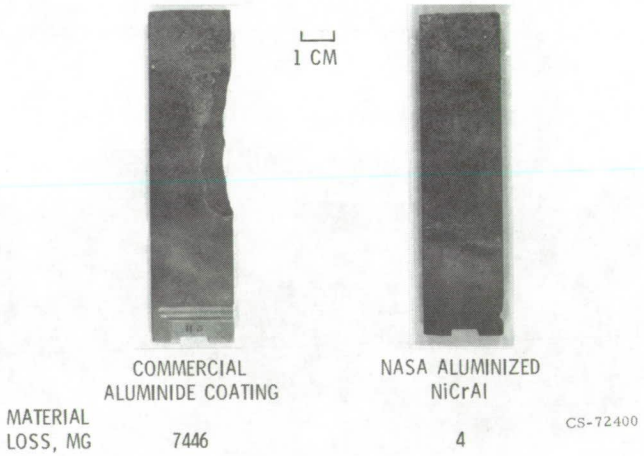

Figure IX-31. - Performance of coatings in accelerated hot corrosion test. Sonic gas-stream temperature, 1650° F; sea-salt content, 5 ppm; number of 1-hr cycles, 200.

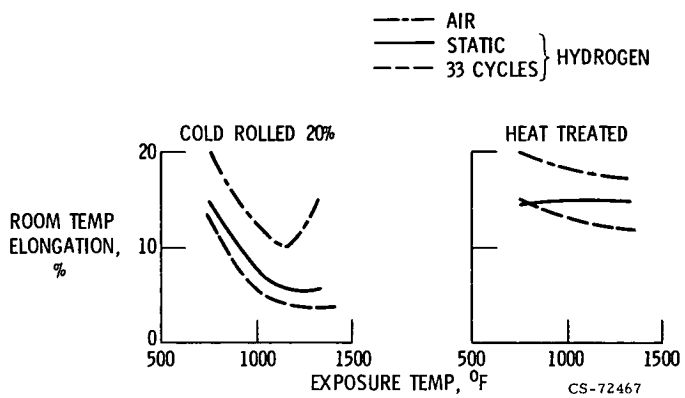

Figure IX-32. - Effect of hydrogen environment on room-temperature elongation of nickel alloy Inconel 718 - both cold-rolled and heat treated.

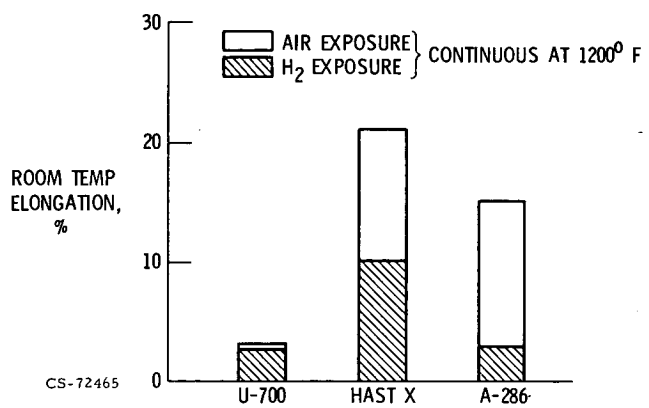

Figure IX-33. - Effect of hydrogen environment on room-temperature elongation of three alloys after 1000-hr exposure.

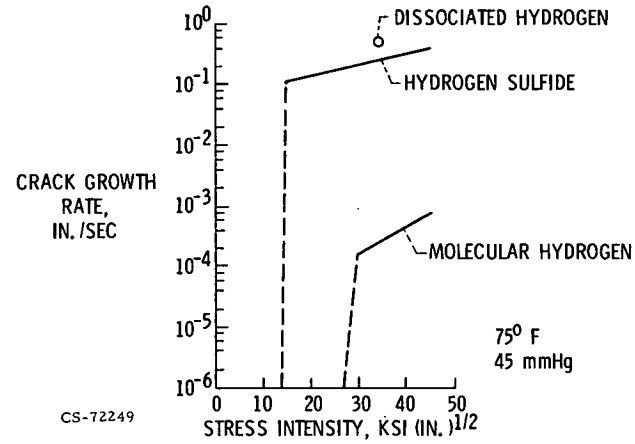

Figure IX-34. - Effect of environment on crack growth rates of AISI 4130 steel.

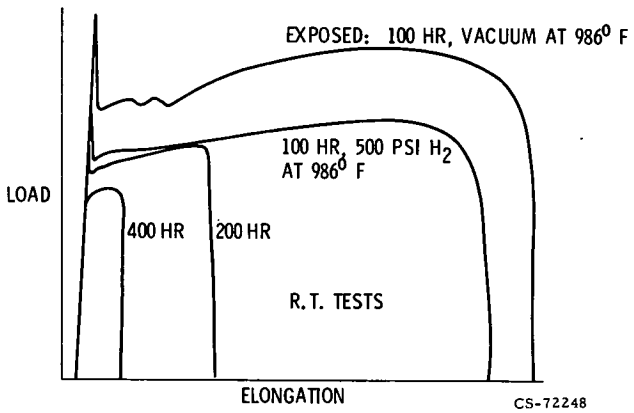

Figure IX-35. - Hydrogen attack on SAE 1020 steel.

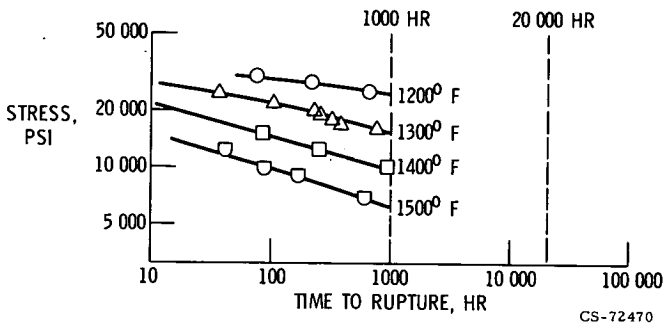

Figure IX-36. - Short-time, creep-rupture isotherms for 316 stainless steel.

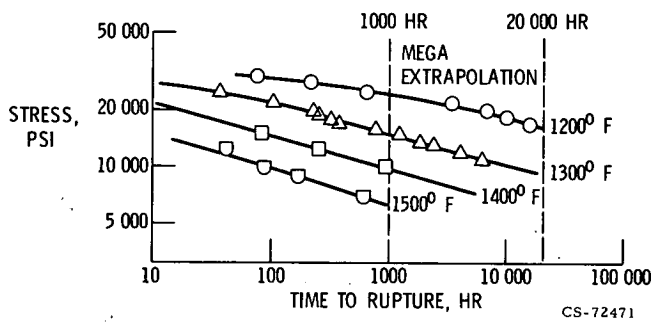

Figure IX-37. - Comparison of MEGA extrapolation with long-time, creep-rupture data for 316 stainless steel.

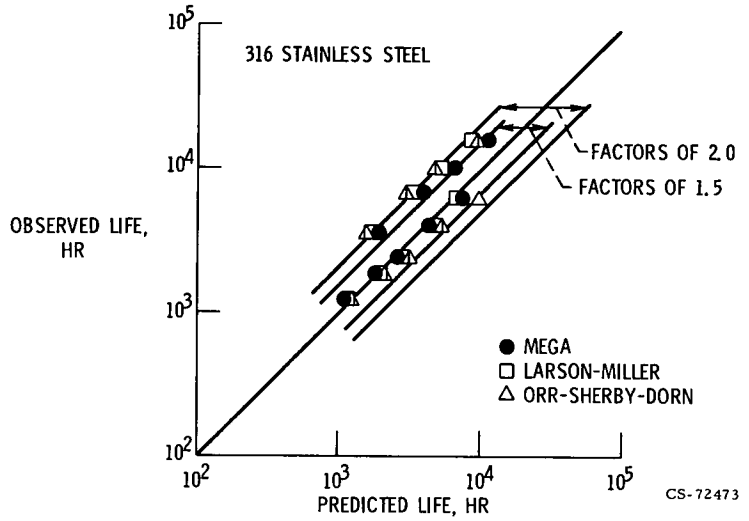

Figure IX-38. - Predictability of long-time, creep-rupture life of 316 stainless steel using three parameter approaches.

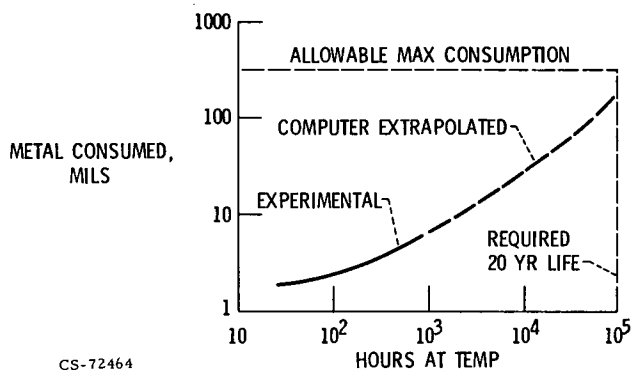

Figure IX-39. - Extrapolation of oxidation life for Ni-40Cr at 2000^{0} F.

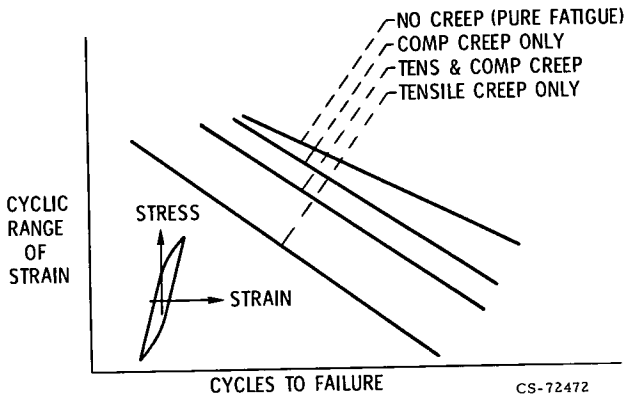

Figure IX-40. - Characterization of material behavior by Strainrange Partitioning.

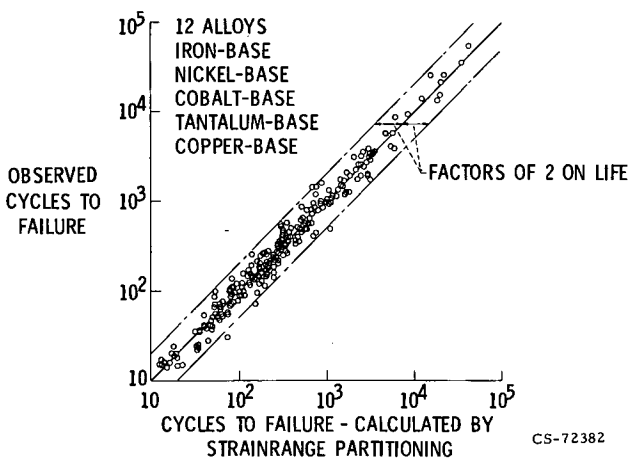

Figure IX-41. - Predictability of cyclic life by Strainrange Partitioning.

Page intentionally left blank

Page intentionally left blank

X. RELIABILITY AND QUALITY ASSURANCE

Walter F. Dankhoff

A useful introduction to a discussion of the reliability and quality assurance system used by NASA is to highlight some of the prime characteristics of space missions and the hardware involved. One of the most outstanding characteristics of a space mission is that it is a "one-shot" operation. The failure of a part or a component in flight can be catastrophic; that is, it can result in the loss of the space vehicle and the failure of the mission. Another characteristic of space missions is that they require large investments of money in both the spacecraft and its launch vehicle, as well as in all the other operations that are required for a successful mission. Also there is little opportunity to correct a malfunction of a system operating in space. Unmanned space missions, in particular, have this characteristic. Since the system used in an unmanned space mission is not brought back to earth, either in a successful mission or in a mission in which there is a malfunction, we are seriously handicapped in analyzing and determining the cause of the malfunction. In this situation, the engineers have to depend on the data that were transmitted to the ground stations during flight. They also depend heavily on the data that were previously collected during the fabrication, assembly, and test operations of the specific vehicle.

It is assumed that the reader is generally familiar with the systems and hardware that are used in the space program. Shown in figures X-1 and X-2 are the vehicles that are used to launch all medium to heavy payloads in the NASA unmanned space program. The Atlas-Centaur (fig. X-1) has been a workhorse for NASA in launching medium-weight payloads. A more recently developed NASA launch vehicle is the Titan-Centaur (fig. X-2). This vehicle, which has the performance capability of handling heavier payloads (up to 34 000 lb) than the Atlas-Centaur, is made up of the Air Force Titan IIIE and the NASA Centaur stage. Within these vehicles, there are a large number of subsystems and complex equipment. This complexity is shown by the forward end of the Centaur stage (fig. X-3), which is used to mount

much of the Centaur electronic and flight control equipment. Figure X-4 shows one of these electronic boxes, the systems electronic unit, in an open position. This example gives some idea of the number of parts involved in these units and the tight packaging that is required.

The spacecraft and satellites used in NASA space missions require an even more sophisticated design approach in regard to minimum weight than do the launch vehicles. The reason is that every pound of spacecraft has to be boosted into earth orbit and, in some cases, on a planetary or other mission trajectory. Therefore, design for minimum weight and, in many cases, minimum size is the dominant consideration. An example of an unmanned spacecraft is the Communications Technology Satellite (fig. X-5), which is under development. This communications satellite will use the highest power communication signal ever to be transmitted from a satellite to the earth. This project is a combined venture between the Canadian Government and NASA. It will be used to communicate to remote and sparsely populated regions of Canada and the United States. The Lewis Research Center is the coproject manager for NASA. Another example of an unmanned spacecraft is the SERT II (fig. X-6). This spacecraft was developed and launched by the Lewis Research Center and explored long-duration operation of an ion thruster propulsion system in space.

In addition to the space program, NASA has an extensive program in aeronautics. The Lewis Research Center has the primary responsibility for aeronautical propulsion. For those parts of the aeronautical program that involve flight or major ground tests of total systems, such as jet engines, reliability and quality assurance requirements similar to those used in the space program are applied. One of the current aeronautical propulsion flight programs at Lewis is the Refan Project. The purpose of this project is to demonstrate the feasibility of modifying a Pratt & Whitney JT8D turbofan engine to operate at lower noise levels; that is, noise levels which would be more acceptable to the communities around our nation's airports. The modified engine recently underwent flight tests on a DC-9 aircraft (fig. X-7).

The proven concepts of reliability and quality assurance are also applied, as appropriate, to other NASA programs. For instance, in the case of the energy program, some demonstration projects, such as the 100-kilowatt wind turbine generator (fig. X-8), use appropriate parts of the reliability and quality assurance program. This particular project is discussed in further detail

in paper XI of this conference report.

Of course, it is recognized that the characteristics of space missions and the systems utilized are quite different from those of the gas industry operation. The gas industry operation could be characterized as a repetitive, long-life operation. But there is some similarity with the space program in that large investments are also required for the initial installation and check-out of the systems used in the gas industry. Also in order to achieve long equipment life under repetitive usage, equipment must require minimum maintenance and experience a minimum number of breakdowns. Therefore, attention to and investment in the reliability, quality, and, of course, safety of the equipment and systems is also mandatory in the gas industry.

The one-shot operation that characterizes the space program has dictated some extremely high requirements for the quality of the equipment and its operational reliability. In fact, the complexity of the subsystems and the number of parts involved has demanded a relatively high reliability just to make the subsystems functional. Then, in order to ensure mission success, extremely high reliability is required of the parts and components that make up the subsystems and flight vehicles. NASA has had to expend large amounts of energy, time, and money to obtain this level of reliability in equipment and operations. However, this is a cost-effective investment because the cost of a failure is extremely high - the loss of a mission. Therefore, over the years, NASA has developed a system which is rigorously applied to our major projects to assure the reliability and quality of the vehicles and equipment involved in space missions. The remainder of this paper is devoted to a description of this system and its elements. As much as possible, the implementation of these elements is illustrated through actual experiences, particularly in launch vehicle operation.

Of course, as was previously recognized, there are differences in the characteristics of the gas industry operation, as compared to the space program. However, a review of the overall system and some specific examples of application of the NASA reliability and quality assurance program should reveal some concepts that could be usefully applied to the gas industry.

For purposes of discussion, the reliability and quality assurance system used by NASA can be divided into 10 key activities:

(1) Management - emphasis and overview

(2) Design - designing in reliability, quality, and safety

(3) Testing - development, qualification, and acceptance
(4) Fabrication and assembly - quality control
(5) Procurement - quality control
(6) Discrepancy reporting, analysis, and corrective action
(7) Data acquisition and retrieval systems
(8) Auditing and surveillance
(9) Flight readiness reviews
(10) Postflight evaluation

MANAGEMENT - EMPHASIS AND OVERVIEW

Through all phases of a project, there is a continuous emphasis by management on reliability and quality assurance. NASA management holds periodic reviews to ensure that reliability and quality assurance systems are in place and operating and that the quality and reliability requirements of the hardware are indeed being met.

Further, in order to ensure that proper attention and emphasis is given to the reliability and quality assurance aspects of NASA projects, these functions are assigned to an organizational element that is independent of the project management. The simplified diagram of the Lewis Research Center's organization shown in figure X-9 is typical of the approach used by all NASA centers. The four operating directors report directly to the director of the center, and each is accountable for the projects that fall within his particular area of responsibility. The reliability and quality assurance functions in support of each project are the responsibility of a separate organizational element, and the director of this organization reports directly to the director of the center.

Another key concept in NASA's approach is to establish the reliability and quality assurance requirements early in the initial phases of each project. A reliability and quality assurance plan is then developed to ensure that these requirements are met.

DESIGN - DESIGNING IN RELIABILITY, QUALITY, AND SAFETY

The reliability of a system is designed into it, starting with the conceptual design and continuing throughout the entire design phase. One way this is accomplished is by the assignment of reliability, quality, and safety engineers as an integral part of the design team. This is essential, since the average design engineer cannot be expected to have the awareness and capability to conduct all the analyses that are needed. Many different analyses, such as hazard analyses, worst-case analyses, and failure modes and effects analyses, are required to ensure that the particular design meets its reliability and safety requirements.

Another feature of the design approach is the use of a series of design reviews starting at the time the conceptual design is completed and continuing through the preliminary design, the intermediate design, and the final design. This review is conducted not only by the engineers involved in the design, but by other design engineers and manufacturing experts, as well as by test and inspection people, and so forth.

In order to ensure that the designs are based on criteria and specifications which meet the requirements of the system, these design criteria are spelled out in some detail in the beginning. Typical design criteria that would normally be developed during this phase are

(1) Structural factors of safety
(2) Electronic parts derating policy
(3) Codes or standards
(4) Functional specifications
(5) Environmental specifications
(6) Duty cycle
(7) Electromagnetic interference

Most of these criteria are generally familiar to the readers; however, electronic parts derating may not be quite so familiar. This policy requires that, rather than electronic parts being used at their rated condition (normal operating condition), they are put into a circuit where they will operate at a lower voltage than the design point, thereby enhancing their life and reliability. Of course, for these parts as well as all other parts, the normal codes and standards, functional specifications, environmental specifications, duty cycles, and electromagnetic interference would be developed.

During the design phase, usually right after the intermediate design review, a failure modes and effects analysis of the design begins. The purpose of this analysis is to answer the following questions:

(1) How can a part or a component fail?

(2) For each mode of failure, what effect would the failure have on the system's performance?

(3) How critical is this effect - what would be the impact on a mission?

(4) Can the potential of a failure be obviated?

This failure modes and effects analysis therefore asks the basic question, "What if?" - What if the weakest point in a subsystem fails? What if a component malfunctions?

The launch vehicle hydraulic schematic shown in figure X-10 illustrates what is involved in a failure modes and effects analysis. As can be seen, it is basically a simple, straightforward hydraulic system. A pump takes hydraulic fluid from a reservoir, raises its pressure, and passes it through a check valve to the engine gimbal actuator and then back to the reservoir. In order to measure the operating pressures of this system, three transducers are used - two on the high-pressure side, and the other on the return side. During the failure mode and effects analysis of this hydraulic system, one of the questions asked was, "What if a high-pressure transducer failed?" The transducer used in this system is shown in figure X-10. It consists of a spirally wound Bourdon tube that moves an electrical potentiometer. The tube is subjected to the operating pressure of the system, which in this case was 3000 psi. The tube was rated at 3500 psi, which seemed to be a sufficient margin. It was found that the weakest point in the Bourdon tube was where the tube was brazed to the inlet fittings. If this were to break, the case in the transducer would be subjected to full line pressure. A substantial leak would result since the electrical connector was only soldered in this transducer design. In a short time, therefore, the supply of hydraulic pressure would make the actuator inoperative and result in loss of control of the vehicle. This possibility was, of course, unacceptable for it would result in a mission failure. This failure potential in the hydraulic system design was corrected by selecting a transducer with a case that could withstand the full line pressure in the event of a failure of the sensing element.

This type of analysis is conducted many times at all levels of assembly of the design. In this way, the system design is modified to provide inherent

reliability. One other important element is provided by the results of this analysis; that is, as each potential failure mode is identified, the test requirements for acceptance testing are established to ensure that the particular hardware meets the minimum requirements necessary to preclude a failure or malfunction.

TESTING - DEVELOPMENT, QUALIFICATION, AND ACCEPTANCE

Testing is extremely important and occupies a large part of any program to ensure the reliability of a system. The development testing starts prior to finalization of the design. This overlap is necessary because the objective of development testing is to prove the adequacy of the design to meet all the requirements that were set down at the beginning of the design phase. Also, the early development testing often reveals inadequacies in the design, and design changes are required to correct the situation. These development tests include functional tests, many environmental tests, stress limit tests, and life tests. These tests, as applicable, are conducted on piece parts, components, subassemblies, and total systems.

Once a design has been produced which under tests has demonstrated its ability to meet specifications, it is ready to go on to flight qualification testing. A unit (i.e., a part, component, or subassembly) is built in accordance with the final design, using the specified manufacturing processes and hard tooling that will be used to build the flight units. This unit then is subjected to flight qualification testing, which includes the same elements as in development testing; that is, functional, environmental, stress limit, and life tests. In qualification testing, the unit is normally subjected to conditions more severe than it is expected to experience in normal flight operations. For example, in vibration testing, it is normally required that the design be capable of surviving at least $1\frac{1}{2}$ times the expected flight vibration levels. An example of a unit, in this case the Centaur inertial measurement group, undergoing a flight qualification test is shown in figure X-11.

Once a unit has successfully passed flight qualification testing, the manufacturing of flight units may begin. The same tooling and manufacturing specifications are used for building the flight units as were used for the flight qualification unit. Then an acceptance test is made to demonstrate the ac-

ceptability of each unit for assembly into a flight system. The test parameters for acceptance tests are normally not as high as those for qualification tests but are somewhat higher than those expected in flight operations. Again, the acceptance tests are conducted at several assembly levels from piece parts to complete systems and vehicles. For example, figure X-12 shows an acceptance test of a Pratt & Whitney RL-10 rocket engine, which is part of the Centaur propulsion system. Checkout and acceptance tests of Atlas and Centaur stages are shown in figure X-13. And, in figure X-14, tests continue on the Atlas-Centaur, as it sits on pad 36 at the Eastern Test Range, to determine its readiness for launch.

FABRICATION AND ASSEMBLY - QUALITY CONTROL

During the manufacturing process, continuous effort is made to ensure that the end products are of high quality. A major part of this effort, which is generally known as quality assurance, is in-process inspection. At various points during fabrication and assembly, the hardware is physically inspected to determine whether it conforms to the drawings and meets the specifications. In addition, at selected points, there are often functional tests of the hardware as well as other nondestructive tests. Shown in figure X-15 is a Centaur tank during a spotwelding operation. During this process, each and every spotweld is X-rayed to determine its acceptability as measured against a set of spotwelding criteria.

In addition to the normal in-process inspection, mandatory inspections are required at selected critical points in the manufacturing process. These mandatory inspections are conducted by government personnel. Usually, NASA delegates this responsibility to the cognizant government agency at the contractor's plant. These mandatory inspection points, which are established during the manufacturing planning process, are actually redundant inspections; that is, a reinspection to ensure that no discrepancies are getting by the initial inspection. In contrast to the relatively large-size hardware involved in the fabrication and assembly of the Centaur and Atlas propellant tanks (figs. X-15 and X-16), a large part of the launch vehicle buildup is associated with small complex parts, components, and subsystems ("black boxes"). Manufacturing high-quality "black boxes", such as the Centaur

inertial reference unit (fig. X-17), requires continuous and meticulous attention on the part of the workmen and the inspectors. This is probably illustrated to the highest degree in the buildup of the Centaur digital computer. The buildup of this computer starts with an extremely small integrated-circuit chip, which is sometimes called a die. This chip is about the size of the head of a common pin. Many of these chips are assembled by means of an epoxy adhesive onto a microelectronic modular assembly, as shown in figure X-18. The chips are the black spots that can be seen on the module, which is approximately 1 inch square. Several of these modules are assembled into a plug-in circuit module (fig. X-18), which is then mounted in the racks of a digital computer (fig. X-19).

During this whole process, in-process inspections are conducted at many points. Scanning electron microscope inspections of samples of the integrated-circuit chip are conducted prior to assembly of these chips into the microelectronic modular assembly. Each microelectronic modular assembly receives an optical inspection, as shown in figure X-20. What the inspector would see during this optical inspection in shown in figure X-21. The black squares are the small dice. Also visible are the leads, which have been bonded to the dice, and the circuits of the modular, assembly. It is, of course, important that each of these leads, which were bonded by an ultrasonic process, have a secure bond at its point of attachment. In spite of a concentrated inspection effort, there have been problems with these microelectronic modular assemblies because of loose or detached lead bonds. One reason for this is the large number, literally tens of thousands, of the lead bonds that are in each digital computer unit. Another reason is that the microelectric modular assembly does not experience all its operating conditions until it is tested at a higher level of assembly.

As an aid to controlling the quality of the hardware during the manufacturing phase, records are kept of the number and percentage of defects experienced during each major manufacturing process. The purposes of accumulating these data are, first, to monitor and control the quality of the hardware during each manufacturing process and, second, to provide records which might be useful in case of the malfunction or failure of a particular piece of hardware at a future date. These data are normally summarized and presented in the form of a curve, such as that shown in figure X-22. This curve shows the number of defects per thousand man-hours as

a function of time. Obviously, the production plastics process had a problem during the months of July and August. The upswing shown in July would have triggered off some action by management to determine the cause of the problem and get it corrected. September's and October's performance indicates the action was effective.

PROCUREMENT - QUALITY CONTROL

Since the reliability of a total system, that is, a launch vehicle or spacecraft, can be no better than the parts or the components that make up the system, the same emphasis on high reliability and quality must be applied to the procurement of material, parts, and components. In general, the same reliability and quality requirements and standards are applied to the vendors and suppliers as are applied to the prime contractors.

One of the best ways to ensure that the products delivered by a vendor will be of adequate quality is the careful evaluation and selection of the vendor in the beginning. Therefore, it is a common practice, if the vendor or source has not been qualified previously, to send a source selection team to the vendor's plant to determine their suitability and qualification for delivering the product needed. Once a procurement order has been placed with a vendor, it is the responsibility of the prime contractor to closely monitor the activities and product of the vendor in order to preclude the emergence of any problems. Also, prior to the delivery of the product, an acceptance test must be conducted, usually at the vendor's plant, to prove that the product meets the procurement specifications. In some cases, if the vendor does not have the equipment necessary to conduct the acceptance test, it is more economical to conduct the acceptance test on the equipment available at the prime contractor's plant. In any case, a rigorous receiving inspection is conducted on all materials and products received at the prime contractor's plant.

Because a high percentage (often 70 percent) of the critical items (parts and components) that go into a space system are procured from commercial vendors, it is essential that management have considerable insight into procurement operations. One means of doing this is to compile data on the rate of rejection of procured lots of hardware and to plot these data on a curve similar to that shown in figure X-23. This curve is a compilation of

all the procurements of a typical aerospace contractor and shows the percentage of rejection for each month. As can be seen, the rejection rate was low in the first part of the year, increased during the summer months, and finally decreased again toward the end of the year. Thus, the particular procurement department met its yearly goal of 4.1 percent rejection. In studying how the rejection rate was forced downward, it turned out that there was no one simple answer but a diligent application of all the quality requirements and practices, particularly to the problem vendors.

DISCREPANCY REPORTING, ANALYSIS, AND CORRECTIVE ACTION

In order to improve the quality of hardware by correcting the causes of manufacturing discrepancies and failures, it is necessary to have a system which identifies and documents these discrepancies and failures. In addition, this system must provide a mechanism for analyzing the causes of the discrepancies and failures and for taking the necessary corrective action. One way this is accomplished is to record the defects that are experienced in individual operations or areas in the manufacturing and assembly processes and to present these data in the form of tables and curves. An example of such a curve was shown in figure X-22, as part of the discussion of fabrication and assembly - quality control. That example was for plastic production. Another example, that of vehicle final assembly and checkout, is shown in table X-1 and figure X-24. In this example, it can be seen that there is an upswing in the defects per thousand man-hours in the September-October period which is above the goal that had been set for this operation (fig. X-24). An analysis of this situation revealed that this was a period in which there was a significant change in personnel because of seniority rights being exercised. The corrective action in this case was increased on-the-job training to enhance the proficiency of the personnel. This type of monitoring of the quality of the hardware is just one element of a total corrective action system and is typically employed in space operations.

An integrated corrective action system is depicted in figure X-25. Although this system seems fairly complex, it might make it clearer to "walk through" the system by using a typical discrepancy or problem. A discrepancy or problem can be generated in any one of several areas, either at the

vendor, on the factory floor, or possibly in the test facility. If an inspection at a manufacturing process point reveals a discrepancy in the hardware, this is first documented on some sort of form. In this case, the form is called a quality assurance report. The issuance of such a report would require corrective action directed by a quality engineer that could be accomplished directly on the factory floor for a minor discrepancy. The disposition of the hardware is normally accomplished by the action of a Material Review Board. If the discrepancy is significant, the problem is documented in a problem report and is tracked to its resolution by the corrective action center. A failure analysis, which might include experimental testing, is conducted when the situation justifies it. This failure analysis identifies the cause of the problem and establishes the necessary corrective action. If the problem has more serious implications for a potential flight or future vehicle, the problem is referred to the next level, which is normally a management-level review board. This board must approve the results of the failure analysis and the corrective action before the problem can be closed out.

During this total cycle at appropriate points, starting with the quality assurance report, data are assimilated for purposes of tracking and future reference. Often, as shown on the left side of figure X-25, the data are assimilated in a computer for efficiency and ease of retrieval. The computer then can be interrogated by operational personnel or management for needed quality information. In some cases, a terminal is provided at a NASA installation for direct access to the stored information, such as the status of failures or problems. The use of these data acquisition and retrieval systems is discussed in the next section of this paper.

As an example of what is involved in a typical failure analysis, consider the solenoid valve shown in figure X-26. This normally closed solenoid valve failed to close when the solenoid was deenergized with an inlet pressure of 750 psig. This failure occurred during testing but was of such a nature that it could have occurred on the launch pad or during flight. Because of this and the fact that it affected all vehicles that were assembled at that time, a failure analysis was instigated. Because of some previous experience of contaminants in the system in which the valve was located, it was suspected that the cause of the failure might have been contaminants. Therefore, the valve was carefully disassembled to inspect for traces of contaminants. None were found, but several examples of workmanship defects were found. In

figure X-27 is shown some screwdriver damage to the pilot seat retainer. Other defects caused by poor workmanship are shown in figure X-28; toolmarks were found on the main poppet near the inlet port. This and similar damage near the outlet port seemed to be caused by attempts to pry the poppet open. However, as is often the case, the failure could not be traced to these obvious workmanship defects. The cause was more subtle than that. The final conclusion was that it was a design problem. The design allowed a stackup of dimensional tolerance in the main poppet to the extent that it bound and did not allow the valve to close when the solenoid was deenergized. The corrective action was a design change by the vendor and also increased emphasis on good workmanship and quality control.

Another type of discrepancy reporting and corrective action system in which NASA participates is the national "Alert" system. The purpose of this system is to provide other government and industry personnel with appropriate information so that similar potential problems may be avoided. The system also provides manufacturers with information on application problems pertaining to their products so that they may take corrective action. If, for example, the problem of the solenoid valve just discussed was concluded to be generic to all these particular solenoid valves, the vendor would develop an alert and distribute it throughout the national system.

DATA ACQUISITION AND RETRIEVAL SYSTEMS

As was mentioned in the previous section, it is absolutely essential that quality data be acquired throughout the manufacturing and assembly process of the hardware. These data are required to track the quality history of the hardware and also to initiate corrective actions to improve the quality of the hardware in the future. In addition, these data are absolutely vital in investigating the cause of problems or failures in ground testing or in flight.

In reviewing the readiness of a vehicle for launch or flight, the past history of the hardware is scrutinized. It is common practice to develop what is known as a "history jacket" for each critical component on the vehicle. (A critical component is a component that is vital to successful operation of the vehicle.) Included in a history jacket are data on any discrepancies which occurred during the fabrication and assembly process, any functional test

failures or failures at high levels of assembly, the corrective action and resolution of any failures or problems, configuration data, and so forth.

The accumulated quality data are also used by quality engineers and others to evaluate the potential of significant problems or concerns in future hardware production or in hardware that has already been assembled on a vehicle. An example of the kind of data that could be retrieved (in this case from a computer) for such an evaluation is shown in tables X-2 and X-3. Table X-2 shows the history of the 1970-75 problem reports on Atlas and Centaur for valves that were classified as critical components. The problems are categorized, and the number of occurrences of each problem category on the valve are recorded for this time period. The three major types of defects that were experienced were component failure to operate within requirements, 37 occurrences; component internal leakage, 13 occurrences; and an out-of-tolerance relief valve setting, 12 occurrences. This information provides the quality engineer with some insight as to where his continuing quality problems are and where additional efforts could result in a higher quality product. The history of the disposition of this hardware, which would normally be decided by a Material Review Board, is shown in table X-3. The hardware was usually repaired to a condition where it was acceptable (39 occurrences) rather than reworked to meet drawing specifications (20 occurrences) or returned to vendor (21 occurrences). Again, this history provides the quality engineer with further insight into the problems on these critical valves and what actions need to be taken.

It should be emphasized here that because of the numerous parts and components in a subsystem or a vehicle and the large amount of information that must be recorded and tracked, the digital computer has proven to be an efficient tool. The computer can acquire data and make it available to all the operating and management personnel, as well as government personnel, who need to have access to this kind of information. The trend is toward increased use of computers for more efficient data acquisition and retrieval.

AUDITING AND SURVEILLANCE

Over and above all these operations, there is a system of continuous and periodic audits. There are several kinds of audits: internal audits conducted

by the contractor; vendor audits, where the prime contractor audits the vendor's operations and product; and audits of either the vendors or prime contractors by the government. The internal audits are normally conducted by quality assurance personnel. There are several types of internal audits. First, there are manufacturing process audits, which try to determine whether the manufacturing operation is being conducted in accordance with the manufacturing process specifications and also to determine whether the manufacturing process specifications are up to date. Second, there are audits of the quality assurance system itself to determine whether the system is being adhered to, for example, to determine whether the proper inspections are being conducted and the proper documentation of discrepancies are being made. Third, another important audit is that of the actual hardware. The hardware is reinspected by the auditing team to determine whether it meets all requirements or whether some of the discrepancies are getting through the inspection system. A good auditing program will also cover other operations, such as engineering and testing.

In order to be effective, the findings and results of these audits must be made available to the elements of the organization that can interpret them and instigate corrective action. Thus, the results (data) of the audits are compiled and presented in such a manner as to facilitate interpretation and tracking. An example of such a presentation for a typical aerospace operation is shown in figure X-29. This graph shows the percentage of nonconformances found in all launch vehicle manufacturing processes as a function of time for 1974. The general downward trend of this curve from about 8 percent to approximately 1 percent is a very desirable trend. This improvement may well have been the result of these manufacturing process audits and the ensuing corrective actions. In order to provide some insight as to how this record compared with that of the previous year, shown on the same figure is a similar curve for 1973. Similar graphs for all audits conducted in a given period of time would provide management with some understanding as to the effectiveness of their operations and what appropriate action might be needed.

Similar kinds of audits can be conducted at vendors' plants, and the findings and results should be presented in a similar manner in order to control the quality of the material and hardware being received from vendors.

In addition to these internal self-audits, it is customary for the govern-

ment, on a periodic basis, to conduct audits of the operations of the prime contractors and in some cases of the vendors also. At Lewis, there was recently instigated a system of government audits called "over the shoulder" audits. In these audits, government quality engineers are sent to contractors' plants to participate in the contractors' internal audits and to conduct "spot" independent audits. The "over the shoulder" audit is more efficient in its use of government manpower and is less disruptive to the contractors' operations. For example, if it is found by the government quality engineers participating in the internal audits that the audits are being conducted on a thorough and effective basis, the need of an in-depth audit by many government personnel is nullified.

FLIGHT READINESS REVIEWS

Flight readiness reviews are conducted prior to each launch. These reviews include a formal and rigorous evaluation of the flight readiness of both the spacecraft and launch vehicle to ascertain its condition and readiness to successfully meet its prescribed mission. These reviews are conducted in several ways. One is the use of a team of engineers from the contractor and the government who review both the documented history of the particular vehicle from the history jackets and the condition of the vehicle hardware. In addition, all open problem reports are reviewed to ensure that they will be properly closed out prior to flight or that they do not have any impact on the particular vehicle. During this review process, the team identifies any item of concern which could possibly have an impact on the success of the mission. Then, there are a series of formal management reviews at which time these findings are considered. These management reviews take place at several management levels before final recommendation to launch. This approach is very time and manpower consuming, but it is necessary in view of the cost of a vehicle failure.

POSTFLIGHT EVALUATION

After each flight there is a postflight evaluation of the data to determine

whether any anomalies occurred during the flight and to instigate any needed corrective action for future flights. On a successful flight this is normally a routine review. Unfortunately, there are flight failures. When one occurs, a very in-depth and extensive review is conducted to determine and correct the cause of the failure. The overall responsibility for this review is assigned to a failure review board, and teams are appointed to conduct a detailed failure analysis. Since, the flight vehicles are not recovered, the engineers conducting the analysis have to depend on data that were telemetered to the ground during the flight plus data that were accumulated during the fabrication, assembly, and testing of all the hardware that was part of the subject vehicle.

In order to provide some understanding of how these failure analyses are conducted, we will review the recent flight of Titan-Centaur (TC-1). This flight, which was the proof flight for the Titan-Centaur, would have been successful, except that the propulsion system on the Centaur stage failed to operate. A schematic of the Centaur D-1T propulsion system is shown in figure X-30. The system is a cryogenic, liquid hydrogen - liquid oxygen, rocket propulsion system. It employs a boost pump to raise the pressure from the tank operating pressure to an acceptable level for the operation of the main rocket engine pumps.

A tool that is used in a failure analysis is the construction of a failure tree such as that shown in figure X-31. The analysis starts at the top of the tree with a block that shows that this particular engine produced improper thrust. ("Improper thrust" is an understatement in that the engine hardly produced any thrust at all.) Shown on the next line are three blocks which indicate three conditions that could result in improper thrust. The engineers were able to rule out two of these conditions, and the suspect then was "insufficient propellants to the engines." This kind of analysis and reasoning was carried out on successive levels until the cause of the problem was identified as a malfunction of the boost pump system.

Some of the telemetry data that were available to analyze the performance of liquid hydrogen and liquid oxygen boost pumps are shown in figures X-32 and X-33. As shown by the top curve in figure X-32 there was proper turbine inlet pressure; so the energy to drive the liquid hydrogen pump was available. The data for the pump rotational speed indicated that there was no rotation. However, there was a differential pressure rise across the hydro-

gen pump, which could mean that the rpm data were erroneous; that is, the sensing element malfunctioned. These data indicated that the hydrogen boost pump was not the cause of the propulsion failure, and attention was then directed to the liquid oxygen boost pump data shown in figure X-33.

These data looked the same as those for the liquid hydrogen pump, except that in this case there was no differential pressure rise across the pump as well as no indication of pump rotation. With two sets of information indicating that the liquid oxygen boost pump did not operate, it was concluded that the cause of the propulsion system failure was the failure of the liquid oxygen boost pump to operate. The failure analysis was continued to determine why the pump failed to operate. The exact cause could not be tied down, but the conclusion was that the most probable cause was the freezing of water that had accumulated in the turbine assembly as a result of preflight ground tests. (Other probable causes were investigated, such as the possibility of a foreign object being wedged in the turbine assembly.)

It is hoped that this example has provided some insight into the approach used to evaluate a major flight failure.

CONCLUDING REMARKS

The system that NASA employs to assure the reliability and quality of the vehicles and equipment involved in space missions is a total system. As such it is concerned with each operation, from design to the final assembly and flight operations. The importance of reliability, quality, and good workmanship are continuously emphasized. At every level of assembly, from the part or component to the final vehicle, consistent and meticulous attention is given to every part and component before it goes on to the next level of assembly. Wherever discrepancies are discovered, the cause is determined, corrective action is developed, and the component is checked to see that the action has been carried out.

It is believed that the total system approach to reliability and quality assurance is desirable and necessary for any major operation, such as that of the gas industry. All the elements of the NASA system may not be applicable or needed, but it is believed that a systematic and conscientious evaluation of all steps in a given operation would reveal those steps where an application of some of the methodologies developed for the space program would be of benefit.

TABLE X-1. - DEFECTS OCCURRING IN VEHICLE FINAL ASSEMBLY AND CHECKOUT

	MONTHS									
	J	F	M	A	M	J	J	A	S	O
DEFECTIVES	10	13	24	15	14	14	16	14	22	32
MANHOURS (THOUSANDS)	16.3	17.0	19.5	14.1	15.3	19.7	15.5	17.1	21.7	20.0
DEFECTIVES/1000 M/HR	.6	.8	1.2	1.1	.9	.7	1.0	.8	1.0	1.6
CUMULATIVE AVG PERFORMANCE (12 MO)●	.9	.9	.8	.8	.9	.9	.9	.9	.9	1.0

CS-72732

TABLE X-2. - HISTORY OF PROBLEM REPORTS ON ATLAS AND CENTAUR CRITICAL COMPONENTS (VALVES), 1970-75

DEFECTS	OCCURRENCES
COMPONENT FAILS TO OPERATE WITHIN REQUIREMENTS	37
COMPONENT LEAKS INTERNALLY	13
RELIEF VALVE SETTING OUT OF TOLERANCE	12
SEAL LEAKS	8
SCRATCHED/GOUGED	5
VALVE TIMING OUT OF TOLERANCE	2
LEAKS	2
PROCEDURE NOT FOLLOWED	2
MAJOR SURFACE DAMAGE	1
IMPROPER TORQUE	1
REGULATOR OUTPUT PRESSURE OUT OF TOLERANCE	1
FLOW RATE TOO HIGH	1
FLOW RATE TOO LOW	1
TOTAL	86

CS-72676

TABLE X-3. - DISPOSITION OF PROBLEMS ON ATLAS AND CENTAUR CRITICAL COMPONENTS (VALVES), 1970-75

DISPOSITION	OCCURRENCES
REPAIR	39
RETURN TO VENDOR	21
REWORK	20
USE AS IS	5
SCRAP	1
TOTAL	86

CS-72663

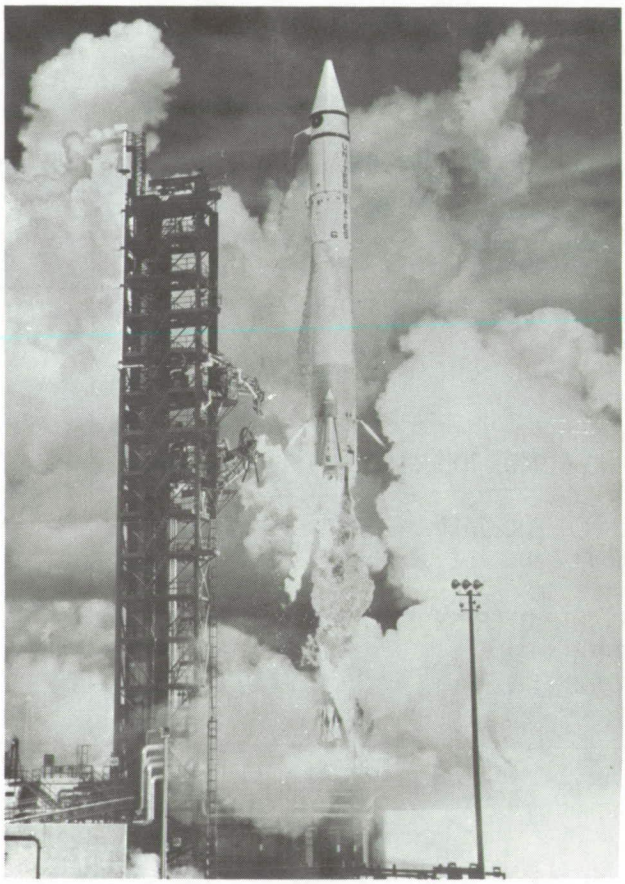

Figure X-1. - Atlas-Centaur launch vehicle.

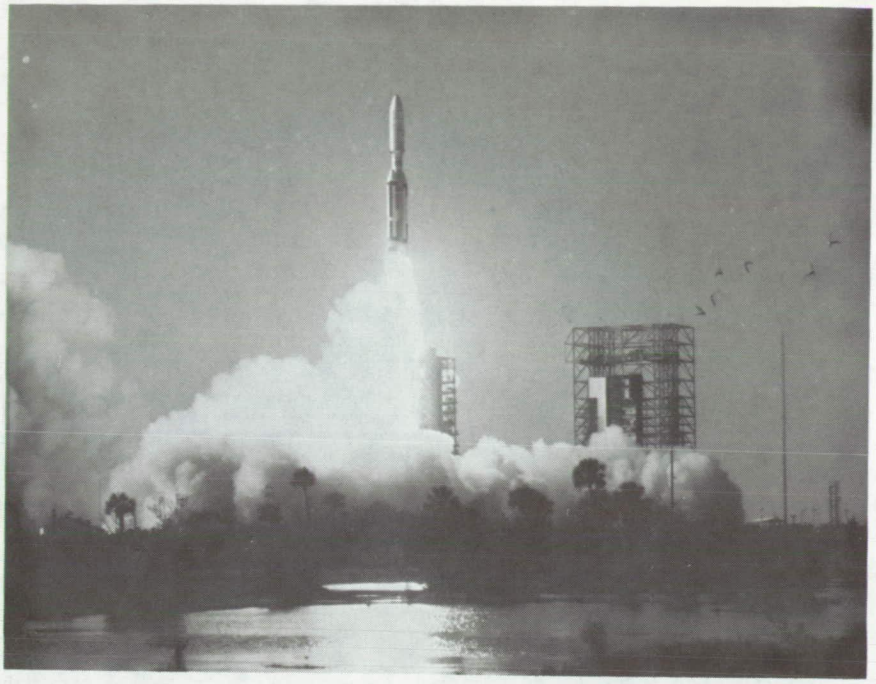

Figure X-2. - Titan-Centaur launch vehicle.

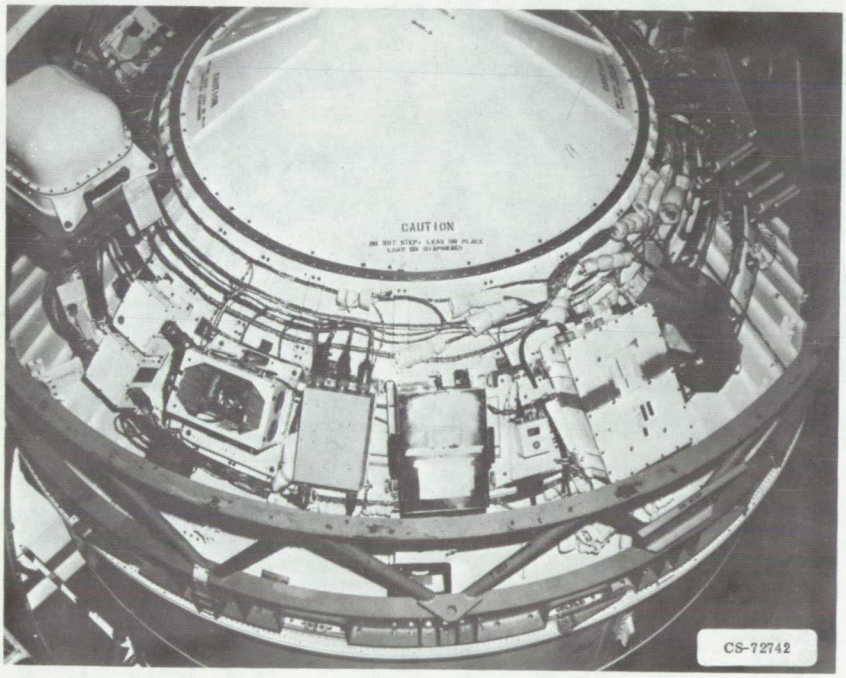

Figure X-3. - Centaur equipment module.

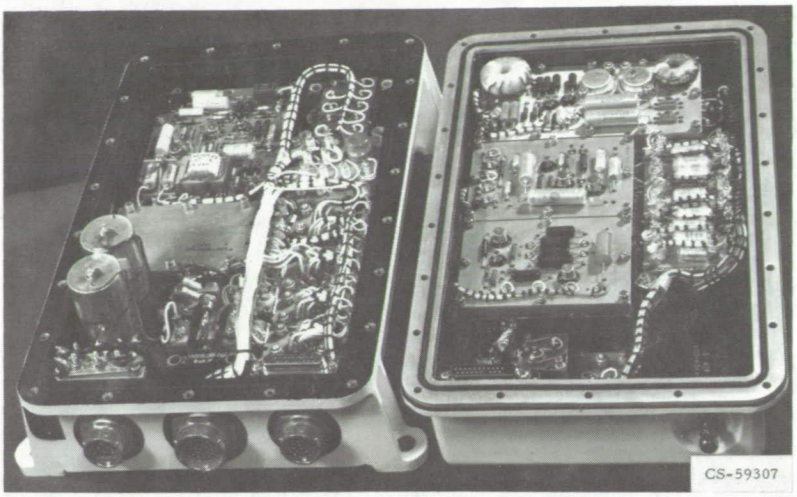

Figure X-4. - Centaur systems electronic unit.

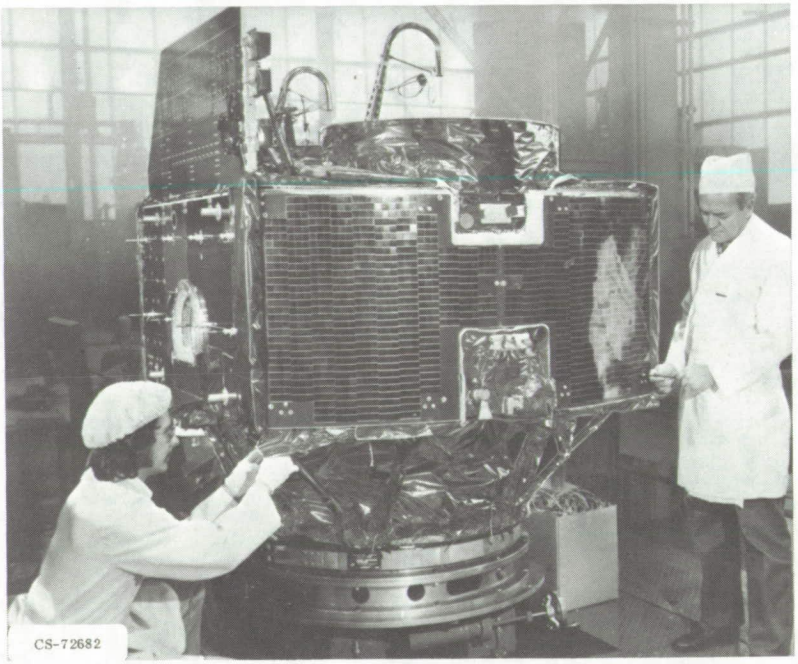

Figure X-5. - Communications Technology Satellite.

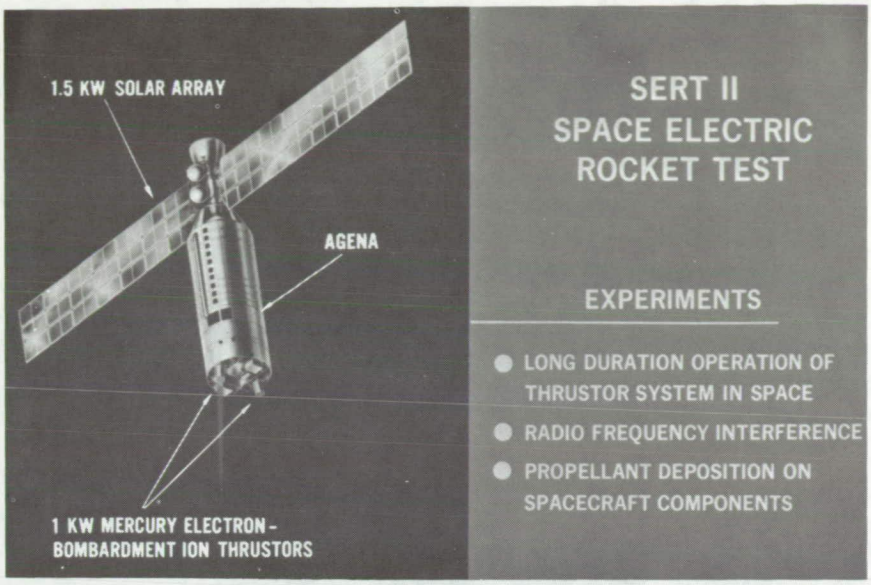

Figure X-6. - SERT II satellite.

Figure X-7. - Refan engine in flight test.

Figure X-8. - Scale model of 100-kilowatt wind turbine generator.

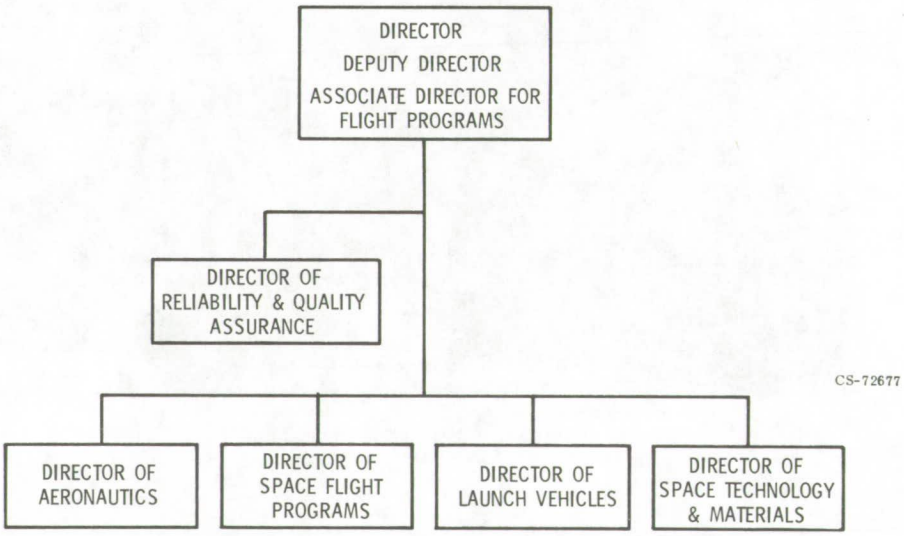

Figure X-9. - Simplified diagram of Lewis Research Center organization.

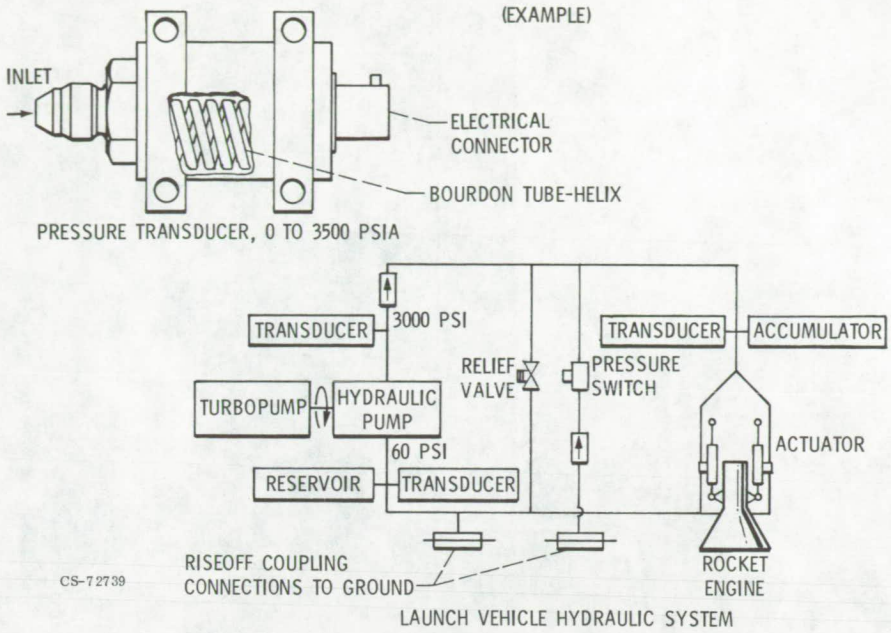

Figure X-10. - Schematic of launch vehicle hydraulic system.

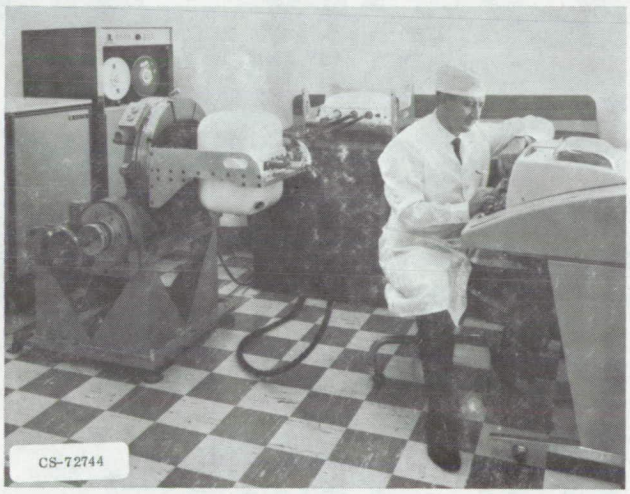

Figure X-11. - Flight qualification testing of Centaur inertial measurement group.

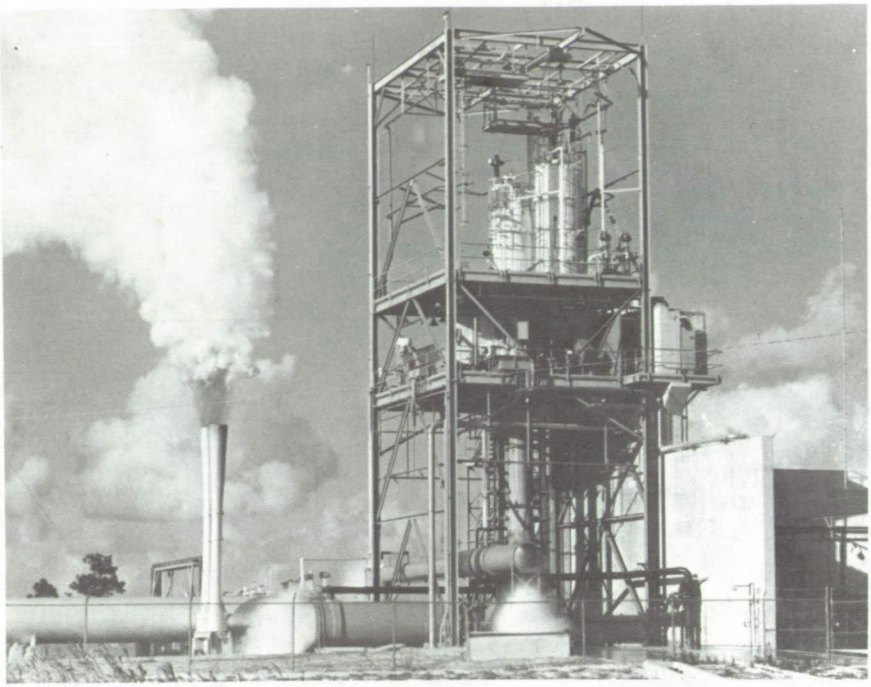

Figure X-12. - Centaur RL-10 rocket engine in test stand.

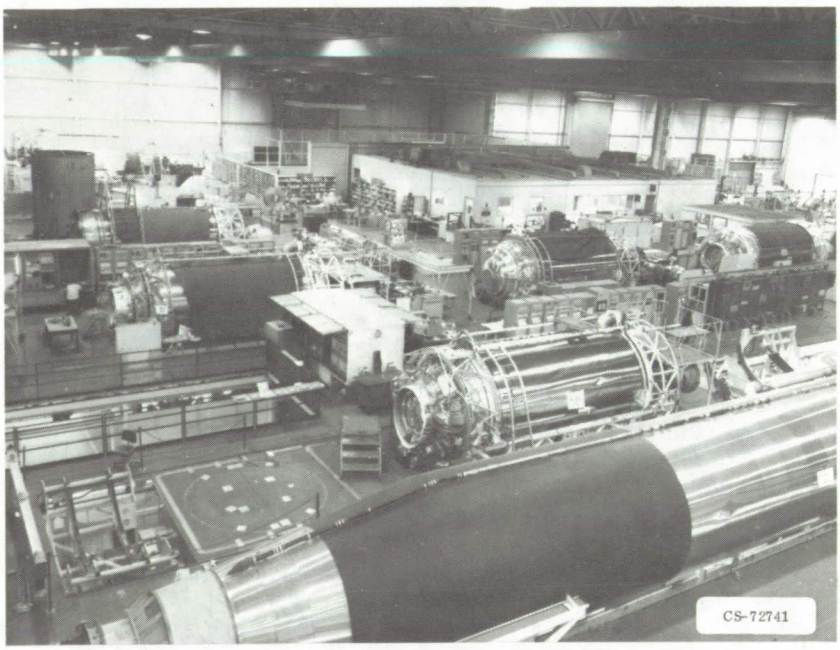

Figure X-13. - Checkout and acceptance testing of Atlas and Centaur stages.

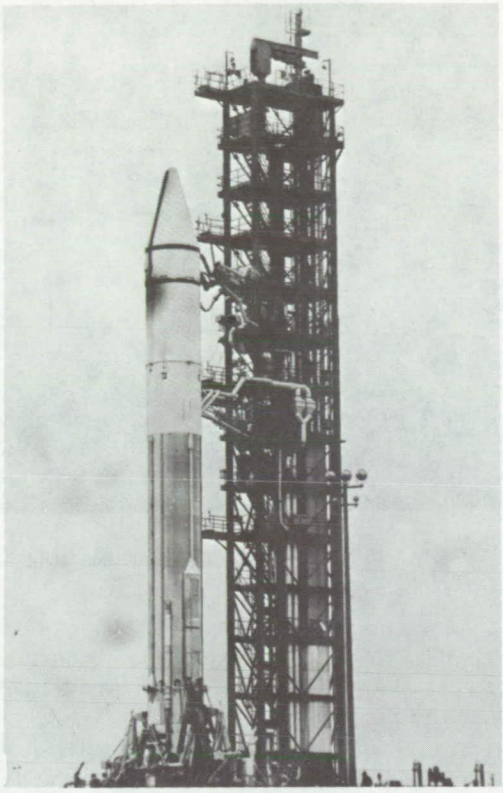

Figure X-14. - Atlas-Centaur on launch pad.

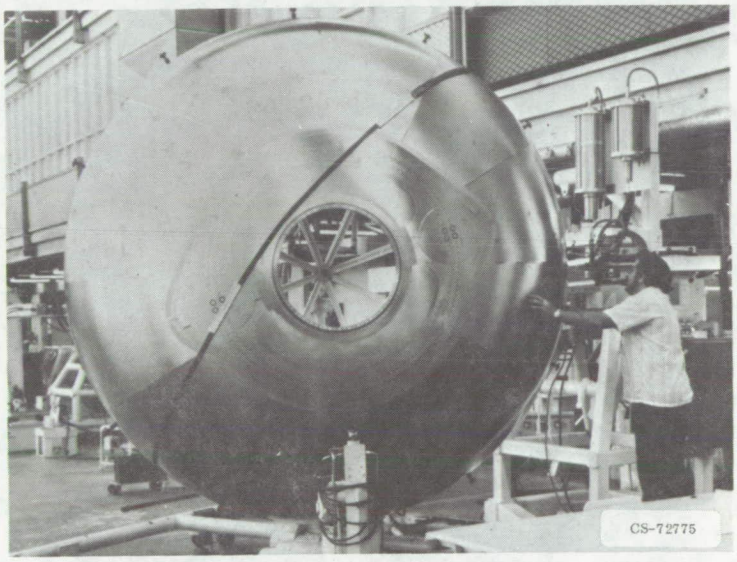

Figure X-15. - Spotwelding of Centaur aft bulkhead.

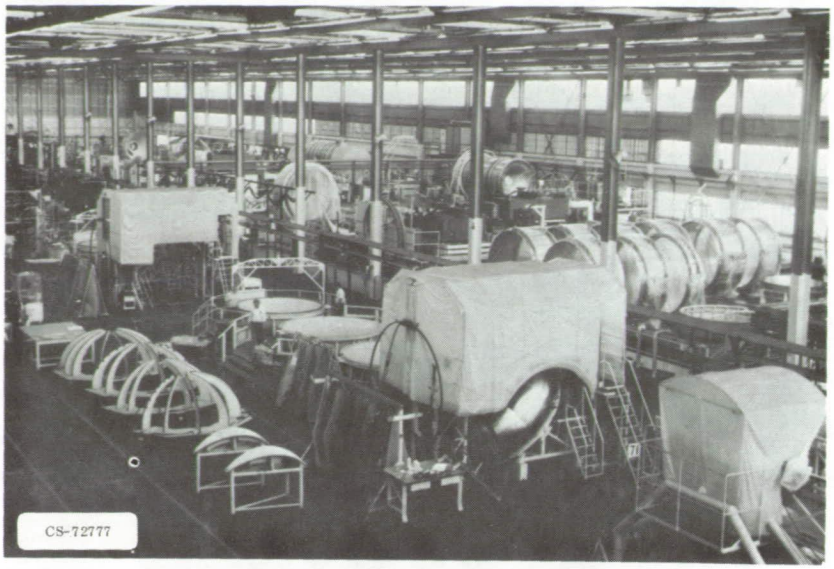

Figure X-16. - Atlas-Centaur tank production facilities.

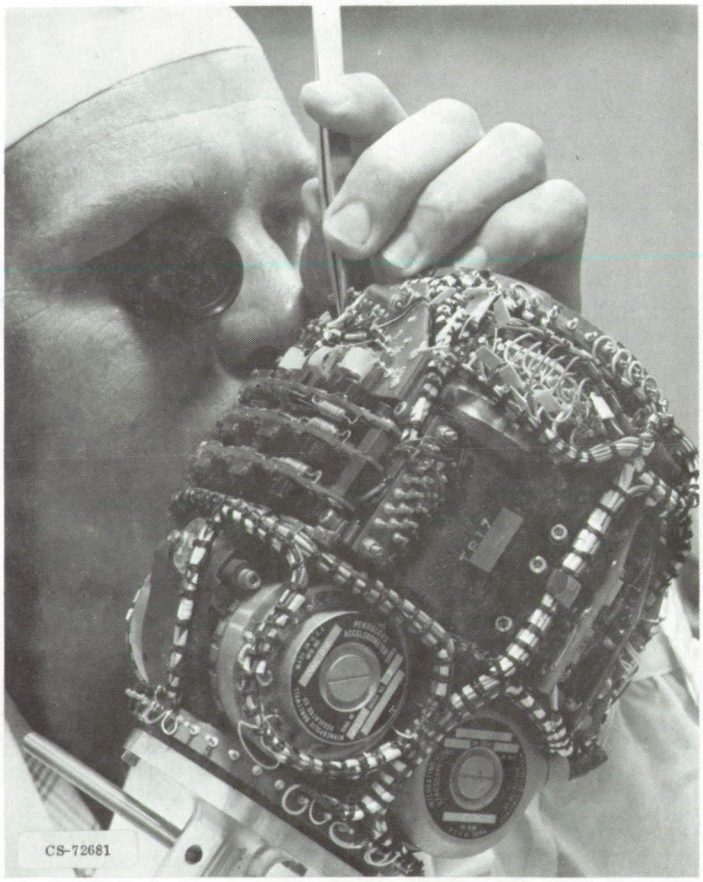

Figure X-17. - Centaur inertial reference unit.

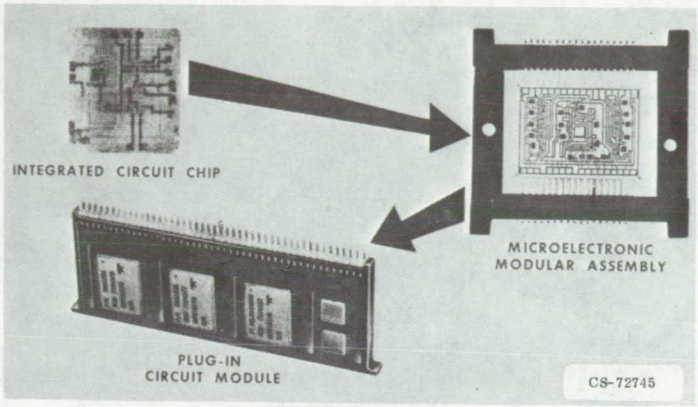

Figure X-18. - Assembly of components for Centaur digital computer.

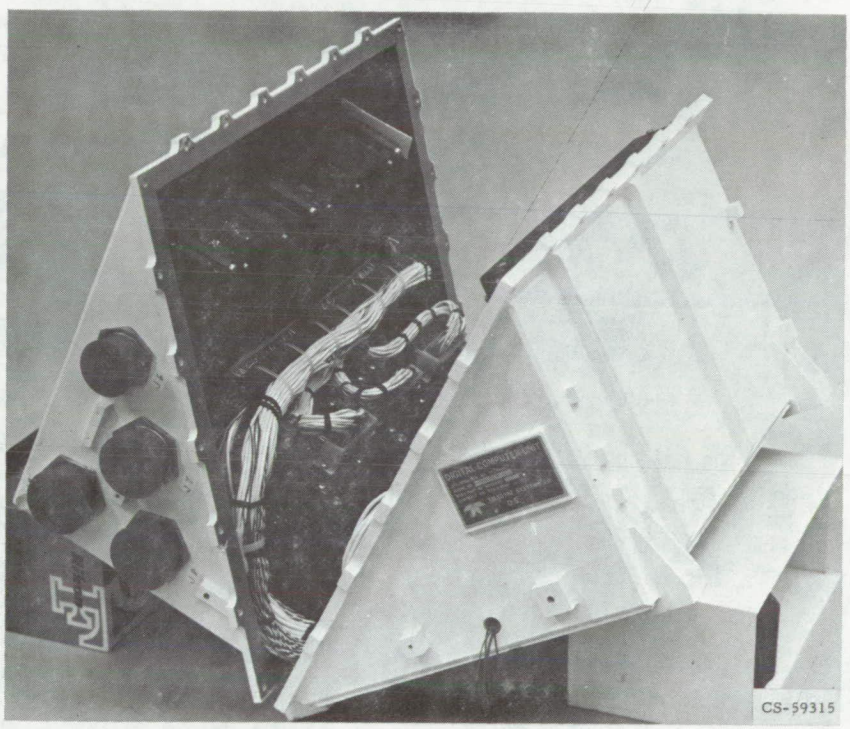

Figure X-19. - Centaur digital computer unit.

Figure X-20. - Optical inspection of microelectronic modular assembly.

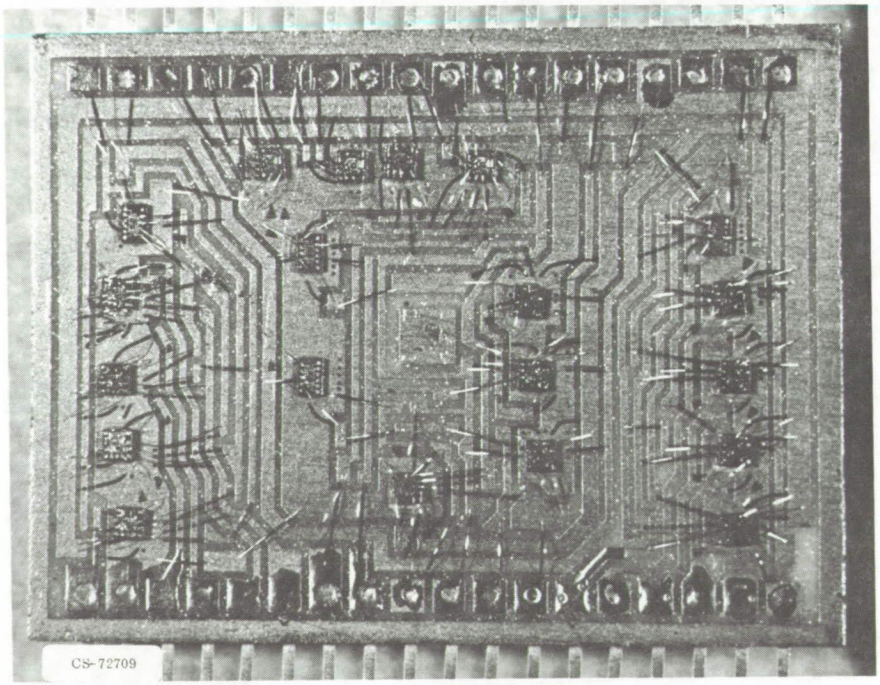

Figure X-21. - Magnified view of microelectronic modular assembly.

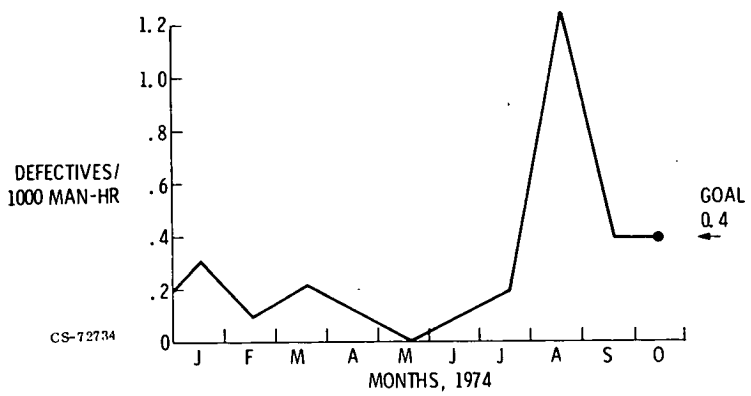

Figure X-22. - Defects per 1000 man-hours in production plastics process.

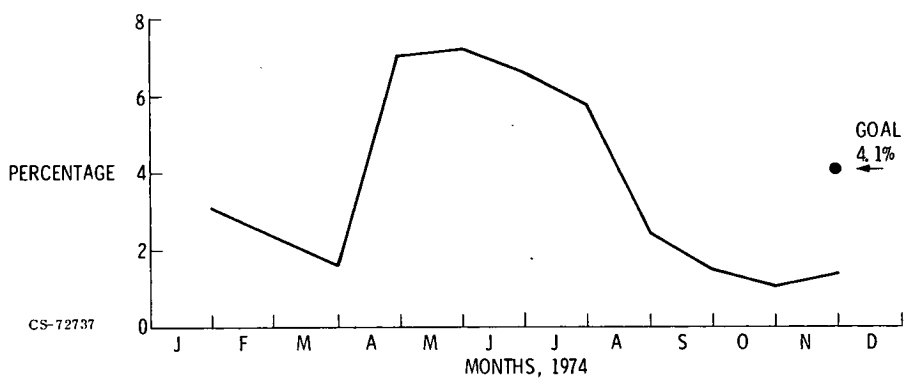

Figure X-23. - Percentage of lots rejected in typical procurements by aerospace prime contractor.

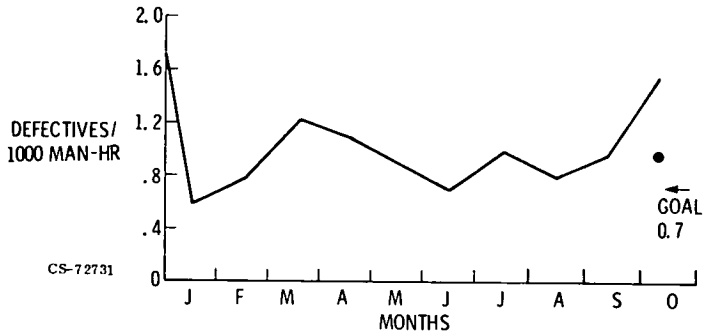

Figure X-24. - Defects occurring in vehicle final assembly and checkout.

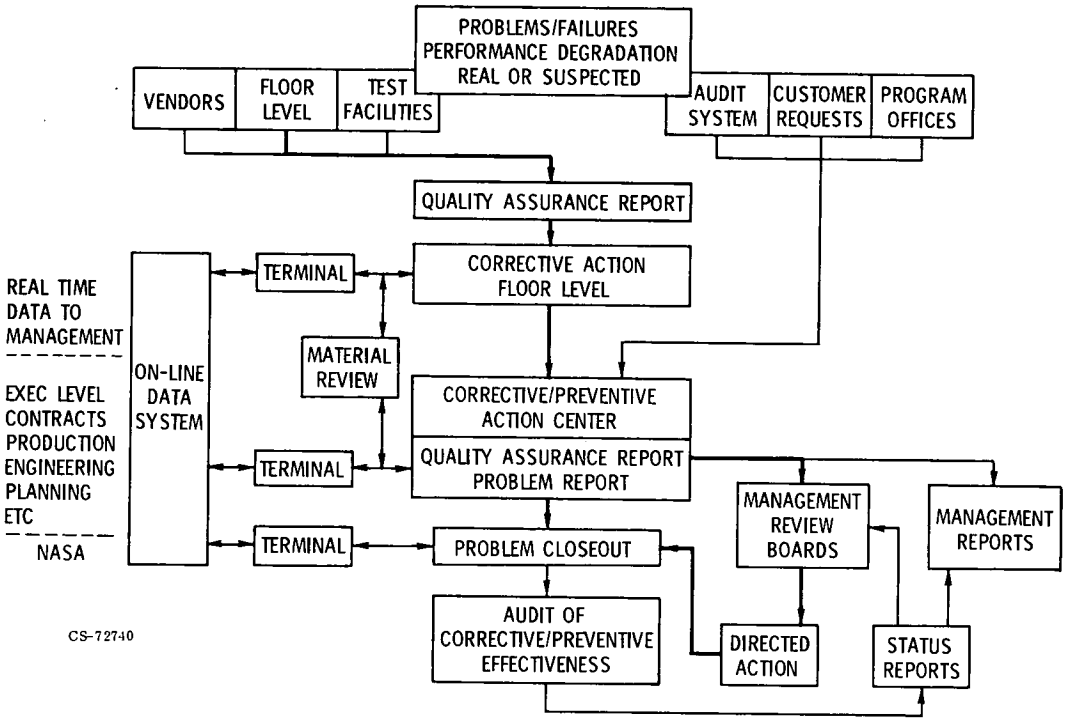

Figure X-25. - Integrated corrective action system.

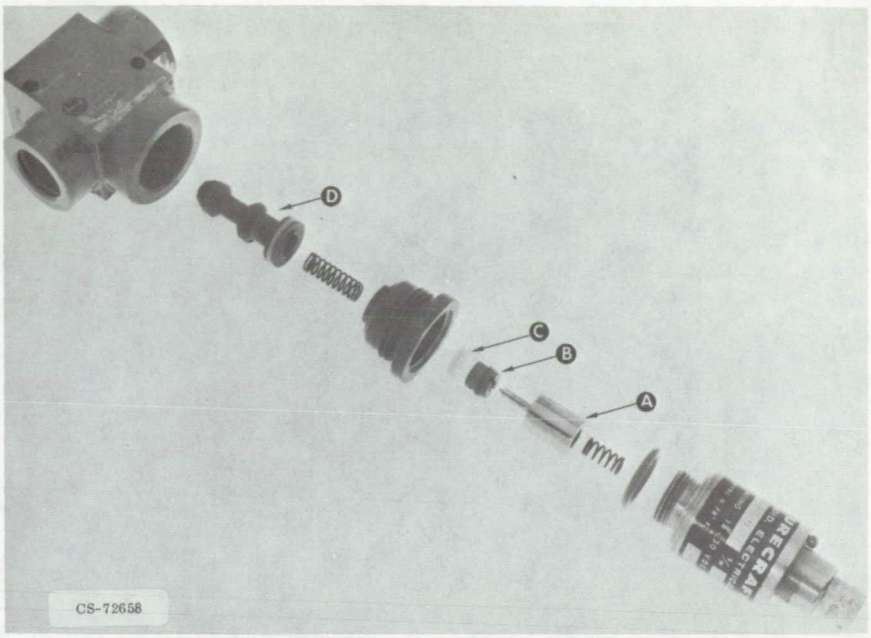

Figure X-26. - Exploded view of solenoid valve.

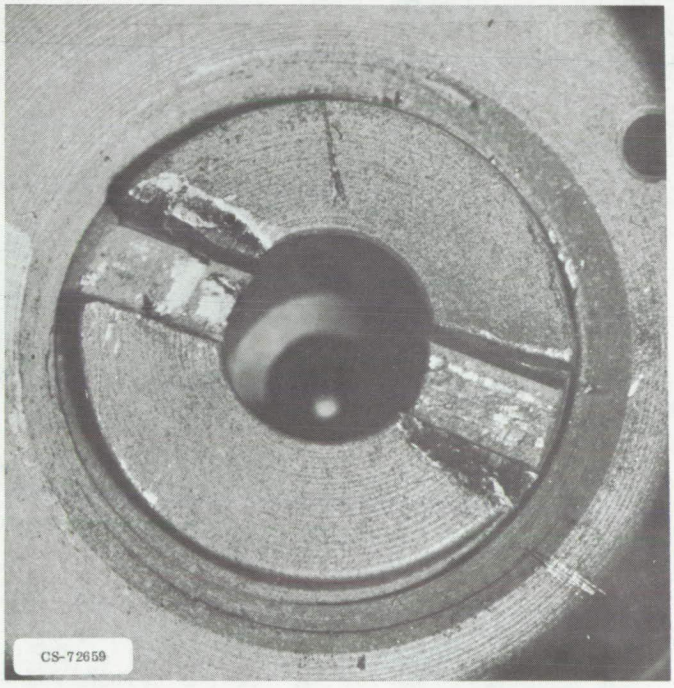

Figure X-27. - Screwdriver damage to solenoid-valve pilot seat retainer.

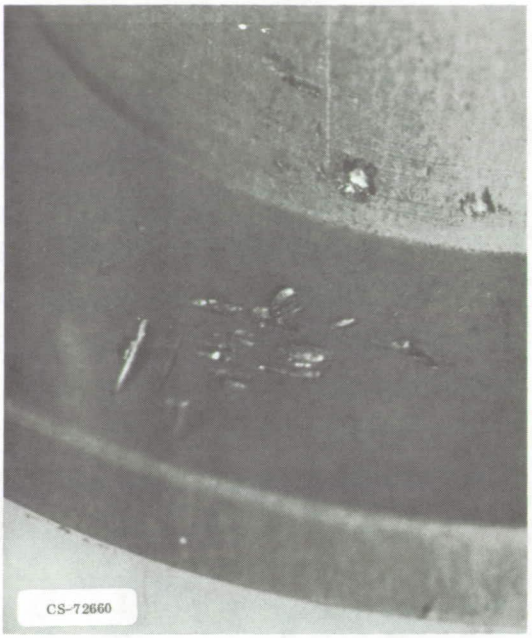

Figure X-28. - Toolmarks found on main poppet, near inlet port of solenoid valve.

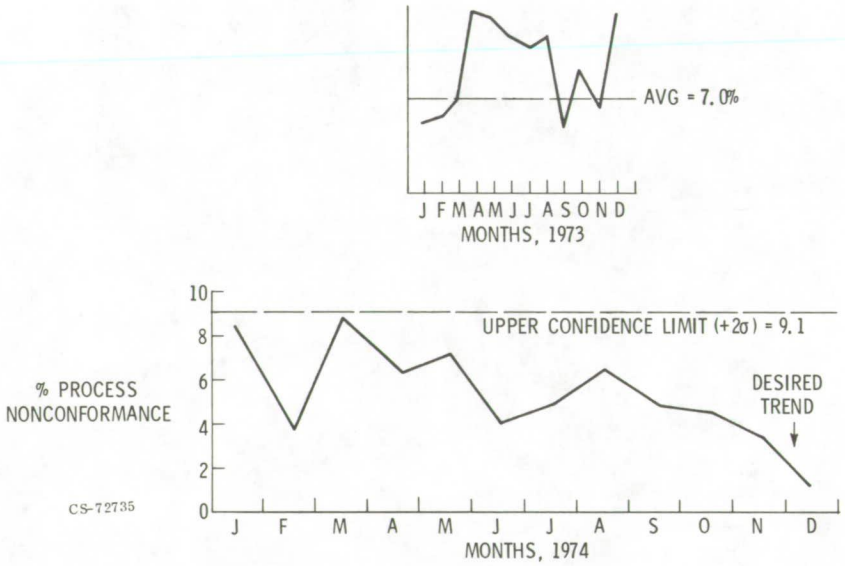

Figure X-29. - Audits of launch vehicle manufacturing process.

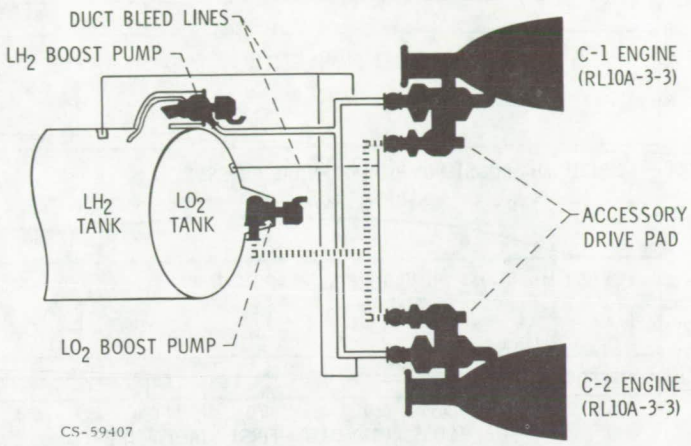

Figure X-30. - Schematic of Centaur D-1T propulsion system.

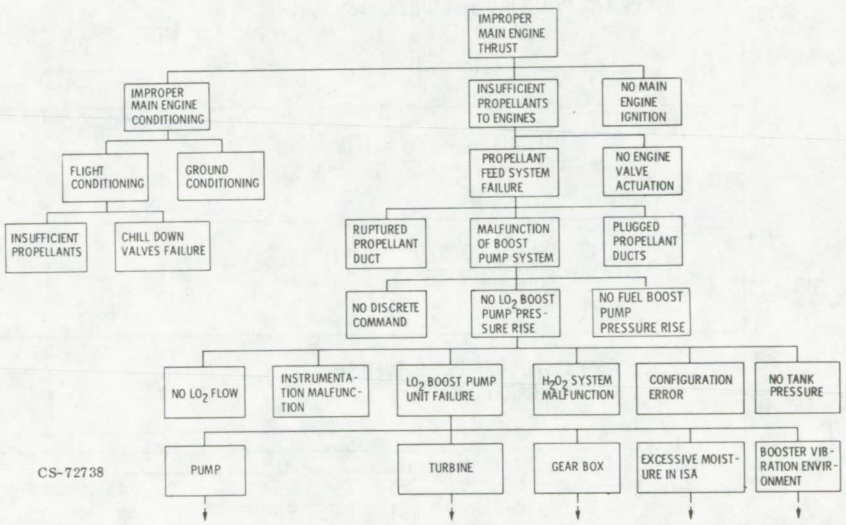

Figure X-31. - Titan-Centaur (TC-1) failure tree.

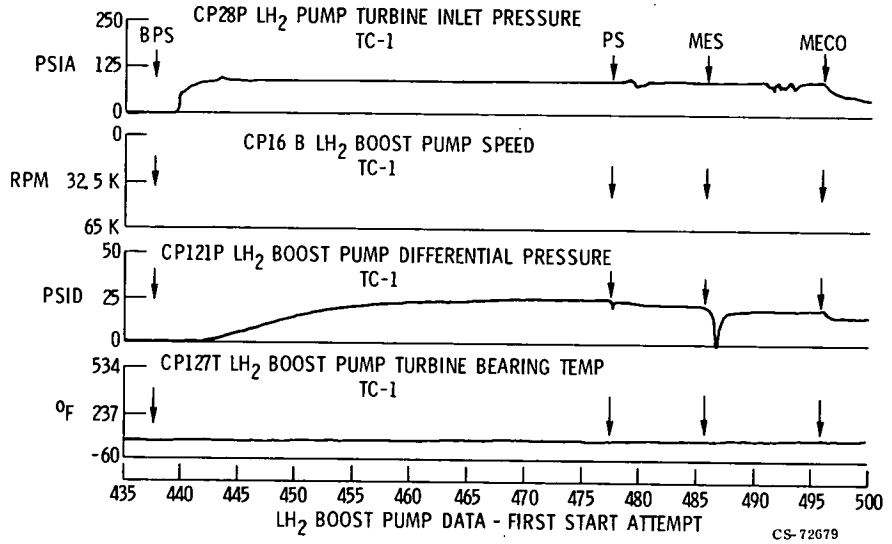

Figure X-32. - Titan-Centaur (TC-1) liquid hydrogen boost pump data for first start attempt.

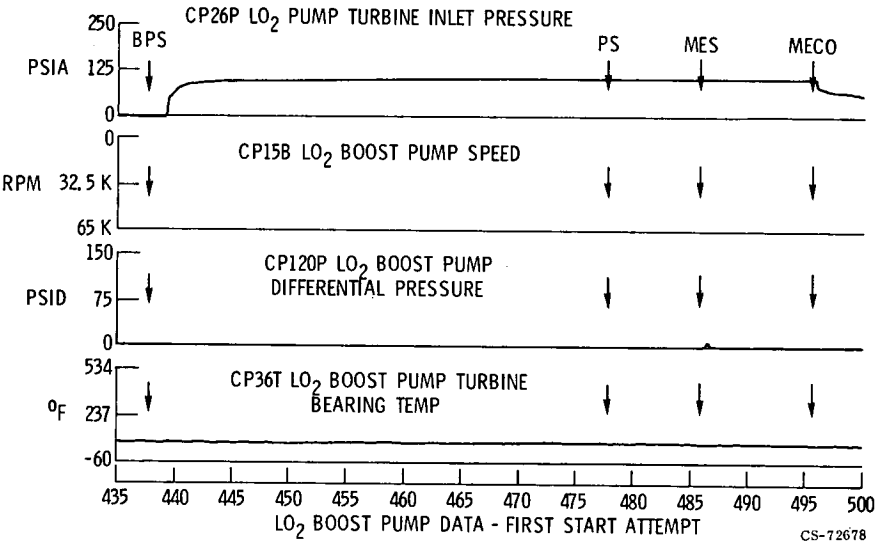

Figure X-33. - Titan-Centaur (TC-1) liquid oxygen boost pump data for first start attempt.

XI. ADVANCED ENERGY SYSTEMS

Robert G. Ragsdale, Donald Bogart, Edgar S. Davis,
and William J. Masica

There is considerable technology now in place, or very near term, that is of interest to the gas industry. More advanced energy technology is on the way, moving nearer, but not yet on the near horizon. This discussion focuses on such technology, which could impact on the energy scene in the coming decade.

There are, of course, many energy technology investigations presently underway - too many to be covered in this discussion. We have therefore selected those technologies most appropriate to the gas industry, specifically, using nuclear heat to make synthetic fuels, energy storage, modular-integrated utility systems, and solar energy technology.

A new application of a relatively mature technology is the use of nuclear reactors to make synthetic fuels such as methane or hydrogen. Various ways of storing energy are under investigation. A joint Department of Housing and Urban Development (HUD)-NASA activity is being carried out at the Johnson Spacecraft Center to study a modular-integrated utility system. NASA is also involved in solar energy studies, particularly in solar heating and cooling. In a specific solar project, the Jet Propulsion Laboratory is working directly with the gas industry in southern California. Our involvement in wind energy electric conversion systems is more a matter of general interest than of direct applicability to the gas industry.

SYNTHETIC FUEL PRODUCTION USING NUCLEAR HEAT SOURCES

If the United States is to continue to rely primarily on fossil fuels, especially coal, high priority must be given to the conversion of coal to synthetic gases and liquids. The prospect of clean fuels from coal is so im-

portant that several government agencies have been asked to participate. This paper describes how NASA and various departments in the Energy Research and Development Agency (ERDA) are assessing their experience and technology so as to contribute to the synthetic fuel programs.

The area of interest is producing synthetic fuels from coal by using nuclear heat. Large increases in U.S. coal production are going to be difficult to achieve. The use of nuclear heat saves the coal, for example, that is ordinarily burned for process heat in making synthetic natural gas (SNG). Therefore, if nuclear heat is used, the SNG yields from available coal supplies are increased.

Many projections indicate that the United States will have to double coal production from the present rate of 0.6 billion tons per year by 1985. This means that the coal industry must more than duplicate itself in 10 years. If we account for present mines that will be exhausted, 70 percent of 1985 production must come from new mining capacity.

There are many impediments to increased coal production in the United States. From a technical viewpoint, the present coal mining technology is acknowledged to be obsolete. Even if the technology were available, the time lag between accepting new technology and implementing it is about 5 to 10 years. Economic considerations suggest that the capital investment by the coal industry must rise from $5 billion in 1974 to $25 billion per year in 1985 (1974 dollars) if this new mining capacity is to become a reality. The social implications are deep. The coal industry will need 125 000 more coal miners and more mining engineers. New communities will have to be established out West. Institutionally, new incentive programs that include joint industry-government cost sharing will have to be worked out. New and old legislation has a profound impact. The Health and Safety Act of 1969 changed the industry. The Surface Mining Control and Reclamation Act of 1974 has yet to make its impact. The political problem of reaching a concensus on future energy programs seems almost impossible. Eventually, the energy user and environmentalist factions of society will have to be brought together.

It is these impediments to increased coal production that have generated new ideas for using nuclear energy. Figure XI-1 shows the impact of nuclear heat on coal conversion. Three schemes are compared - the first is repre-

sentative of current coal gasification technology. In this technology, now under development, coal is required for three functions: (1) to generate the process heat; (2) to produce hydrogen to feed the conversion process; (3) to make the SNG product. Therefore, this scheme needs three carbon atoms to produce one carbon-bearing molecule, for a carbon conversion of about 35 percent.

The next scheme uses coal gasification but adds nuclear process heat. Coal is still used to produce hydrogen and SNG. Here two carbon atoms are required to produce one carbon-bearing molecule, for a carbon conversion of 50 percent. This scheme reduces carbon dioxide (CO_2) emissions and converts more of the coal to product by using nuclear process heat.

The last scheme uses nuclear heat to produce hydrogen by thermal decomposition of water, in addition to the nuclear process heat used for coal conversion. Here all the coal input is converted, for a carbon conversion of 100 percent. The incentives for nuclear coal-conversion plants are as follows:

(1) Maximum use is made of whatever coal production capacity the country will have.

(2) The ash and CO_2 wastes from nuclear coal-conversion plants are reduced by 1/2 to 2/3 relative to an all-fossil coal gasifier.

(3) The nuclear coal-conversion plant uses coal and nuclear technologies that are now under development.

(4) With a feasible water-splitting process, there is potential for low-cost hydrogen and oxygen in addition to SNG.

The seriousness of this proposal to use nuclear heat for coal gasification is demonstrated by the nuclear process heat assessment presently being undertaken by government and industry. The technology for very-high-temperature reactors has been reviewed by the major reactor manufacturers - General Electric, General Atomic, and Westinghouse. The prospects of using nuclear heat for reduction of iron ores for iron and steel production are being evaluated by the American Iron and Steel Institute (AISI). Reference coal-conversion processes and those that may be adapted to nuclear process heat are being studied by the Office of Coal Research (OCR) and the Oak Ridge National Laboratory. NASA is responsible for assessing various methods of hydrogen production from both coal and water and has study contracts with the Institute for Gas Technology (IGT), General

Atomic, and Westinghouse. Refinery and petrochemical applications are also being evaluated by several oil companies. The total assessment is under the direction of the Division of Reactor Research and Development of ERDA. Overall responsibility for coordinating the various efforts, evaluating the technologies involved, conducting cost/benefit studies, and providing recommendations on future program activities is assigned to the Oak Ridge National Laboratory.

It may be asked why NASA is involved in the study of hydrogen production. NASA has been concerned with hydrogen since the beginning of the space era and has tackled the problems of storing, transporting, pumping, and combustion of hydrogen for both chemical and nuclear rockets. Currently, Langley Research Center is studying the logistics and economics of using hydrogen for commercial aircraft. In the future, NASA will require large quantities of cryogenic hydrogen for the space program. Since past and present hydrogen production relies on reforming natural gas, which may not be available for this purpose, it is in the national interest for NASA to support new processes that have the promise of low-cost and efficient production of hydrogen.

One of these new processes being studied under NASA contract is shown in figure XI-2. This coal-solution gasification process has been conceived and designed by the Stone and Webster Engineering Company. It uses nuclear heat from a high-temperature, gas-cooled reactor (HTGR) under development by General Atomic. The coal-solution process converts coal to aromatic liquids and pipeline gas. The process can use any kind of coal that is first ground, slurried, and then dissolved in an organic solvent with partial addition of hydrogen. The liquid coal is hydrocracked and hydrogasified by further additions of hydrogen to make the low-sulfur aromatics and methane. A portion of the methane is cycled to a high-temperature, gas-cooled reactor that supplies heat both to generate steam and for the steam-methane reforming reaction. The resulting hydrogen-rich gas stream is sent through a hydrogen purification process which contains a carbon monoxide (CO) shift and CO_2 stripping sections. The purified hydrogen is then fed into the coal-solution gasification process. The coal processing and reactor portions of the plant can be sized to produce either pipeline gas or hydrogen. Under NASA contract, General Atomic is now studying how the plant size and coal inputs vary with steam-methane reforming temperatures from 1200^{o} to

2000^{o} F.

Within the gas industry in the United States, the Institute of Gas Technology has been an advocate of pipeline hydrogen - which they call "the fuel for the nuclear age." They look forward to a time when hydrogen can be made economically from water without the use of any fossil feedstock. Two methods of using nuclear energy to make hydrogen from water are being studied. Hydrogen can be made by electrolysis. Nuclear heat makes electricity that is converted to direct current that drives electrolyzers to decompose water into H_2 and O_2. The thermal efficiency for converting heat energy to hydrogen energy by electrolysis is presently about 20 percent. With technology advances in both the nuclear electrical and electrolyzer plants, we may expect efficiencies of about 40 percent. Hydrogen can also be made thermochemically by using nuclear heat to drive multistage chemical processes to produce H_2 and O_2. Thermal efficiencies for these processes can range from 30 to 60 percent. These thermochemical water-splitting processes are still in the laboratory stage; but research and development on both the process chemistry and the high-temperature nuclear reactors required is justified by the promise that such processes may have overall thermal efficiencies above 50 percent.

One process being studied by Westinghouse under NASA contract produces hydrogen by a combination of low-voltage electrolysis and a thermochemical recycling process. This water decomposition process consists of two chemical stages. The first uses sulfur dioxide to depolarize the anode of an electrolyzer and to liberate H_2 at the cathode.

$$SO_2 + 2H_2O \rightarrow H_2 + H_2SO_4$$

Sulfuric acid (H_2SO_4) is formed and for a 1-molar concentration of sulfuric acid, the potential theoretically required is only 0.17 volt. At slightly higher voltages, more concentrated sulfuric acid solutions could be formed. It takes about 1.5 volts to electrolyze water by present methods, so that large electrical savings are possible. In order to complete the cycle, the H_2SO_4 formed has to be concentrated and thermally decomposed to make SO_2 and O_2.

$$H_2SO_4 \rightarrow H_2O + SO_2 + \frac{1}{2}O_2$$

Equilibrium for this reaction is toward the right above 1400° F. Operating temperatures and catalysts to drive the reaction to completion are being studied by Westinghouse. The NASA contract with Westinghouse is concerned with the conceptual design of a full-scale plant based on this process so as to get a reasonable indication of required research and development and estimates of the economics.

Figure XI-3 shows the major components of the Westinghouse water decomposition process. The pressurized electrolyzer is fed with direct current, makeup water, and SO_2; hydrogen is taken off under pressure and sulfuric acid is removed. The acid must be greatly concentrated and then thermally decomposed in a reactor heat exchanger. The decomposed gas mixture is fed to a liquefaction cascade for oxygen recovery and the SO_2 and some H_2O are recycled into the electrolyzer. Work on this water decomposition process has just begun; results should be available by the end of this year.

As mentioned earlier, NASA has been involved with hydrogen energy systems for many years. We have developed launch, propulsion, and onboard power systems for space vehicles that operate on hydrogen. NASA is also involved with hydrogen fuel systems for conventional aircraft. Therefore, it was natural and timely for NASA to apply this experience in an agency-wide technology study of hydrogen energy systems as they apply to national energy needs. Figure XI-4 is a diagram of the NASA Hydrogen Energy Systems Technology Study. The study is under the direction of the NASA Office of Energy Programs with the NASA Jet Propulsion Laboratory as the leading center. Each NASA research center is factoring in its experience and expertise through a working panel. These efforts are being coordinated with other government agencies, utilities, and industrial groups. The assessment areas consist of hydrogen utilization, production, economics, storage, transmission, and distribution. The safety considerations and plans for implementation are also being studied. The related NASA contracts are those with IGT, Linde, the University of Kentucky, General Atomic, and Westinghouse.

The results of this study and the assessment being directed by ERDA will guide further government participation in these areas. As these efforts mature, more knowledge about nuclear process heat and hydrogen systems will become available.

ENERGY STORAGE

NASA is investigating energy storage concepts for a variety of aerospace and terrestrial applications, including the storage of compressed air, hydrogen, and electrochemical energy.

Compressed-air storage concepts are receiving much attention today and deservedly so. A representative concept is shown in figure XI-5. Off-peak electric power generated by fossil fuel, by nuclear fuel, or even from intermittent energy sources, such as a network of windmills, can be used to run a compressor stage to pump air underground. Storage sites might be either excavated or natural gas caverns, perhaps even leached salt caverns or porous rock formations. Here the compressed air would be stored for later use in a combustor stage to run a turbine-motor generator during hours of peak demand. The addition of a hydrostatic head maintains constant supply pressure and thus simplifies system design and aids system efficiency.

NASA is conducting conceptual design studies of compressed-air storage systems (fig. XI-6). The initial efforts are quite conservative, that is, using state-of-the-art compression ratios of 30 to 1 and turbine inlet temperatures of 2060° R. We are attempting to use the compressor stages during and after cooling to preheat the compressed air during the generation cycle. Normally, heat from compressor cooling is discharged as waste heat. If this heat can be stored in the form of latent or sensible heat for preheat addition, system efficiency would increase from 25 percent to better than 27 percent. More importantly, fuel consumption would decrease by more than 20 percent.

Compressed-air storage is currently very attractive, It is economically and operationally competitive with all other energy storage systems. Unlike normal gas turbines, the compressor and turbine stages are uncoupled and therefore may be designed and optimized separately. The basic technology for the system exists, and long life is one of its more attractive advantages. Additionally, the concept has fast startup response, making it an ideal companion for base-plant operation. The disadvantages are related to the underground storage site. There are unknown problems associated with long-term cyclic mechanical and thermal stressing of underground caverns. Contamination may be a problem. The Brown-Boveri

and Stal-Laval corporations are seriously considering compressed-air storage demonstration plants. NASA is presently formulating an engineering study of this concept which may also lead to a large-scale demonstration.

In the field of hydrogen energy storage systems, the most extensive system development work is being conducted by the Brookhaven National Laboratory (fig. XI-7) and the Public Service Electric and Gas Company. A complete test facility for demonstrating the hydrogen energy storage system concept on a utility system is in operation at Public Service's energy laboratory. There, hydrogen is produced by electrolysis and is stored in a hydride reservoir. A Pratt & Whitney 12.5-kilowatt fuel cell uses the stored hydrogen to produce electricity. NASA is conducting system studies to explore alternatives to this energy storage concept. There are, for example, alternate ways of producing, storing, and converting hydrogen. Of particular interest are alternate conversion systems which would replace the fuel cell and inverter with a combustion chamber and turbine generator. Either a hydrogen-air combustor or a hydrogen-oxygen combustor with water added as a diluent to reduce the steam temperature to acceptable turbine inlet conditions are possible alternatives.

The state-of-the-art of hydrogen combustion for power applications is actually quite advanced. To name a few - an aircraft engine, the J-57, was modified to run on hydrogen; a hydrogen-oxygen auxiliary power system was designed and built for the Space Shuttle; and 4- to 10-megawatt hydrogen steam electric generators have been routinely tested. The hydrogen-oxygen Space Shuttle auxiliary power system (fig. XI-8) was recently built and tested by the Air Research Corporation for the Lewis Research Center as a backup hydraulic power system. The system is about 3 feet wide and 4 feet high. It produces hydraulic power capable of being modulated from 0 to 400 horsepower with a 100-millisecond response time. The power modulation tests demonstrated that the controls technology required for hydrogen combustors and turbines is well in hand.

A stoichiometric H_2-O_2 combustor run with water diluent (fig. XI-9) has been tested at the Lewis Research Center. When it is mated with an appropriate turbine and generator, this combustor can produce over 4 megawatts of electric power. Especially notable is its compactness. The unit sizes of the stoichiometric combustor and a conventional air-fed boiler with

the same power output are compared in figure XI-10. Also, because the H_2-O_2 powerplant is a closed-cycle system, it eliminates stack losses and results in higher thermal system efficiency.

The potential applications of hydrogen combustor - turbine generator systems are much broader than baseload or peak power generation. They can be used in steam replacement systems. They may even aid in more fully recovering fossil fuels from underground reservoirs. The systems use state-of-the-art components and have high specific energy and minimum environmental impact. Our preliminary economic and performance assessments show that these systems are competitive. If system efficiency can be increased from the present value to the predicted future value of about 47 percent, these systems will be most attractive.

An advanced energy storage concept being actively investigated is an electrochemical storage system which employs an electrically rechargeable flow cell (fig. XI-11). The heart of the flow cell is a redox couple, that is, two oxidation-reduction reactions in which the ions of the pair remain soluble in their electrolytes in both their reduced and oxidized states. The flow cell itself consists of two compartments, each containing an electrolyte and an inert carbon electrode. The compartments are separated by a permeable, selective ion exchange membrane. The anolyte and catholyte solutions are circulated through the cell from storage tanks. The membrane allows ions to pass from one compartment to the other, preserving electroneutrality and generating electricity. The cell is recharged by reversing the flow of input current.

NASA is conducting a technology program to develop the redox flow cell concept. Thus far, the concept looks very attractive because it has all the advantages of batteries with the addition of very deep discharge cycles but without apparent cycle life limitations. Efficiencies as high as 70 percent are predicted. The technology problems are, admittedly, numerous. A satisfactory membrane with low ionic resistance, good selectivity, and long life is not currently available. The predicted power density of 648 W/m^2 has yet to be obtained in the laboratory. And while promising redox couples have been identified, property data are not available. It may be some time before a redox flow cell is a practical reality. Its development will, however, represent a significant advance in energy storage technology.

MODULAR-INTEGRATED UTILITY SYSTEMS

One key to the efficient utilization of energy lies in the integration of the various utility functions into a single system. This is not a new idea to NASA. Each of our manned spacecraft was a small "community" that required the same utility services as would an ordinary community. And, of course, in space, efficiency and reliability are key requirements. Recently, NASA has been applying this energy systems know-how to a terrestrial community.

This 3-year program, started in 1973, is a joint Department of Housing and Urban Development (HUD)-NASA activity to define a modular-integrated utility system (MIUS). The objective of this program is to demonstrate efficient integration of utility functions in an apartment complex. Utility functions to be integrated are electrical, water, solid and liquid waste, and space heating and cooling.

The basic process utilizes a prime mover to drive an electrical generator, as illustrated in figure XI-12. The high-temperature waste heat is used for space heating and cooling (through utilization of an absorption cooler). The low-temperature waste heat is used for water heating and waste drying. The dried sewage and rubbish is then used, along with fossil fuel as needed, as the fuel for the prime mover. Presently, NASA has completed concept feasibility studies, HUD is carrying out a site selection activity, and NASA has initiated verification tests at the Johnson Spacecraft Center using a MIUS integration and subsystem test (MIST) facility. The basic components of this facility, as illustrated in figure XI-13, duplicate or simulate those that would exist in an actual MIUS installation.

The potential payoff of MIUS is considerable: energy savings, 35 percent; water savings, 18 percent; effluent reduction, 28 percent; and trash load reduction, 80 percent. Technological improvements could further enhance the concept. NASA is continuing to investigate gaseous fuel production by pyrolysis, slurry transport and anaerobic digestion, and multifuel fuel cells in hopes of providing the information base for future, improved MIUS systems. As illustrated in figure XI-14, one such advanced system could utilize solar energy if and when that technology becomes available.

Figure XI-15 depicts how a MIUS utility system could be architecturally integrated into an apartment complex. It is obvious that successful im-

plementation of this idea will involve institutional and social issues, in addition to the technological ones. However, the idea looks promising, and the payoff appears to warrant additional effort.

SOLAR ENERGY

It is generally accepted that solar energy could, in principle, be used to supply virtually all of our energy needs. The real question is whether solar energy can become sufficiently economical and reliable to actually displace other energy sources now in use. The answer to that question is the subject of a number of investigations currently underway.

There is more than enough energy in the form of sunshine (fig. XI-16), and it is convertible to all the forms of energy we need (fig. XI-17). The solar energy falling on 7 percent of U.S. land - an area equal to the size of Texas - could supply all of our projected 1985 energy needs, assuming an overall conversion efficiency of 5 percent. This energy could be transformed into electricity or into clean fuel forms such as oil or gas or it could be used directly to heat and cool buildings.

Solar heating and cooling of buildings appears to be the solar technology that is nearest to commercial maturity. There are already a number of residential structures that utilize solar energy. Some typical ones are illustrated in figure XI-18.

NASA has underway a number of activities aimed at creating and advancing the technology for low-cost, efficient, reliable solar heating and cooling systems. Those activities, which are described in the following pages, are a general solar research and technology program, a major office building project, a solar-assisted gas water heater project, and program planning activities related to the Solar Heating and Cooling Demonstration Act of 1974.

Solar Technology Program

At the Lewis Research Center, NASA is conducting a research activity to advance the technology for solar heating and cooling systems. This effort

involves testing and evaluation of solar collectors under both simulated and real-sun conditions, development of solar collector coatings to enhance the thermal performance and life of collectors, experimental modeling on a laboratory scale of entire solar heating and cooling systems, and systems analysis and utilization studies to determine which collectors show the most potential to be cost effective in various applications.

A solar simulator (fig. XI-19) has been constructed to test solar collectors under known, controllable, and reproducible conditions. The simulator utilizes a bank of 140, 300-watt lamps that provide a very close duplication of the wavelength distribution of "air-mass 2" sunlight. The intensity can be varied from that corresponding to a cloudy day in Cleveland (150 Btu/hr/ft^2) to high noon in Tucson (350 Btu/hr/ft^2).

This controlled "sunshine" falls on a 16-ft^2 test pad area. Coolant flow rate and inlet temperature are varied over predetermined ranges during a test. The collector test pad has two-dimensional movement so that it can be set to provide any desired incidence angle. During 1974, the first year of simulator operation, over 20 different collector configurations were tested. Most of these were collectors obtained from various industrial sources. We have found this test facility to be a strong and valuable tool for comparing various collectors on a consistent basis.

After being tested in the simulator, some collectors are selected for further testing under real-sun conditions. Figure XI-20 shows one of two identical outdoor test stands. Each of these stands can test five collectors at one time, obtaining separate data on each collector. Coolant flow rate, inlet temperature, and tilt angle can be varied independently for each collector if desired. In this facility, we study performance degradation rates and other weathering effects, all-day performance characteristics compared to instantaneous performance, night-time operation, and icing effects in wintertime.

The performance of a solar collector depends strongly on the optical properties of the surface of the absorber plate. High performance can be obtained by coating the absorber plate with a "solar selective" material that has a high absorptivity in the wavelength range of sunlight and a low emissivity in the emitting wavelength range of a 200° F blackbody. Thus, a good absorber surface will absorb nearly all of the sunlight falling on it but will re-emit little of it.

Figure XI-21 shows an aluminum absorber plate coated with a black-chromium solar selective coating. We have found black chromium to give the same high performance as does the more often mentioned black nickel. Black chromium appears to be much more durable under the varying temperature and humidity conditions encountered in a solar collector. To date, we have measured the optical properties of over 100 different test specimens involving many combinations of various coatings (such as paint; enamel; anodized surfaces; and electroplated copper, nickel, chromium, and zinc compounds) and plate materials (such as copper, aluminum, steel, and glass).

Which collector is best cannot be decided until "best" is defined. That definition will involve some complicated mix of factors such as initial performance, cost, life, reliability, and performance degradation rate. However, the best efficiency measured to date was produced by a collector with a black-nickel-coated aluminum plate covered with two sheets of glass treated with antireflective coatings. The following table shows the performance obtained with this collector, which was produced by Honeywell, Inc., under contract to the NASA Lewis Research Center:

OUTLET WATER TEMP, ^{o}F	230
COLLECTOR EFF, %	58
SOLAR FLUX, BTU/HR-FT^2	300
PRESENT COST, \$/FT^2	16
PROJECTED COST, \$/FT^2	4

CS-72363

So far as we know, this is the highest efficiency yet reported for a flat-plate solar collector. Further, utilization studies show that this collector is cost effective in a residential heating and cooling application when compared with

a collector employing black paint and ordinary glass. Though it has yet to be substantiated, we feel that a steel absorber plate coated with black chromium and covered with an inner cover of Tedlar, or a similar material, and an outer cover of antireflective coated glass would yield the most cost-effective solar collector for heating and cooling applications. The following table shows how such a 1000-square-foot collector would perform on a 2000-square-foot house in two different geographical locations:

	% OF LOAD PROVIDED BY SOLAR	
	HEATING	COOLING
PITTSBURGH	65	100
ATLANTA	100	80

CS-72357

Langley Office Building Solar Project

NASA plans to utilize solar energy to provide a significant portion of the heating and cooling needs of a new office building that is now under construction at its Langley Research Center in Hampton, Virginia. As shown in figure XI-22, the 53 000-square-foot office building will utilize solar energy supplied by 15 000 square feet of solar collectors located in an adjacent field. This collector test bed is designed and instrumented so that as many as 15 different kinds of solar collectors can be tested simultaneously.

This project is a joint Lewis-Langley activity. Lewis has the general responsibility of providing the technology base to support this project, including the specific job of selecting and providing the solar collectors to be tested in the field. Langley is responsible for installation of the solar system and for operation and data acquisition. Lewis is responsible for interpretation of the data and publication of the results. It is currently planned to have the solar energy system ready for shakedown tests at the time of build-

ing occupancy, now scheduled for February 1976. Solar collector selection is presently underway.

Project SAGE

Through its Jet Propulsion Laboratory (JPL), NASA is working with the Southern California Gas Company to investigate the use of solar energy to augment a conventional gas water-heating system. The objective of the project is to prepare the way for commercialization of solar-assisted-gas-energy (SAGE) water heating. One million dollars will be spent on project SAGE from February 1973 to December 1976. Participants include the University of California at Los Angeles (UCLA), the California Institute of Technology (Caltech), the National Science Foundation (NSF), and the Fredericks Development Corporation in addition to the Southern California Gas Company and NASA.

Testing of various configurations for solar water heating systems for an apartment building has been carried out on a pilot plant at JPL. The system which has the best ratio of performance to cost is shown in figure XI-23. A heat exchanger is located between the tank and the hot-water circulation loop. The tank and the solar collector system are isolated from the domestic water supply by the heat exchanger, thereby minimizing the cost of the tank and collector. The tank and collector are not subjected to domestic line pressure, water hammer, corrosion, and scaling associated with simpler systems. Compared to a system without a heat exchanger the efficiency of the system is reduced by about 15 percent. This loss in efficiency is more than balanced by the savings in the cost of the tank and the cost of the collector per square foot.

The pilot plant is a full-scale system sized for a 10-unit apartment complex. The pilot plant has 450 square feet of collector and a 580-gallon storage tank. The solar collector is an array of 32 panels which measure 2 feet by 7 feet by 4 inches deep. The panels are manufactured by Unitspan. Each panel is a galvanized steel box containing an absorber plate, insulation, and glazing. The collector absorber plate is a copper sheet with tubes soldered to the back side and painted on the front side with 3M Co. Black Velvet.

insulation is approximately $2\frac{1}{2}$ inches of fiberglass. Glazing is two layers of glass, the outermost of which is double strength and tempered. Four of these panels are plumbed together in series to form a module, and eight modules are plumbed in parallel to make up the collector array. Each module is a separate physical unit and all are inclined 37° above horizontal toward the south.

To a gas utility, the seasonal and hourly variation in demand for auxiliary fuel is important. A preliminary evaluation of the demand for auxiliary fuel has been made on a simulation model of the system. Estimates were based on a 32-unit apartment building and 1400 square feet of collectors. Using hourly weather observations from the weather station at Burbank, California, for the year 1961 (a year with a space heating requirement typical of the long-term average for the Southern California Gas Company territory), performance of a baseline system was simulated with a time interval of 20 minutes. For this simulation, the daily hot-water demand was assumed to be 58 gallons per apartment unit, and the cold water inlet was assumed to be constant at 60° F. A single, typical average hourly demand profile was used for all days of the simulation. The results of this simulation are presented in figure XI-24. The monthly share of water heating carried by solar energy varied between a low of 52 percent in December to a high of 77 percent in April.

The relatively steady nature of the supply of solar energy when averaged over 1 month is very important. Of the order of 78 percent of solar energy collected by the system in 1961 could have directly displaced production and transmission capacity in the gas utility system. Thus, the "steady supply" component of solar energy is more significant than the "when available" component in the water-heating application.

Finally, the equipment will be tested in the field, and marketing and institutional problems that challenge rapid and widespread use of SAGE water heating will be addressed. SAGE water heating systems will be installed and tested on both an existing apartment building and a new apartment building. These systems will be installed by collaborating members of the building industry.

Because of the sensitivity of the building industry to first cost, the Southern California Gas Company marketing staff will compare utility ownership of equipment to other business arrangements. The best business approach

for offering SAGE water heating to the market is to be determined.

Because of the current situation in the world energy market, the institutions which influence the energy market are reevaluating energy policies. The existing policies under which the energy market operates favor continued dependence on fossil fuels and retard introduction of solar energy systems. Alternative government policies, incentives, and regulations needed to encourage application of SAGE water heating are to be evaluated.

Figure XI-25 compares estimates for SAGE water heating made in 1973 to actual costs for the two most prevalent types of water heaters in use in Southern California apartments. The 1974 estimates for SAGE water heating equipment are about double the 1973 estimates (i. e., $600 compared to $300 per apartment unit). The increase in the estimate is caused by inflation in the cost of off-the-shelf components and labor and hardening of cost estimates for a conventional, metal-box, double-glazed, steel-absorber solar collector, which start at $6.70 per square foot. There is still considerable hope that the cost of a collector suited to the apartment application can be fabricated and delivered to the site for $2.00 per square foot. This would reduce the estimated cost for the SAGE system to $360 per unit.

Based on experience with pilot plant construction and performance, the 1974 cost of solar energy for water heating was competitive with that of electricity. In order to be strictly competitive in cost with natural gas, solar technology must improve and the price of gas must rise.

The resistance of the housing industry to innovations has been studied. Case studies have been combined with an extensive review of the literature. Eleven generic barriers to acceptance of innovations have been formulated from these case studies. Specific operational tactics for overcoming these barriers will be formulated in conjunction with a panel of experienced major personnel in the housing industry.

In this final testing and marketing phase, the center of effort will move to the gas company. JPL will provide technical direction and analytical support to the project. Supported by staff from Caltech and UCLA, JPL will formulate industry requirements and evaluate policies and incentive options. After this, JPL will phase out of the SAGE project with the Southern California Gas Company. Possible future JPL roles include technical direction and support to the gas utility industry in the implementation of SAGE water heating in other areas; research for utility research agencies such as the Electric

Power Research Institute (EPRI) on components for solar-assisted water heating (tank operation, storage, collectors); research and development of other solar heating, ventilating, and air conditioning systems; and planning and execution of research- and action-oriented projects related to energy conservation in the building industry.

Solar Heating and Cooling Demonstration Act of 1974

In September 1974, the President signed the Solar Heating and Cooling Demonstration Act into law, prior to the more recent formation of ERDA. It authorized a 5-year, $60 million nationwide demonstration program. NASA was to develop and procure the solar heating and cooling systems, and HUD was to provide the structures to be used for the demonstrations.

At that time, NASA designated its Marshall Space Flight Center in Huntsville, Alabama, to take the lead within NASA to procure and provide to HUD the hardware systems to be utilized in the demonstrations. A solar "test house" (fig. XI-26) has been in operation for approximately 1 year and has produced much valuable system operating experience.

With the formation of ERDA, the basic NASA responsibilities in solar heating and cooling demonstration have been transferred to that agency. A possible NASA role in that demonstration activity is presently being discussed by NASA and ERDA. Along with other government agencies, NASA has been working with ERDA to develop a national heating and cooling program plan that would include demonstrations as a major program element.

Wind Energy

As a part of the nation's solar energy program, ERDA is carrying out a program to develop wind energy devices. The Lewis Research Center is responsible for carrying out a portion of that technology program. The major elements of the Lewis activity include a 100-kilowatt experimental wind turbine generator; supporting research and technology; and the first industry-built, utility-operated wind turbine generators.

In order to get some early learning experience about how to instrument,

test, and operate a wind turbine, a commercial machine was purchased. Figure XI-27 shows this 4-kilowatt wind generator in operation. In the summer of 1975, we plan to put into operation a 100-kilowatt test wind turbine. Figure XI-28 shows a model of that device. The centerline of the generator will be 100 feet above the ground. The diameter from blade tip to blade tip will be 125 feet. Figure XI-29 shows the templates, fixtures, and forgings for the first metal blades to be used.

With this test wind turbine, we plan to evaluate various new component technology ideas for reducing the cost of reliable wind generators. The primary source of these new ideas will be a supporting research and technology program now being initiated by NASA for ERDA. A major program goal is to turn over the first industry-built machines to electric utilities in the summer of 1977. These machines, probably in the size range of 1- to 3-megawatts, will be operated by the utilities and will be connected into actual power grids. To this end, Lewis recently held a conference to acquaint the electric utility industry with the program goals and plans and to invite their active participation. More such conferences will be held at appropriate times, since we view this as a joint government/utility program, and not an activity that we can or should carry out alone.

CONCLUDING REMARKS

This paper has briefly described the status of some of NASA's efforts to develop the technology for advanced energy systems. The challenge is great. Much has been done, but much more remains to be done. It will be a difficult task to move technology from the research and development stage into the commercial arena with success. The assistance and active participation of the appropriate industry elements - like the gas industry - is a necessary element for success.

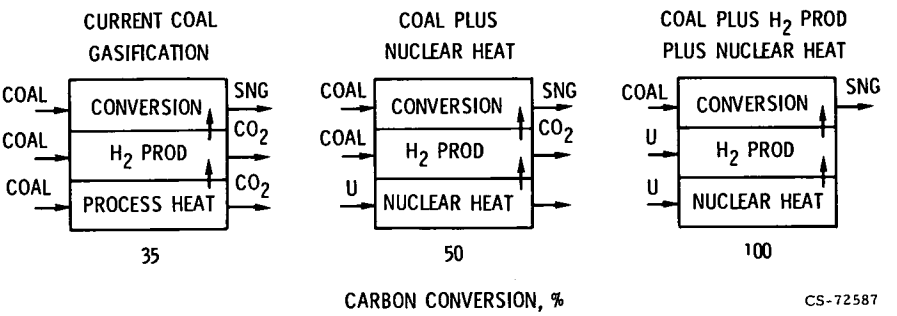

Figure XI-1. - Impact of nuclear heat on coal conversion.

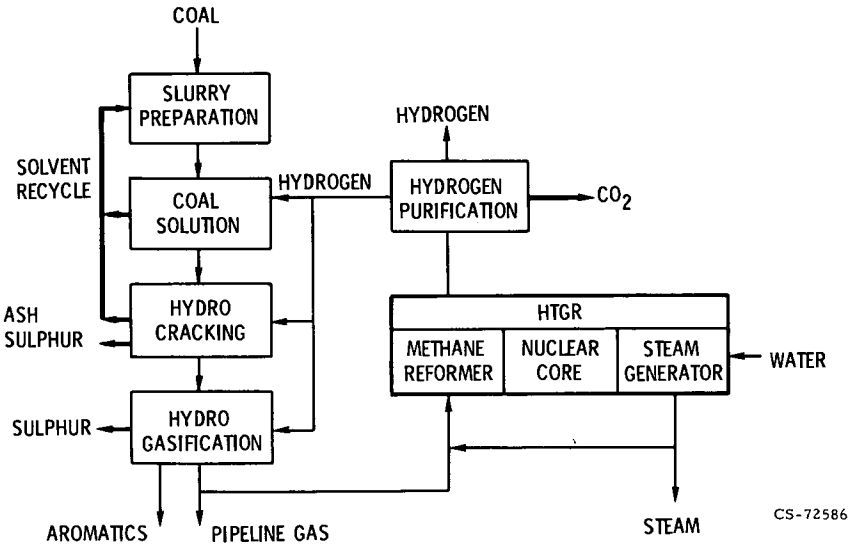

Figure XI-2. - Coal-solution gasification process.

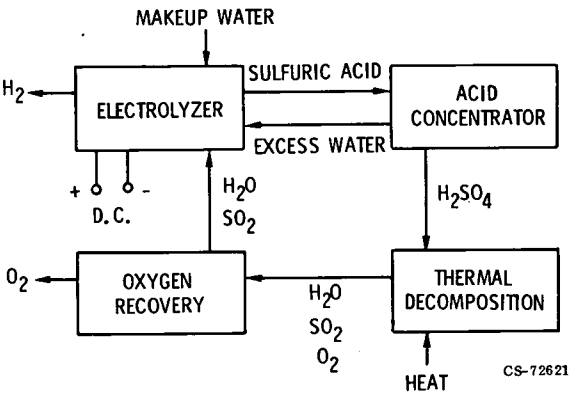

Figure XI-3. - Major components of water decomposition process.

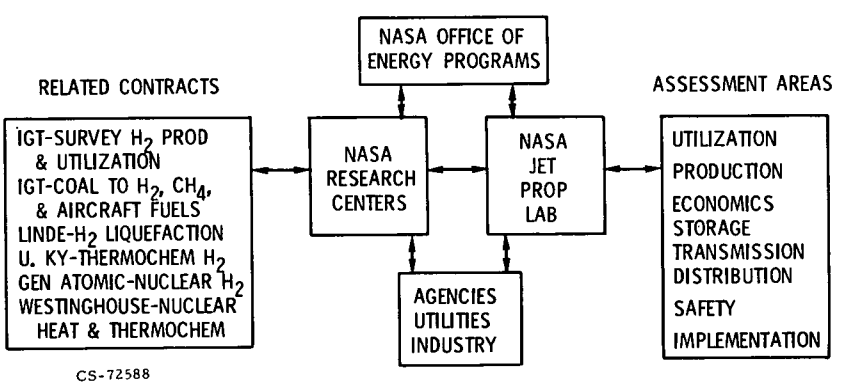

Figure XI-4. - NASA hydrogen energy systems technology study.

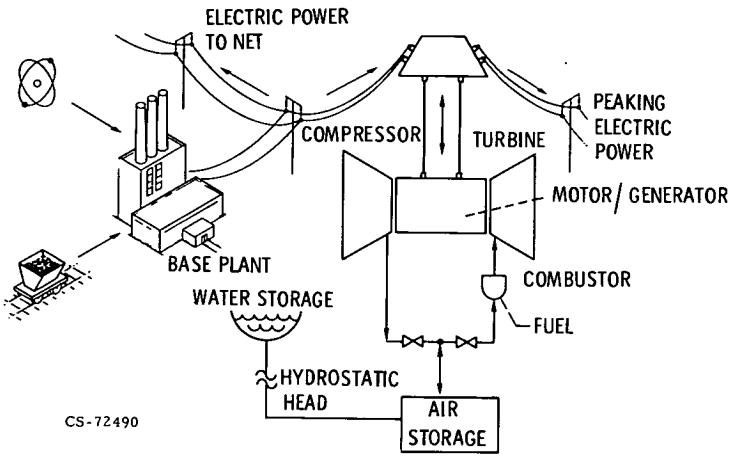

Figure XI-5. - Schematic of compressed-air storage facility.

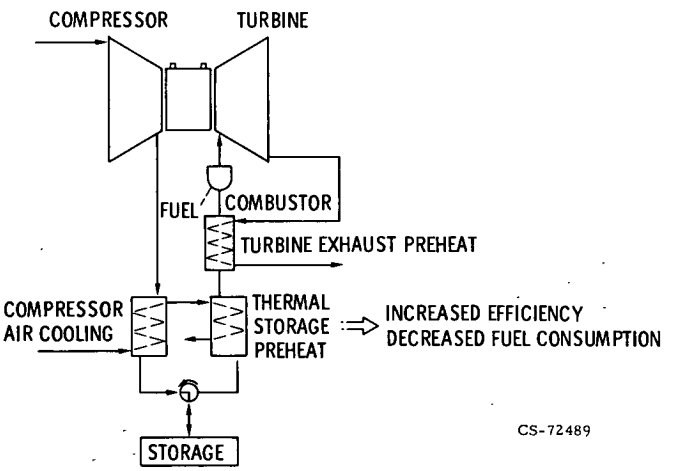

Figure XI-6. - Compressed-air storage concept.

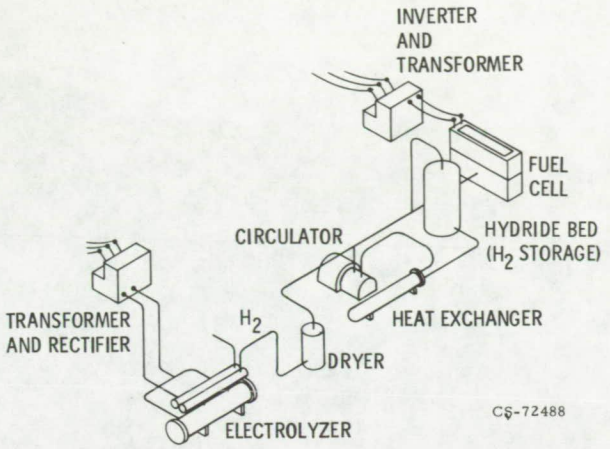

Figure XI-7. - Brookhaven National Laboratory hydrogen energy storage plant.

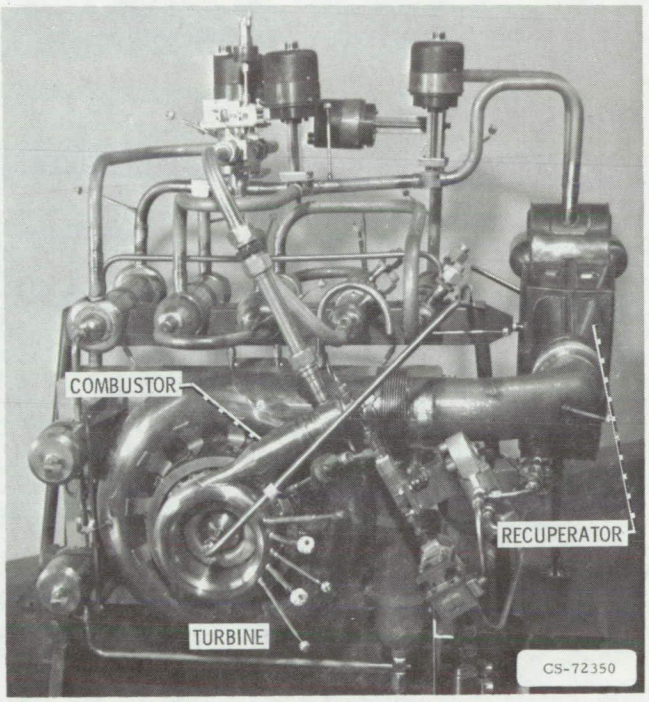

Figure XI-8. - Space Shuttle hydrogen-oxygen auxiliary power system.

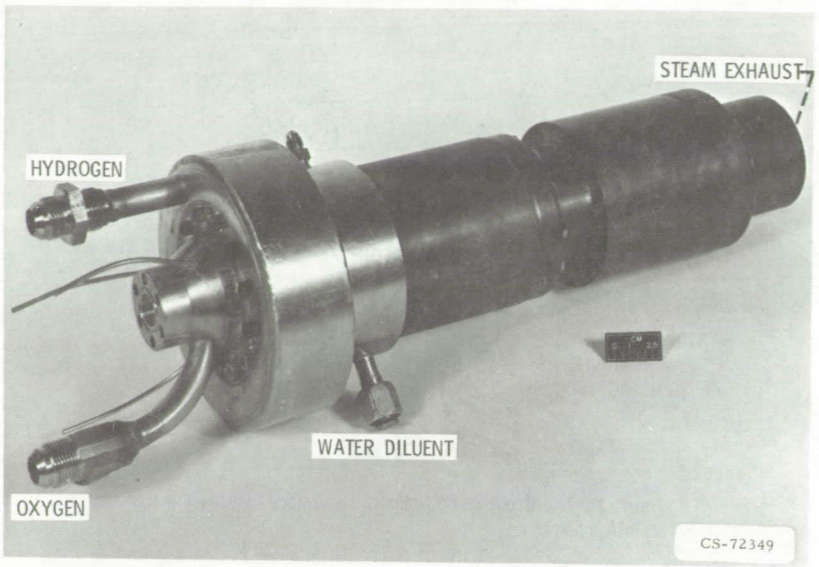

Figure XI-9. - Hydrogen-oxygen stoichiometric combustor.

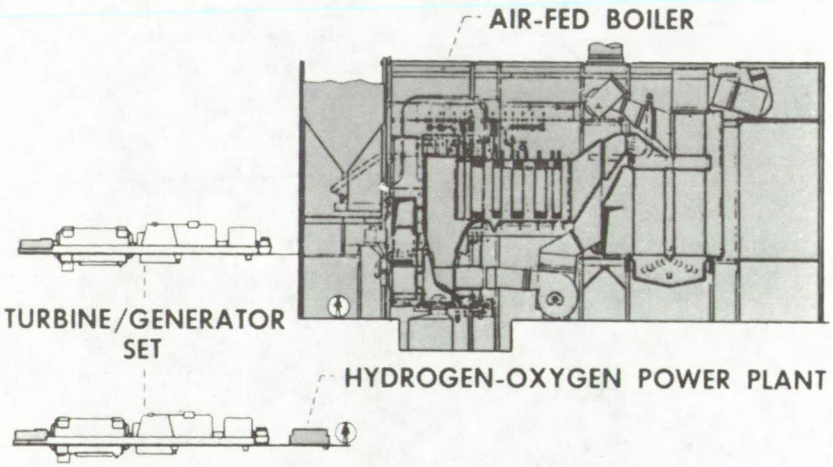

Figure XI-10. - Comparison of powerplant size.

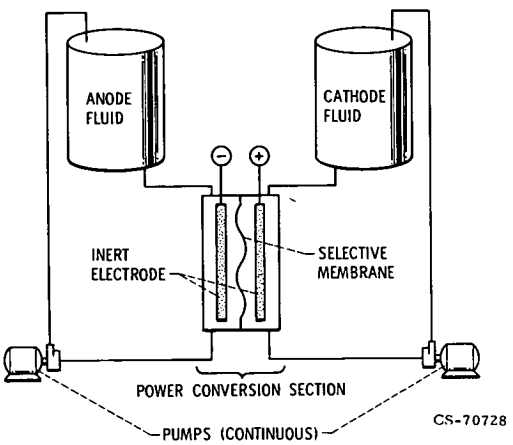

Figure XI-11. - Two-tank electrically rechargeable redox flow cell.

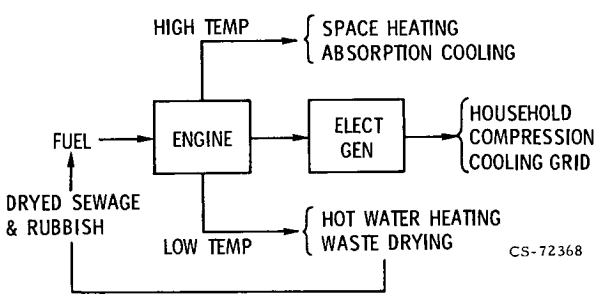

Figure XI-12. - Diagram of basic modular-integrated utility system (MIUS) concept.

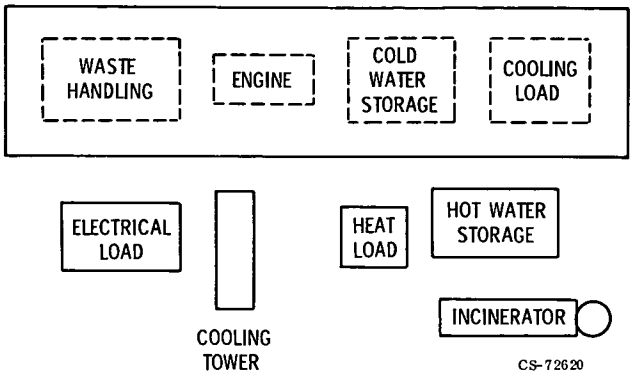

Figure XI-13. - MIUS integrated system test (MIST) facility.

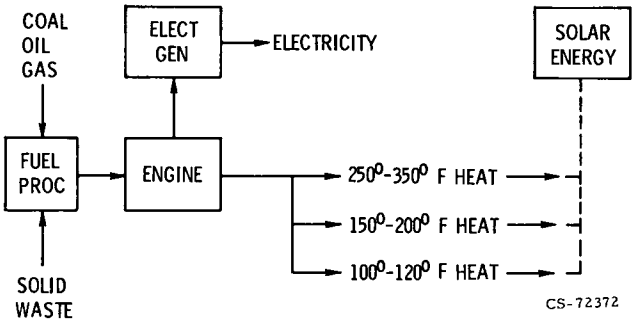

Figure XI-14. - Advanced concept for modular-integrated utility system (MIUS).

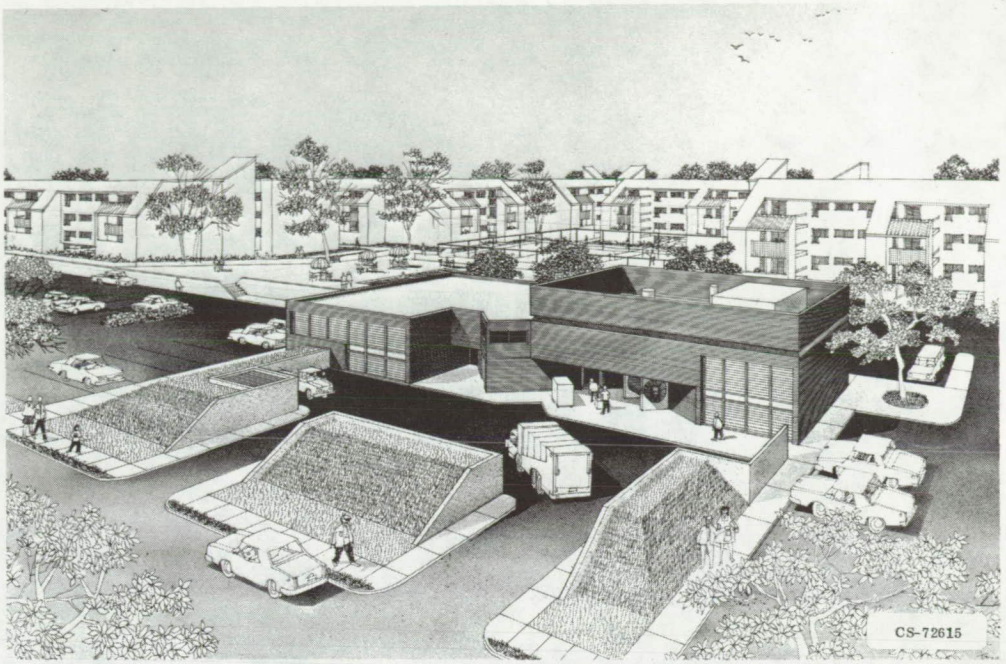

Figure XI-15. - Architectural integration of MIUS system into apartment complex.

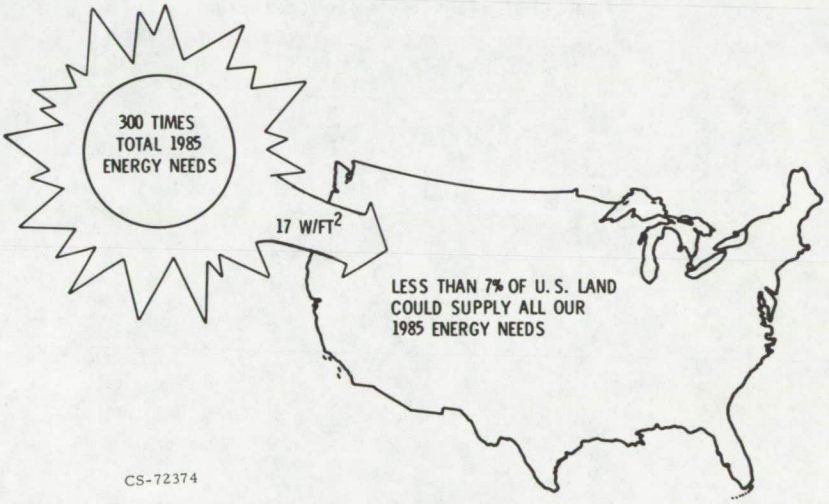

Figure XI-16. - Abundance of solar energy.

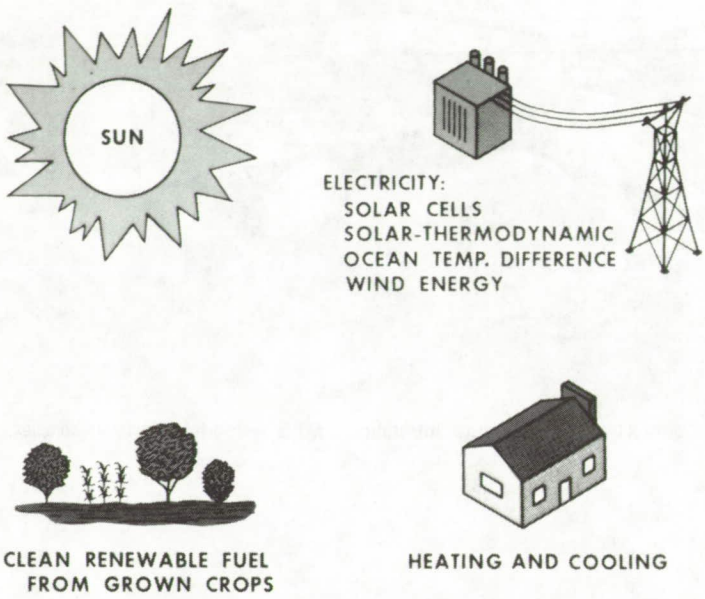

Figure XI-17. - Forms of energy provided by sun.

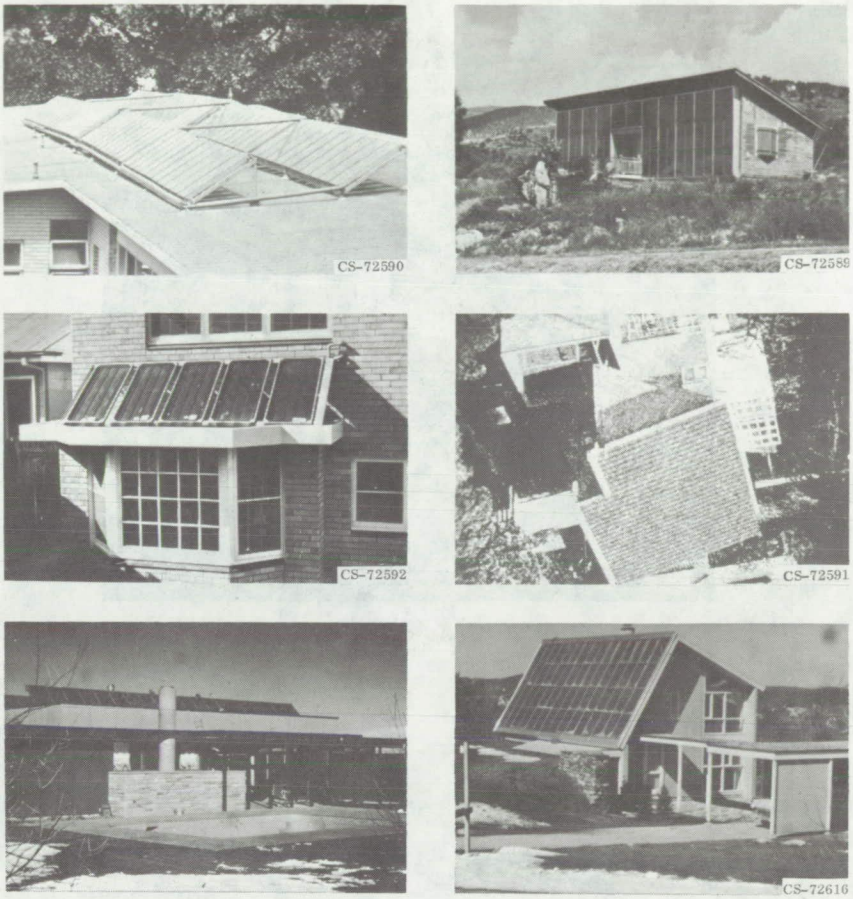

Figure XI-18. - Examples of solar collectors used on houses.

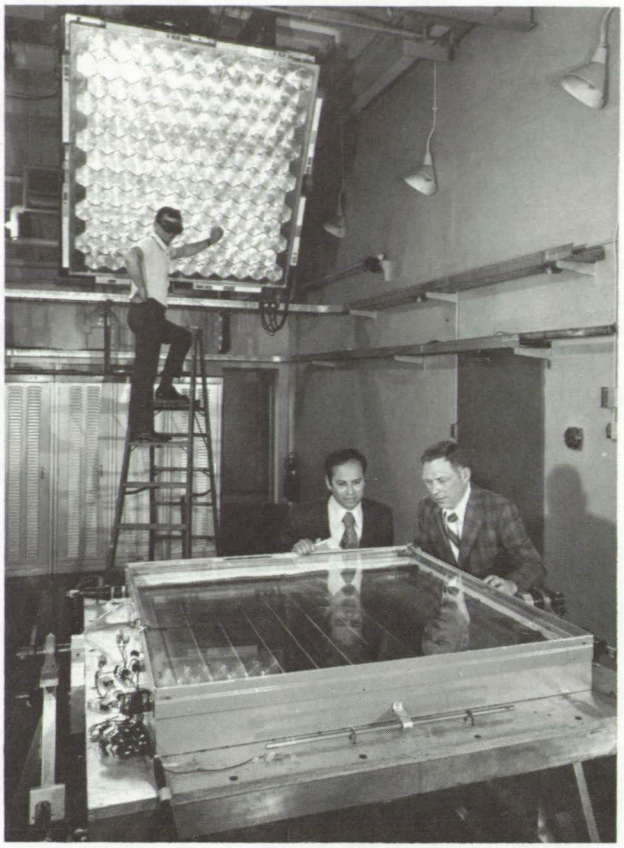

Figure XI-19. - NASA Lewis Research Center solar simulator.

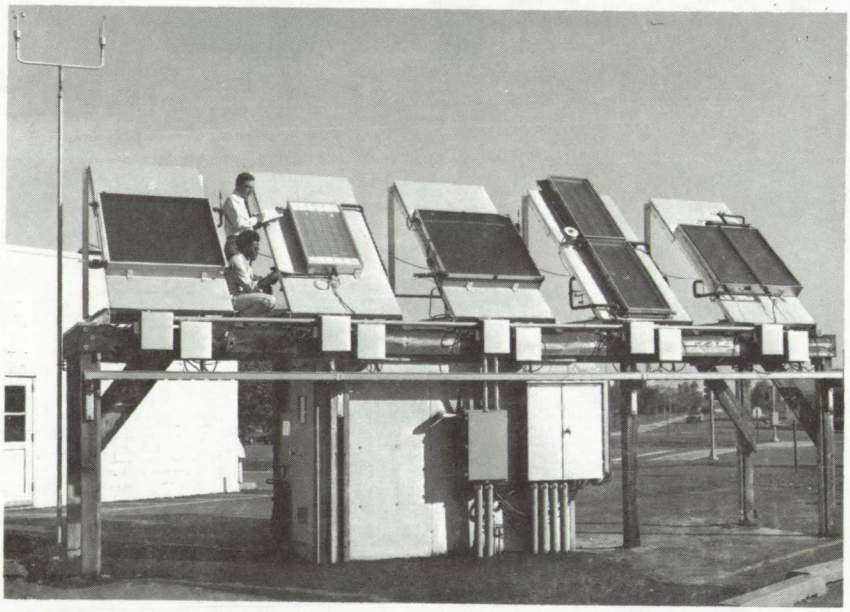

Figure XI-20. - Outdoor collector test stand.

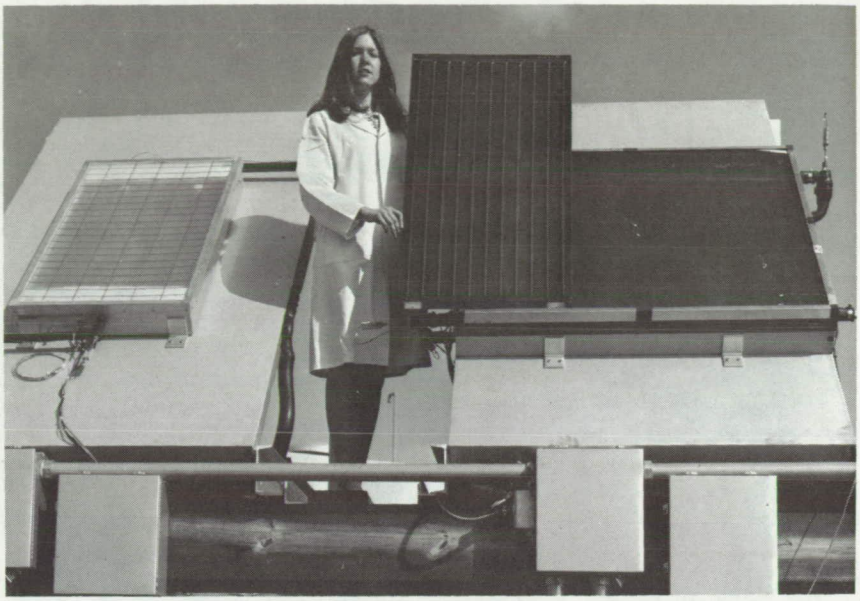

Figure XI-21. - Absorber plate with black-chromium coating.

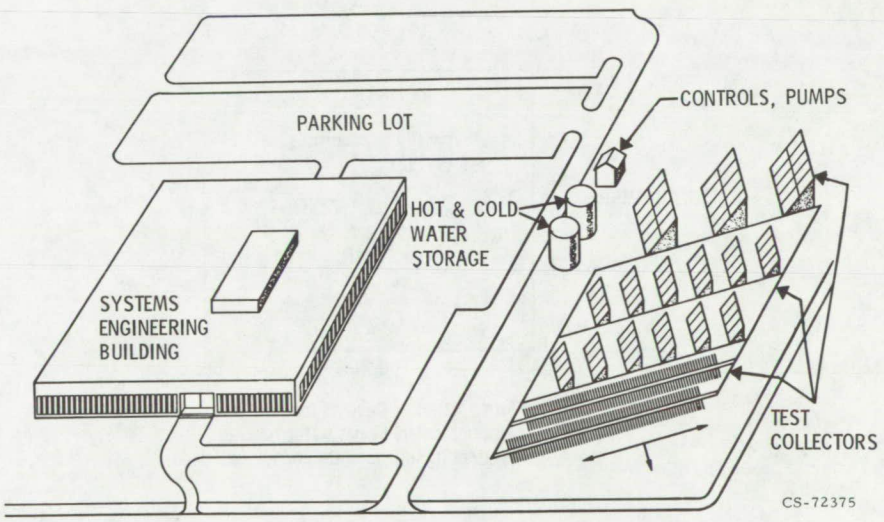

Figure XI-22. - NASA Langley Research Center office building solar project.

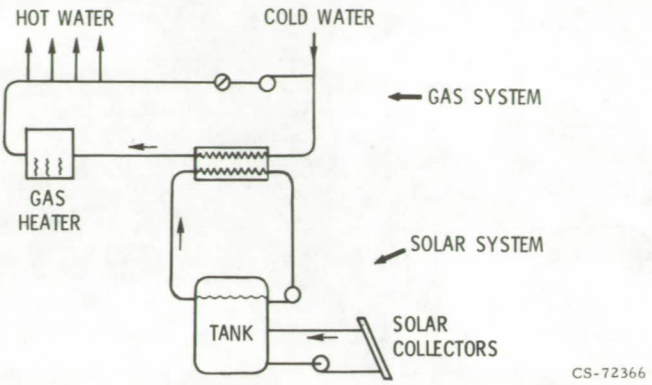

Figure XI-23. - Solar-assisted gas energy (SAGE) water heating system.

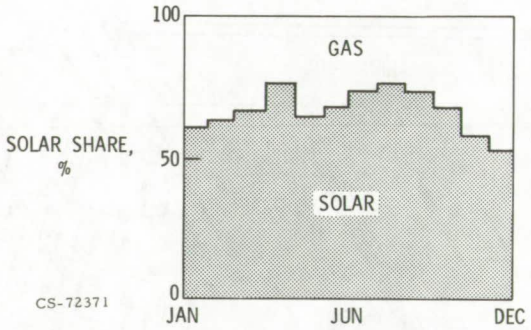

Figure XI-24. - Demand for auxiliary energy (solar) by gas water heating system in southern California.

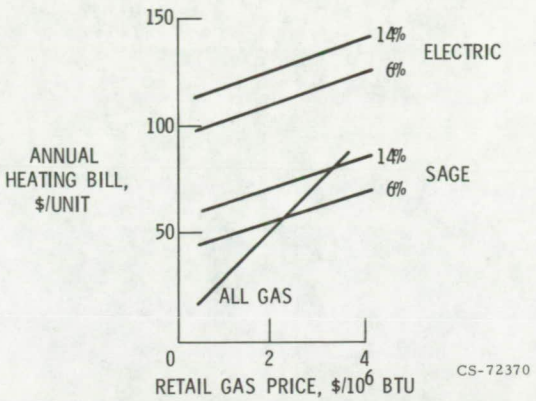

Figure XI-25. - Comparison of cost of SAGE water heating with costs of all-gas and electric water heating.

Figure XI-26. - NASA Marshall Space Flight Center solar test house.

Figure XI-27. - Four-kilowatt wind turbine generator.

Figure XI-28. - Scale model of 100-kilowatt experimental wind turbine generator.

LOCKHEED METAL BLADE

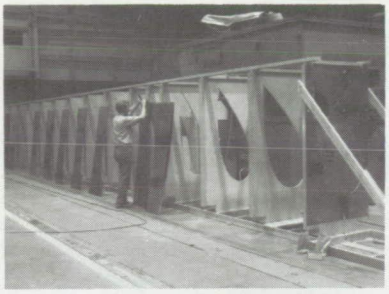

BLADE TEMPLATES

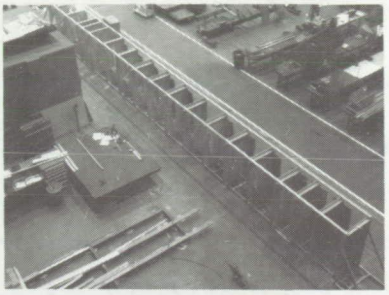

ASSEMBLY FIXTURE

BLADE ROOT END FORGINGS

CS-72491

Figure XI-29. - Steps in assembly of metal blade for 100-kilowatt experimental wind turbine generator.

☆ U. S. GOVERNMENT PRINTING OFFICE: 1975-659-661/42 Region No. 5-11

NATIONAL AERONAUTICS AND SPACE ADMINISTRATION
WASHINGTON, D.C. 20546

OFFICIAL BUSINESS
PENALTY FOR PRIVATE USE $300

SPECIAL FOURTH CLASS MAIL
Book

POSTAGE AND FEES PAID
NATIONAL AERONAUTICS AND
SPACE ADMINISTRATION
NASA-451

U.S.MAIL

POSTMASTER: If Undeliverable (Section 158 Postal Manual) Do Not Return

"The aeronautical and space activities of the United States shall be conducted so as to contribute . . . to the expansion of human knowledge of phenomena in the atmosphere and space. The Administration shall provide for the widest practicable and appropriate dissemination of information concerning its activities and the results thereof."

—NATIONAL AERONAUTICS AND SPACE ACT OF 1958

NASA TECHNOLOGY UTILIZATION PUBLICATIONS

These describe science or technology derived from NASA's activities that may be of particular interest in commercial and other non-aerospace applications. Publications include:

TECH BRIEFS: Single-page descriptions of individual innovations, devices, methods, or concepts.

TECHNOLOGY SURVEYS: Selected surveys of NASA contributions to entire areas of technology.

OTHER TU PUBLICATIONS: These include handbooks, reports, notes, conference proceedings, special studies, and selected bibliographies.

Details on the availability of these publications may be obtained from:

National Aeronautics and Space Administration
Code KT
Washington, D.C. 20546

Technology Utilization publications are part of NASA's formal series of scientific and technical publications. Others include Technical Reports, Technical Notes, Technical Memorandums, Contractor Reports, Technical Translations, and Special Publications.

Details on their availability may be obtained from:

National Aeronautics and Space Administration
Code KS
Washington, D.C. 20546

NATIONAL AERONAUTICS AND SPACE ADMINISTRATION

Washington, D.C. 20546

GPO 944-370